8-1-1995

Experimental and numerical investigation of a double concentric bluff body flameholder

Peter Eliot Zeender

"Experimental and Numerical Investigation of a Double Concentric Bluff Body Flameholder"

by

Peter Eliot Zeender

A Thesis Submitted

in

Partial Fulfillment

of the

Requirements for the

MASTER OF SCIENCE

in

Mechanical Engineering

Approved by:

Professor: Satish Kanlikar
(Thesis Advisor)

Professor: _____
(Dr. Alan Nye)

Professor: _____
(Dr. Ali Ogut)

Professor: _____
(Deptartment Head)

DEPARTMENT OF MECHANICAL ENGINEERING
COLLEGE OF ENGINEERING
ROCHESTER INSTITUTE OF TECHNOLOGY

AUGUST 1995

PERMISSION GRANTED:

I, Peter Eliot Zeender, do hereby grant permission to the Wallace Memorial Library of the Rochester Institute of Technology to reproduce this thesis entitled "Experimental and Numerical Investigation of a Double Concentric Bluff Body Flameholder" in whole or in part, for educational use only.

December 15th, 1995

_____

Peter Eliot Zeender

FORWARD:

This work has been almost two years in the making, and it has proved to be the academic highpoint of my engineering career. The list of people I would like to thank for all their help, inspiration, support and understanding is too enormous to put to pen. I would like to make special note of a few though, as this work would be incomplete without their mention.

I would like to thank Dr. Kandlikar, for putting up with me for so long. He has been instrumental in maintaining an academic environment that makes work such as this posssible. His endless support and guidance are greatly appreciated. I would like to thank Dr. Ogut and Dr. Nye for aiding me in putting this work into its final presentable form. I extend great appreciation to the RIT Machine Shop, especially Dave Hathaway, Jim Greanier and Tom Locke for everything they have done for me. I want to extend a special thanks to Janet Zandy, for directing my vision to the concerns of the world outside of engineering, a gift that has helped to change my life.

I want to extend my love and thanks to all of my family; Mom, Dad, Aaron, Nathan, the fam, Grandma and Grandpa for giving me the support I needed to bring this work to fruition. A very special thanks to my best friend Tracy Avgerinos for more than I can put into words.

Thanks to all my academic peers and friends, who have played such a vital role in my life these past five years. And lastly, though by no means the least, my thanks to Dr. Abdel Hafez, a mentor without whom this work could never have been concieved. It was hisguidance and friendship that put me on the path I am today, I for that I am grateful.

ABSTRACT:

In the present investigation, the flow through a double concentric bluff body flameholder is examined. The flameholder is studied numerically, using commercially available computational dynamics software CFDS-Flow3D; and experimentally, using a burner test stand constructed for the study.

The capabilities of the software are first validated by a numerical recreation of experimental work done by Huang and Lin (1994) on a single bluff body flameholder. This work is then extended by converting the numerical models to include a propane jet, serving as a reference for the double bluff body models.

The flameholder is numerically modeled under both cold flow and combustion conditions for a propane diffusion flame, for four separate conditions of operation. An experimental analysis is also conducted with the test stand to verify the results of the numerical combustion model. The numerical results for the flame shape and envelope agreed closely with the experimental data.

TABLE OF CONTENTS:

LIST OF FIGURES:

LIST OF TABLES:

NOMENCLATURE:

B = body force (for turbulence model)

BA = aerodynamic blockage ratio

BR = geometric blockage ratio

C_1, C_2, C_3, C_μ = coefficients for turbulence model

D_A = outer diameter of airflow obstruction (disc) for single bluff body models

D_O = outer diameter of airflow obstruction (disc) for double bluff body models

E = flameholder blockage ratio conversion coefficient

f = mixture fraction

F_{ST} = stoichiometric mixture fraction

F/A = fuel air ratio

F/A_{Stoic} = stoichiometric fuel air ratio

G = energy production due to body force (for turbulence model)

H = total enthalpy

k = turbulent kinetic energy

m_f = mass fraction of fuel

m_o = mass fraction of oxidant

m_p = mass fraction of product

P = shear production (for turbulence model)

S = flame speed

t = time

T = temperature

u_a = axial velocity of annular jet, from Huang and Lin (1994)

u_c = axial velocity of central jet, from Huang and Lin (1994)

U = gas stream velocity

U_A = axial velocity of annular jet

U_C = axial velocity of central jet

U_{MC} = axial velocity of central jet, modified for CFD geometry

Greek Symbols:

ε = turbulent energy dissipation rate

ρ = density

μ = viscosity

μ_{eff} = effective viscosity

μ_T = turbulent viscosity

λ = thermal conductivity

Φ = equivalence ratio

Subscripts:

a = annular jet (Huang and Lin)

A = annular jet (for velocity)

A = airflow obstruction, single bluff body (for diameter)

c = central (Huang and Lin)

C = central jet

eff = effective

MC = central jet, modified for CFD

O = airflow obstruction, double bluff body

ST = stoichiometric

Stoic = stoichiometric

T = turbulent

1.0 INTRODUCTION:

The use of a bluff body obstruction for non-premixed diffusion flames is a common method for increasing flame stability in gas turbine combustion chambers, aircraft engines, furnaces and many other industrial applications. In order to maintain efficient and stable combustion over a wide range of operating conditions, most combustion chambers require a flame stabilizer of some sort. Generally, these stabilizers serve to broaden the range of combustion conditions while maintaining acceptable levels of efficiency and stability, by decreasing the direct effect of the air stream on the flame. This is most commonly accomplished by the use of either an air swirler, or a bluff body obstruction in the air stream. This work is an examination into a unique configuration of bluff body stabilizer, with bluff bodies applied to both air and fuel streams, the Double Concentric Bluff Body Flameholder.

The standard configuration for a bluff body flameholder is to place an obstruction (a disc, v-gutter, cone, or other similar obstruction) directly in the air flow of the combustion chamber. This serves to create a recirculation zone directly behind the obstruction, in the wake region. At this point, fuel is injected into the recirculation zone to create the flame. The benefit of the bluff body obstruction comes directly from the recirculation zone, and is twofold. First, the recirculation zone is an area of decreased axial velocity, which greatly increases flame stability and hinders flame blowoff, this is the most direct benefit to flame stability. Second, the recirculation zone is a region of intense mixing, as fresh air is both pulled back into the zone from downstream to mix with the fuel. An added benefit of this design is that during combustion hot gases are also pulled back into the recirculation zone along with fresh air,

serving both to preheat and ignite the fuel. All of these factors tend to increase combustion efficiency and stability, as well as increase the operation range.

Bluff body stabilization can be used for both liquid and gaseous fuels. For gaseous fuels, the fuel is injected directly into the recirculation zone through the injection nozzle, while for liquid fuels an air atomizer is commonly used to disperse the fuel into a fine mist for efficient combustion.

The Double Concentric Bluff Body Flameholder incorporates the bluff body method of stabilization into both the air stream and the gaseous fuel stream. The expected result of this configuration is the formation of an additional recirculation zone above the fuel inlet, which should cause an increase in fuel-oxidant mixing over the single bluff body configuration, as well as enhanced flame stabilization characteristics. This being the case, this configuration warrants further investigation in order to better understand its performance. As the structure of the recirculation zone is of critical importance to the stability of the flame, the present investigation will be focused around this region.

2.0 OBJECTIVES:

The main objectives of the present work are:

1. To model the single bluff body visualization study of Huang and Lin (1994) using commercially available computational fluid dynamics code, as verification of the capabilities of CFDS-Flow3D, as well as to serve as a comparison for the double bluff body analysis.

2. To model the flow characteristics of a Double Concentric Bluff Body Flameholder using CFDS-Flow3D, under both cold flow and combustion conditions.

3. Construct a double concentric bluff body burner test stand, to be used for the experimental section of the study.

4. Conduct an experimental study of the flame to obtain temperature profiles, and compare these with the computational work.

5. Determine possible benefits to fuel-oxidant mixing and recirculation of the Double Concentric Bluff Body configuration over the single bluff body configuration.

3.0 LITERATURE SEARCH:

3.1 Principles of Combustion:

Combustion is a reaction process that is governed by both physical and chemical conditions. It is the process whereby a fuel reacts with an oxidant in order to release its latent energy through an exothermic reaction. The fuel and the oxidant are the reactants of the process, and the products of the reaction generally include carbon byproducts (carbon monoxide and dioxide), water, light, and significant amounts of heat. There are many conditions that affect the combustion process, as are there often many effects of the process (most generally some form of flame or explosion). The amount of fuel and air present is a defining factor of combustion, as are the burning rate of the mixture, the flame speed, and the velocity of the surrounding gases. The most common effect of the process is a flame, the visible embodiment of the reaction and the release of light and heat. The flame itself has many important characteristics, most notably its combustion efficiency, adiabatic and maximum temperatures, and levels of stability and turbulence.

3.11 Chemistry of Combustion:

As stated previously, combustion is an exothermic chemical reaction. Methane, for example, reacts with oxygen as follows:

$$CH_4 + 1.5O_2 \longrightarrow CO + 2H_2O \qquad (3.1)$$

to form carbon monoxide, water, heat and light. Or as follows:

$$CH_4 + 2O_2 \longrightarrow CO_2 + 2H_2O \qquad (3.2)$$

to form carbon dioxide, water, heat and light. Notice in both cases that heat is released and there is no unreacted fuel or oxygen.

While oxygen may seem the ideal oxidant, at least chemically, it is generally easier, safer, and much more economical to use air instead. Air reacts with propane, for example, as follows:

$$C_3H_8 + 7\,(O_2 + 3.76N_2) \longrightarrow 3CO_2 + 8H_2O + 26.32N_2 \qquad (3.3)$$

to form carbon dioxide, water, heat, light, with leftover nitrogen (for this example, air is assumed to contain 79% Nitrogen and 21% oxygen). This case, where there is exactly enough air to react in combustion with all the fuel to produce complete combustion, is called the stoichiometric ratio of air and fuel.

There are three possible mixture ratios of oxidant and fuel that can be employed to ensure the desired reaction: stoichiometric (as seen above), excess air, or insufficient air. The stoichiometric condition is when there is precisely the required amount of air to completely combust the fuel. The excess air condition is when there is more air than stoichiometrically necessary to combust the fuel (often many times the required amount). This results in complete combustion of the fuel, as well as a large amount of air remaining after the reaction. The insufficient air condition is when the amount of air involved in the reaction is less than the amount necessary to completely combust the fuel, often leaving significant portions of the fuel uncombusted, with little or no leftover air (only heated product gases).

At this point it is helpful to define the fuel-air ratio (F/A), which is the ratio of fuel to air by mass for any given combustion process. The fuel-air ratio can be further classified

as either the stoichiometric F/A or the actual F/A. The stoichiometric FAR being that under stoichiometric conditions, and the actual fuel-air ratio being simply that actually used in a given reaction (excess or insufficient air).

The equivalence ratio (Φ) is another important property of a combustible mixture, and is defined as follows:

$$\Phi = \frac{(F/A)_{ACTUAL}}{(F/A)_{STOICHIOMETRIC}} \tag{3.4}$$

The equivalence ratio is used primarily to place a mixture into one of the three categories described above. An equivalence ratio of one denotes a stoichiometric mixture, that greater than one denotes a rich (insufficient air) mixture, and that less than one denotes a lean (excess air) mixture.

3.12 Flames:

A flame is loosely defined as a combustion process that gives off both light and heat. It is the most common embodiment of a combustion reaction. The most visible portion of the flame is at the edge of the luminous zone, and is called the flame front or flame envelope. This is the very outer shell of the flame, and is the area where the surrounding air meets the fuel and combustion begins to take place. The bulk of the reaction between the air and the fuel takes place here, and consequently this is generally the region of highest temperature and product concentration. The concentration profiles for the oxidant, fuel and products across a diffusion flame front and inside the flame at a constant height above injection ports (above any recirculation zone) are shown in Figure 3.1.

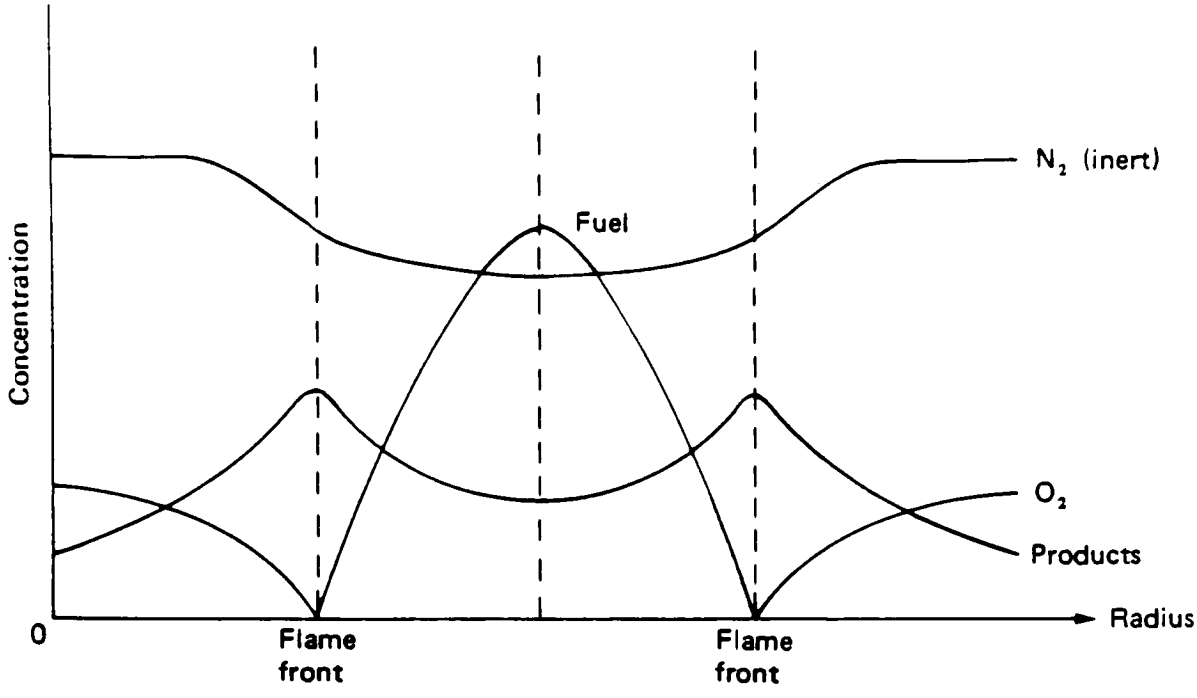

Figure 3.1 Standard Diffusion Flame Concentration Profiles

The flame is initially characterized by how the fuel and air are physically brought together, as either a premixed flame or a diffusion flame. For a premixed flame, the air and the fuel are intimately mixed in non-combustion conditions, then ignited and supplied with additional air to insure complete combustion. For a diffusion flame, the air and the fuel are unmixed prior to ignition, and mix directly at the flame front itself (or in the recirculation region as will be seen later in the Sections 5, 6 and 7).

The flame is further characterized by the flow characteristics of the injected fuel mixture (for premixed) and/or the characteristics of the gas stream in which the fuel is injected (for diffusion). Flames are also classified as laminar or turbulent. Laminar flames tend to be much steadier and stable, with a well defined flame length and shape; while turbulent flames are often unsteady and wrinkled, with an overall oscillating flame length. Turbulent flames do, however, offer some distinct advantages over laminar flames. Their burning rate is much higher as their turbulent and wrinkled nature greatly increases the amount of surface area on the flame front, and there is generally more intense fuel oxidant mixing caused by the turbulent nature of the flame. Both of these characteristics tend to increase flame efficiency, but decrease flame stability. As this is the case, in practical applications measures must be taken to stabilize turbulent flames before these benefits can be realized.

3.13 Flame Stabilization:

The basic principle involved in flame stabilization is quite simple. Every flame has a flame speed (S), which is a property based primarily on the burning rate of the mixture.

The flame speed is a measure of how quickly the flame can consume incoming fuel. If combustion is initiated in a flowing stream, and if the gas velocity U is higher than this flame speed S, the flame will move downstream at a speed of U minus S. If the burning velocity is higher, than the flame will move upstream with a speed of S minus U. Only when U equals S (or if U is less than S and there is an obstruction to block the flame from traveling upstream) will the flame be stationary and stable. In order to achieve the required stability for a flame in conditions adverse to combustion, such as in high velocity gas streams and low inlet temperatures (as in aircraft engines) or for a wide range of operating conditions (as in gas turbine engines), one must use some form of flame holder.

The function of a flame holder is to create, in a high speed gas stream, a region whose velocity is lower than the burning velocity of the mixture (the recirculation zone). Flame blowout occurs when the burning velocity of the flame is below the gas speed at all points in the flow field. Thus the primary design objective for good stability is to maximize the ratio of burning velocity to flow velocity; incidentally this is also a major requirement for high combustion efficiency.

The most common form of flame stabilizer is the bluff body flameholder. Bluff body flameholders operate by the insertion of a non streamlined body into the gas stream; causing a recirculation zone of greatly decreased gas velocity (U) immediately after the body, followed by a turbulent wake region that follows further downstream. This, in effect, increases flame stability by effectively lowering U for the area of the gas stream in which the combustion will take place. A shear region is created between this recirculation zone and the gas stream. This shear region pulls fresh air in from the jet stream and passes

it into the recirculation zone for stable combustion. Most of the hot combustion products then travel downstream through the wake, though some are pulled back into the shear region and are passed into the recirculation zone to heat up the reactants. Figure 3.2 gives sample visualized flow around some standard bluff bodies, by Isaac, Chidananda and Sridhara (1976).

As this form of flameholder is usually located in a duct, hence a very important characteristic becomes its geometric blockage ratio (BR) as:

$$BR = \frac{\text{Duct Free Flow Area}}{\text{Blockage Area}} \tag{3.5}$$

and a relation for the blockage ratio to the aerodynamic drag is as follows:

$$\frac{1}{(1-BA)^2} - 1 = E(BR)(1-BR)^2 \tag{3.6}$$

as BA is the aerodynamic blockage, and E is a constant based on the flameholder geometry. For concentric obstructed jets:

$$BR = \frac{D_O^2 - D_I^2}{D_D^2 - D_I^2} \tag{3.7}$$

3.2 Bluff Body Flameholders:

There has been a significant amount of research reported on bluff body stabilized flames through the years, and Lefebvre (1983) reports that extensive data and empirical formulations are available in order to predict the performance of a bluff body stabilized diffusion flame.

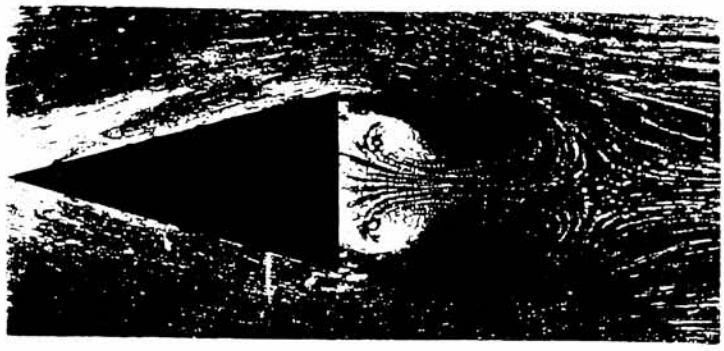

(a)

(b)

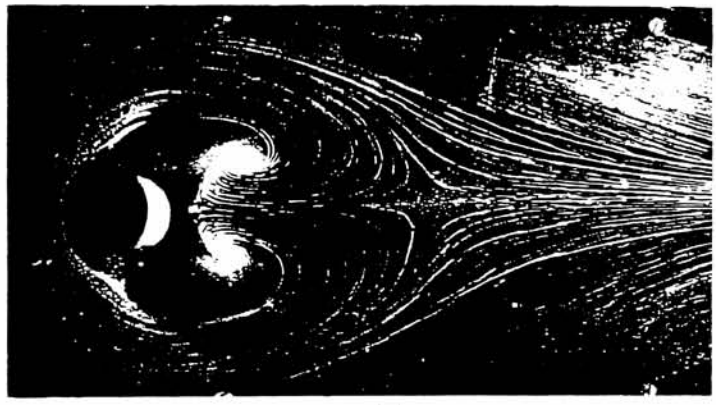

(c)

Figure 3.2 Flow Pattern around various Bluff Bodies
(a) 30° V-gutter, BR = 0.31
(b) 30° Round-nose, BR = 0.25
(c) Jet Curtain Flameholder, BR = 0.19
From Isaac, Chidananda and Sridhara (1976)

The bluff body flameholder has been studied in both cold flow and combustion conditions, as both yield insights into its performance. A cold flow analysis of a flameholder is generally an examination of the recirculation and mixing characteristics of the system under non-combustion conditions. A combustion analysis is performed under combustion conditions, and generally focuses on flame shape, stability and combustion efficiency. It is seen that the focus of most research in this area is the structure, strength and size of the recirculation zone, and its effects on flame stability and efficiency. Li and Tankin (1987) provide a good overview of some of the research done in both cold flow and combustion, as well as provide details of their own visual studies. A significant amount of research has been reported in this area, and recent work of interest to this study is briefly discussed below.

Nikjooy, So and Peck (1988) offer finite rate chemistry models (analytical) to predict the reaction region of swirl stabilized and single bluff body obstructed non-premixed flames, as well as comparisons to their experimental data. They found not only that their finite rate chemistry model was adequate to predict jet stabilized flames, but also that a k-epsilon turbulence model proved to be sufficient for non-premixed flames over a fair range of operation.

Pan, Schmoll and Ballal (1992), conducted a detailed analysis of the turbulence properties and of the recirculation zone structure of a conical bluff body flameholder, confined within a can-type combustion chamber. They presented experimental data encompassing the differences in the recirculation zone between open air and confined flames.

Shefer, Namazian and Kelly (1989, 94) present some of the effects of bluff body stabilization in several visualization studies. They present results not unlike those of Huang and

Lin (1994) as will be seen in Section 3.3, noting the significance of momentum dominance on the structure of the recirculation zone.

There are significant amounts of ongoing research in this area, but most seems to be aimed at performance analysis of specific engines and combustion chambers, rather than fundamental investigations into the principles of flame stabilization.

3.3 Review of Single Bluff Body Cold Flow Analysis

The visual study of Huang and Lin (1994), on the recirculation zone of single bluff body flameholder is of particular interest to this investigation, and is used not only to validate the CFD software, but also as a comparison for performance of the flameholder. Their experimental setup consisted of a central air jet of 3.4 mm outer diameter, and an annular jet of 30 mm outer diameter, obstructed by a 20 mm diameter disc of 0.44 blockage ratio. Using a smoke wire technique, Huang and Lin were able to determine the shape and size of the recirculation zone created by two concentric jets under various inlet conditions (for both the central and the annular jet). Four typical characteristic regions were identified - that of weak flow, prepenetration, transition, and penetration. Figure 3.3 illustrates these characteristic regions. The most influential factor of these regions is the dominance in axial momentum of one jet over the other, this being the major influence on stability. The weak flow region (Region I) is characterized by a very weak recirculation zone, as the velocities of the two jets are too low to create significant recirculation. The prepenetration region (Region II), is characterized by a strong recirculation zone, which is formed as the momentum of the reverse axial flow from the annular jet overcomes that of

the central jet. This region is further categorized into three sub-regions (A), (B) and (C); with the progression leading towards a less dominant annular jet, and a recirculation zone smaller in structure. The transition region (Region III) is that in which the momentum of the central jet begins to overpower the momentum of the annular jet, and it begins to pierce through and break up the recirculation zone. It has also been observed that this region is generally very chaotic and unstable, often accompanied by violent and random distortions in the shape of the recirculation zone. The penetration region (Region IV) is characterized by a split recirculation zone, where the momentum of the central jet overpowers that of the annular reverse axial flow, and the central jet column pierces completely through the recirculation area. This causes a division in the recirculation zone, resulting in a ring shaped zone, appearing as two smaller sub zones between the central and annular jets when viewed across the cross section.

Table 3.1 shows the results of the visualization study, most notably that the height of the recirculation zone steadily decreases as the operating conditions of the flameholder move towards the penetration region, from 1.10 and 1.20 D_A for cases II (B) and II (C) down to 0.70 for case IV (B).

Table 3.1) Sample Results of Huang and Lin, Visualization Study

Case	U_A (m/s)	U_C (m/s)	BR (-)	Approx. Height of Rec. Zone (D_A)
II (B)	0.75	1.79	0.44	1.10
II (C)	0.56	2.03	0.44	1.20
III	0.32	1.52	0.44	1.00
IV (B)	0.47	2.96	0.44	0.70

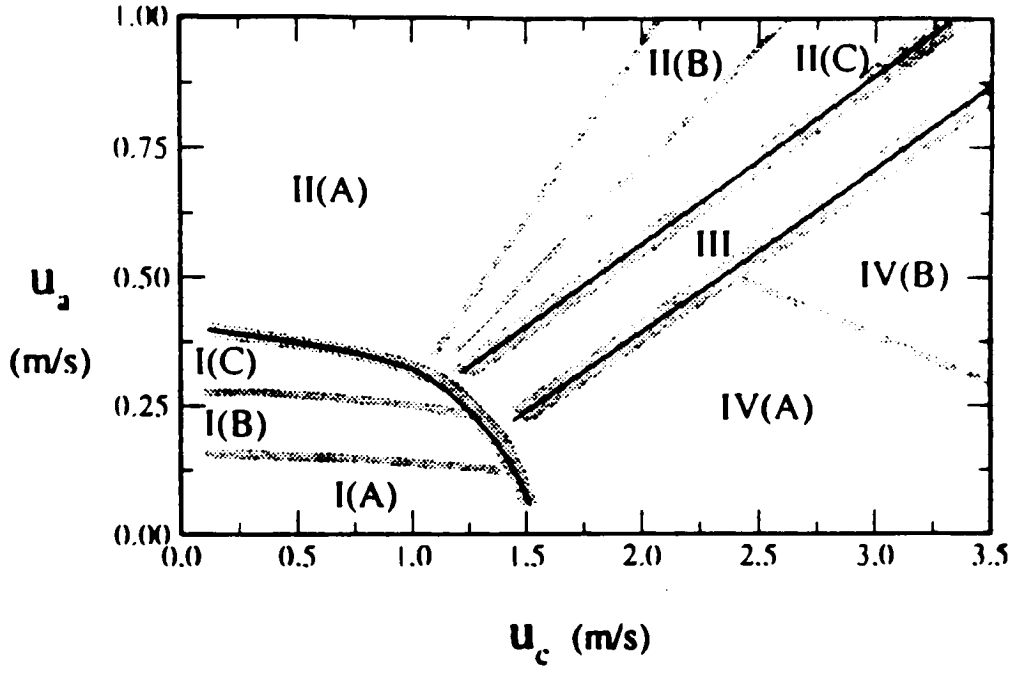

Figure 3.3 Characteristic Regions of Flow, Huang and Lin (1994)

4.0 COMPUTATIONAL FLUID DYNAMICS OVERVIEW:

4.1 Operation Principles of CFD:

A commercial CFD code, CFDS-Flow3D, was used to perform the numerical analyses in the present investigation. CFDS-Flow3D is a finite volume CFD code, with the capabilities of solving three-dimensional, compressible and turbulent flows of multiple gas and/or liquid constituents. The code solves the conservation equations of mass, momentum and energy (Navier Stokes equations) in discrete cells, based upon user defined boundary conditions, to obtain the steady state solution for the flowfield. Specifically, these equations are the continuity equation

$$\frac{\partial \rho}{\partial t} + \nabla \cdot (\rho U) = 0, \tag{4.1}$$

the momentum equation

$$\frac{\partial \rho U}{\partial t} + \nabla \cdot (\rho U \otimes U) = B + \nabla \cdot \sigma, \tag{4.2}$$

sigma being the stress tensor

$$\sigma = -p\delta + \mu(\nabla U + (\nabla U)^T), \tag{4.3}$$

and the energy equation

$$\frac{\partial \rho H}{\partial t} + \nabla \cdot (\rho U H) - \nabla \cdot (\lambda \nabla T) = \frac{\partial p}{\partial t}, \tag{4.4}$$

The code employs either a k-epsilon model or one of several variations of a Reynolds stress model for turbulence, and the k-epsilon model is used exclusively for this investigation. The k-epsilon model uses an eddy viscosity hypothesis for the turbulence of the fluid flow. This

model alters the solution of the Navier Stokes equations by replacing the fluid viscosity with an effective viscosity, that accounts for the turbulence of the fluid flow, as

$$\mu_{eff} = \mu + \mu_T. \tag{4.5}$$

For this model it is assumed that

$$\mu_T = C_\mu \rho \frac{k}{\varepsilon}. \tag{4.6}$$

The transport equations for the turbulence kinetic energy (k) and the energy dissipation rate (ε) are:

$$\frac{\partial \rho k}{\partial t} + \nabla \cdot (\rho U k) - \nabla \cdot ((\mu + \frac{\mu_T}{\sigma_k}) \nabla k) = P + G - \rho \varepsilon \tag{4.7}$$

and

$$\frac{\partial \rho \varepsilon}{\partial t} + \nabla \cdot (\rho U \varepsilon) - \nabla \cdot ((\mu + \frac{\mu_T}{\sigma_\varepsilon}) \nabla \varepsilon) = C_1 \frac{\varepsilon}{k} (P + C_2 \max(G,0)) - C_3 \rho \frac{\varepsilon^2}{k} \tag{4.8}$$

A mixed-is-burnt model is employed for gaseous combustion. This solution method is designed for modeling diffusion flames, and approaches the solution from the context that oxidant and fuel cannot occupy the same space without reacting. This model solves for the instantaneous mixture content of each cell in terms of the fuel, oxidant and product, as well as the variance in these values between iterations. Each cell may only contain either fuel and products or oxidant and products (either a rich or a lean mixture), as all reactants instantaneously create products and release the heat of combustion of the fuel. For fast rate chemical reactions, the mixture fraction (f) can be defined as:

$$f = \frac{\aleph - (F/A_{Stoic})^{-1}}{1 - (F/A_{Stoic})^{-1}} \tag{4.9}$$

where

$$\aleph = m_f - \frac{m_O}{F/A_{Stoic}} \tag{4.10}$$

and the stoichiometric mixture fraction (F_{ST}) is defined as

$$F_{ST} = \frac{1}{1 + F/A_{Stoic}} \tag{4.11}$$

The mixture fraction is further related to the mass fractions of fuel (m_f), oxidant (m_o) and products (m_p) by the following

$$m_f = \frac{f - F_{ST}}{1 - F_{ST}}, m_o = 0, \text{and } m_p = 1 - m_f \tag{4.12}$$

for fuel rich cells, and

$$m_f = 0, m_o = 1 - \frac{f}{F_{ST}}, \text{and } m_p = 1 - m_o \tag{4.13}$$

The mixture fractions and their variances (which are calculated with an extensive probability function) are calculated along with the conservation laws until convergence criteria (the minimization of residuals for all variables) are obtained for the steady state solution.

A separate computational model is used for each of the numerical analyses presented, one for the single bluff body analysis (for both the validation and the propane analyses), one for the double bluff body cold flow analysis, and one for the double bluff body combustion analysis. The single bluff body model is based on the geometry of the experimental setup of Huang and Lin, and the double bluff body model is based on the geometry of the experimental setup as presented in Section 7.0. Each model consists of a three-dimensional solution field that

encompasses the desired region of the flow field, internal solid cells to model the nozzle geometry, and boundary conditions to model the flow conditions. The solution field is divided into discrete cells (control volumes) for computational solution. As only a two-dimensional axisymmetric model in the axial and radial directions is needed for each analysis, the solution field is a single cell in height and a two-dimensional solution method is employed by the solver.

The boundary conditions employed for the air and fuel inlets of the nozzle were turbulent uniform velocity boundaries, placed at the base of the nozzle. Ambient pressure boundaries were employed along the sides of the model to simulate an open air diffusion flame. A mass flow outlet at the top of the model allows all mass entering the system (solution field) to leave, in accordance with the law of conservation of mass.

4.2 Numerical Model for Single Bluff Body:

The computational model for the single bluff body validation analysis (Section 5.0), consists of a solution field of 6 cm by 10 cm, divided into 6000 cells, 60 cells equally spaced horizontally in 100 vertical rows. The model encompasses a full cross-section of the flameholder, and the solution method recognizes the model as an axisymmetric section. Figure 4.1 shows the outline of the model geometry, figure 4.2 shows the placement of the boundary conditions, and figure 4.3 shows the structure of the grid (cells). The nozzle geometry was modeled as solid cells, with no slip boundary walls, and has a 30 mm exit diameter for the annular jet, obstructed by 20 mm disc (D_A) as in the experimental setup of Huang and Lin. The exit diameter of the central jet was increased to 4 mm (from 3.4 mm) in order to serve as a better comparison for later sections, as it allowed for a grid structure more similar to later models. The magnitude of the central jet velocity (U_C) has been modified for all cases (and retermed the modified central jet velocity (U_{MC})), to maintain the same volume flowrate as those studied experimentally by decreasing the axial velocity in accordance with the increase in area. The nozzle section accounts for the lower 3 cm of the model, leaving 7 cm of solution field in the wake region. The velocities of the central (U_{MC}) and annular jets (U_A) are given in Table 4.1. The only appreciable difference between the cold flow validation model and the cold flow model with propane is that a second fluid is present, so the solution method must account for fluid mixing.

Table 4.1) Single Bluff Body Analysis

Case	U_A	U_C	U_{MC}	BR	k	ε
II (A)	0.75	1.4	1.0	0.44	0.00196	0.10026
II (B)	0.75	1.79	1.28	0.44	0.00329	0.18499
II (C)	0.56	2.03	1.45	0.44	0.00423	0.26983
III	0.32	1.52	1.09	0.44	0.00237	0.11327
IV (B)	0.47	2.96	2.12	0.44	0.00899	0.83651

Table 4.2) Double Bluff Body Cold Flow Analysis

Case	Φ	BR	U_A	U_C	k	ε
Alpha	1.0	0.53	2.732	2.282	0.01491	0.21702
Beta	1.5	0.53	2.732	3.423	0.01491	0.21702
Chi	1.0	0.44	2.732	2.282	0.01491	0.21702
Delta	1.5	0.44	2.732	3.423	0.01491	0.21702

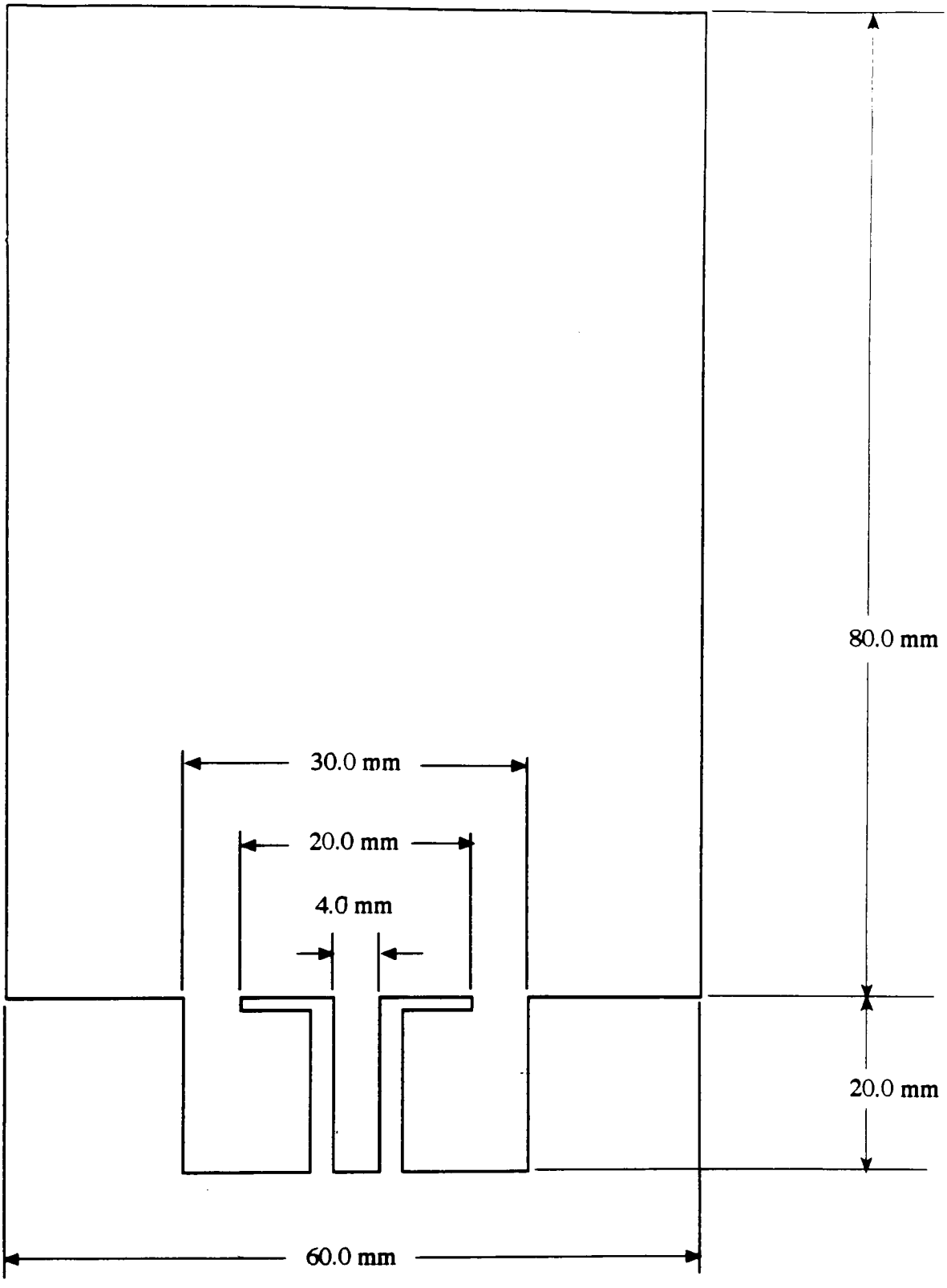

Figure 4.1 Model Outline for Single Bluff Body

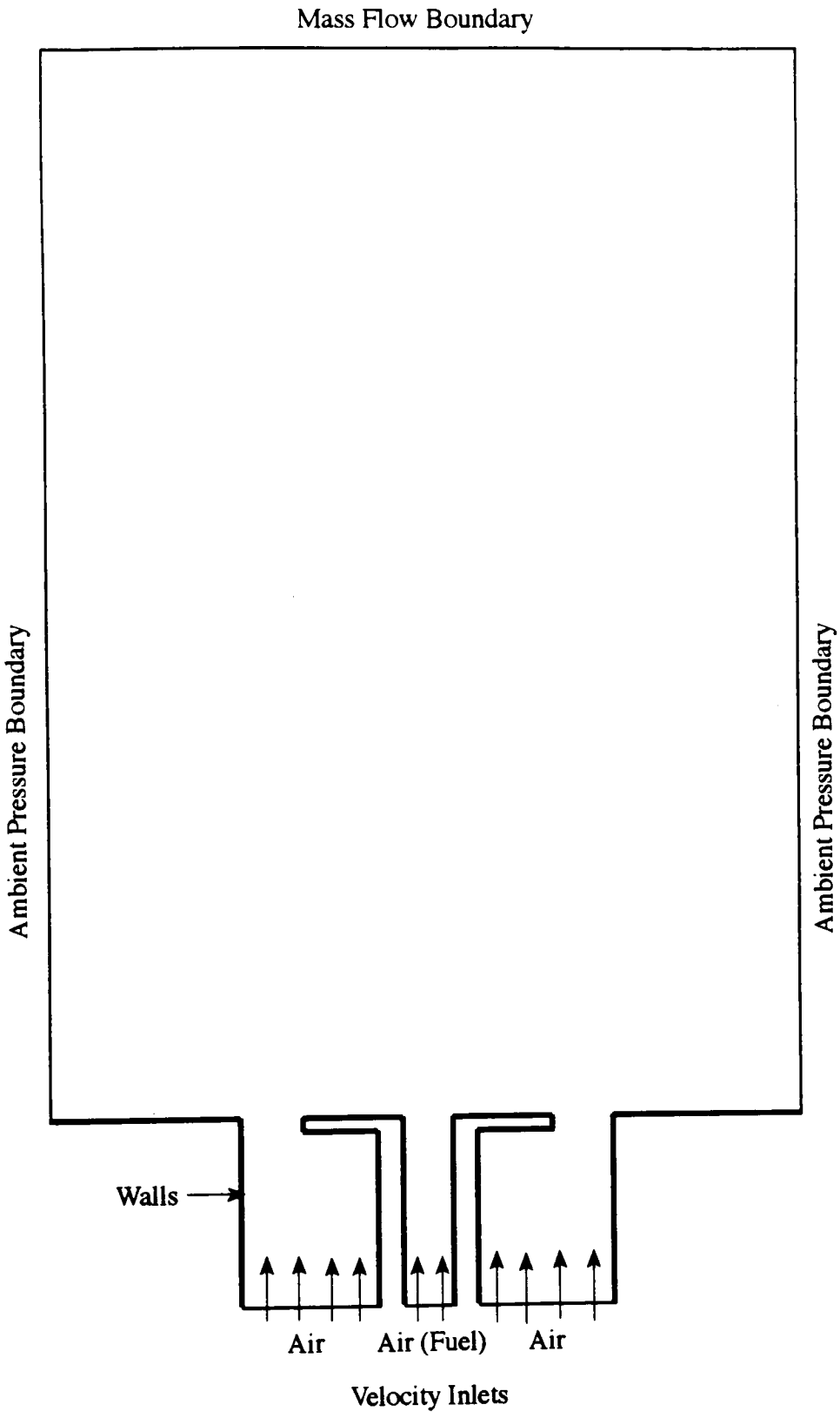

Figure 4.2 Boundary Conditions for Single Bluff Body

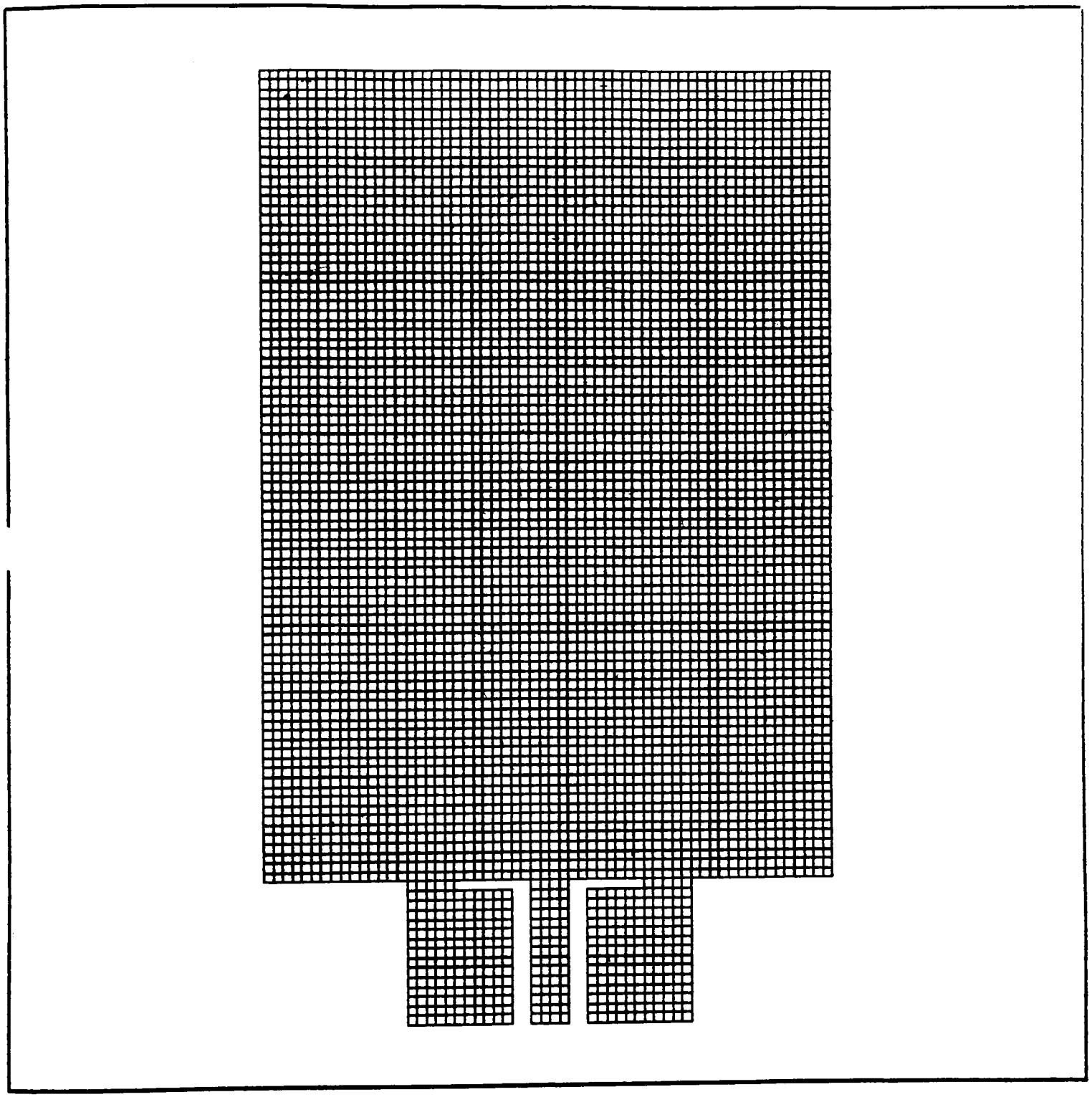

Figure 4.3 Grid Structure for Single Bluff Body

4.3 Numerical Model for Double Bluff Body - Cold Flow:

The computational model for the cold flow double bluff body analysis (Section 6.1) is 3 cm wide by 10 cm tall, and consists of 12000 cells, 60 cells equally spaced horizontally in 200 vertical rows. Figure 4.4 shows the outline of the model geometry (note that D_O is dependent on the geometric blockage ratio of the disc, and is 28.0 mm for BR = 0.53 and is 26.0 mm for BR = 0.44), figure 4.5 shows the placement of the boundary conditions, and figure 4.6 shows the grid structure. The blockage ratio for the central jet obstruction is 0.57. There are two significant differences between this model and that of the single bluff body flameholder. First, the grid density was increased to account for the finer geometry of the central bluff body; and second, the model only encompasses an axisymmetric section from the centerline outward, essentially half the size of the previous model. A symmetry plane has been added at the centerline of the flameholder in order to model the effects of the entire cross-section. The nozzle geometry was modeled in the same manner as the previous models (as solid cells), and again encompasses the lower 3 cm of the model, leaving 7 cm of solution field for the wake region. The central (U_C) velocity is for propane and annular (U_A) velocity is for air, and two separate geometric blockage ratios (for the air obstruction) were examined, all are as given in Table 4.2. Otherwise the solution method is identical to that of the single bluff body propane extension model.

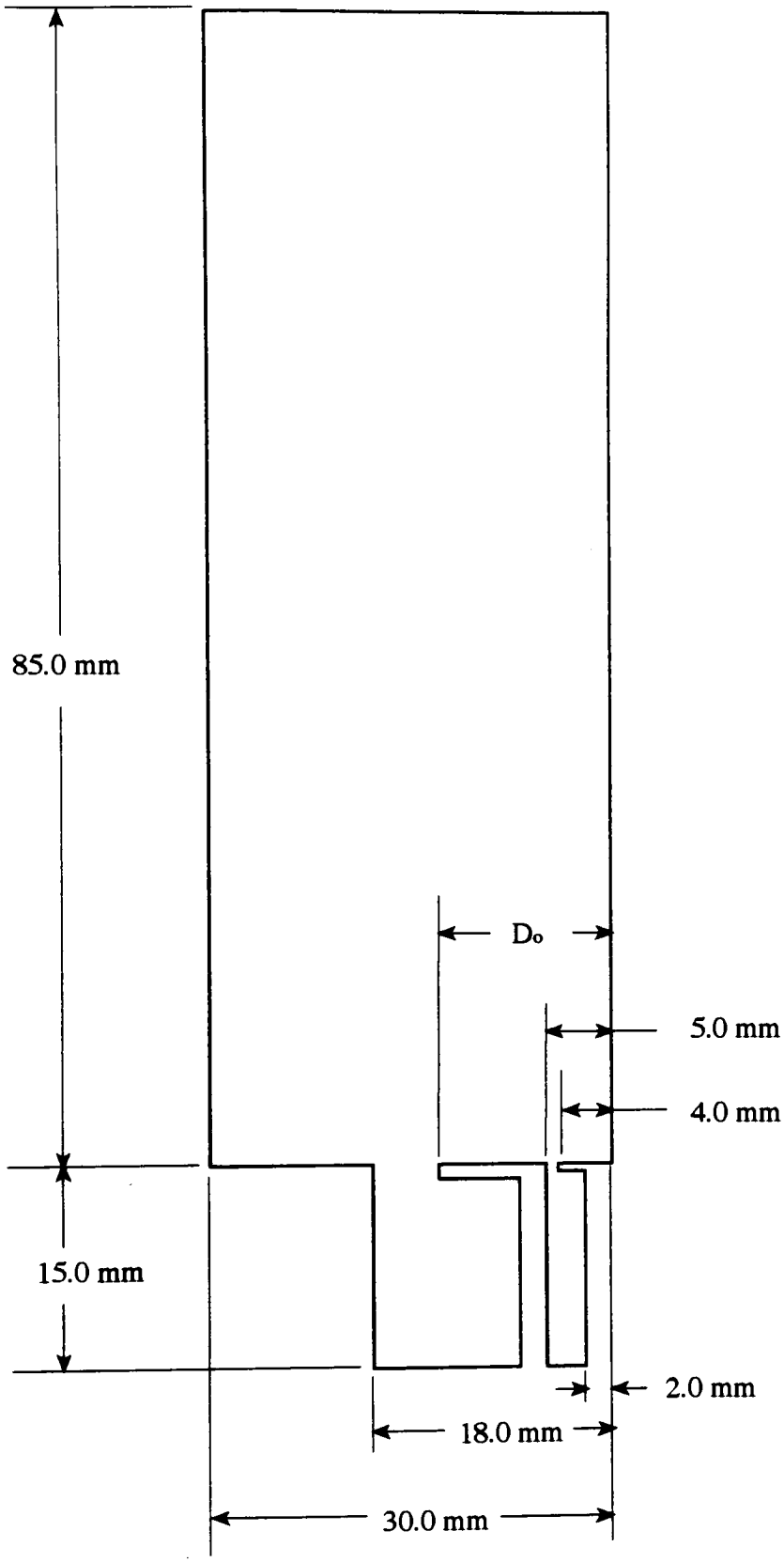

Figure 4.4 Model Outline for Double Bluff Body - Cold Flow

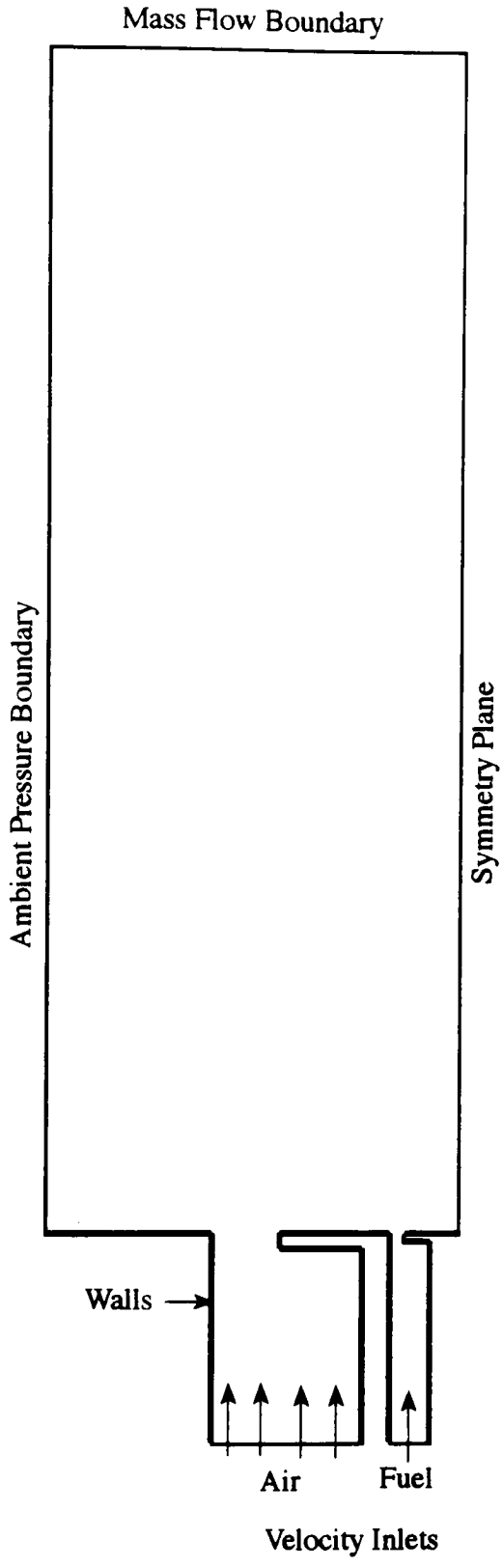

Figure 4.5 Boundary Conditions for Double Bluff Body - Cold Flow

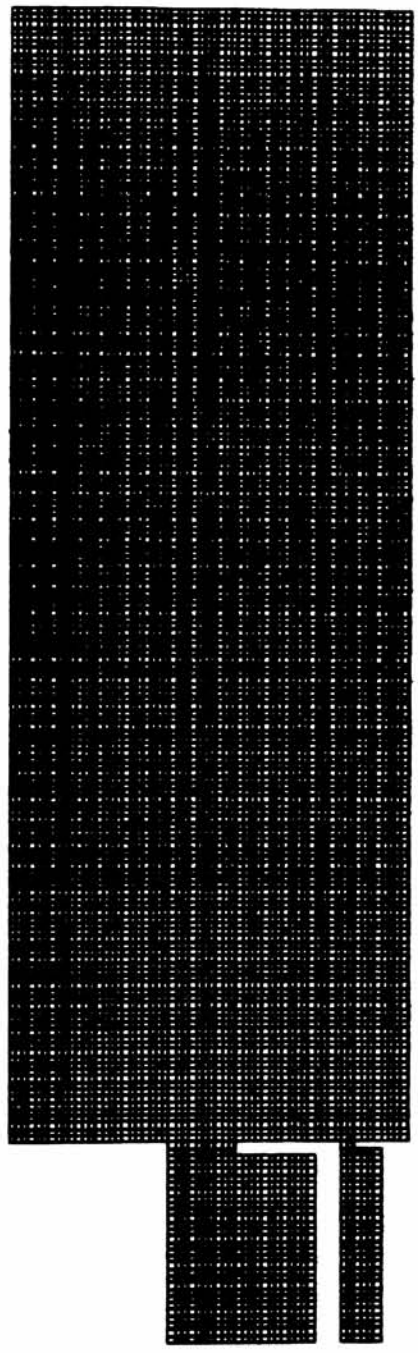

Figure 4.6 Grid Structure for Double Bluff Body - Cold Flow

4.4 Numerical Model for Double Bluff Body - Combustion:

The computational model for the double bluff body combustion analysis (Section 6.2) consists of three solution fields (termed blocks in the CFDS-Flow3D command code), joined together. The first contains the internal solids and flow passages for the nozzle, while the other two are for the downstream region. As the first section is of significantly less width than the third, the second section is tapered to allow for smooth transition between them. The first section is 5 cm wide by 1.5 cm tall, containing 3000 cells, 100 equally spaced horizontally by 30 equally spaced vertically (note that each section/block contains the same number of horizontal cells for continuity). The second section is 3 cm wide at the base, 20 cm wide at the top, 13.5 cm tall, and contains 4000 cells. The third section is 20 cm wide by 25 cm tall and contains 4000 cells, divided into 40 rows in a vertical geometrical progression. The geometric progression increases the height of each cell in accordance with its distance form the base, so the grid is essentially finer at the base of the block, and courser at the top of the block. Figure 4.7 shows the outline of the model geometry, figure 4.8 shows the placement of the boundary conditions, figure 4.9 shows the grid structure of the model, and figure 4.10 is an enhanced view of the grid structure in the first block.. This model is significantly larger than each of the previous models (geometrically speaking), and again encompasses the axisymmetric section from the centerline outward, with a symmetry plane at the centerline. The nozzle geometry is defined in much the same manner as the previous sections. Again, the central velocity (U_C) is propane, and the annular velocity (U_A) is air, and two geometric blockage ratios are studied, all are as given in Table 4.2.

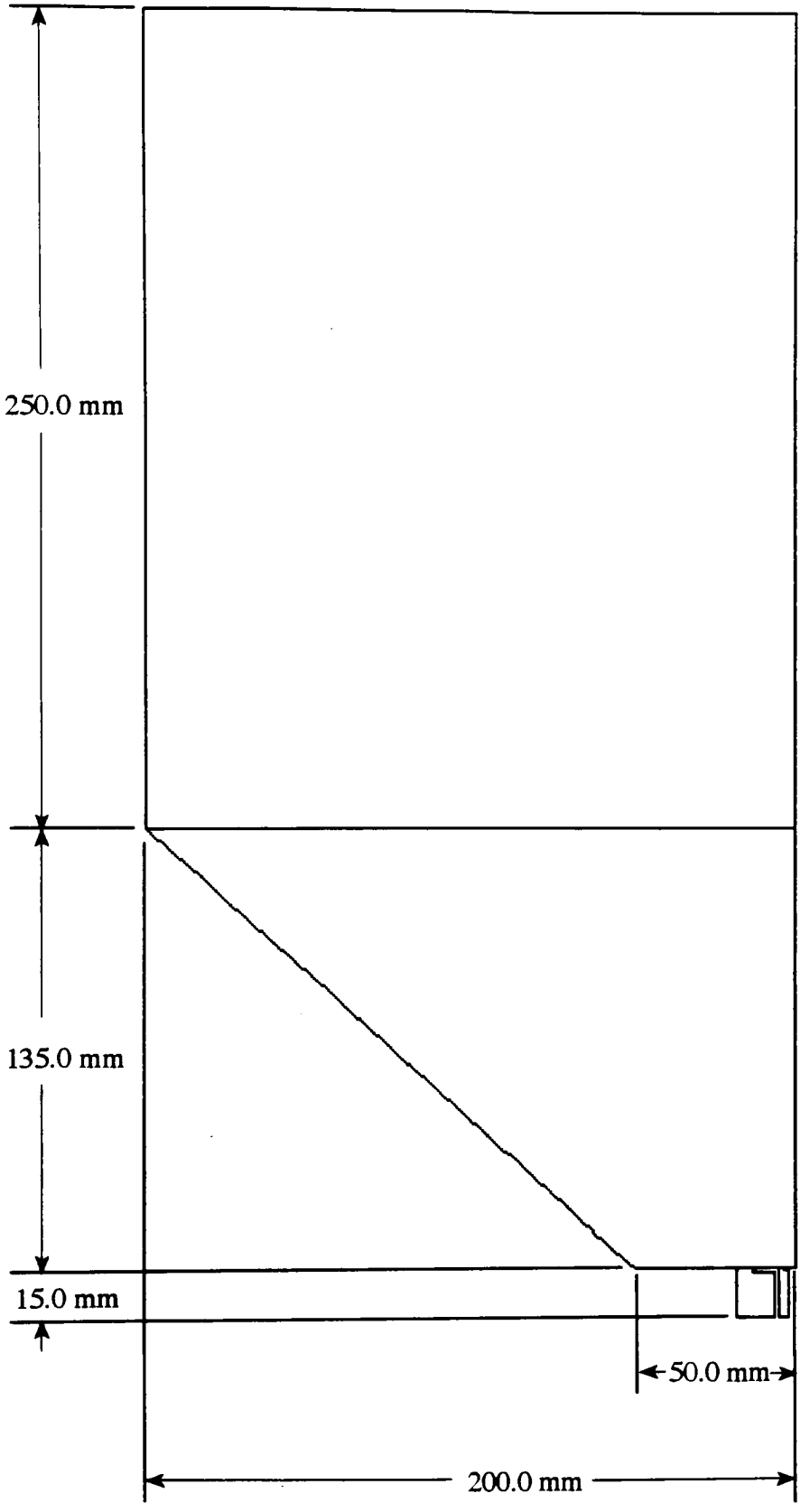

Figure 4.7 Model Outline for Double Bluff Body - Combustion

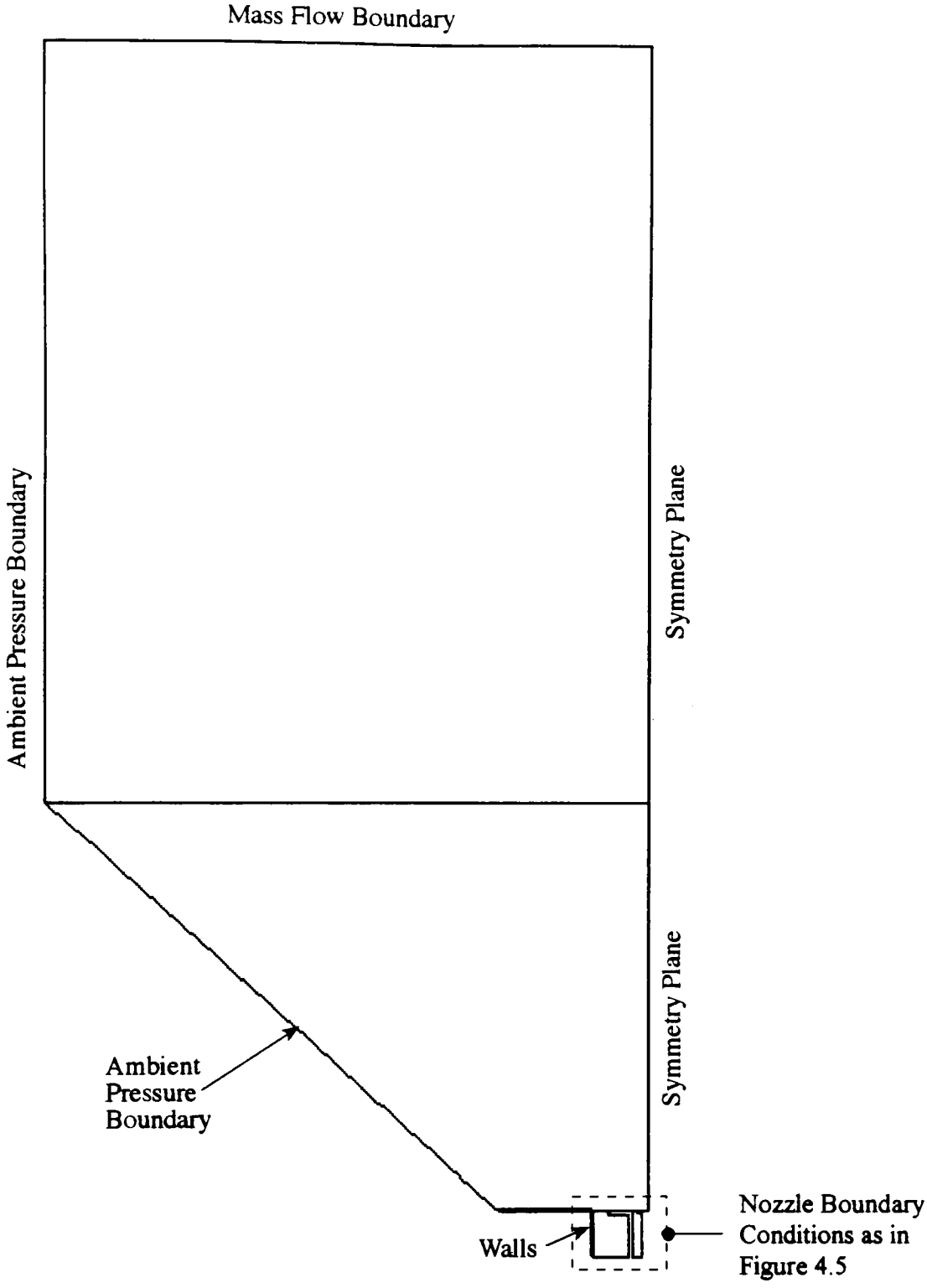

Figure 4.8 Boundary Conditions for Double Bluff Body - Combustion

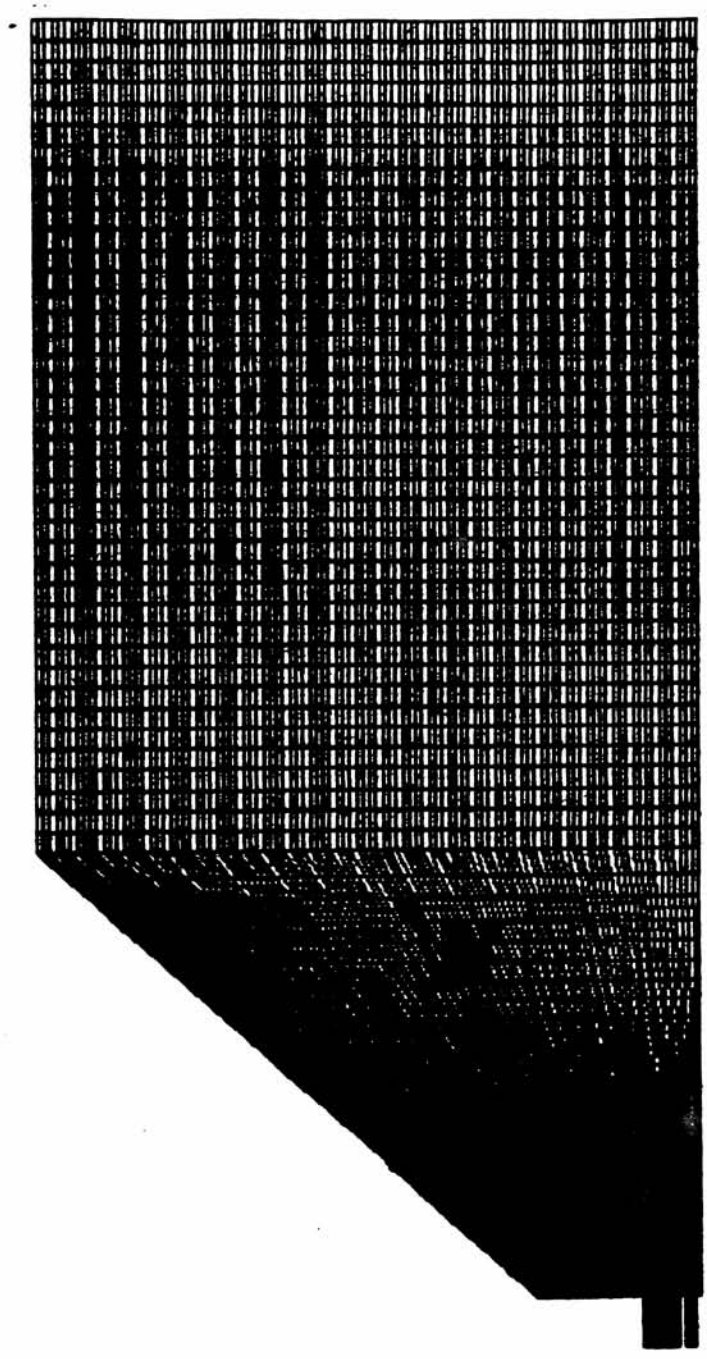

Figure 4.9 Grid Structure for Double Bluff Body - Combustion

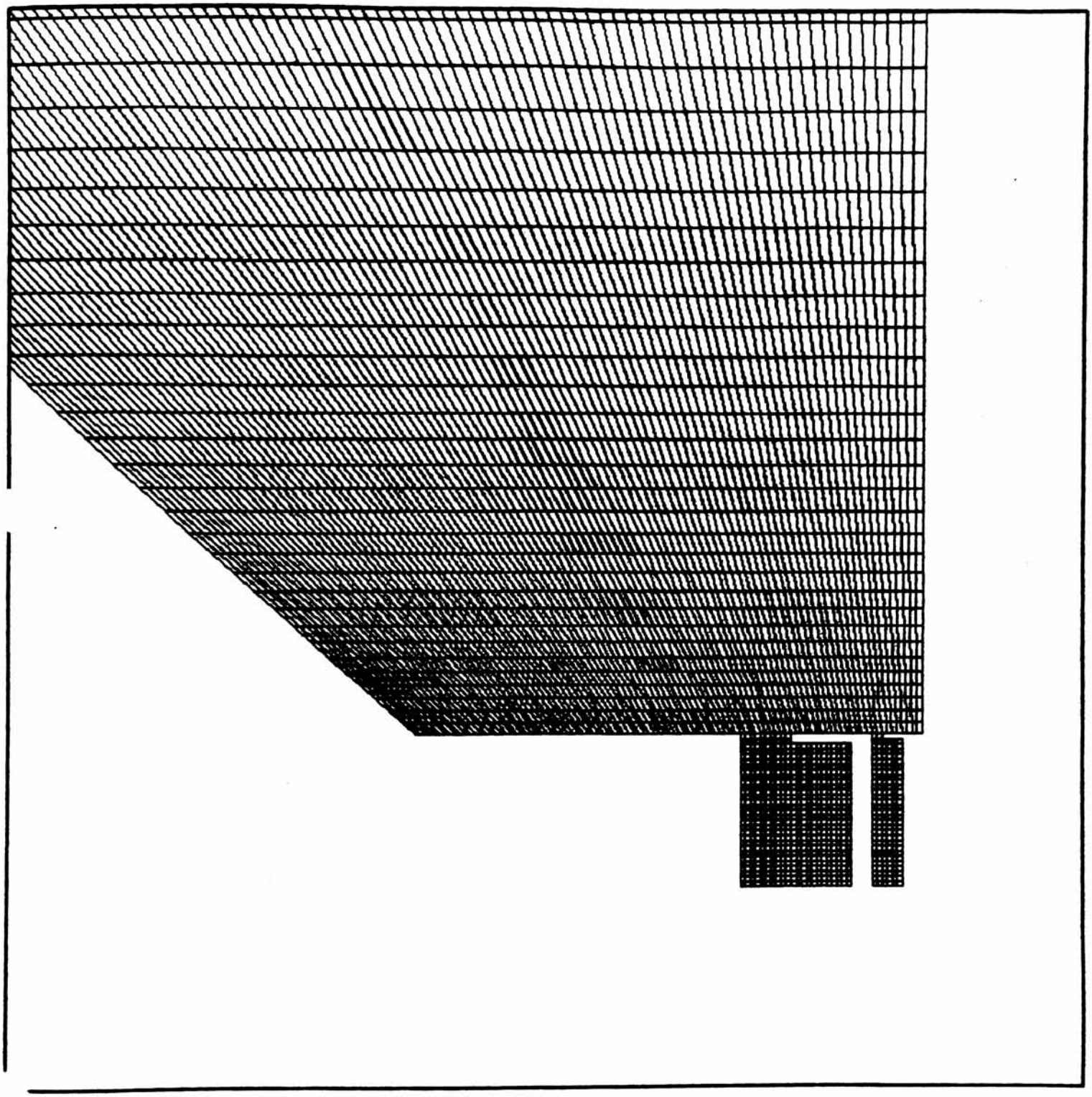

Figure 4.10 Grid Structure for Double Bluff Body - Combustion, Enhanced View

4.5 Output from the CFD Code:

CFDS-Flow3D offers solution output in two forms, tabular data output in the form of a data file (as seen in Appendix X), or graphical output, in the form of vector and contour plots of the data. For the purposes of comparison the latter is most appropriate, and the majority of the computational results given in this study will be presented as vector and contour plots. These plots are available for each variable that is solved for in the code. For the cold flow models of the single bluff body and the double bluff body flameholders, the variables solved for included: u velocity, v velocity, pressure, density, viscosity, k, ε, enthalpy and a single mass fraction (percent of fuel in cell by mass). For the double bluff body combustion models, the variables included all of the above, as well as: temperature, three mass fractions (one for percent oxidant, one for percent fuel, one for percent products), and two combustion scalars (mixture fractions).

5.0 NUMERICAL VALIDATION ANALYSIS:

5.1 Cold Flow Analysis of Single Bluff Body:

In order to verify the capabilities of the Computational Fluid Dynamics Solver Code, part of the experimental research of Huang and Lin was recreated numerically with the code. This was undertaken to verify the capability of the code to accurately model the recirculation zone, and later to serve as a basis of comparison for the double bluff body configuration. The initial object of this validation was to clearly reproduce the three characteristic flow regions found by Huang and Lin, and show the effects of momentum dominance on the recirculation zone. Five individual cases were studied, based on those of Huang and Lin, and are as defined in Table 4.1. Of all the output available from the code, the axial (V) velocity contours provide the clearest depiction of the structure of the recirculation zone, while velocity vector plots of the region show the effect of the recirculation zone. Figures 5.1 through 5.10 depict the velocity vectors and V velocity contours of the five cases studied.

Cases II (A), (B), and (C) are representative of the three sub-regions of the prepenetration region. Figures 5.1, 5.3, 5.5, 5.7 and 5.9 (the velocity vector plots) clearly show recirculation behind the bluff body obstruction, but the V velocity contour plots yield much better information as to the structure of the recirculation zone. For Case II (A), Figure 5.2 clearly shows a stable recirculation zone dominated by the reverse flow of the annular jet. This is evident by the purple regions which denote negative axial velocity (or recirculation). The zone has the expected closed toroidal shape similar to that shown

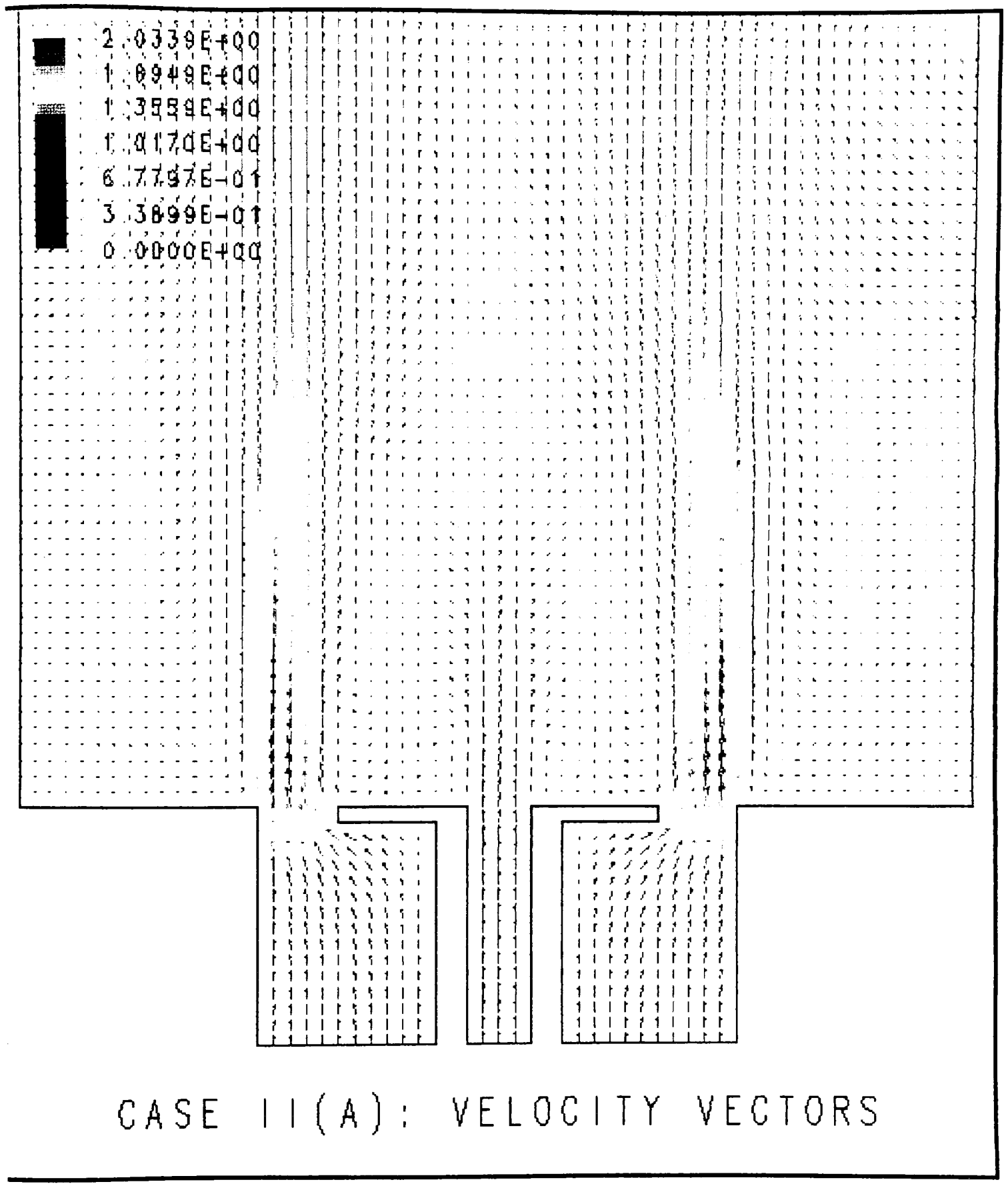

Figure 5.1 Case II(A): Velocity Vectors (m/s)

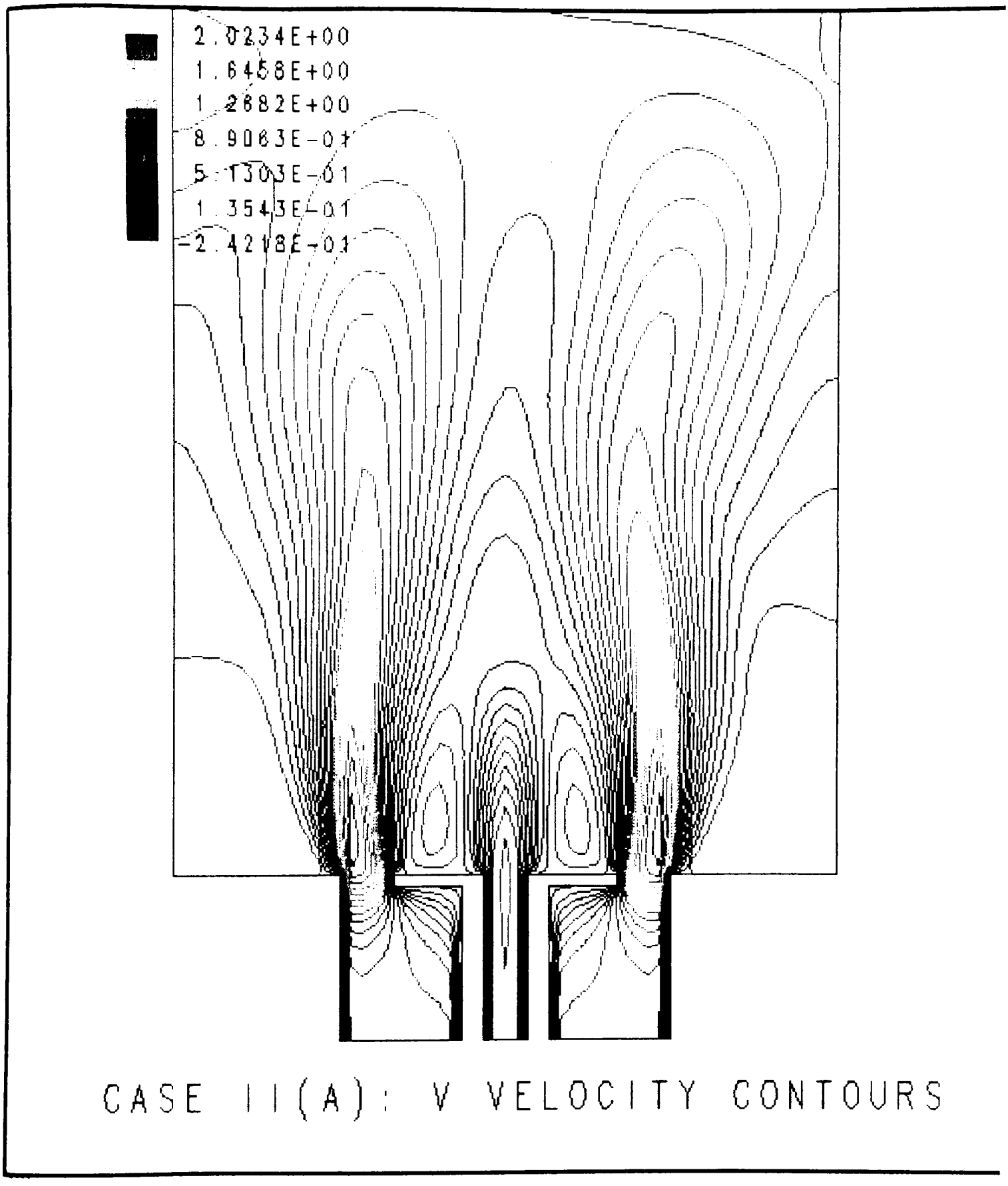

Figure 5.2 Case II (A): Axial Velocity Contours (m/s)

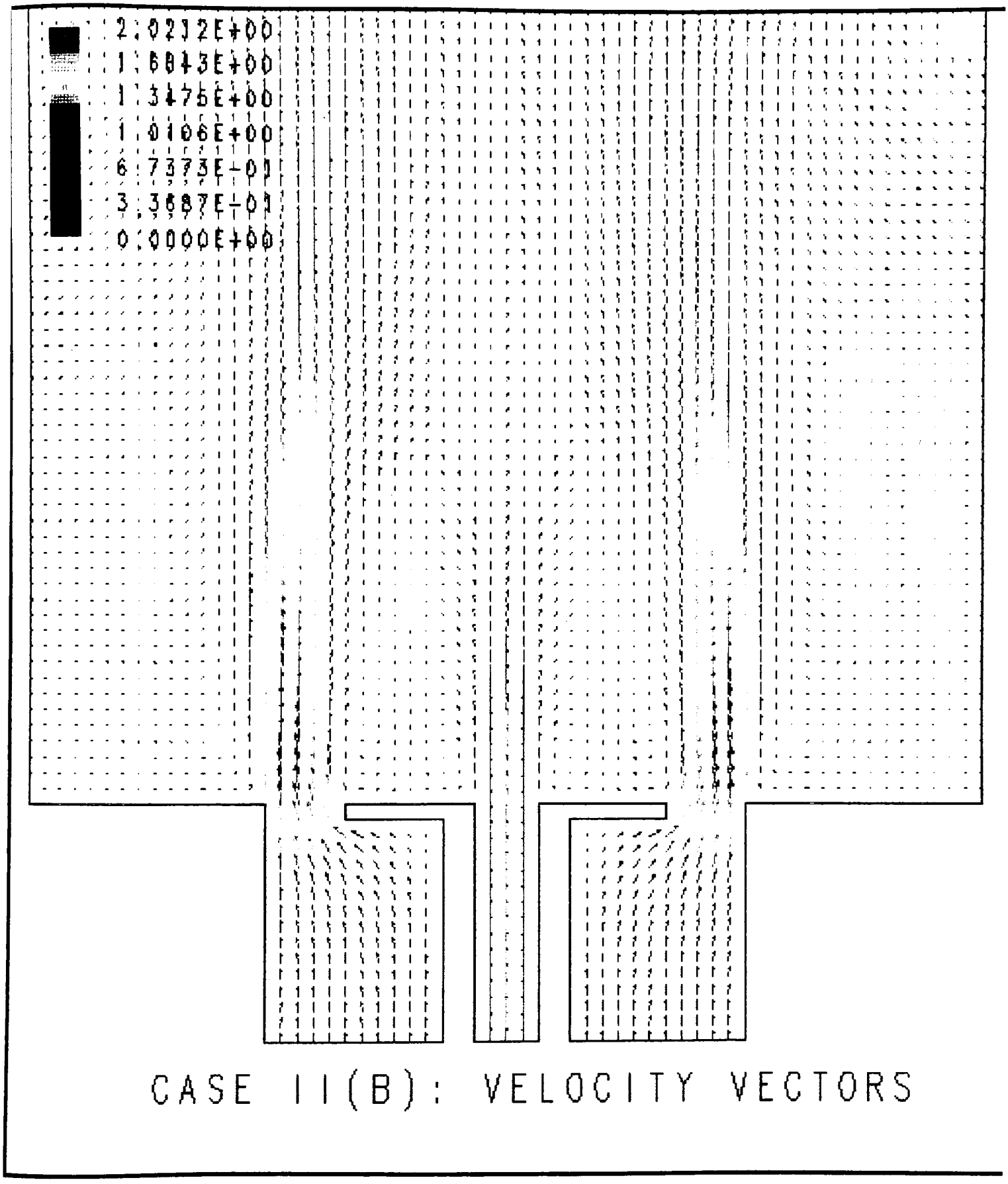

Figure 5.3 Case II (B): Velocity Vectors (m/s)

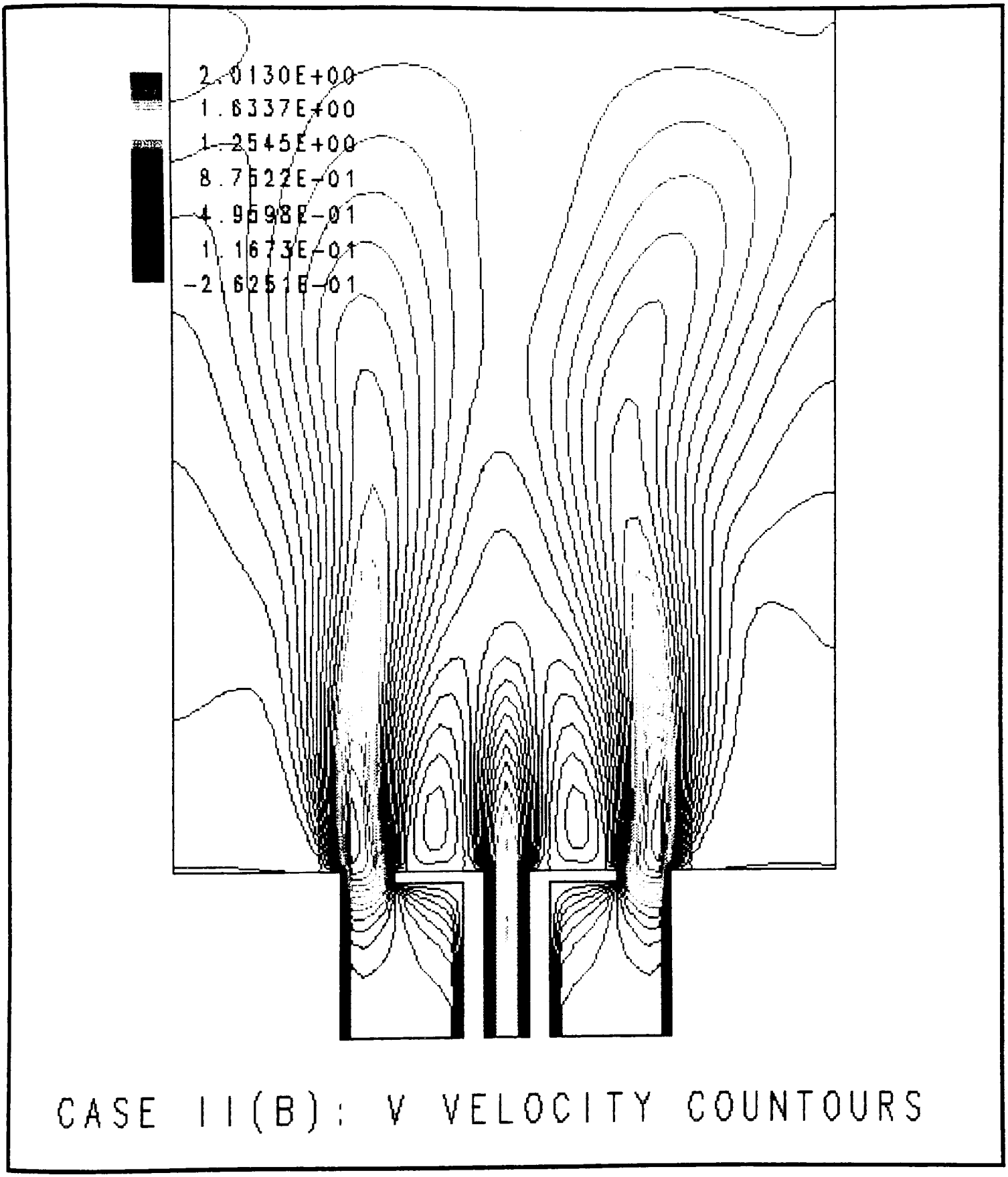

Figure 5.4 Case II (B): Axial Velocity Contours (m/s)

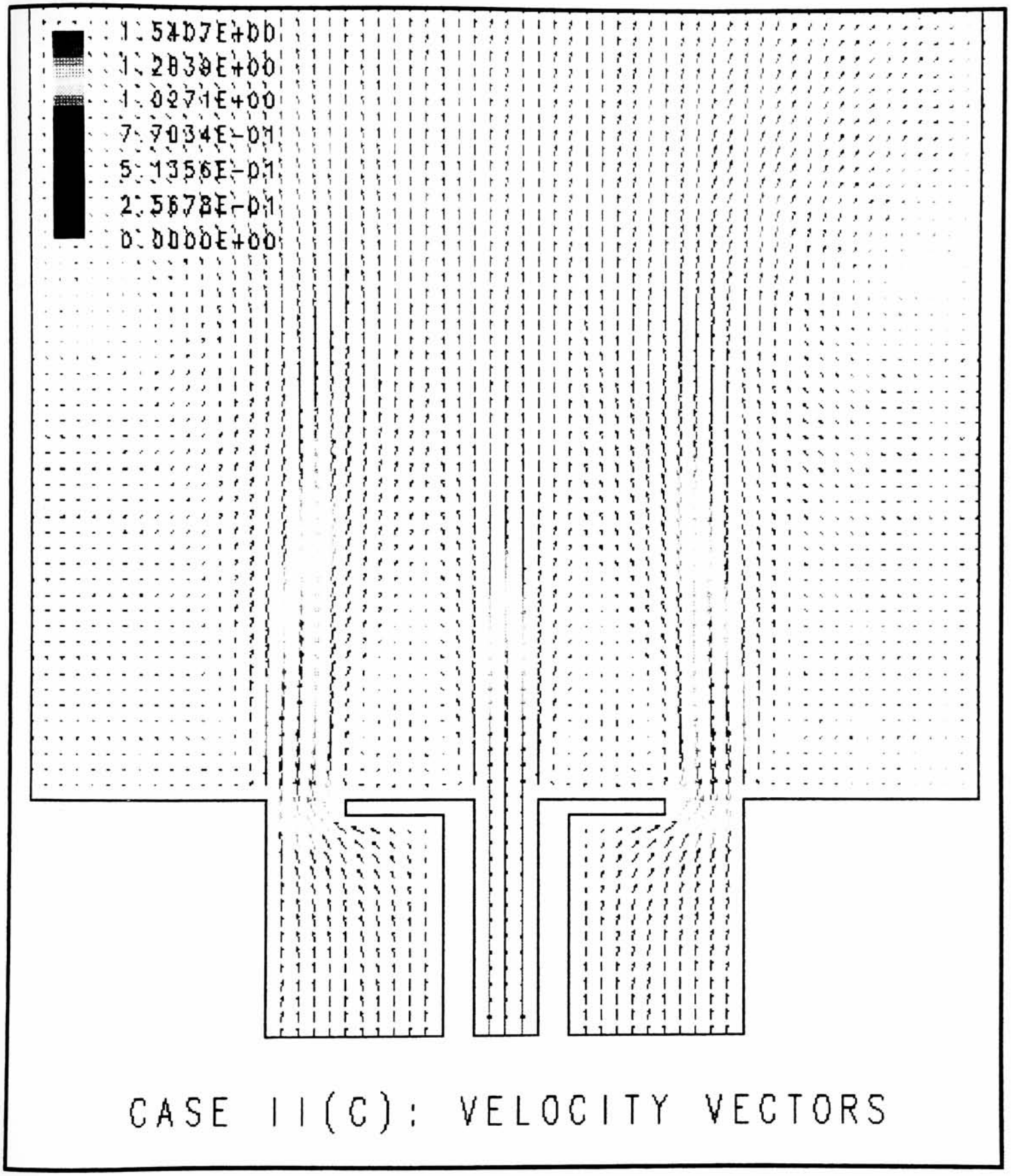

Figure 5.5 Case II (C): Velocity Vectors (m/s)

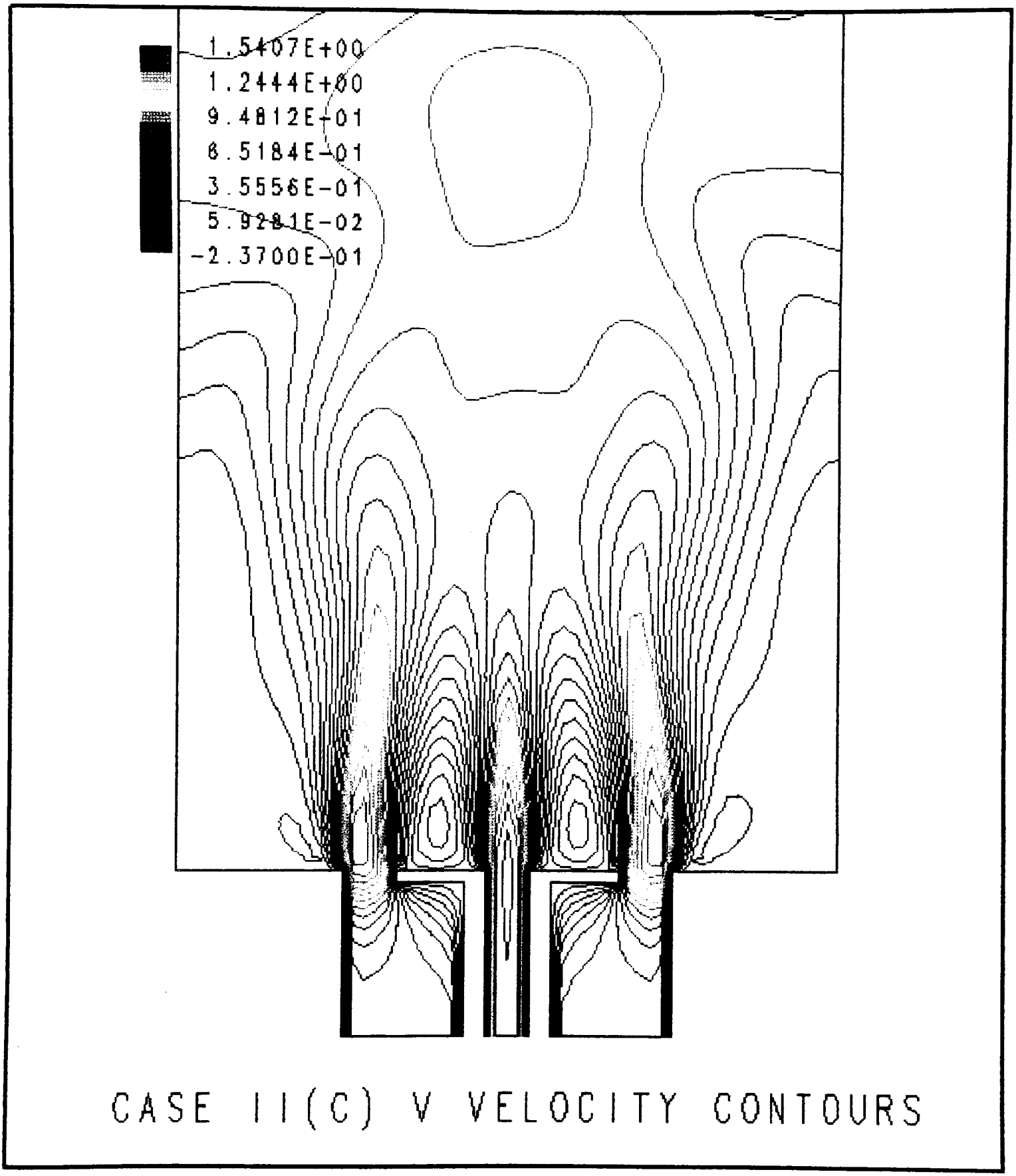

Figure 5.6 Case II (C): Axial Velocity Contours (m/s)

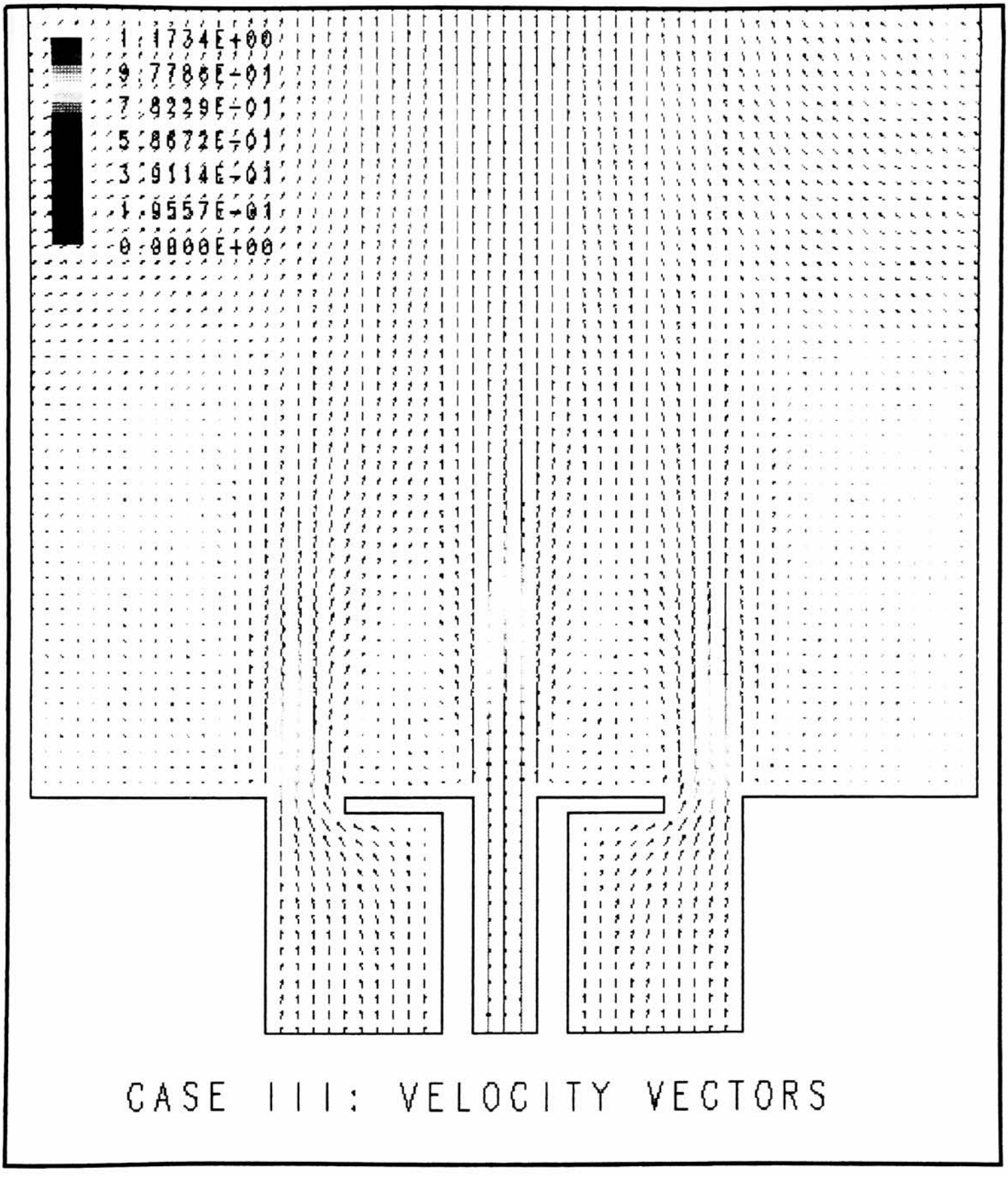

Figure 5.7 Case III: Velocity Vectors (m/s)

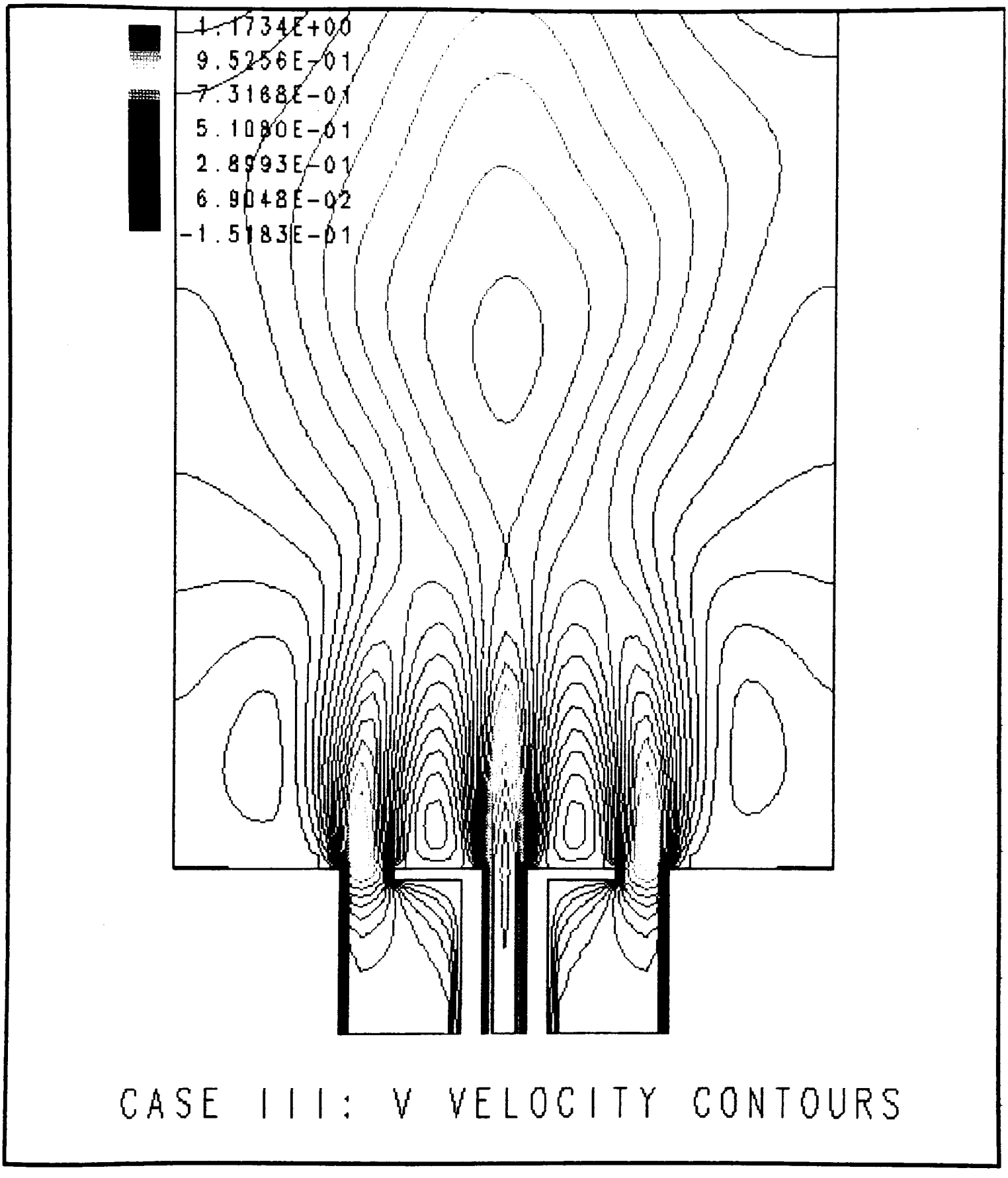

Figure 5.8 Case III: Axial Velocity Contours (m/s)

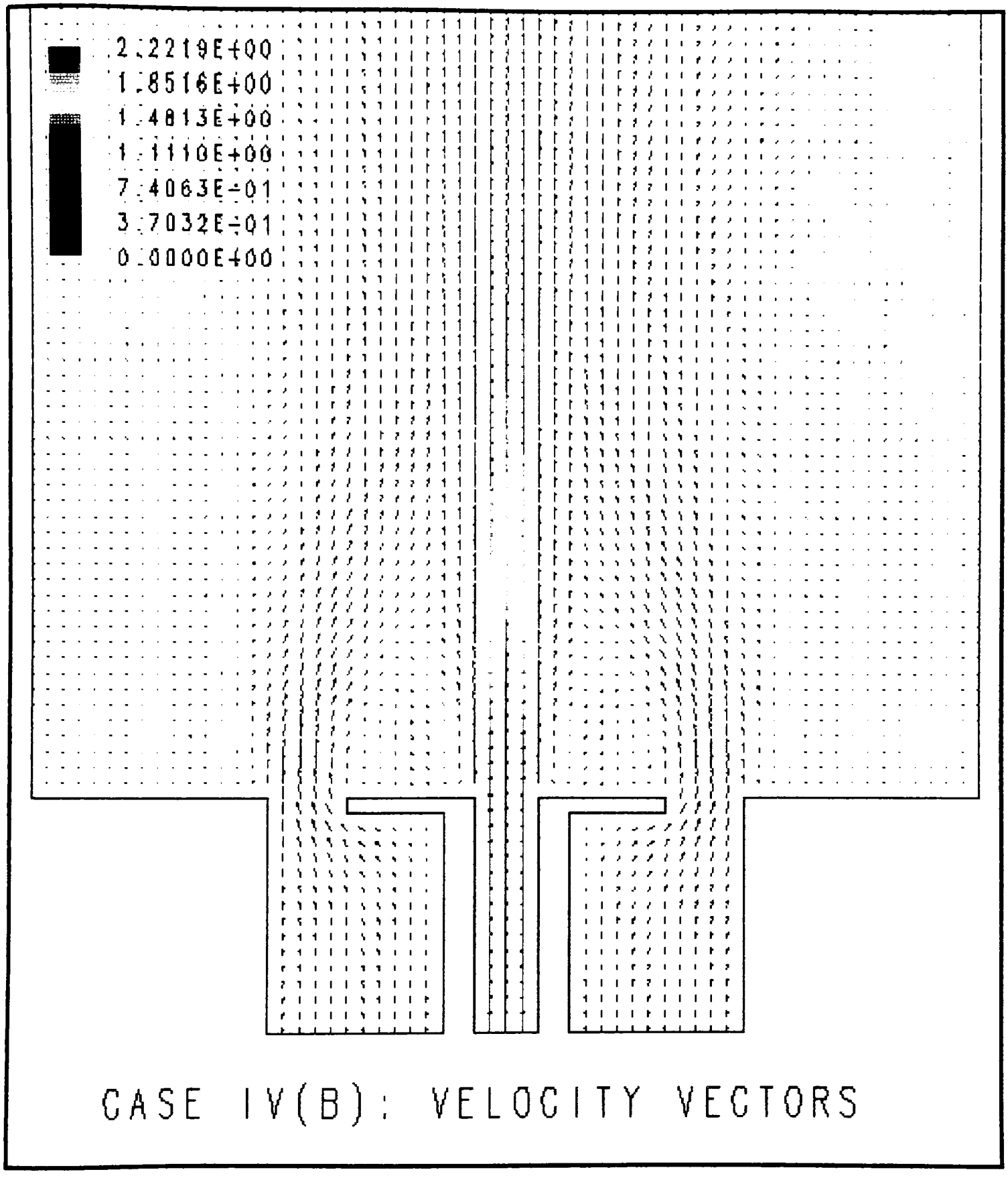

Figure 5.9 Case IV (B): Velocity Vectors (m/s)

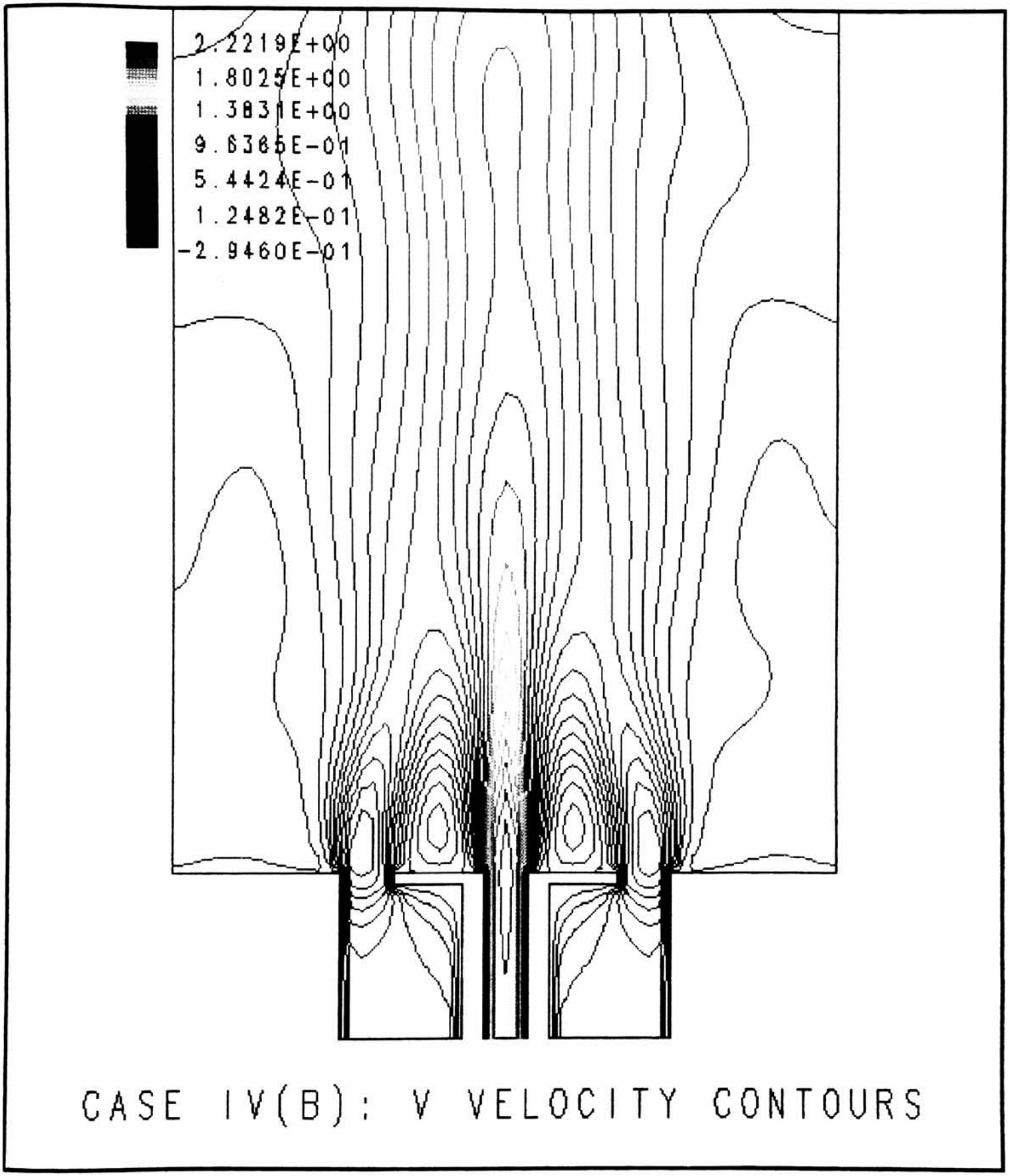

Figure 5.10 Case IV (B): Axial Velocity Contours (m/s)

by Huang and Lin (and others), and the entire central jet is engulfed in the recirculation, with no indications of any penetration. The recirculation zone extends a little under 27 mm downstream of the disc, or about 1.37 D_A. It exhibits a maximum reverse axial velocity of 0.242 m/s, which is approximately 24.2% of the magnitude of the central jet. Cases II(B) and (C) also exhibit this expected trend, as the momentum of the central jet increases, the annular jet begins to lose its dominance over the recirculation. This causes the recirculation zone to slowly lose its toroidal shape and begin divide itself into a ring shaped region (appearing as two separate regions in the axisymmetric figure). In Case (C) the central jet column is just beginning to exhibit the first signs of penetration, as the central jet is starting to push past the annular recirculation zones into the downstream area, foreshadowing the transition region. In Case (B) the recirculation zone extends about 1.22 D_A downstream, with a maximum reverse velocity of 0.262 m/s (20.5% of the magnitude of the central jet velocity) as shown in Figure 5.4; while for Case (C) the zone extends about 0.82 D_A with a maximum reverse velocity of 0.237 m/s (16.3% of the magnitude of the central jet velocity) as shown in Figure 5.6. It can be clearly seen already, that as the central velocity increases, the recirculation zone decreases in size as well as strength.

Case III represents the transition region, and the axial (V) velocity for this case is given in Figure 5.8. At this point the central jet is beginning to penetrate the central recirculation region, dividing the zone into the shape of a ring. This zone appears as two smaller zones, that are in the same areas as the maximum reverse velocities were in the previous cases (in the annulus region between the central and annular jets), but the two are

now completely separated by the central jet. It is likely that this representation for Case III is closer to penetration than to true transition, as the delicate balance of momentum does not cause such chaotic reactions in the computational analysis as was seen in the experimental work of Hung and Lin. The twin recirculation zones extend about 0.72 D_A downstream, and have maximum reverse velocities of 0.152 m/s (13.9% of the magnitude of the central jet).

The penetration region is illustrated by Case IV (B), and is given in Figure 5.10. The central jet is the dominant force of the flowfield, and a smaller, divided recirculation zone is developed between the central and annular jets. The flow is well out of the transition region and is performing very much as shown in the work of Huang and Lin. The recirculation zone has diminished to approximately 0.56 D_A in height, with a maximum reverse axial velocity of 0.295 m/s (again, 13.9% of the magnitude of the central jet).

This computational analysis seems to clearly recreate the results noted by Huang and Lin. The recirculation zone is present, and is of the predicted toroidal shape. The recirculation zone steadily diminishes is size and strength with increased dominance of the central jet. The models also accurately show the penetration region, where the fuel jet divides the recirculation zone into a ring, all very much as shown in the experimental analysis of Huang and Lin. The most significant difference between the two seems to be that the CFD analysis under predicts the size of the recirculation zone. In fact, each separate computational case appears to be closer to the previous experimental case (that is, case II(C) from the CFD analysis most closely resemble case II (B) from the

experimental analysis of Huang and Lin). This is most likely due to the change in momentum effected by the increase in the central jet diameter for the computational recreation.

This validation analysis shows that the CFD code employed for the work is able to accurately model the prepenetration and penetration regions (but not the chaotic fluctuations of the transition region), specifically the effects of the recirculation zone of these regions. As an extension of this set of models, the central jet was changed to propane instead of air, to serve as a basis for comparison to the Double Concentric Bluff Body analysis.

Table 5.1) Sample Tabulated Results of the Single Bluff Body Analysis

Case	U_A (m/s)	U_{MC} (m/s)	Approx. Height of Rec. Zone (D_A)	Maximum Reverse Axial Velocity (m/s)	% Magnitude of Central Jet Velocity
II (A)	0.75	1.00	1.37	0.242	24.2
II (B)	0.75	1.28	1.22	0.262	20.5
II (C)	0.56	1.45	0.82	0.237	16.3
III	0.32	1.09	0.72	0.152	13.9
IV (B)	0.47	2.12	0.56	0.295	13.9

5.2 Extension of Single Bluff Body Analysis to Mixing with Propane

The numerical model is now extended to include the effects of a gaseous fuel in the central inlet instead of air, in order to examine the mixing characteristics of the single bluff body configuration. This will serve as a basis of comparison for the following section on cold flow around the double bluff body configuration.

This computational model is a direct extension of the model used in the previous section. The geometry and the grid structure are identical, as are all of the boundary conditions (except that the central inlet is modeled as Propane). The central inlet was modeled as a uniform turbulent velocity inlet of propane gas, and a mixture fraction equation was added to the solution method. The same cases were studied as in the previous, three in prepenetration (II A, B and C), one in transition (Case III), and one in penetration (IV B); with like inlet velocities to keep the volume flowrates similar. From this set of models, two characteristics of importance are analyzed, first the axial (V) velocity - to determine the size and shape of the recirculation zone, and second the mass fraction concentration of propane throughout the region - to examine the extent of mixing around the flameholder.

The V velocity contours showed almost identical recirculation characteristics for this series of models as was seen in the verification series of models, and as this is the case the data is omitted here. The prepenetration and penetration regions were clearly present, as were the major distinctions between the two. One significant difference however was that in each case the fuel jet exhibited a slightly greater influence on the flowfield than its air counterpart. This is probably due to the slight increase in momentum of the central

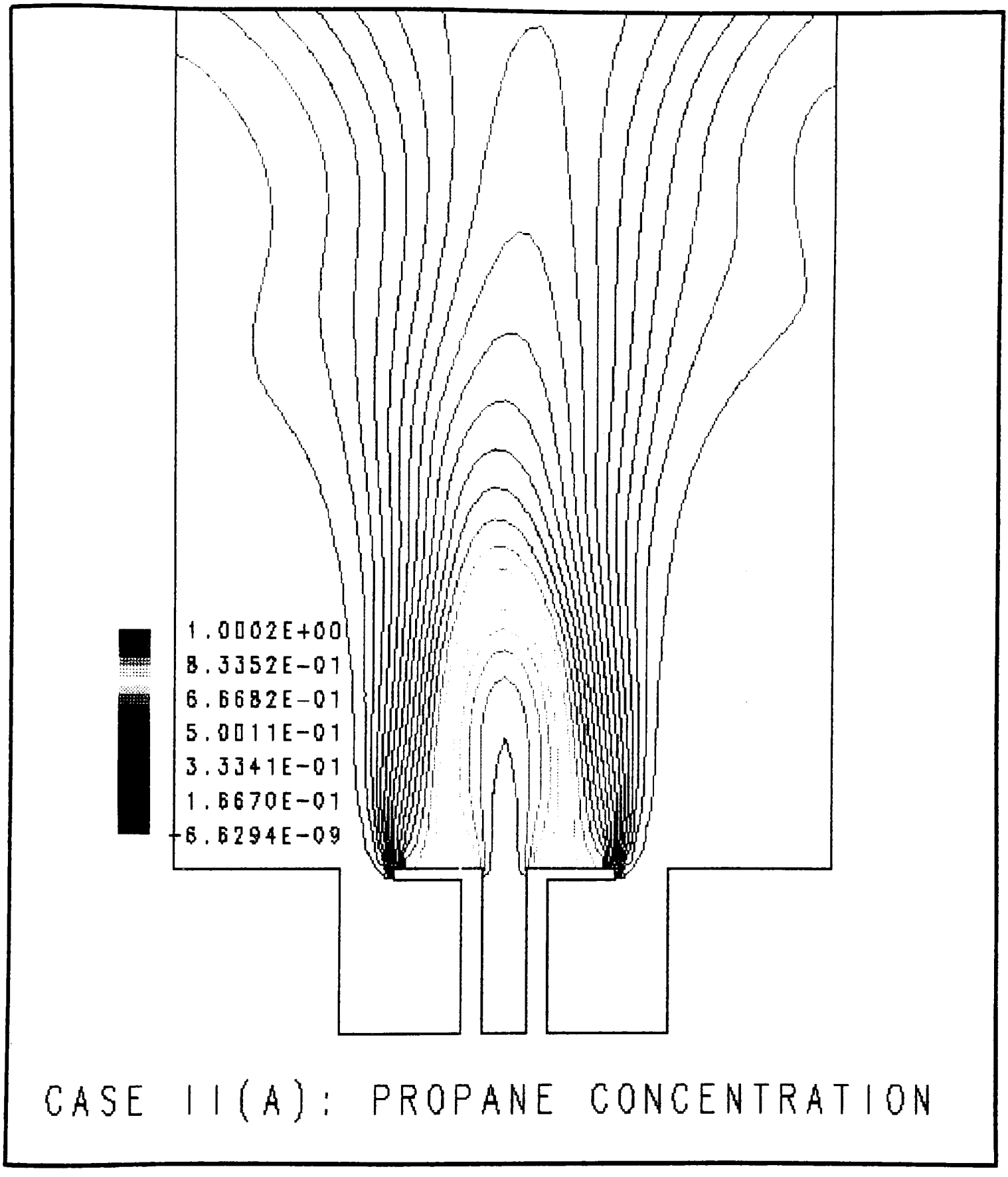

Figure 5.11 Case II (A): Propane Concentration Contours (% Propane by Mass)

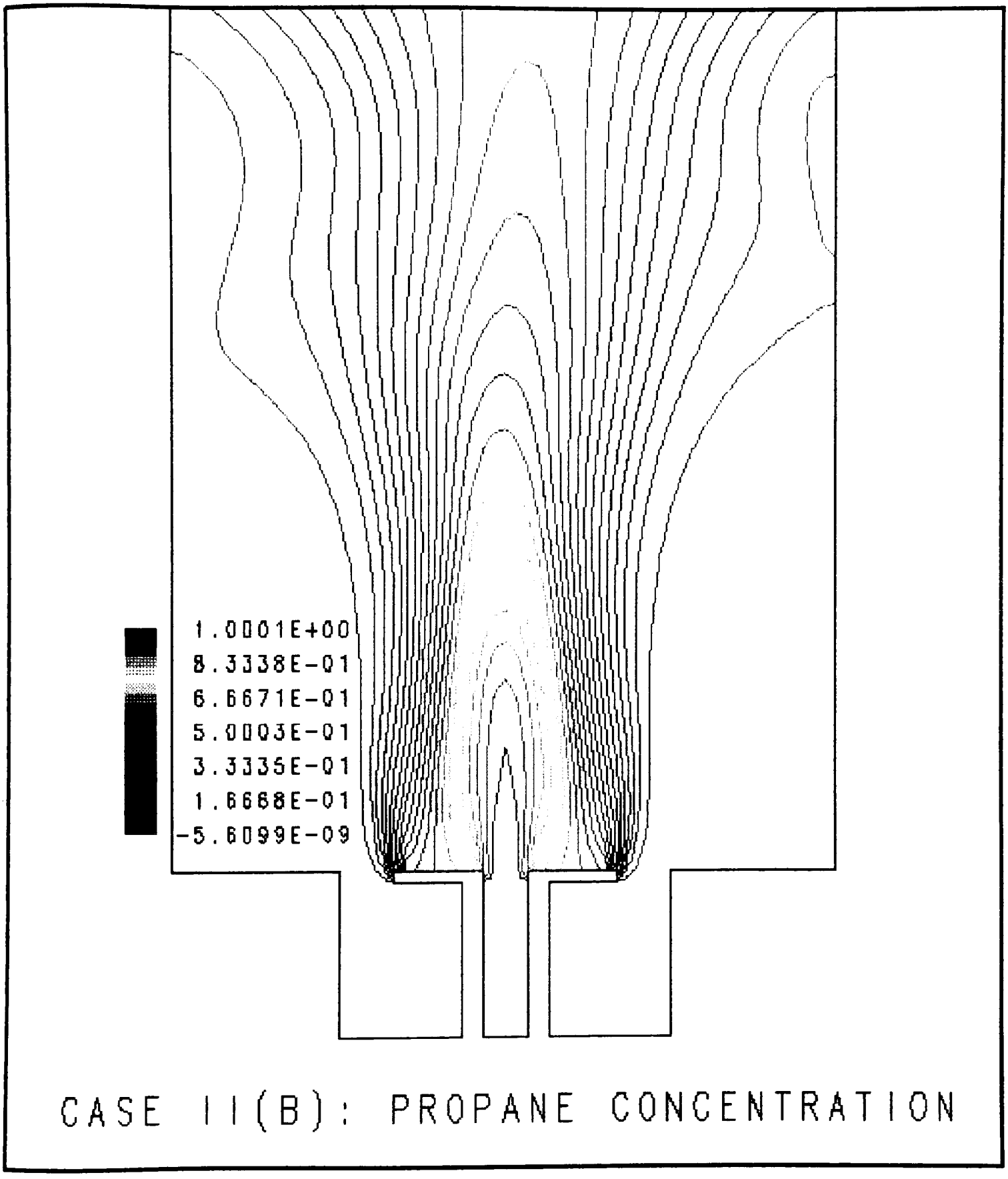

Figure 5.12 Case II (B): Propane Concentration Contours (% Propane by Mass)

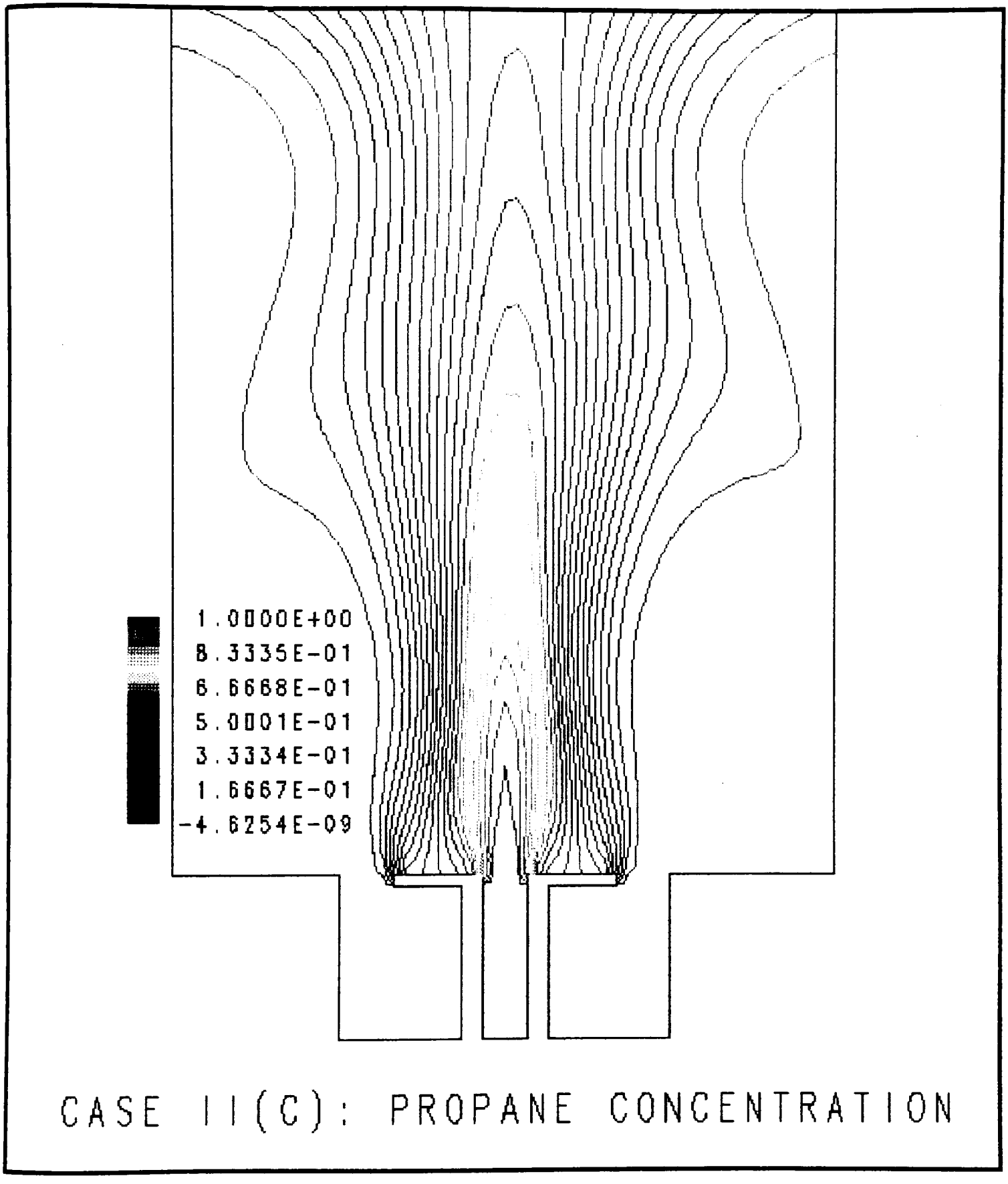

Figure 5.13 Case II (C): Propane Concentration Contours (% Propane by Mass)

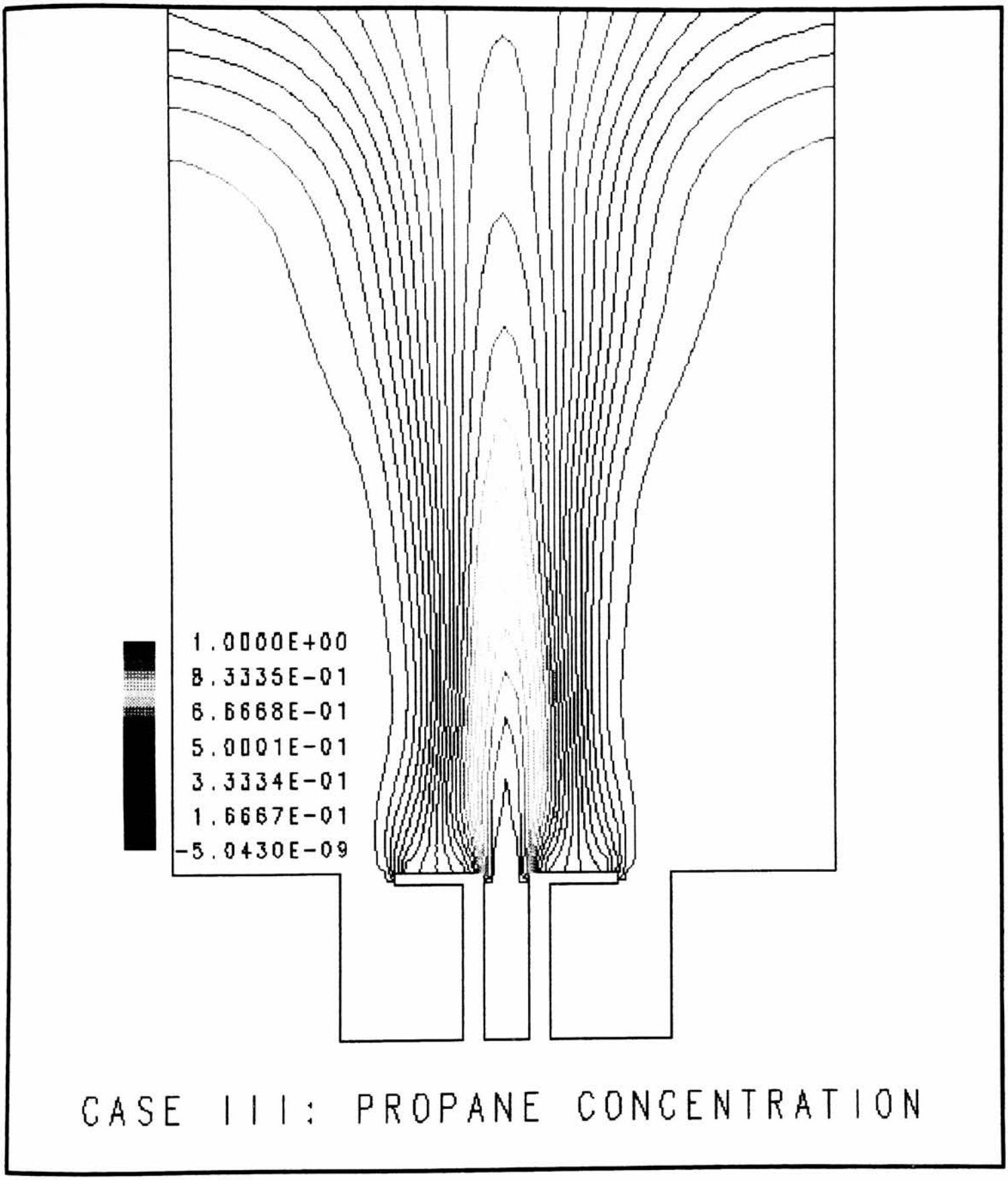

Figure 5.14 Case III: Propane Concentration Contours (% Propane by Mass)

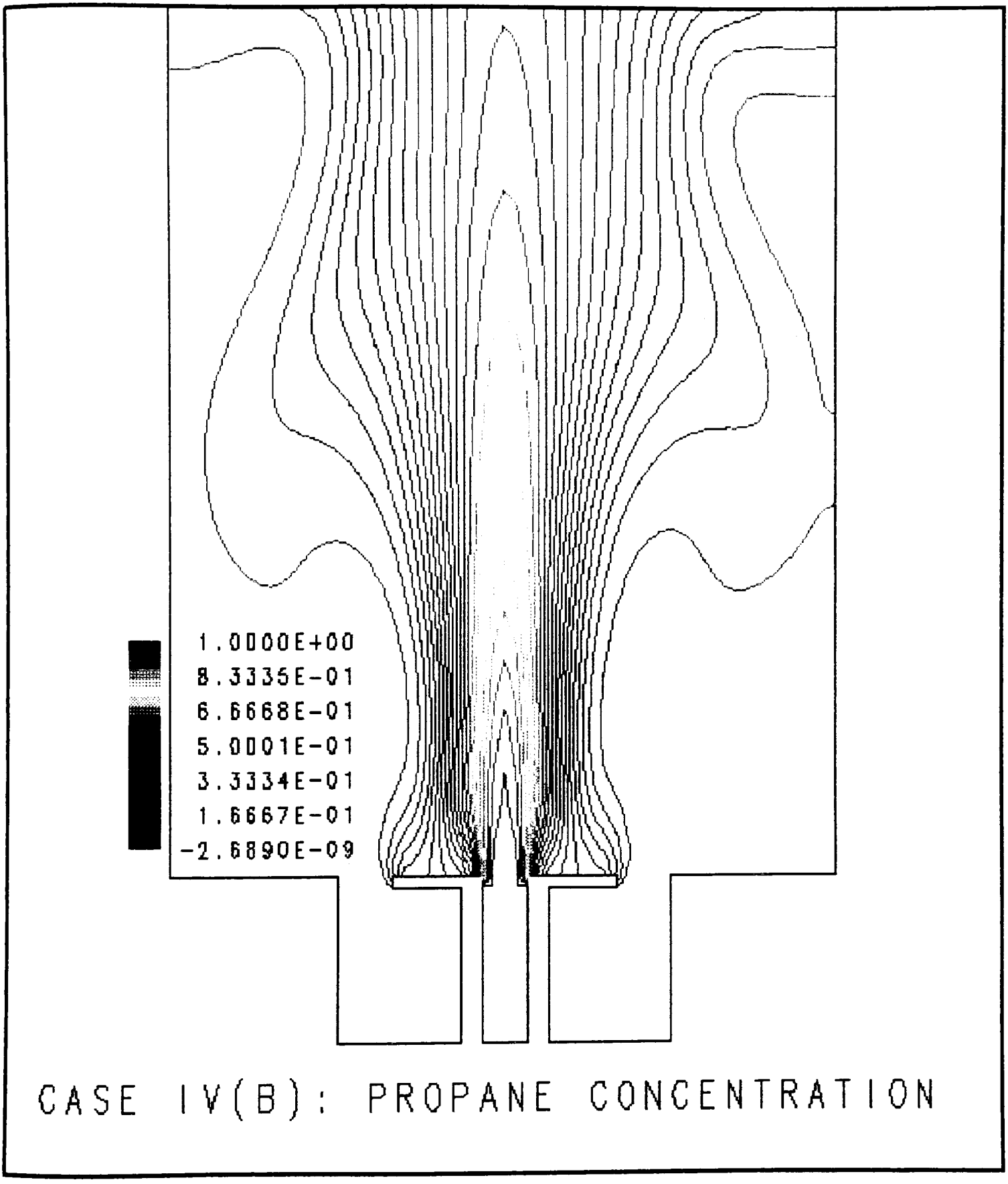

Figure 5.15 Case IV (B): Propane Concentration Contours (% Propane by Mass)

propane jet brought about by its greater molecular weight. Thus, these models display the same general recirculation characteristics, yet each separate case is slightly closer to the penetration region than before.

As the Velocity data does not yield any new information, the extent of the mixing in the recirculation zone becomes the important characteristic of this series of models. Figures 5.11 through 5.15 show the propane concentration (by mass fraction) for the five cases studied.

Figure 5.11 represents Case II (A), the penetration region, and clearly illustrates the advantage that this region holds for flame stability. There is a high degree of mixing between the fuel and oxidant that takes place all throughout the recirculation zone. This is evident as the mixture fraction across the face of the flameholder gradually decreases from pure propane (at the center) to slightly above fifty percent propane (at the outer diameter of the disc).The mixture directly above the disc exhibits much better mixing characteristics than any of the other cases. Most of the mixing takes place inside the recirculation zone, as the air is forced back upon the fuel by the reverse flow of the annular jet. As shown in Figures 15.12 and 15.13, Cases II (B) and II (C) begin to display the characteristics of an important trend that leads from prepenetration to penetration. With a steady increase in the dominant affect of the central (fuel) jet, the extent of mixing in the recirculation zone becomes less and less. The fuel jet becomes thinner and thinner with much less mixing across the face of the flameholder. As the fuel jet begins to penetrate through the recirculation zone,, less fuel is recirculated inside the zone, causing significantly less mixing in that region. Even as the mixing area in Case II (A) appears oval, much in the

shape of the recirculation zone, when it approaches closer to penetration and the recirculation zone gets smaller, the oval tends to become thinner and longer as the propane jet is more concentrated.

Figures 5.14 and 5.15 represent Cases III and IV (A), which continue to exhibit this same trend, and the fact that it intensifies significantly in the penetration region. Both of these regions demonstrate little mixing in the recirculation zone, as the bulk of the mixing is seen through diffusion of the central jet, rather than through direct recirculation. The propane jet is very concentrated. The oval shaped region of mixing from earlier cases has been replaced with a sharply pinched region above the flameholder face, quickly changing to a sheer jet column directly afterwards.

The general trend for mixing in the recirculation zone is clear, that from prepenetration to penetration there is a steady decline in mixing, due mainly to the penetration of the fuel jet through the recirculation zone. The ultimate result of this trend will be less stability and less efficiency under combustion conditions as operating conditions are closer to the penetration region.

At this point it is clear that CFDS-Flow3D is fully capable of modeling the characteristics of the flowfield around a single bluff body flameholder. Basic trends have been established for the behavior of the recirculation zone under various inlet conditions for both the central and annular jet. The effects of the characteristic regions of flow as defined by Huang and Lin (1994) have been shown numerically with the CFD model, with a good degree of correlation, bearing in mind the alterations made to the geometry for the CFD model. The next phase of the investigation is to employ similar CFD modeling

techniques to evaluate the performance of a double bluff body flameholder in both cold flow and combustion, and to compare that to both the single bluff body analysis just presented (for cold flow), and an experimental analysis performed on a double bluff body flameholder under combustion conditions.

6.0 DOUBLE BLUFF BODY NUMERICAL ANALYSIS:

6.1 Cold Flow Analysis

This section deals with the computational cold flow analysis performed on the double concentric bluff body flameholder. A cold flow analysis examines the behavior of the flameholder under non-combustion conditions. This offers insight into the mixing and recirculation characteristics of the system without taking into account the effects of a chemical reaction between the two. A cold flow analysis is often performed as a preliminary study to a full combustion analysis, and gives the flameholder designer a good idea of what to expect from the flame.

This analysis examines four cases, as shown in table 4.2. The first pair are for a geometric blockage ratio of 0.53 and two separate equivalence ratios, while the second pair are for a blockage ratio of 0.44 and the same two equivalence ratios. The equivalence ratios examined are 1.0, the stoichiometric mixture, and 1.5, a fuel rich mixture. All cases are for a fixed air flowrate of 0.1416 m^3/min (300 SCFM). As subsequent possible study on the double concentric bluff body flameholder may involve the addition of secondary air flow, examining a rich mixture will serve as a good basis of comparison for subsequent work.

Figure 6.1 gives the velocity vectors for case Alpha (Φ = 1, Br = 0.53). The most noticeable difference between the performance of this configuration and that of the single bluff body is immediately recognized, as the change in the structure of the recirculation zone(s). The change in structure is more clearly illustrated in Figure 6.2, the axial (V)

velocity contours. It shows that an additional recirculation zone (hereafter termed the central recirculation zone), completely new with this configuration, has been created directly above the central bluff body, and it is much larger than the one between the fuel and air jets (hereafter termed the annular recirculation zone). This recirculation zone is directly caused by the addition of the central bluff body, and shows the first signs of this configurations potential benefits. It extends 1.11 D_O , or outer disc (that used for the air flow obstruction) diameters downstream, and has a maximum reverse axial velocity of 1.77 m/s (77.6 % of the magnitude of the central jet velocity). The annular zone is still present, much as seen in the single bluff body analysis, but it is much smaller than the central zone. It extends only 0.29 D_O downstream, but has a strong maximum reverse axial velocity, also at 1.77 m/s.

Figure 6.3, the propane concentration contour plot for case Alpha, shows that there is extensive mixing in the entire recirculation region, even directly above the central bluff body. The propane jet is completely engulfed in the two recirculation zones, and there is no noticeable jet column at all, as was seen with the single bluff body. There is significantly more air brought into the entire recirculation region to mix with the fuel, and there is a strong increase in the extent of mixing directly above the face of the flameholder than in the single bluff body cases. There are few areas of pure propane, except in the small channel at the nozzle face, as almost all of it has been mixed with the oxidant in either of the two recirculation zones. The strength of the central recirculation zone seems to force propane into the annular recirculation zone, as the propane stream can be seen curving into the annular zone.

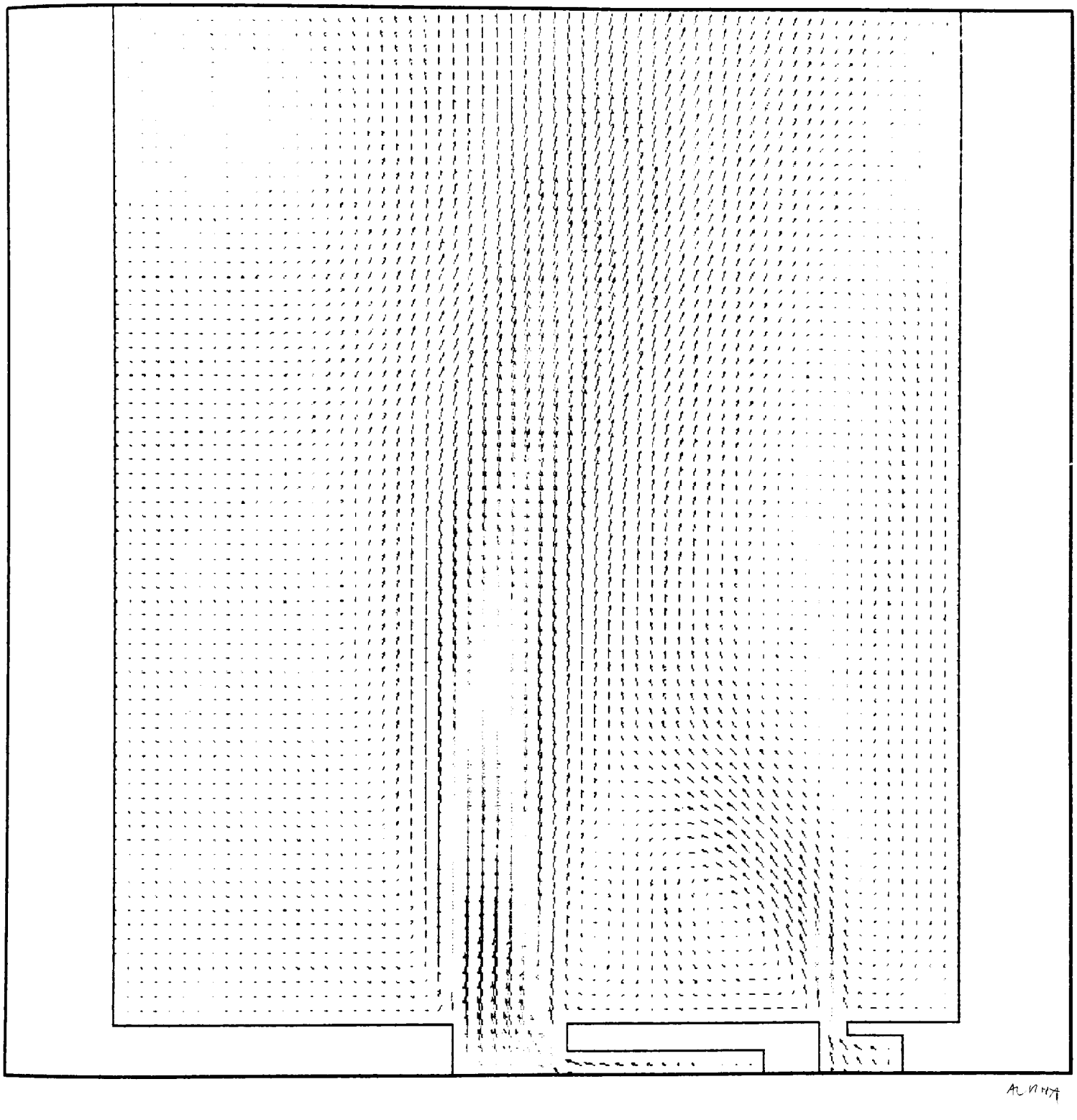

Figure 6.1 Cold Flow, Case Alpha: Velocity Vectors (m/s)

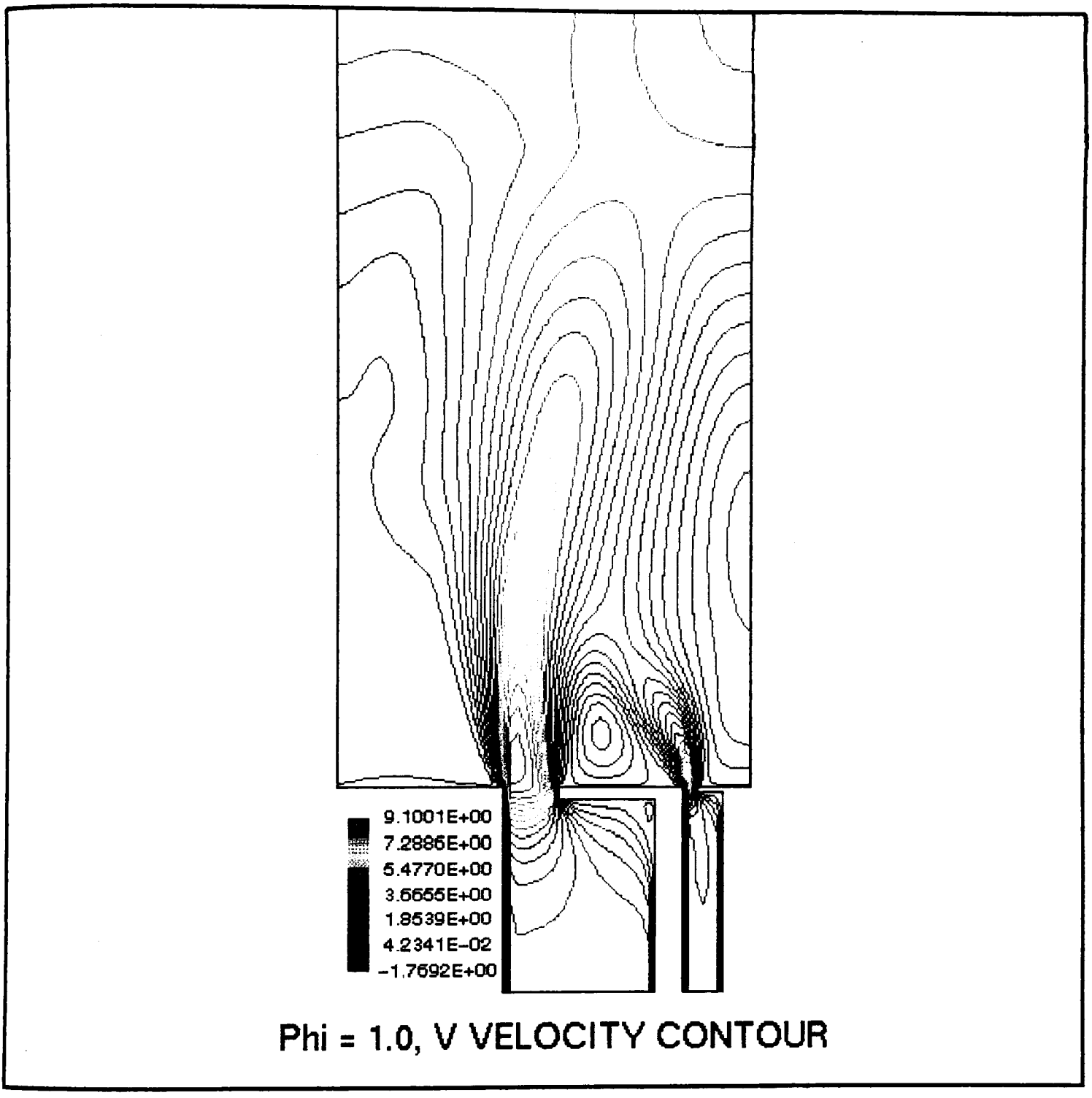

Figure 6.2 Cold Flow, Case Alpha: Axial Velocity Contours (m/s)

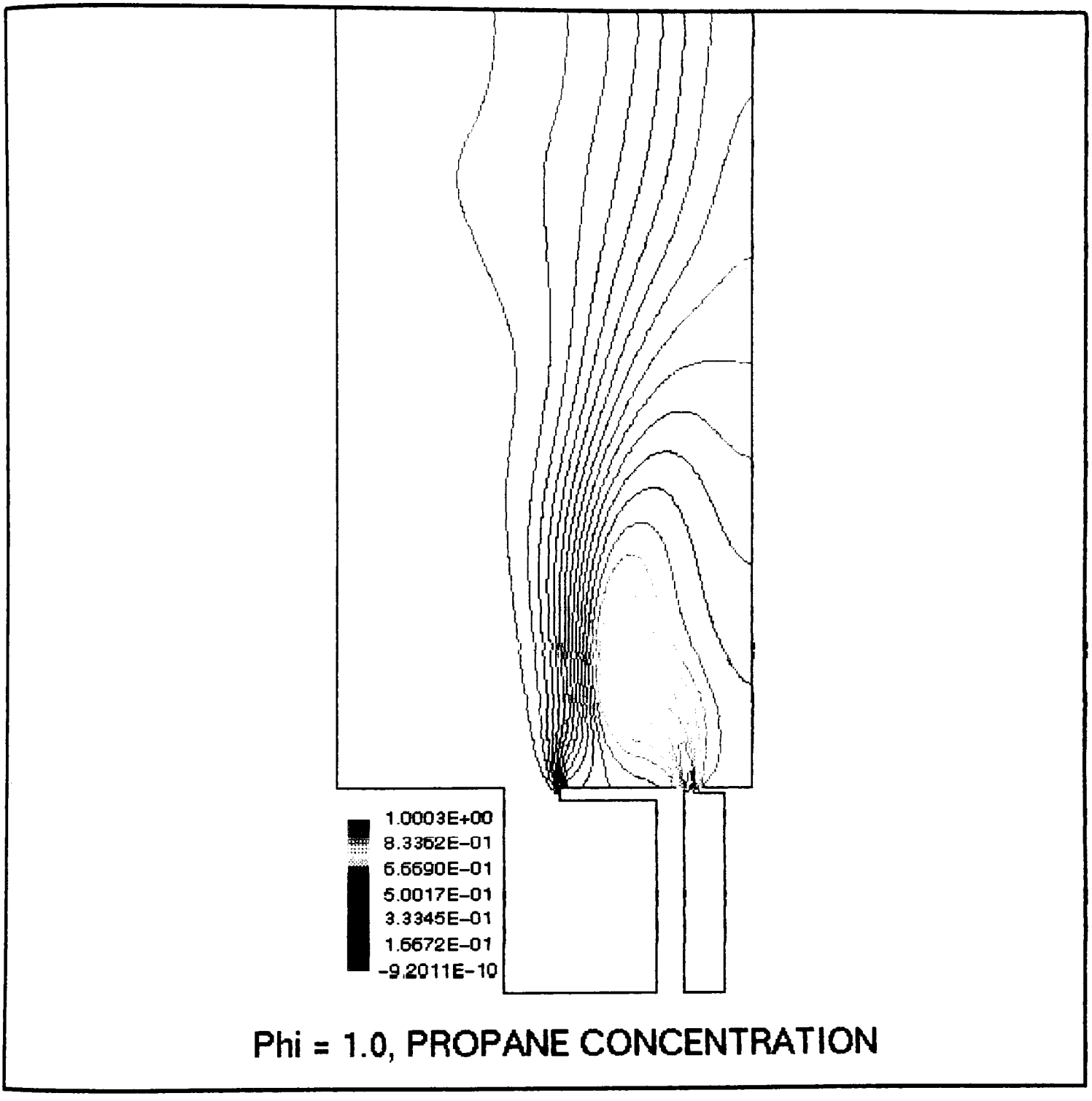

Figure 6.3 Cold Flow, Case Alpha: Propane Concentration Contours
(% Propane by Mass)

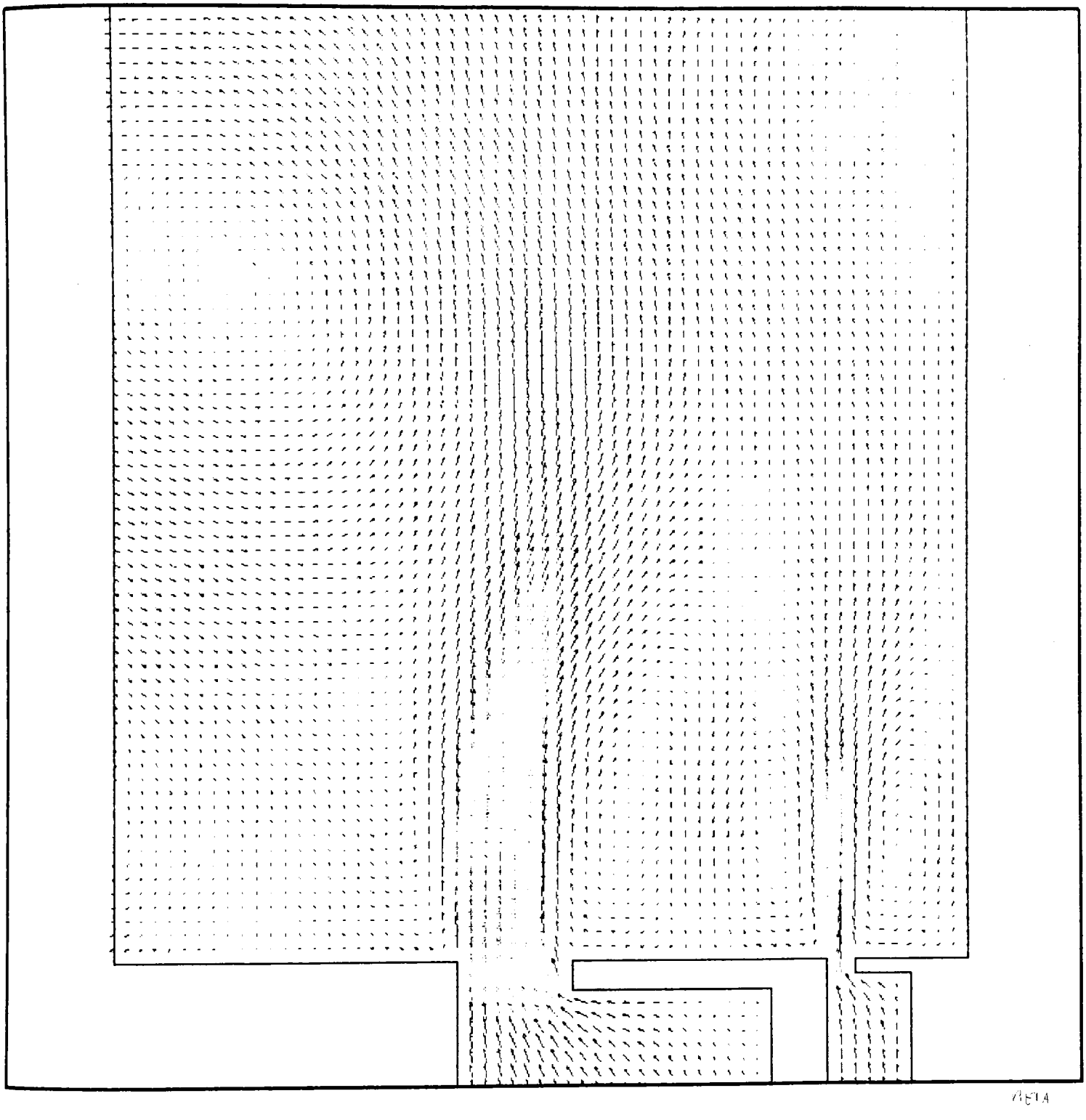

Figure 6.4 Cold Flow, Case Beta: Velocity Vectors (m/s)

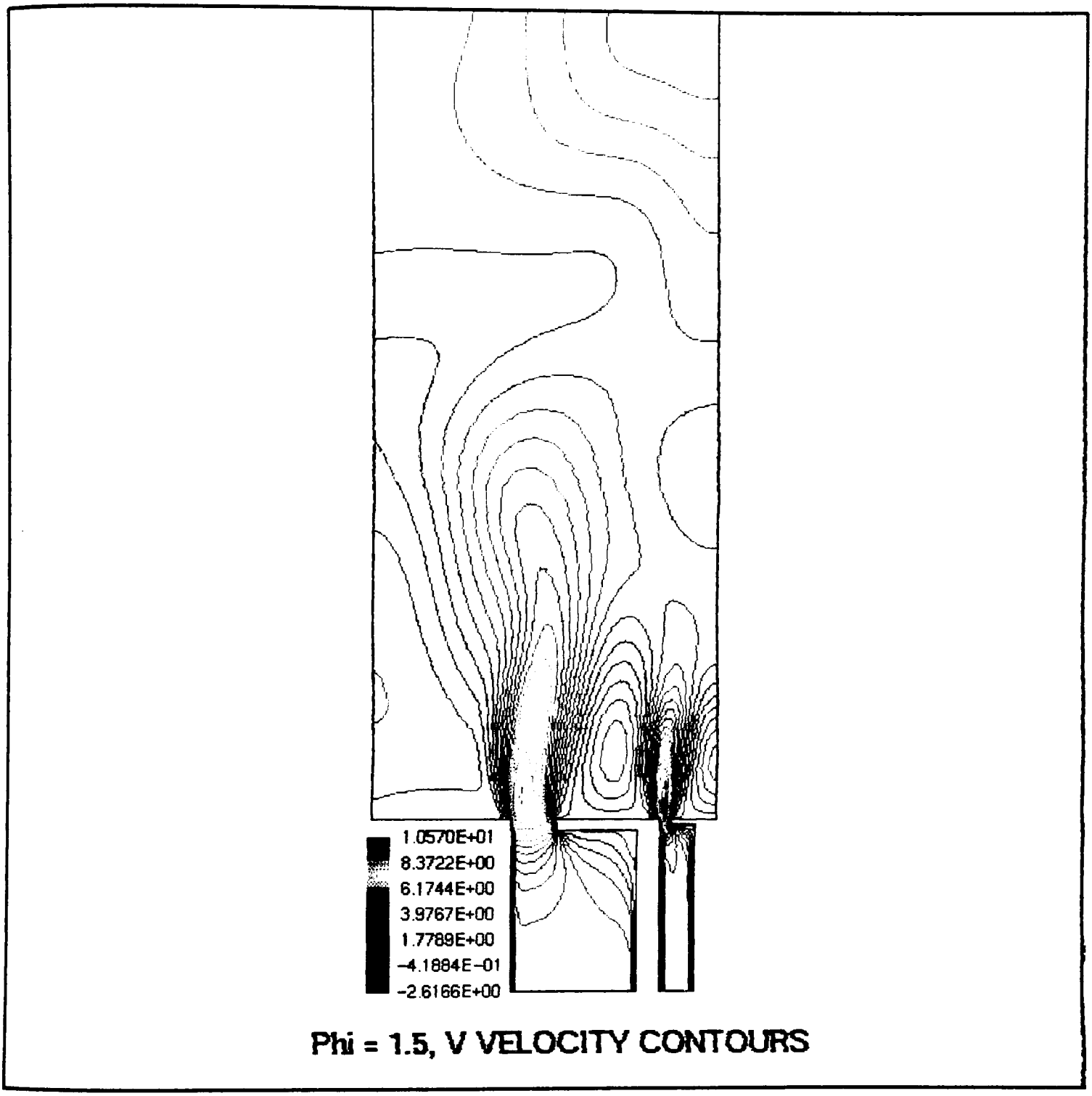

Figure 6.5 Cold Flow, Case Beta: Axial Velocity Contours (m/s)

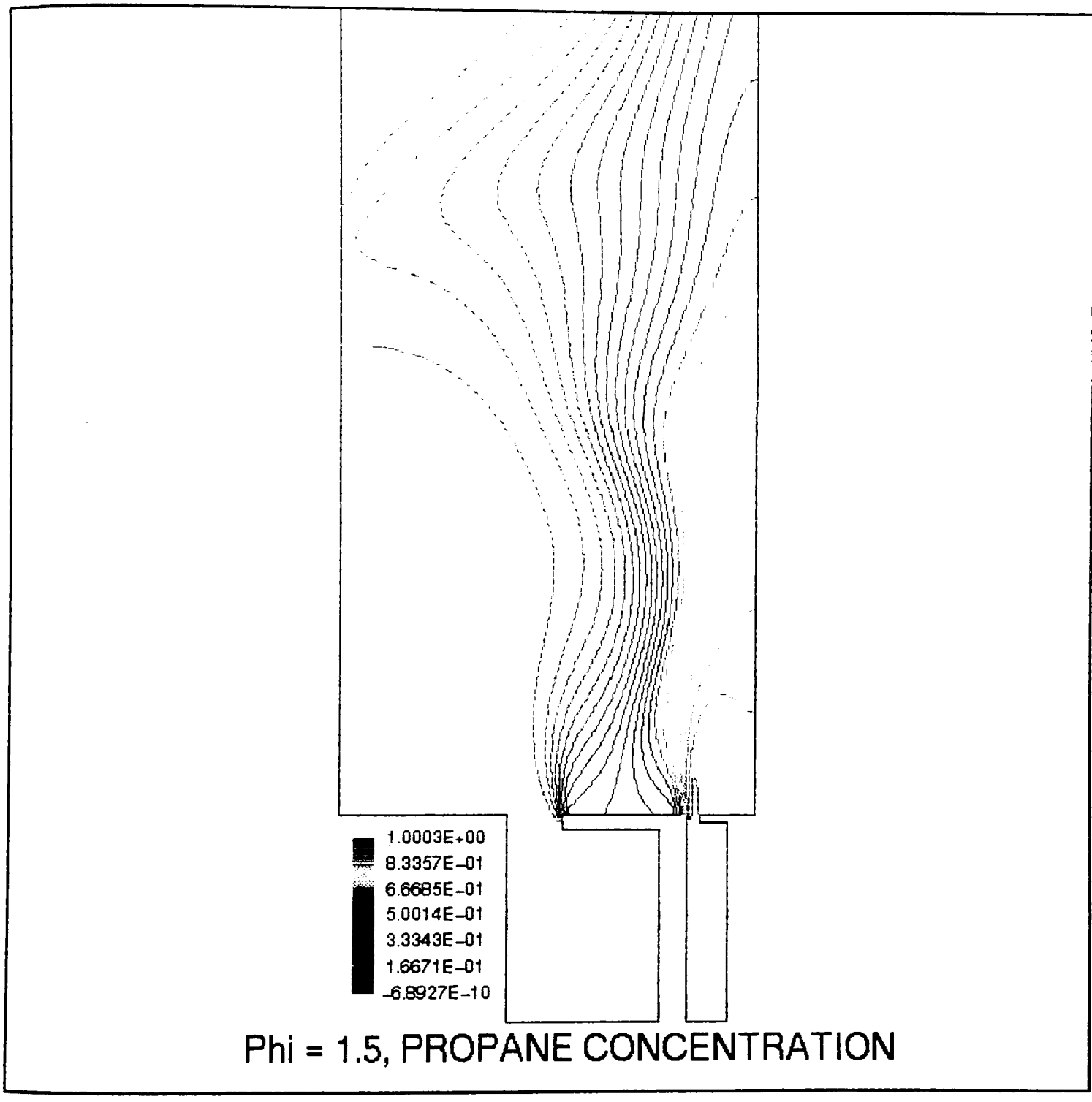

Figure 6.6 Cold Flow, Case Beta: Propane Concentration Contours
(% Propane by Mass)

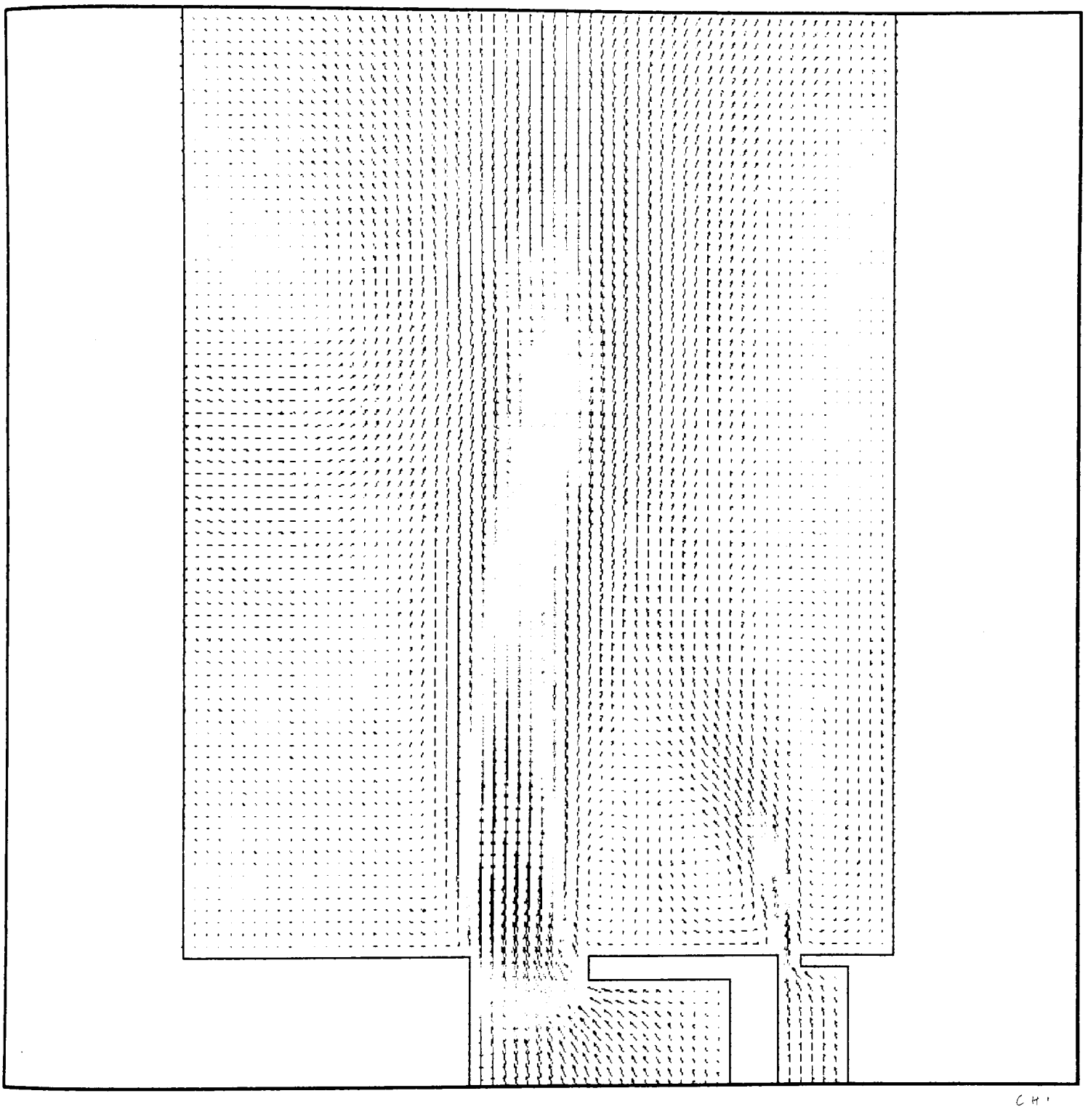

Figure 6.7 Cold Flow, Case Chi: Velocity Vectors (m/s)

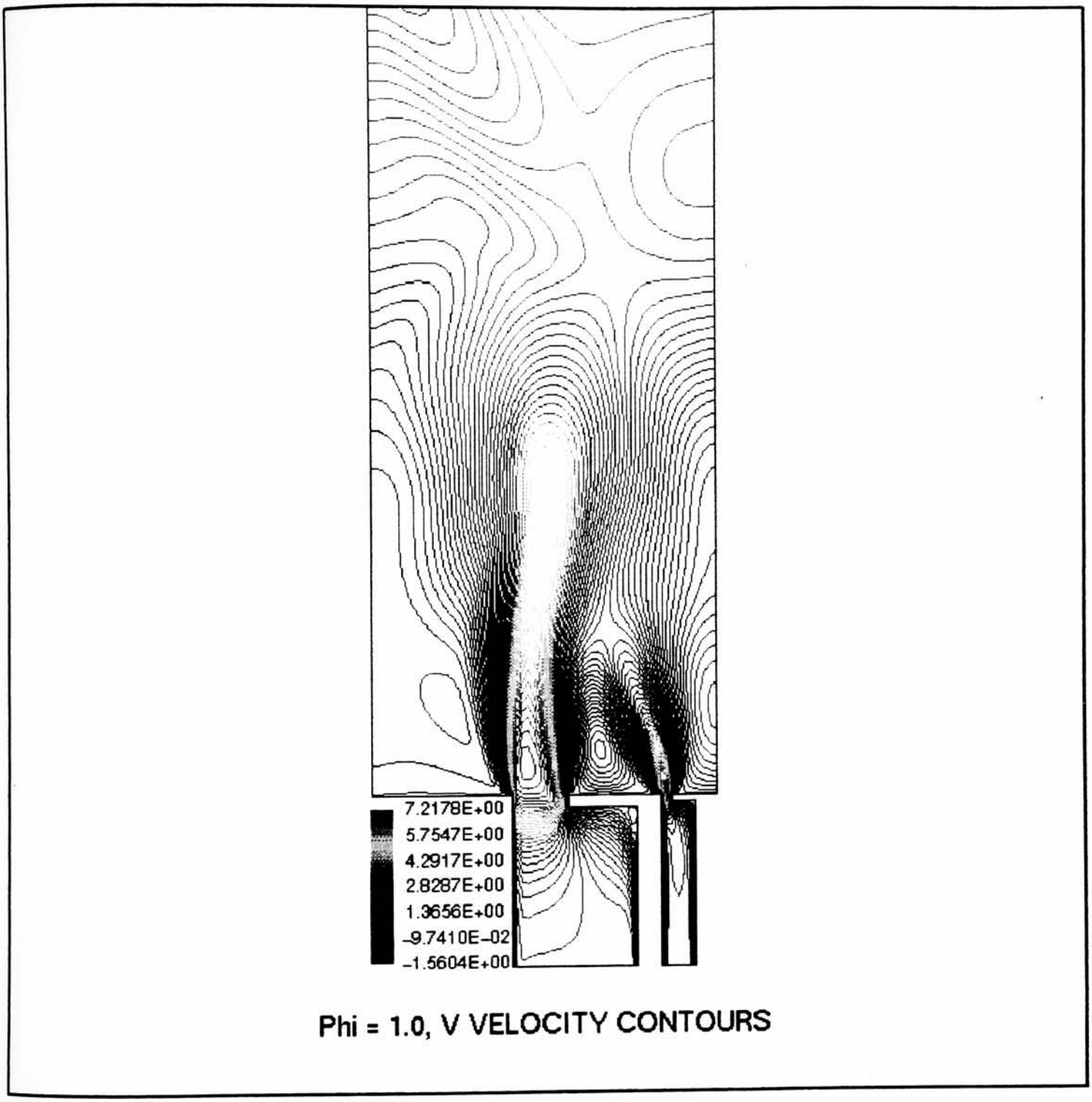

Figure 6.8 Cold Flow, Case Chi: Axial Velocity Contours (m/s)

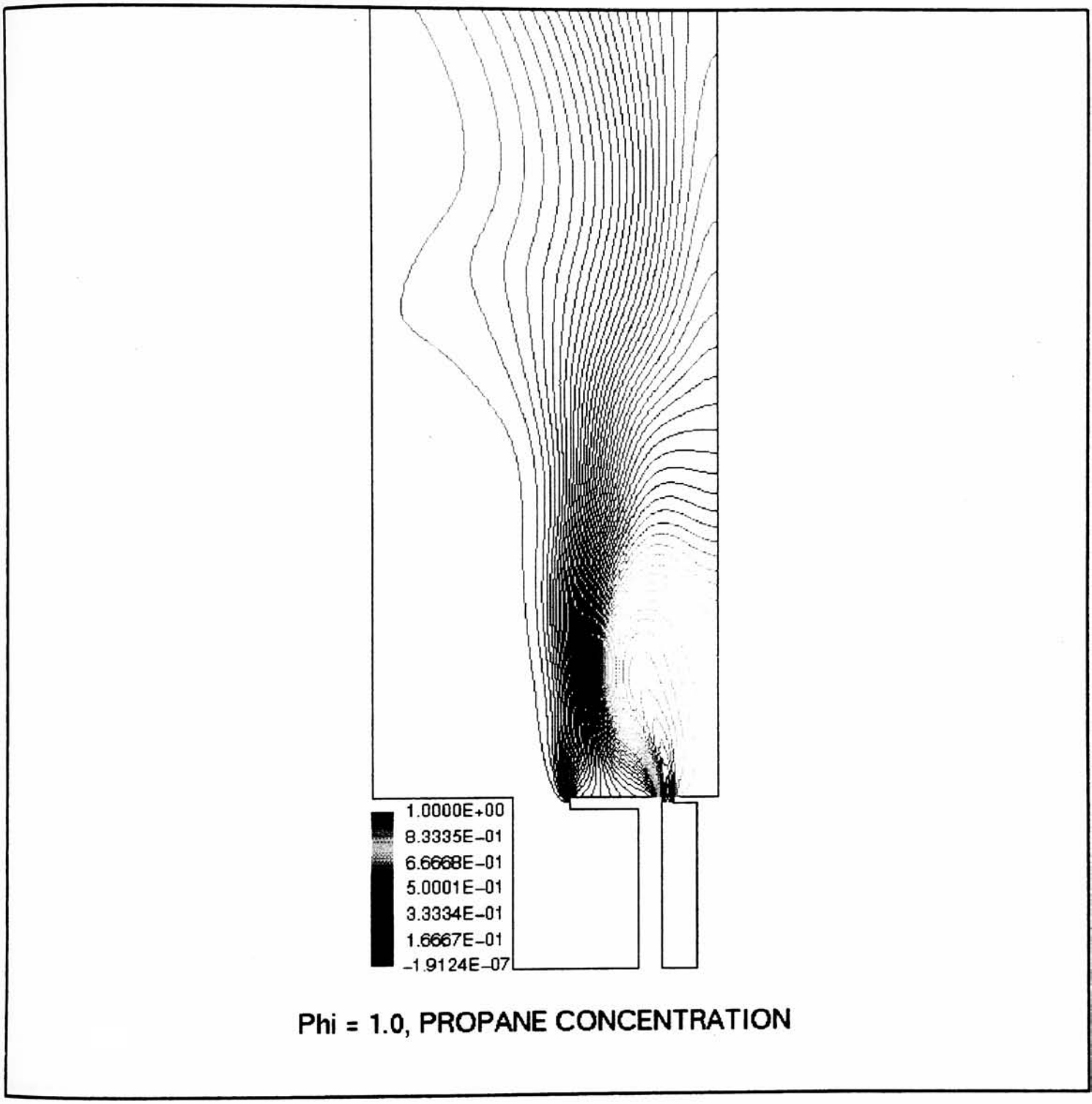

Figure 6.9 Cold Flow, Case Chi: Propane Concentration Contours
(% Propane by Mass)

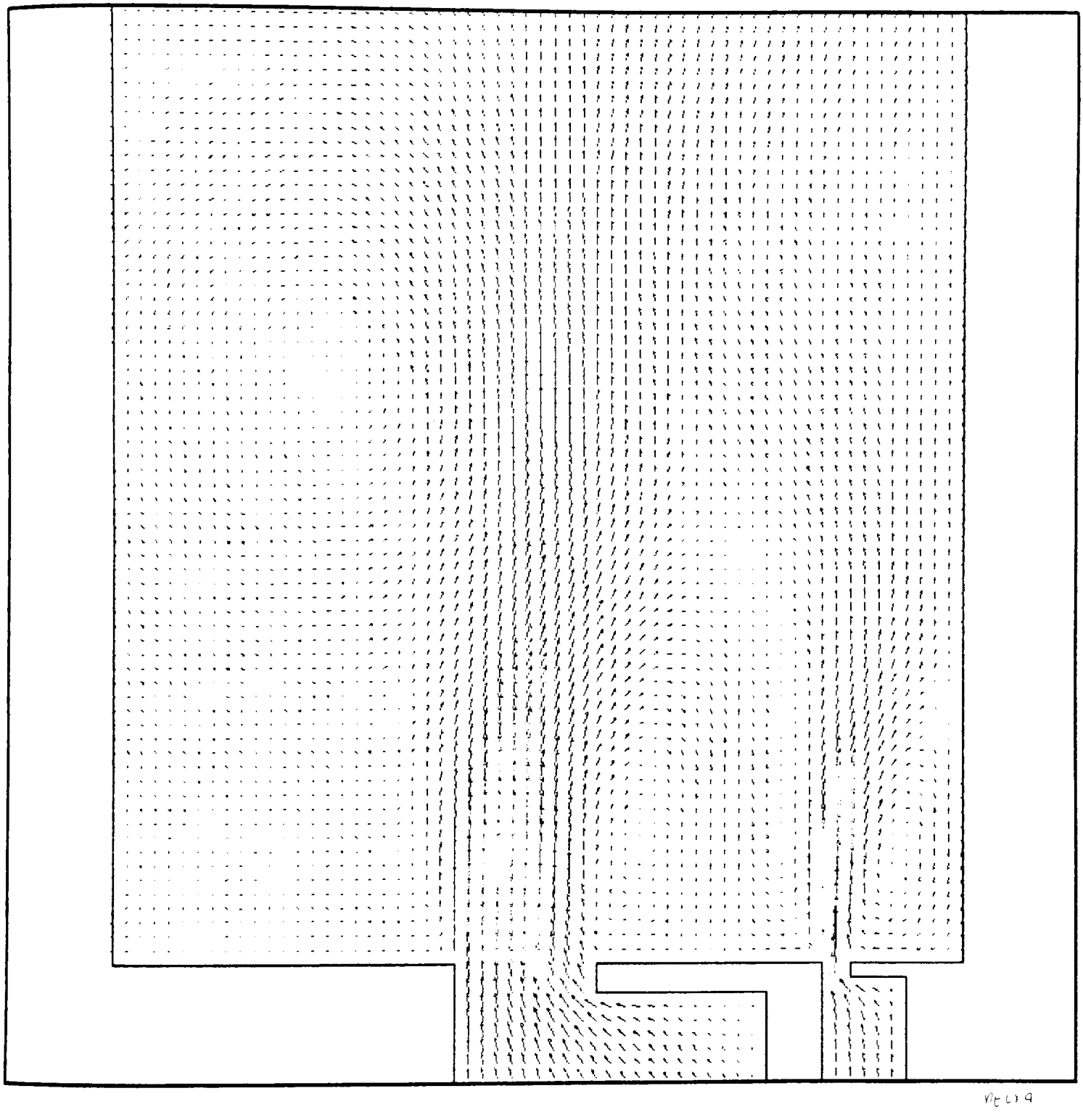

Figure 6.10 Cold Flow, Case Delta: Velocity Vectors (m/s)

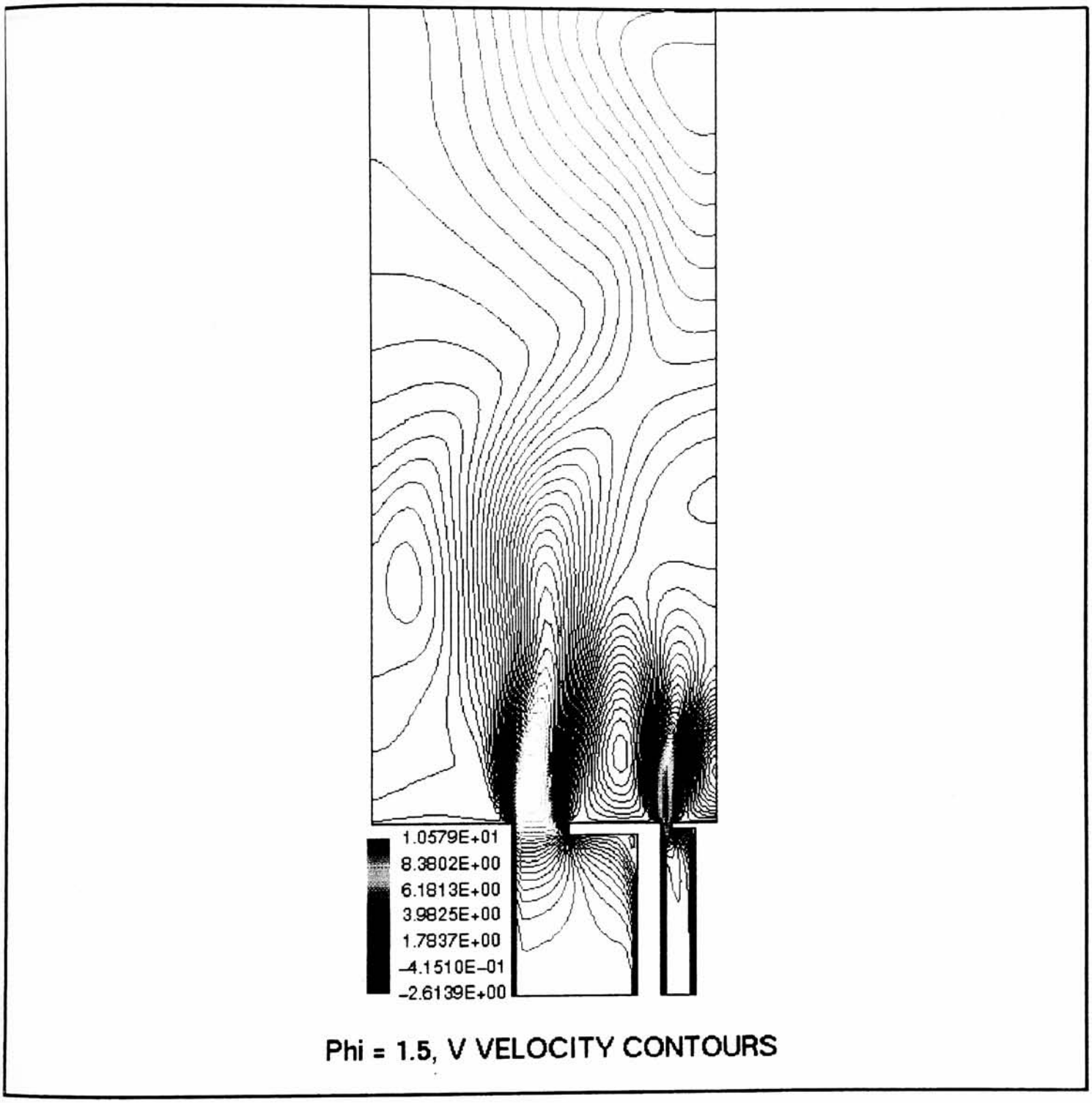

Figure 6.11 Cold Flow, Case Delta: Axial Velocity Contours (m/s)

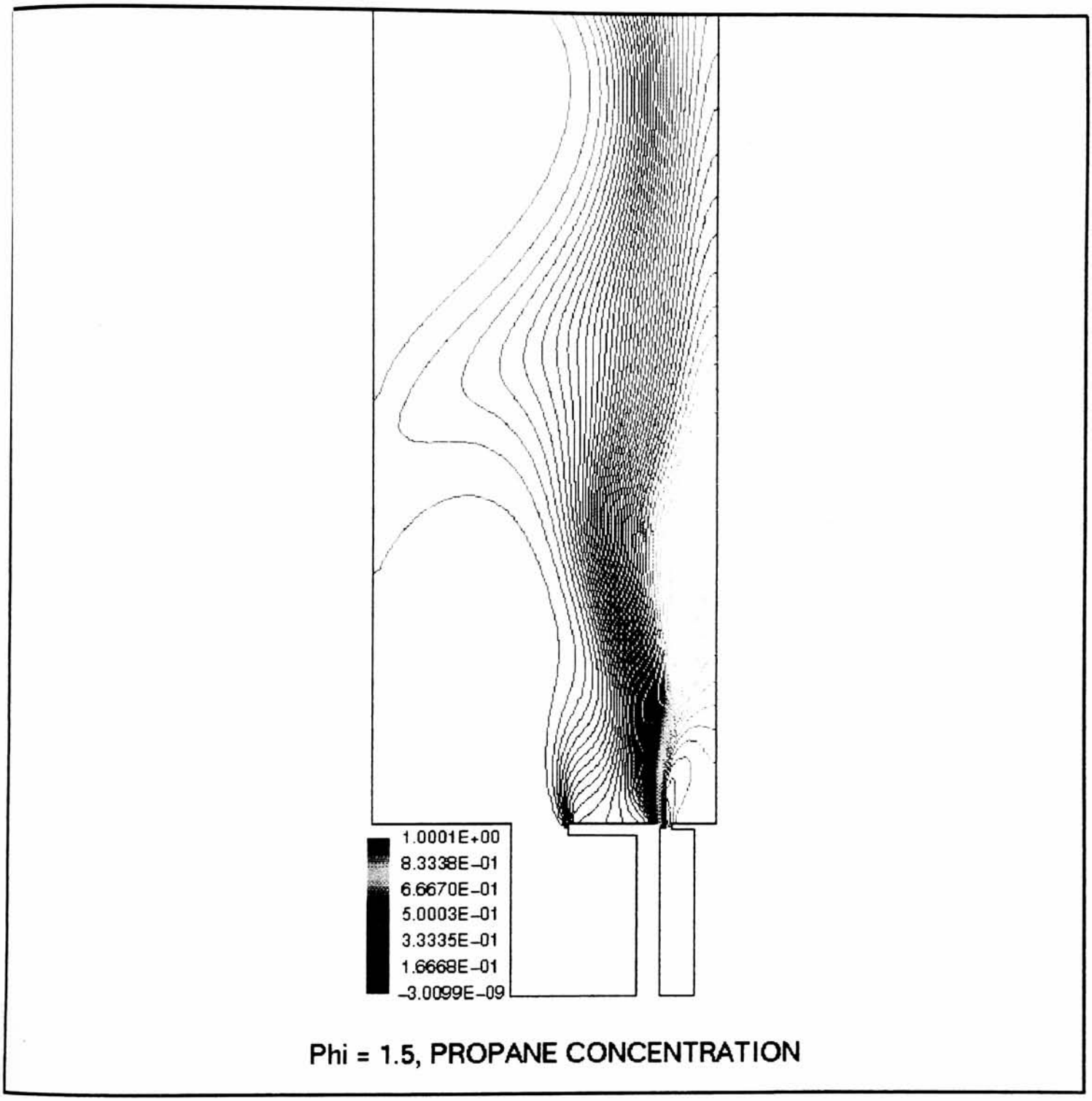

Figure 6.12 Cold Flow, Case Delta: Propane Concentration Contours
(% Propane by Mass)

Figures 6.4 and 6.5 show velocity vector and axial velocity contour plots for case Beta (Φ = 1.5, Br = 0.53). The central recirculation zone above the fuel disc is still present, but it has diminished in size and strength due to the increase of the central jet velocity. Figure 6.5 shows that for this case the fuel jet emerges vertically into the recirculation region, while in the previous case it was drawn outward, into the air jet. This clearly illustrates the increase in fuel jet dominance, which has resulted in a greatly decreased central recirculation zone, but a very similar (if not a little stronger) annular zone. Both zones are now of comparable size and strength; the central extending about 0.35 D_O downstream, with a maximum reverse axial velocity of 2.62 m/s (76.5% of the central inlet velocity), and the annular zone extending about 0.45 D_O, with a maximum reverse axial velocity of 2.16 m/s (63.1% of the central inlet velocity).

Figure 6.6, the propane concentration contour plot for case Beta, clearly shows the affect of penetration by the fuel jet. As the central recirculation zone has diminished in size, it is able to draw less air back onto the face of the central disc. This is markedly less mixing above the central disc than in case Alpha, as most of the region is well above 80% (by mass) propane, as opposed to between 60% and 70% for Alpha. There is also less mixing in the annular zone than in the previous case, as most of the fuel jet column penetrates through the recirculation zones.

Cases Chi (Φ = 1.0, Br = 0.44) and Delta (Φ = 1.5, Br = 0.44) exhibit much the same performance as those of Alpha and Beta, when observed with respect to each other. The annular and central recirculation zones are clearly present in both, and the same trend appears with the increase in fuel jet velocity. The central zone diminishes in size but

increases in strength, and the annular zone actually increases in size and strength. The trend in fuel-oxidant mixing that was seen in the first two cases is also seen; as the fuel jet velocity increases, the amount of mixing in the recirculation zones decreases.

Figures 6.7 and 6.8 give the axial velocity contour and the propane concentration contour plots for case Chi. The central recirculation zone extends 1.27 D_O downstream, with a 1.56 m/s maximum reverse axial velocity (68.4% of the magnitude of the central jet inlet velocity); while the annular recirculation zone extends 0.34 D_O downstream, with a 1.44 m/s maximum reverse axial velocity (63.1% of the magnitude of the central jet inlet velocity). Figures 6.9 and 6.10 give the axial velocity contour and the propane concentration contour plots for case Delta. The central recirculation zone extends 0.34 D_O downstream, with a 2.61 m/s maximum reverse axial velocity (76.2% of the magnitude of the central jet inlet velocity); while the annular recirculation zone extends 0.54 D_O downstream, with a 2.54 m/s maximum reverse axial velocity (74.2% of the magnitude of the central jet inlet velocity).

The significant difference between the first pair of cases and the second pair of cases is the geometric blockage ratio (BR) of the air inlet. The second pair of cases has a lower blockage ratio, and hence a smaller obstruction, causing the air entering the region downstream of the nozzle to enter at a lower velocity, and a lower momentum. The major effect of this is that the fuel jet is more dominant for both equivalence ratios in the second pair of cases than in the first. This can be seen in the performance of the second pair of cases, as in each case the fuel jet is more dominant, resulting in smaller overall recirculation zone size and less mixing throughout the entire region.

The increase in the dominance of the fuel jet has similar effects on the performance of the double bluff body configuration as on that of the single bluff body. Increasing the amount of fuel flow (while holding the amount of air flow constant), and thus the degree of fuel jet dominance, decreases the effects of the bluff bodies with respect to fuel - oxidant mixing. For comparative purposes, the $\Phi = 1.0$ cases (Alpha and Chi) most nearly exhibit characteristics comparable to those of prepenetration region, while the $\Phi = 1.5$ cases (Beta and Delta) most nearly illustrate characteristics comparable to those of penetration. For all of these cases though, the double bluff body configuration exhibits prominent benefits to mixing and recirculation performance, due mainly to the addition of the central recirculation zone. This added zone serves to greatly increase mixing for the stoichiometric cases, as the fuel jet column is forced into the annular zone by the recirculated air in the central zone. The central zone also increases the mixing in the fuel rich cases, but to a lesser degree. There is mixing in the central recirculation zone in this configuration, where there is none in the single bluff body configuration, which is a benefit in and of itself as it makes a region previously incombustible subject to combustion. This is particularly important as it eliminates a region wasted by an incombustible mixture (pure fuel), effectively reducing flame size, and as this combustion is in close proximity to the fuel injection point (the narrow channel between the obstruction and the wall), it also preheats the fuel more effectively.

Table 6.1: Results of the Double Bluff Body Analysis - Cold Flow

Central Recirculation Zone:

Case	U_A (m/s)	U_{MC} (m/s)	Approx. Height of Rec. Zone (D_A)	Maximum Reverse Axial Velocity (m/s)	% Magnitude of Central Jet Velocity
Alpha	2.732	2.282	1.11	1.77	77.6
Beta	2.732	3.423	0.35	2.62	76.5
Chi	2.732	2.282	1.27	1.56	68.4
Delta	2.732	3.423	0.34	2.61	76.2

Annular Recirculation Zone:

Case	U_A (m/s)	U_{MC} (m/s)	Approx. Height of Rec. Zone (D_A)	Maximum Reverse Axial Velocity (m/s)	% Magnitude of Central Jet Velocity
Alpha	2.732	2.282	0.29	1.77	74.0
Beta	2.732	3.423	0.45	2.16	63.1
Chi	2.732	2.282	0.34	1.44	63.1
Delta	2.732	3.423	0.54	2.54	74.2

6.2 Combustion Analysis:

This section covers the computational combustion analysis performed on the double bluff body flameholder. The combustion analysis yields information about the flameholder during its operation, providing valuable data about the stability, size, shape and temperature profile of the flame. Insights into the possible benefits of this configuration over a single bluff body configuration will also be seen. This analysis examines the flameholder under four separate conditions of operation, which are identical to those examined in section 6.1 (cases Alpha through Delta). The performance of the flameholder under these conditions will be subsequently compared to the experimental performance under like conditions in Section 7.3, for validation of the numerical model.

Figures 6.13 shows the temperature contours, and Figure 6.14 gives the products concentration (CO, CO_2, H_2O and NO_X - the last of which takes up much less than one percent of the total) contours for case Alpha. The temperature contours show the steady state temperature of the flame brought about by combustion, while the product concentration gives a relative idea of the extent of combustion in each given area. Areas of high product concentration denote areas of high reaction rate, where the reactants rapidly release the latent energy of the fuel and produce intense heat and flame.

The flame shape can be determined by the combination of these two figures, as can some of the differences between mixing in combustion and mixing in cold flow. Figure 6.13 shows the area of maximum temperature, which coincides with the area of maximum product concentration as seen in Figure 6.14. The combination of these two are used to define the flame envelope (or flame front). This is the region of the most intense reaction

between fuel and oxygen, and is hence the brightest, hottest and contains the highest concentration of products. The area of visible flame extends a short distance beyond the envelope, as shown by the temperature contours down to about 600 K. It is important to note that the temperature of the flame is lower inside the flame envelope than at the flame front itself. This is due to the fact that the interior of the flame is mostly fuel, being unable to react with the oxygen, as no oxygen makes it through the flame front into the interior.

The annular recirculation zone is seen clearly in the temperature profile. It is another region of intense reaction, as the recirculation zone draws in air, fuel and hot product gases for ignition. This intense mixing gives rise to flame temperatures in excess of 1200 K inside the recirculation zone. This is the desired effect of the flameholder, and is the root of the performance benefits brought about by this configuration. The combustion in the recirculation zone not only burns off a good deal of the incoming fuel in a very stable reaction, but also preheats the rest of the fuel inside the flame envelope to increase the combustion efficiency. The shear region (the pinched area where the annular recirculation zone ends and the downstream region begins) is clearly visible, directly after the annular recirculation zone, about 1.5 cm from the face of the flameholder. This feature is a common characteristic of bluff body stabilized flames, and defines the recirculation region during combustion. The flame plumes out to full width quickly after this region, about 7.0 cm wide (3.5 cm radially on the axisymmetric figures).The effects of the central recirculation zone are not as clearly seen in this figure as they are in the next two, as the gases that are recirculated are still well within the flame envelope, and not as hot as those in the annular zone, but there are still important effects to be noted. Even slight increases

in the fuel temperature inside the envelope can increase the combustion efficiency. Directly above the central bluff body, the temperature contours show slight increases in temperature in the central recirculation zone, an effect that is present in a much lesser degree for a single bluff body configuration. The temperature of the fuel increases by about 100 K inside the central recirculation zone, which is a definite benefit to combustion efficiency. The flame reaches a maximum temperature of 1700 K in the heart of the envelope, far downstream in the plume region; while most of the envelope is in the temperature range between 1300 K and 1450 K.

Figure 6.15 shows the propane concentration (by mass fraction) for case Alpha, illustrating mixing inside the flame envelope. Immediately it is seen that no propane passes through the flame front, all of it reacts with air in combustion. The effect of the central recirculation zone appears clearly in this figure, as there is no region of pure propane past the face of the flameholder. The central recirculation zone draws back the heated fuel and products to the face of the central disc, resulting in a mixture of fuel and products in that region. This is the cause of the preheating of this region that was seen in Figure 6.13. The general mixing characteristics are somewhat different from those of the cold flow analysis, as much of the oxygen reacts with fuel near the flame envelope before making it into the central recirculation zone. Instead of air mixing with fuel in the interior regions, there is fuel mixing with products. The general structure of the recirculation zones are still the same, as are the general mixing trends, the significant difference is that there are now three classifications of fluid (air, fuel and products) mixing in the flowfield.

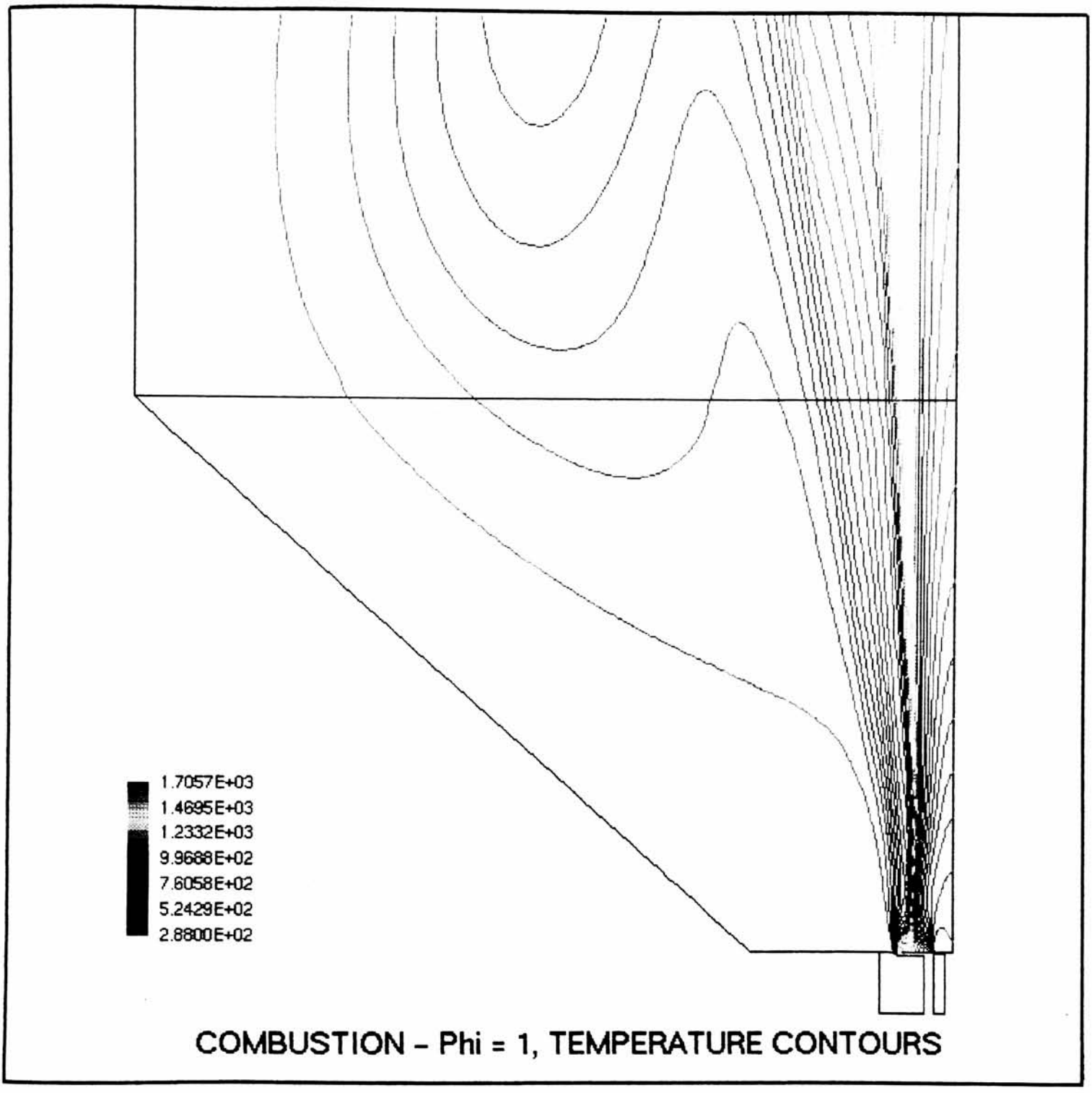

Figure 6.13 Combustion, Case Alpha: Temperature Contours (K)

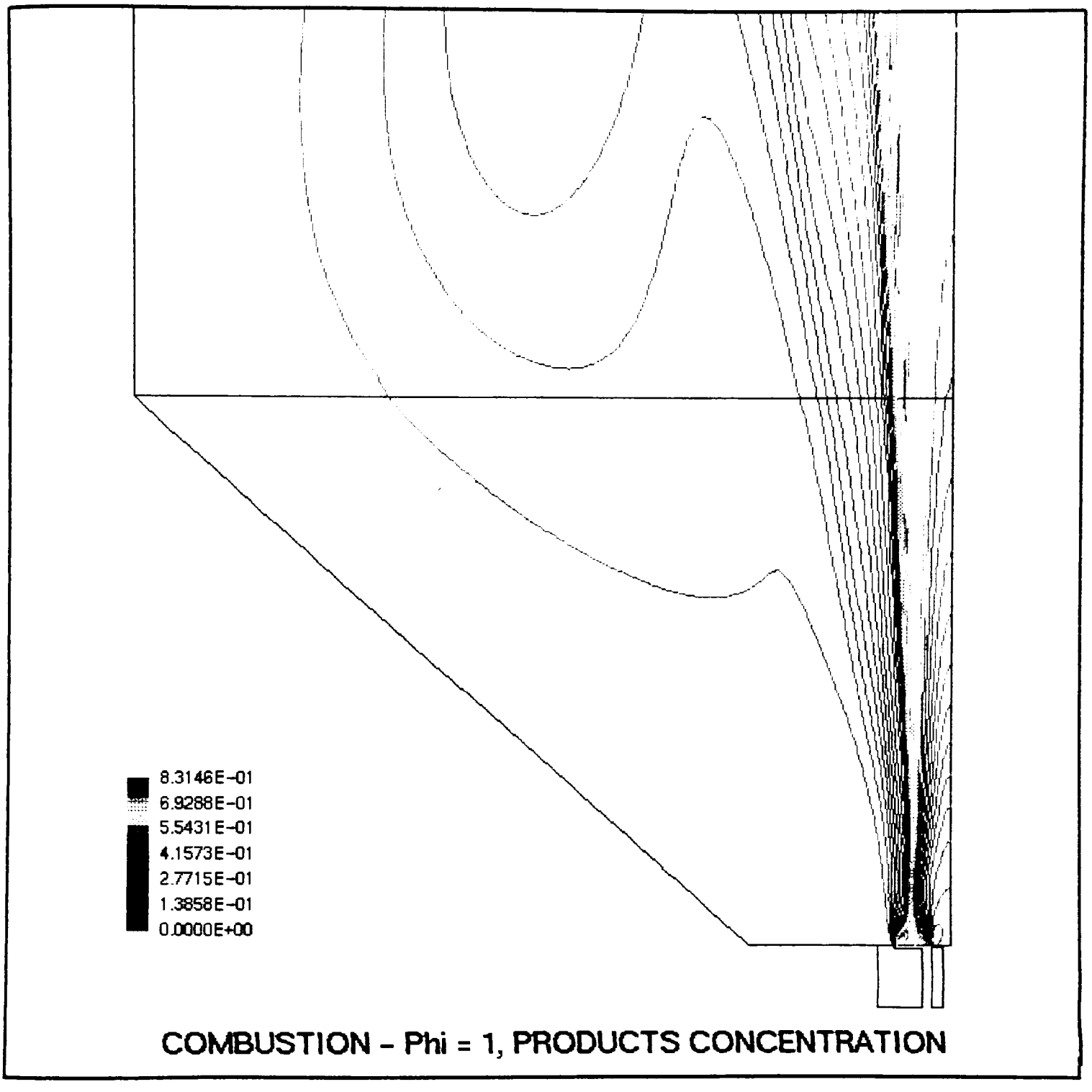

Figure 6.14 Combustion, Case Alpha: Products Concentration Contours
(% Products by Mass)

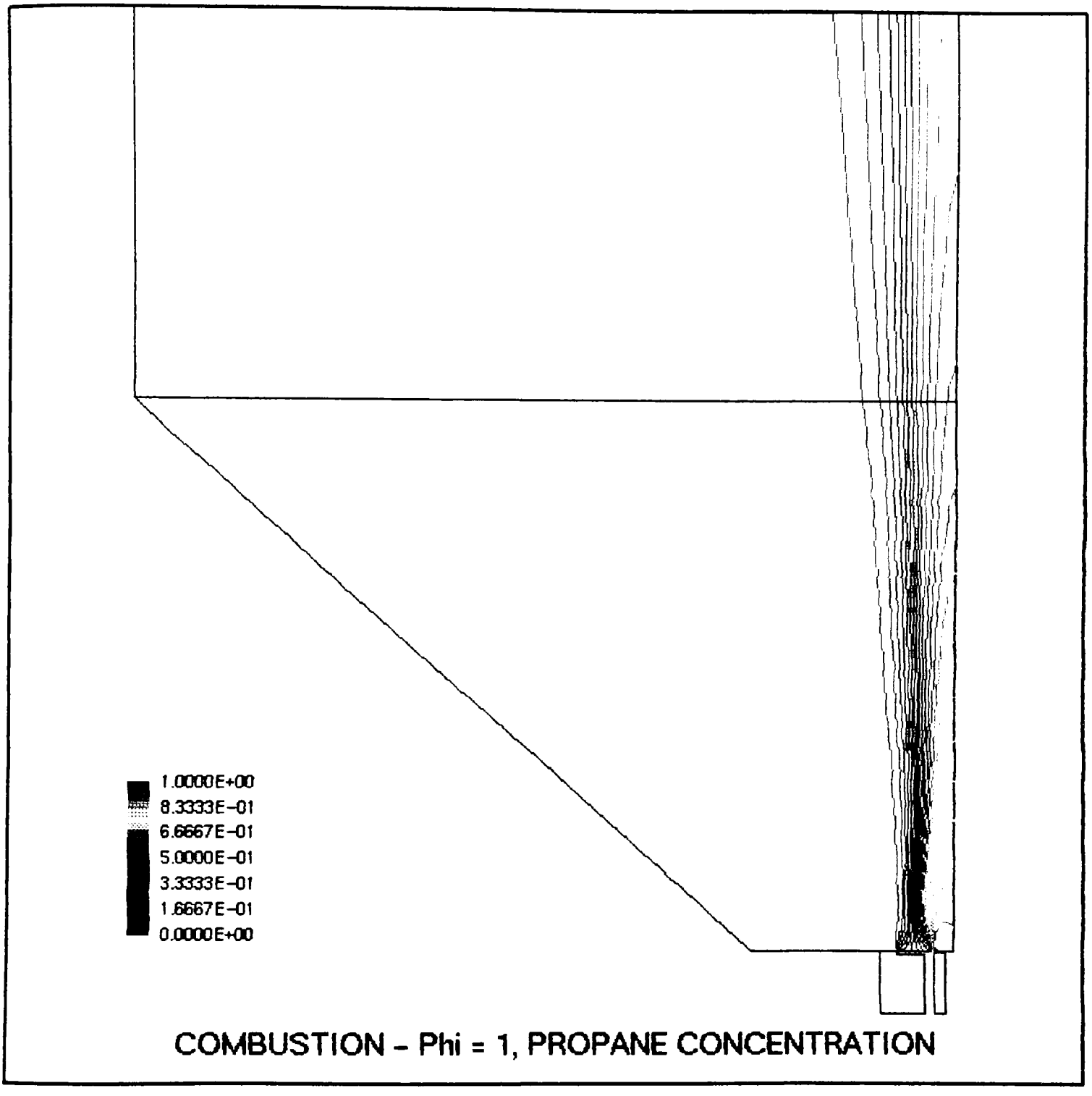

Figure 6.15 Combustion, Case Alpha: Propane Concentration Contours
(% Propane by Mass)

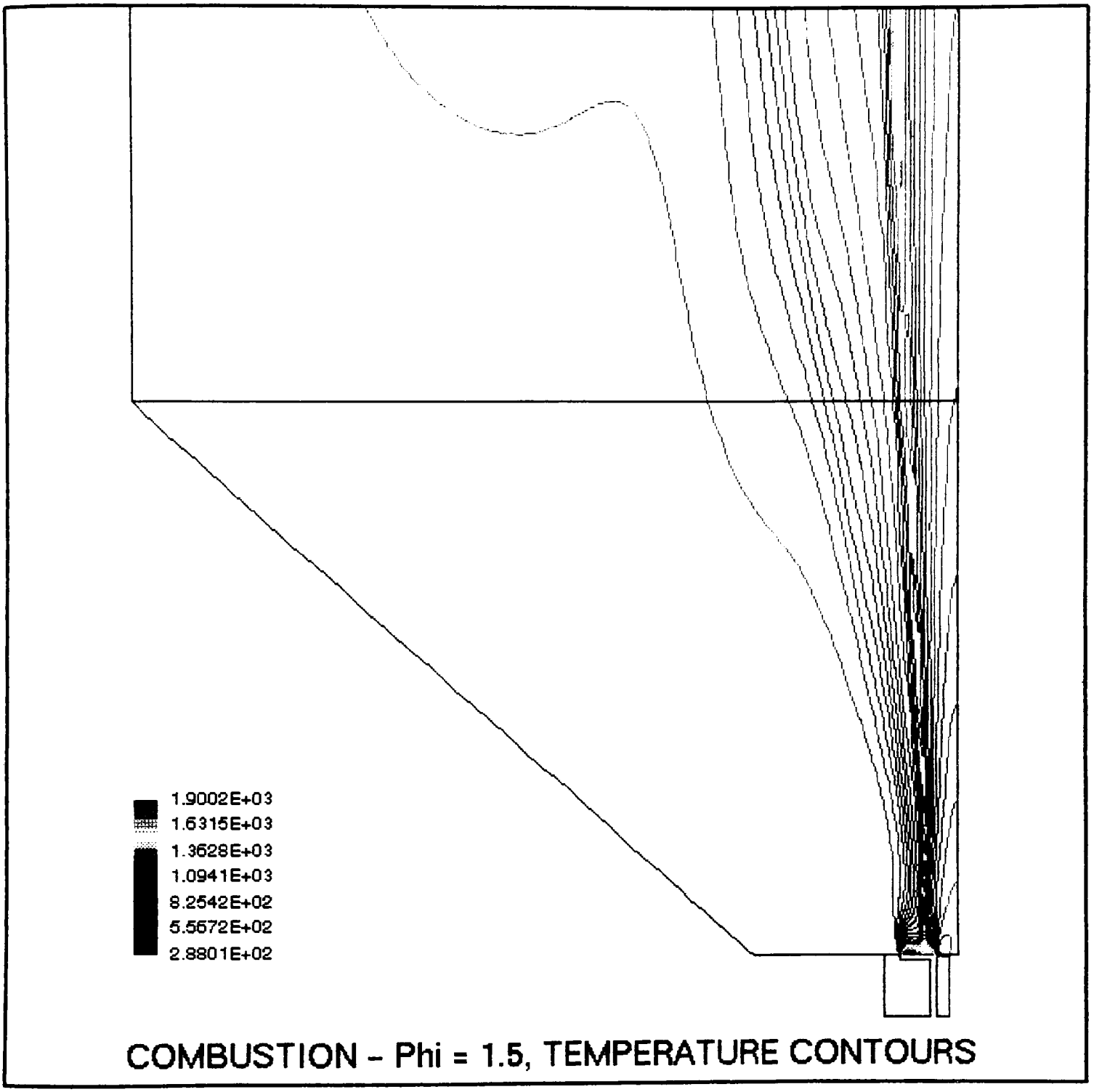

Figure 6.16 Combustion, Case Beta: Temperature Contours (K)

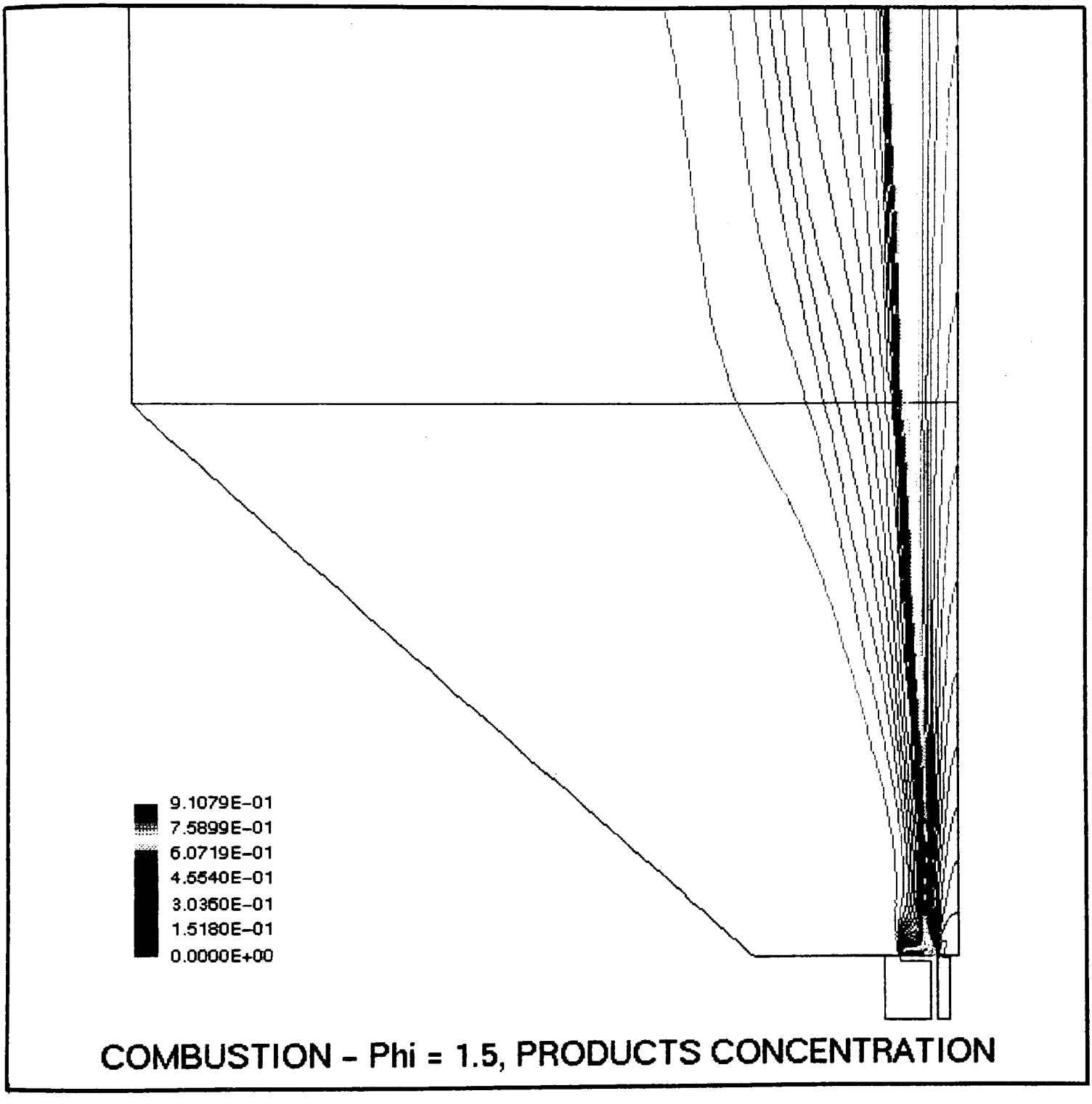

Figure 6.17 Combustion, Case Beta: Products Concentration Contours
(% Products by Mass)

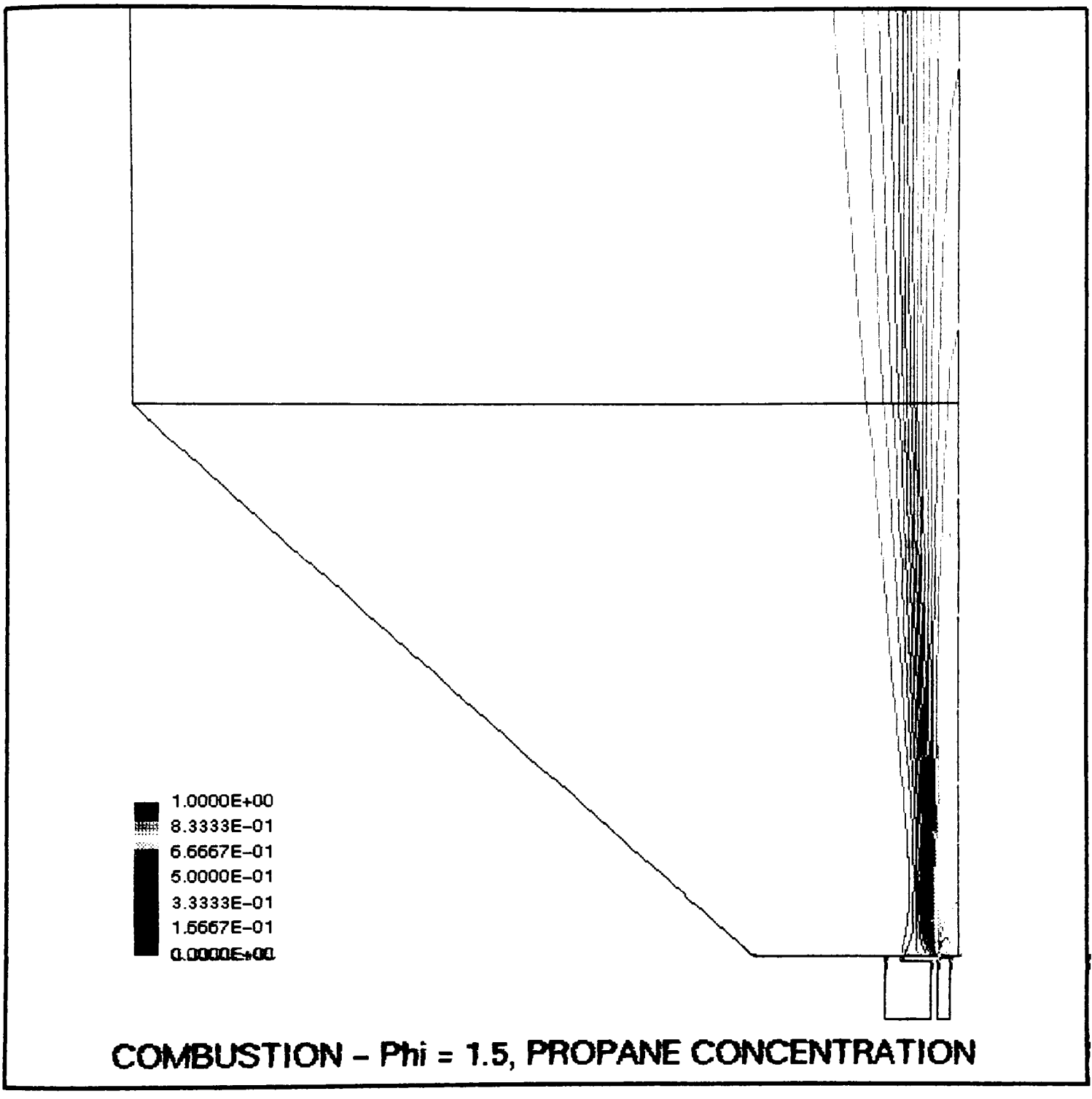

Figure 6.18 Combustion, Case Beta: Propane Concentration Contours
(% Propane by Mass)

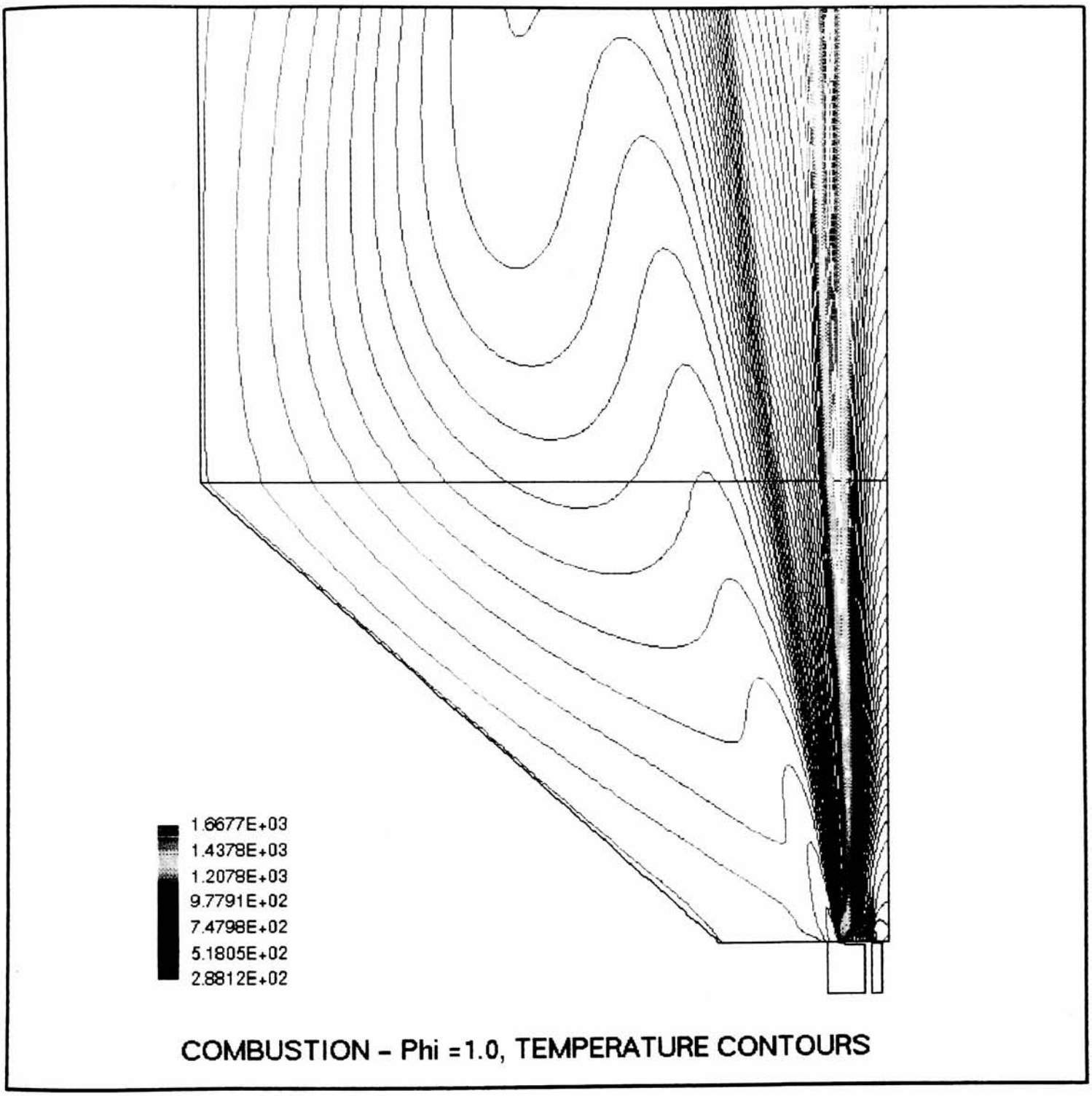

Figure 6.19 Combustion, Case Chi: Temperature Contours (K)

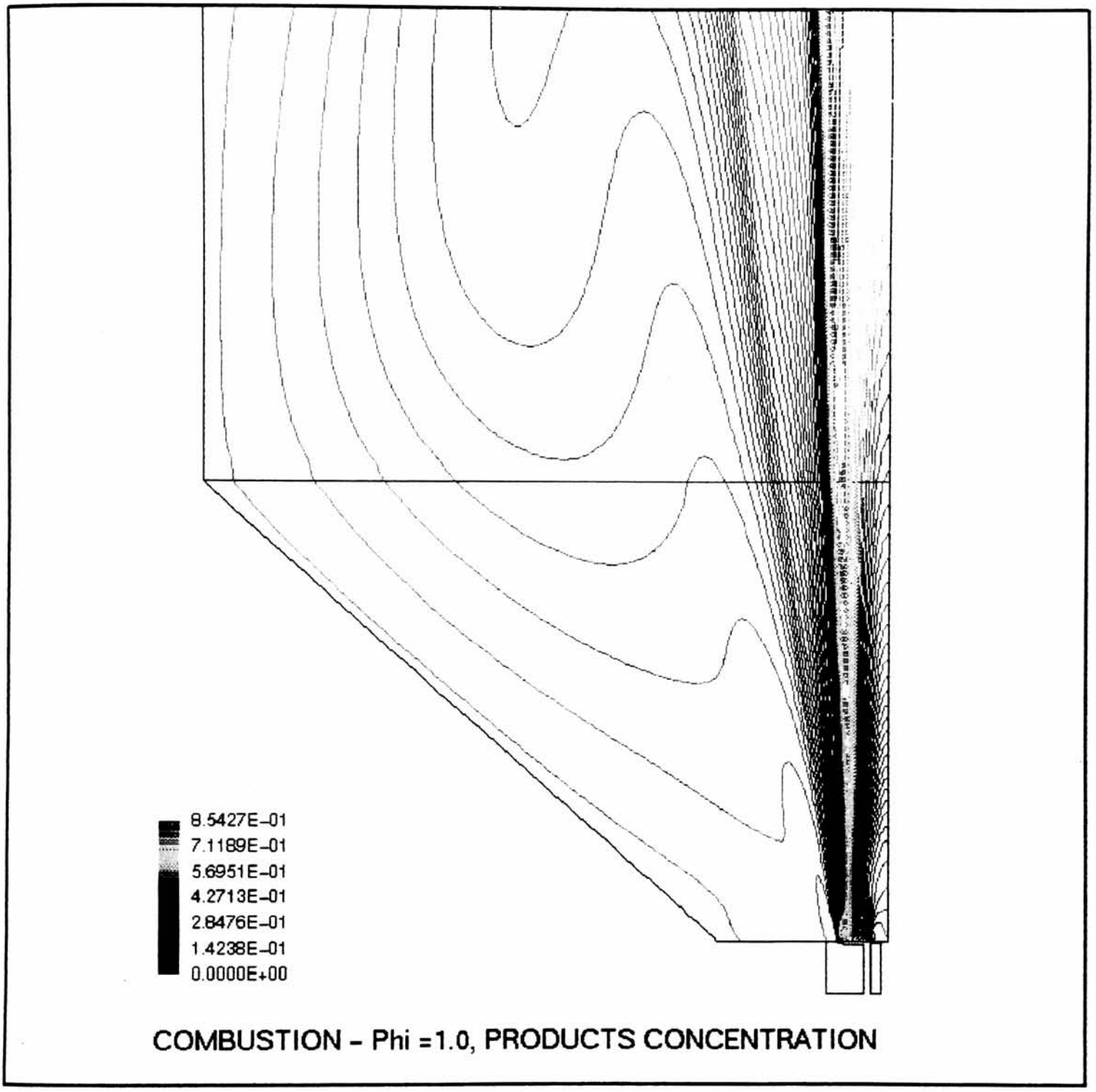

Figure 6.20 Combustion, Case Chi: Products Concentration Contours
(% Products by Mass)

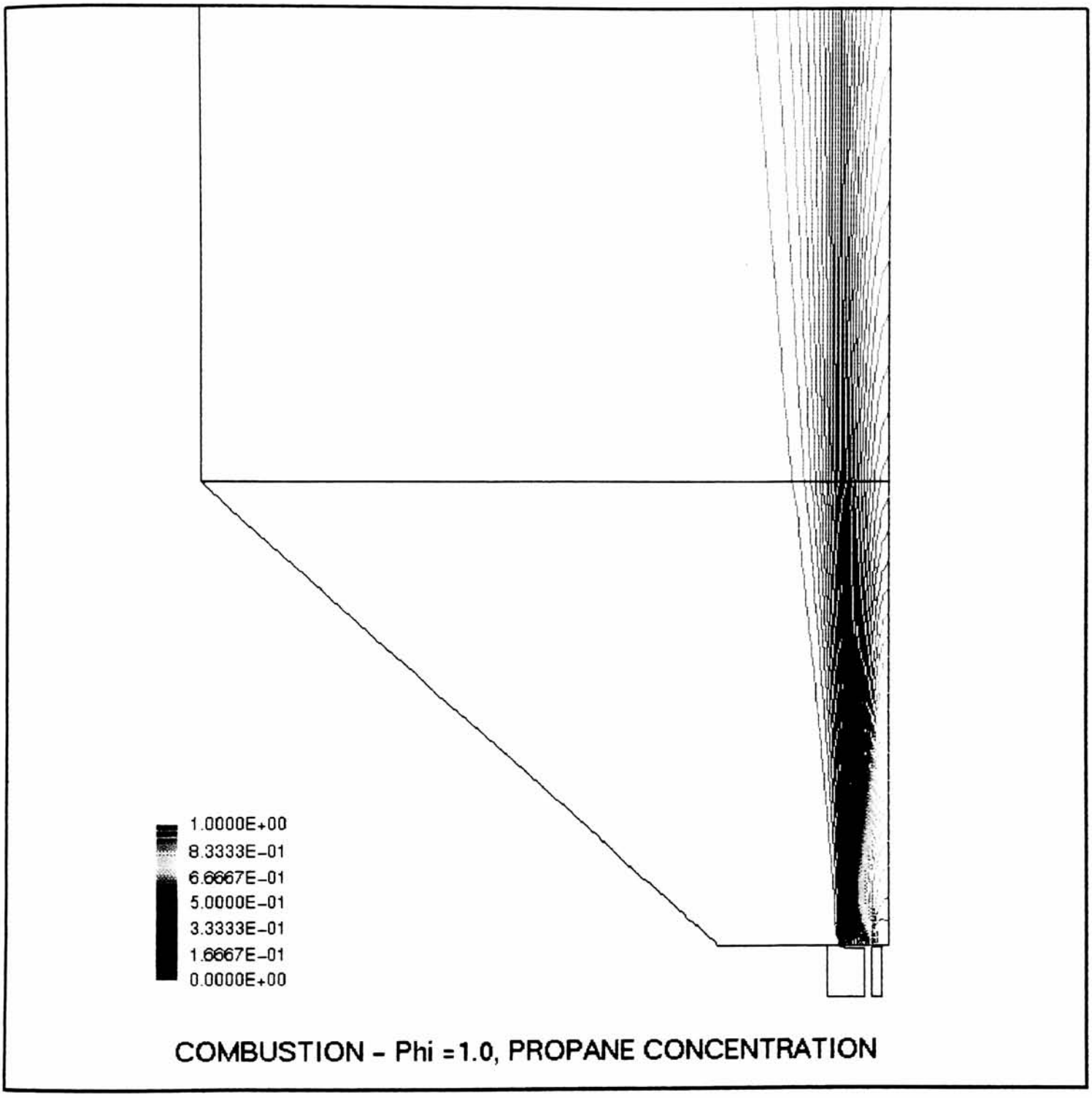

Figure 6.21 Combustion, Case Chi: Propane Concentration Contours
(% Propane by Mass)

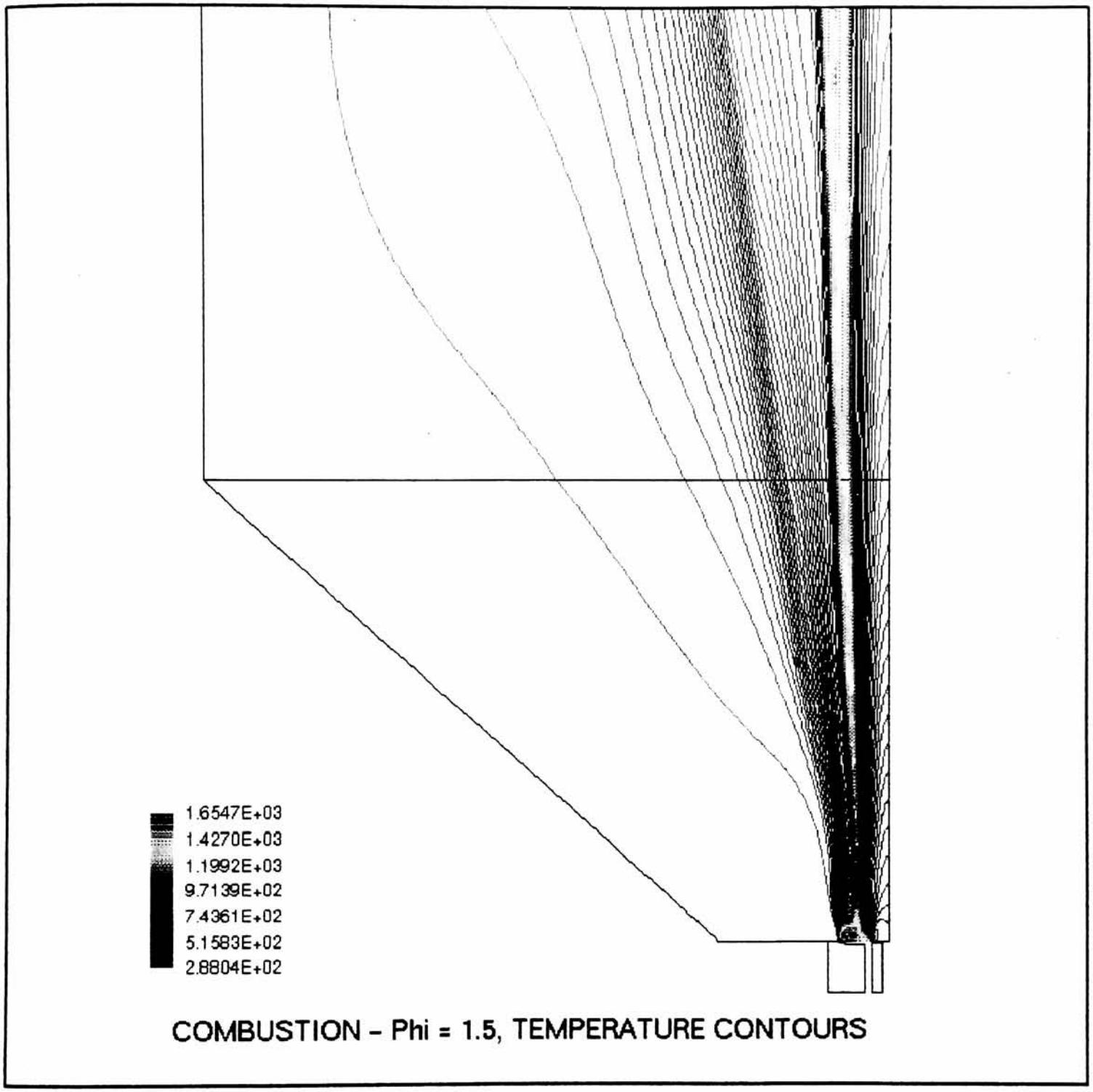

Figure 6.22 Combustion, Case Delta: Temperature Contours (K)

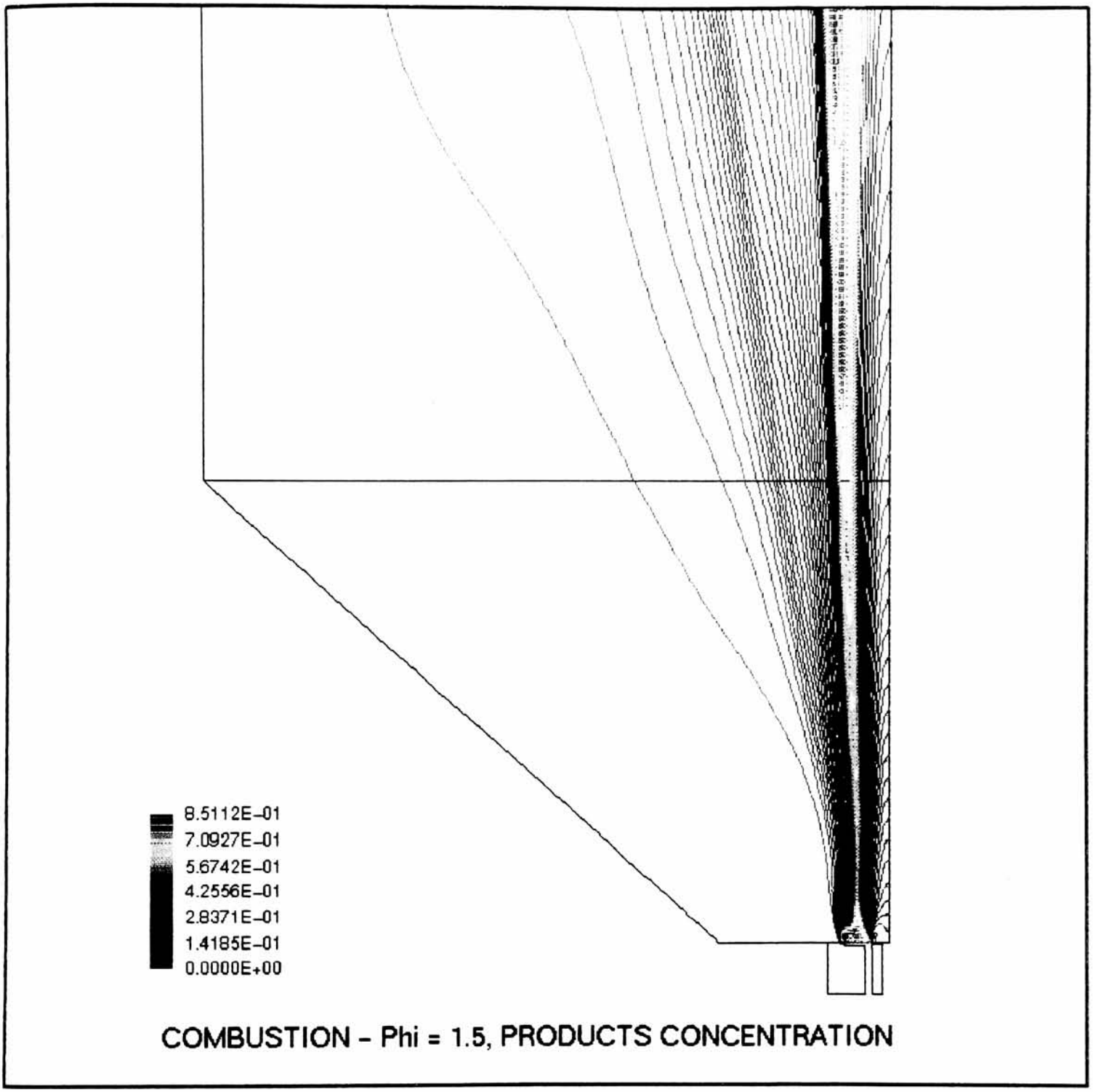

Figure 6.23 Combustion, Case Delta: Products Concentration Contours
(% Products by Mass)

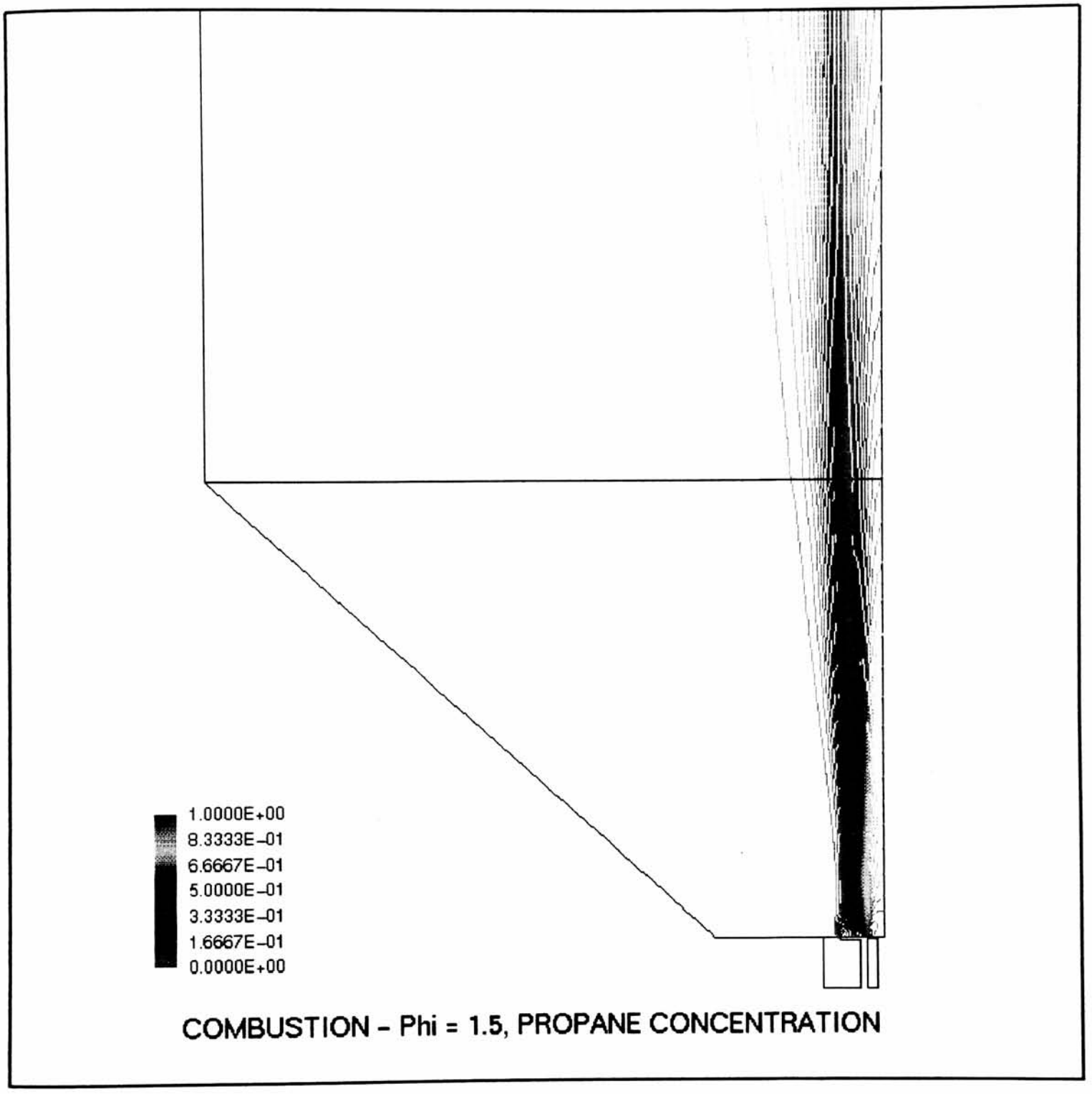

Figure 6.24 Combustion, Case Delta: Propane Concentration Contours
(% Propane by Mass)

Figures 6.16 and 6.17 show the temperature and propane concentration contour plots for case Beta. The overall shape and size of the flame is generally similar to that of the previous case, except at the base of the flame where the difference in the structure of the recirculation zones has the most effect. From these figures it can be seen that the reaction in the annular recirculation zone is very intense, with a much higher temperature and product concentration than in case Alpha. The temperature inside much of the annular zone is around 1400 K, though it increases to almost 1700 K right at the face of the annular disc. The flame is visibly pinched in the middle (much more so than the previous case) at about 2.0 cm from flameholder, and the classic shear region is clearly defined. The result of this is a thin flame envelope directly above the recirculation region, about 2.5 cm wide, that quickly plumes out to about 7.5 cm wide, a little more that the width in the previous case.

The effects of the central recirculation zone are very similar in this case to the previous case, even though its size has diminished considerably. It even appears to be slightly more effective, most likely due to its increase in strength. Figure 6.18, the propane concentration contour plot for case Beta, clearly shows that there are no areas of pure propane past the face of the flameholder. In fact there are even more combustion products brought into the central recirculation zone than in case Alpha. Thus, the central recirculation zone still serves to effectively preheat the fuel entering flame, even though it has diminished in size. The propane flows in a more condensed stream in this case though, as much more fuel penetrates through the recirculation zones to burn later in the flame,

due in part to the fuel rich nature of the operating conditions. This generally makes for a larger flame, as there is more fuel to burn off.

Cases Chi and Delta exhibited similar performance to Alpha and Beta, with only minor difference brought about by the change in the size of the blockage ratio for the annular obstruction. In both cases the flame size and shape were nearly identical, except that the shear region, and the characteristic pinching of the flame that it generally produces were visibly diminished.

Figures 6.19, 6.20 and 6.21 give the temperature, product concentration and propane concentration contours (respectively) for case Chi. For this case there almost does not seem to be a shear region at all, just a steadily increasing flame width. While the annular recirculation zone is still visible, most notably by the high temperature at the outskirts, there is no sharp transition as is normally expected. The temperature in the annular recirculation zone reaches as high as 1300 K, and the temperature of the flame envelope is generally between 1300 and 1400 K, but reaches a maximum at over 1650 K far downstream of the flameholder. There is significant preheating of the fuel due to the central recirculation zone, as in case Alpha, and it is of approximately the same magnitude.

Figures 6.22, 6.23 and 6.24 give the temperature, product concentration and propane concentration contours for case Delta. In this case there is a shear region, but it is not as clearly defined as in case Beta. The annular recirculation zone is a region of very intense reaction, the highest of the four cases, with temperatures as high as 1500 K. The temperature of flame envelope is generally between 1300 K and 1350 K, but it reaches a maximum temperature of about 1650 K, again far downstream of the flameholder. The

increase in the central jet strength has similar effect on the amount of preheating as it did in case Beta, producing a slight increase over case Chi.

Apparently, the increase in the annular blockage ratio of the flameholder has the effect of increasing the size of the annular recirculation zone, as was seen in the cold flow analysis. Which in turn lessens the pinching effect of the shear region. This increase in blockage ratio also seems to favorably effect the annular recirculation zone by allowing for a general increase in combustion in that region, which yields added flame stability, smaller effective flame size, and more efficient combustion.

With the computational analyses for the Double Concentric Bluff Body Flameholder completed, it now becomes necessary to validate the numerical model, in an effort to determine how accurate the model is, and whether or not it will perform as predicted.

7.0 EXPERIMENTAL ANALYSIS:

7.1 Experimental Setup:

The experimental test stand used in this investigation is shown in Figure 7.1. The test stand consists of the double concentric bluff body nozzle, the fuel line, the primary air line, the secondary air line and the thermocouple assembly (for measuring temperature).

The central fuel line is fed from dual high pressure propane tanks, and is regulated with a valve and flowmeter. The line feeds from the dual tanks to the stand through high pressure hose. The line feeds vertically through the stand to the nozzle, where it is injected into the atmosphere through an outlet of 10 mm outer diameter, and obstructed by a disc of 8 mm outer diameter(0.57 BR). Turbulators in the nozzle (a wire mesh) insure a moderate degree of turbulence, and the system is capable of supplying upwards of 0.0472 m^3/min. of propane. Figure 7.2 shows a close-up cross section of the nozzle configuration.

The primary air jet is fed by in-house compressed air lines, is regulated with a valve and flowmeter, and is capable of delivering up to 0.5663 m^3/min. of air. The air travels through high pressure black hose from the wall line to the stand, where it is fed into the nozzle concentric to the fuel jet. The outlet is of 36 mm outer diameter, and is obstructed by a disc of diameter D_O (where D_O equals 28.0 mm for 0.53 BR, or 26.0 mm for 0.44 BR). The test stand is also equipped with a secondary, unobstructed, air line concentric to the primary, capable of delivering another 0.7079 m^3/min. of air for secondary combustion burn off, but it was not used in the investigation.

A graduated traversing arm is employed to grasp the thermocouple probe, and is free to move in both the axial and radial directions, allowing temperature data to be taken in a 12 cm (horizontal) by 64 cm (vertical) field is and around the flame.. The thermocouple probe is a ceramic insulated R-type platinum - platinum/rhodium thermocouple, with a stainless steel sleeve of 1.6 mm outer diameter. It is critical that the outer diameter of the probe be as small as possible in order to cause as little disruption of the flame as possible. A thermocouple reader and display is used to monitor the temperature data, which was recorded manually.

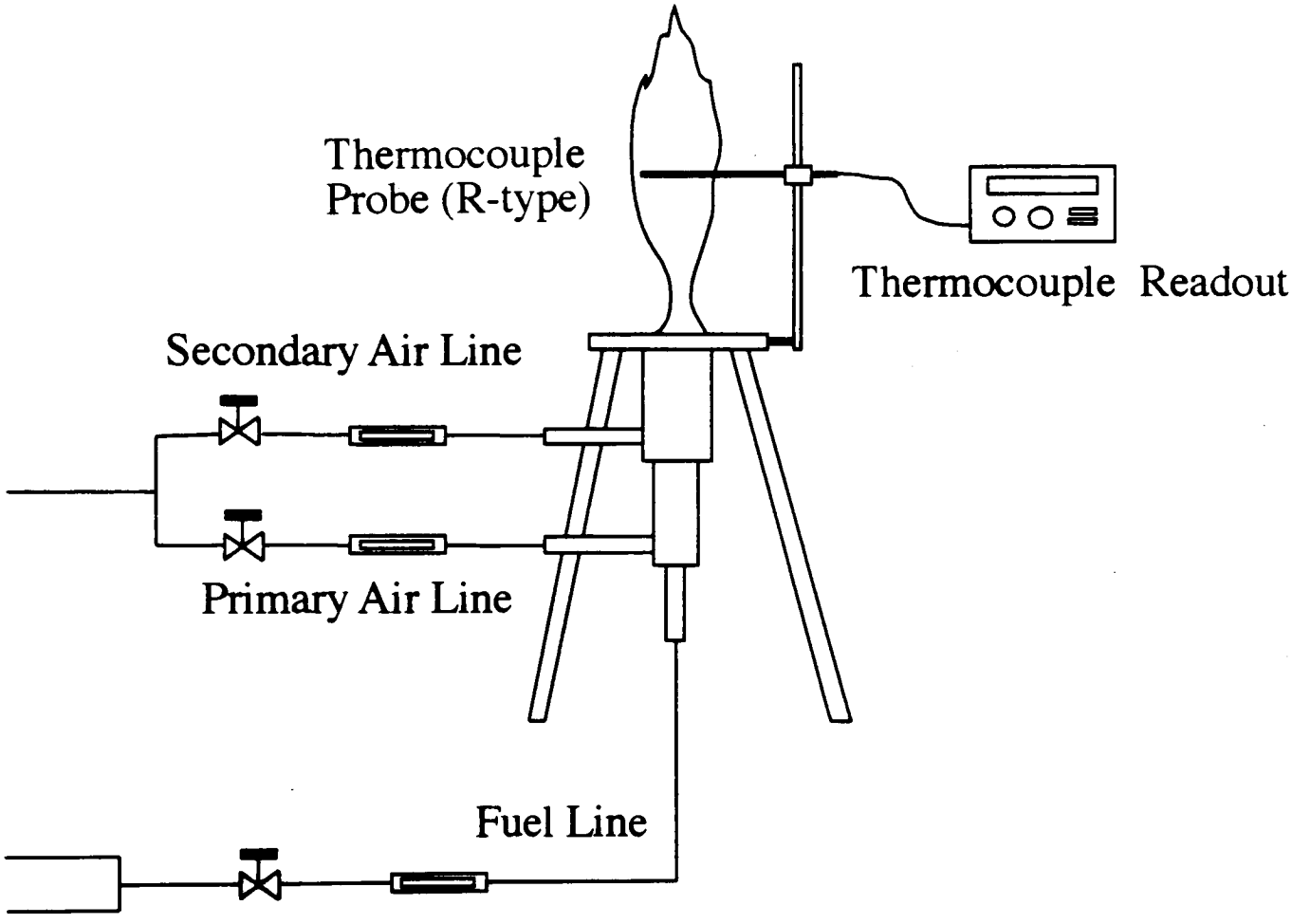

Figure 7.1 Double Concentric Bluff Body Burner Test Stand

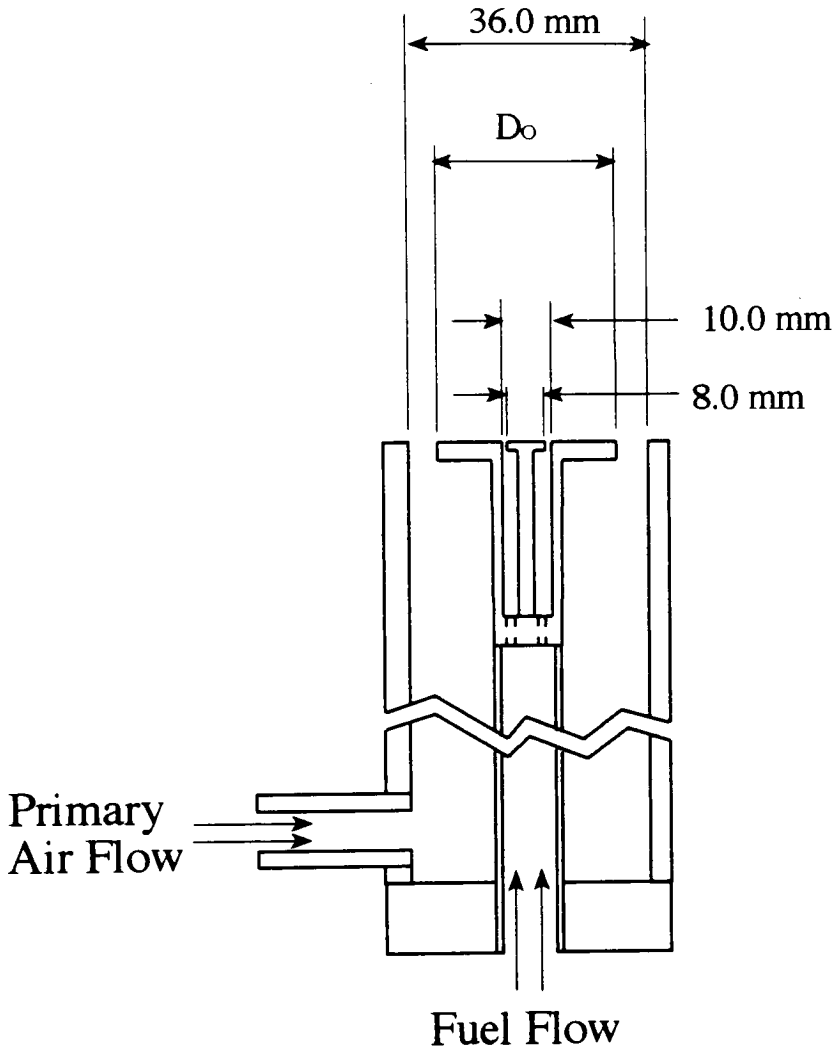

Figure 7.2 Double Bluff Body Nozzle Configuration

7.2 Experimental Procedure:

The experimental investigation was performed in order to obtain temperature data for the flame under operating conditions similar to those of the CFD analysis. Temperature data was collected in a two dimensional axisymmetric cross section of the flame.

As it stands in non-operational mode, the test stand is permanently connected to the in-house pressurized air lines, but not to the pressurized propane tanks. There are several steps that must be taken first to connect the system before combustion can be initiated and data collection can begin.

First the thermocouple probe must be inserted into the traversing arm and clamped down with a set screw. The connecting wire for the thermocouple must be attached to both the probe and the thermocouple readout. Both propane tanks must connected to the manifold by way of the left hand threaded ports. Once the propane tanks are secured and connected to the system, the valves on the tanks can be opened, but only with the flow regulation valve on the fuel line closed (else the system floods with propane). With both the propane line and the thermocouple connected into the system, the air lines are tested to insure that adequate flowrates of air can be supplied for testing.

With the system fully connected and operational, combustion can be initiated and data collection can begin. First the fuel regulation valve is cracked open, just enough to allow a flammable amount of propane through the nozzle. With propane passing through the nozzle, ignition is initiated with hand held lighter (remote gas grill type, four inch long barrel). With the valve cracked and no primary air flow, the flame is approximately 10 cm tall and laminar in appearance. The fuel regulation valve is then increased to the desired

flowrate of fuel, during which time the flame steadily grows in height and becomes turbulent. Once the fuel flowrate is set the primary air flowrate is increased to the desired amount with the air flow regulation valve (in all experimental cases the primary air flow was set at 0.1416 m^3/min). At this point the flameholder is fully operational with a turbulent and stable flame.

The thermocouple probe is then used to determine the temperature across the flowfield containing the flame. Discrete temperature data is taken at 10 mm intervals across the lower portion of the flame (30 mm wide by 350 mm tall), including the recirculation zone and the flame envelope. The temperature data is tabulated manually, along with notes and values for flame size, shape and level of stability. Once the required data is obtained, it is converted into a data file for MATLAB, and displayed as a contour plot using the MATLAB contour function. A sample data sheet is shown in Table 7.1. The experimental data for all four cases (Alpha through Delta) is given in Tables 7.4 through 7.7. The contour plots of the experimental data are given in Figures 7.3 and 7.4.

7.3 Experimental Results:

An experimental analysis was performed using the burner test stand in order to verify the combustion computational analysis for the double bluff body cases. The above stated experimental procedure was followed for all four cases, Alpha through Delta, and the results are shown in Figures 7.3 and 7.4. The temperature data is considered axisymmetric about the centerline of the flame, as in the CFD analysis, and is displayed as contour plots. Due to the turbulent nature of the flame, all of the temperature values were subject to fluctuation, some by as little as ±3 °C and some by as much as ±20 °C. Values were taken as close to the mean value for each temperature data point as was possible.

The flame for case Alpha was visibly stable, approximately 6.5 cm in diameter at the widest point, and approximately 86 cm in length. Both of these measurements showed slight transient fluctuations, but the flame held the same general shape throughout the testing. The recirculation zone was clearly visible, as a toroidal shaped region of intensely hot blue flame, directly above the face of the flameholder. The temperature data for this trial is given in Figure 7.3.

The flame looked very much as was predicted in the computational analysis. The annular recirculation zone was clearly visible, as was the shear region, where the flame envelope pinches in directly after the annular recirculation zone. The region of maximum temperature, in this case between 900° and 975° Celsius, coincides very closely with the region of maximum temperature in the CFD analysis. Both appear directly after the shear region, from about 10 cm downstream of the face onward, the actual region being about 4 cm in diameter and the computed region being about 3.5 cm in diameter. The first

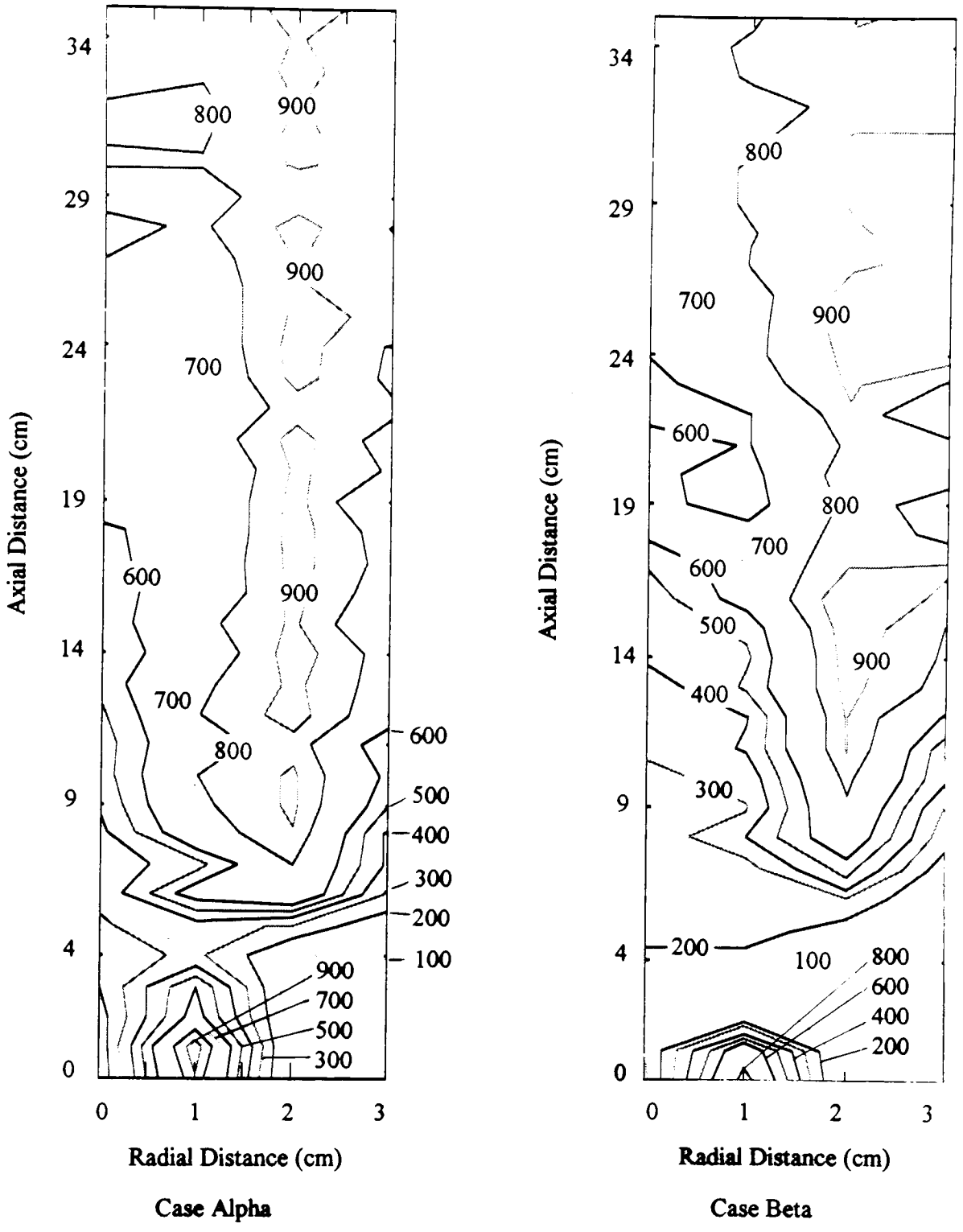

Figure 7.3 Experimental Results, Cases Alpha and Beta:
Temperature Contours (°C)

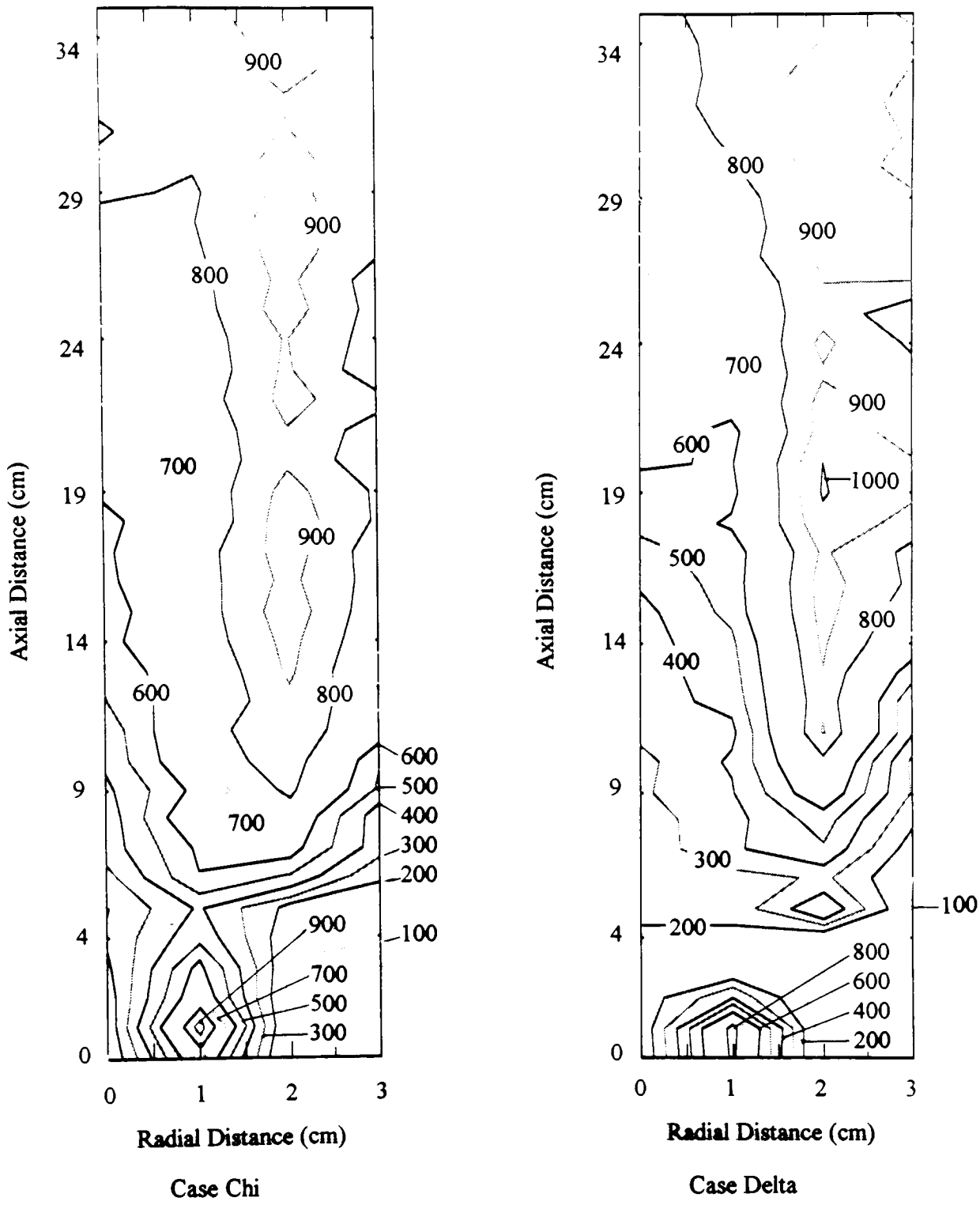

Figure 7.4 Experimental Results, Cases Chi and Delta:
Temperature Contours (°C)

significant shortcoming of the computational model also appears in this region, as it is seen that the CFD analysis predicts temperatures from 1025° to 1175° Celsius in this region, about 100° greater than the actual value.

The recirculation region itself also shows a good degree of correlation between the CFD model and the experimental testing. The computational analysis predicts the increased temperature inside the recirculation zone rather well, predicting a maximum temperature of about 950° Celsius, compared to the experimental value of about 900°. The effects of the annular recirculation zone are also similar to those predicted in the CFD analysis. The incoming fuel is preheated by the central zone, the temperature increasing by 135° Celsius in the first 4 cm past the face of the disc, very close to the effect predicted by the model. The temperature in the center of the flame is generally lower than the rest of the flame (for any constant axial distance) and increases fairly steadily into the flame envelope.

The flame for case Beta was also visibly stable, but showed several significant differences in structure when compared to case Alpha. The temperature contour plot for this case is given in Figure 7.3. The flame was still about 7.0 cm in diameter at the widest point, but the length increased to a full meter. The region of blue flame extended 7.5 cm downstream of the face (axial distance), and the effects of the recirculation zone are seen only 2 cm downstream, as opposed to a blue flame region of 5.5 cm, with the increased temperature effects of the recirculation zone extending 3.5 cm downstream for case Alpha. The increase in fuel jet momentum has diminished the size of the recirculation zone

and caused less mixing in this area, extending the region of blue flame and decreasing the amount of combustion, and hence the flame temperature.

The flame shape is emulated well by the CFD analysis; it shows much decreased recirculation zone, and a thinner neck in the flame, directly downstream of the recirculation zone. The area of maximum temperature starts 12 cm downstream, and is again between 900° and 975° Celsius, as compared to predicted values between 900° and 1100° for that region. The maximum flame temperature in the recirculation zone for this case is 800°, while the temperature from the CFD model is about 1100° in that area. This is the largest discrepancy found in the CFD analysis, and it would appear that the model overestimates the amount of combustion in the recirculation zone at the face of the flameholder, yielding a flame temperature much greater than the experimental value. The effect of the central recirculation zone is once again predicted with a good degree of accuracy. The diminished effects are seen as the fuel is only preheated 100° in the first 4 cm of the flame, as opposed to the 135° for case Alpha. Clearly, the larger the central recirculation zone, the greater the amount of preheating.

Another characteristic of the flame that the CFD analysis does not model satisfactorily, is the temperature of the flame at the shear region. The computational model predicts that a region of high temperature extends from the recirculation zone all the way up to the flame envelope, but this was not seen in the testing. While the recirculation zone is a region of intense reaction, there is a sharp drop in temperature after the zone (in the shear region), from about 2 cm to 5 cm axial distance, where the temperature of the flame is only between 100° and 300° Celsius.

The flames for cases Chi and Delta performed very similarly to those of Alpha and Beta, with some slight exceptions. The experimental temperature contours for the two cases are seen in Figure 7.4.

For case Chi, the flame had an overall length of about 92 cm, and was again 6.5 cm at it's full width. The temperature at the flame envelope fluctuated around 900° for the experimental, as compared to 1025° from the CFD analysis. The effects of the annular recirculation zone extend about 3 cm downstream (axial distance), with an experimental maximum temperature of 940° C, as compared to the predicted temperature of 1050° for the same area. The effects of the central recirculation zone are again clearly present, as the temperature of the fuel increases 120° in the first 4 cm downstream of the face.

For case Delta, the flame had an overall length of about 115 cm, and was a little over 7.0 cm at it full width, the physically largest flame of the four cases. The temperature at the flame envelope fluctuated around 950° for the experimental, and reached a maximum of 1008° C, as compared to 1100° from the CFD analysis. The effects of the annular recirculation zone are again diminished, extending only 1.5 cm downstream, with an experimental maximum temperature of 840° C, as compared to the predicted temperature of 1200° for the same area. as in case Beta, the CFD software appears to significantly over predict the temperature inside the annular recirculation zone. The effects of the central recirculation zone are still clearly present, but again diminished, as the temperature of the fuel increases 85° in the first 4 cm downstream of the face.

From the comparison between the experimental and computational analyses, it can be seen that the CFD code employed for the investigation predicts the flame shape and

recirculation characteristics fairly well, but appears to have difficulty predicting the flame temperature in certain areas, generally predicting 100° or so over, but sometimes far in excess of that. The major trends and effects of the flameholder are clearly present, and yield much insight into possible benefits of this configuration, but the degree of accuracy of the CFD models could use improvement.

Axial Distance (cm)					
	35				
	34				
	33				
	32				
	31				
	30				
	29				
	28				
	27				
	26				
	25				
	24				
	23				
	22				
	21				
	20				
	19				
	18				
	17				
	16				
	15				
	14				
	13				
	12				
	11				
	10				
	9				
	8				
	7				
	6				
	5				
	4				
	3				
	2				
	1				
	0				
		0	1	2	3

Radial Distance (cm)

Values are Temperature, degrees Celsius
Case:

Table 7.1 Sample Experimental Data Sheet

Axial Distance (cm)	0	1	2	3
35	830	835	930	865
34	855	850	905	820
33	885	815	925	833
32	800	785	905	815
31	795	795	925	815
30	805	805	915	845
29	765	775	835	855
28	825	785	935	795
27	800	745	905	835
26	750	715	915	805
25	694	705	925	805
24	675	690	945	880
23	725	670	935	785
22	655	665	855	775
21	640	715	940	825
20	625	635	920	735
19	655	650	940	785
18	585	650	945	615
17	565	685	935	735
16	550	768	925	755
15	525	765	915	725
14	530	685	950	645
13	542	775	920	745
12	480	795	945	740
11	455	740	865	695
10	450	800	915	498
9	420	775	920	570
8	370	725	891	375
7	340	455	795	385
6	320	671	760	275
5	288	368	275	125
4	243	325	95	105
3	200	600	45	45
2	165	655	55	35
1	115	975	30	32
0	105	885	31	32

Radial Distance (cm)

Values are Temperature, degrees Celsius
Case Alpha (Φ = 1.0, Br = 0.53)

Table 7.2 Experimental Data, Case Alpha

Axial Distance (cm)					
	35	757	790	905	885
	34	745	818	890	835
	33	720	815	895	875
	32	705	760	835	865
	31	720	775	910	905
	30	690	820	905	900
	29	665	825	905	925
	28	658	795	895	920
	27	655	805	885	935
	26	645	764	935	908
	25	625	770	940	900
	24	605	775	925	945
	23	550	735	915	785
	22	580	595	890	609
	21	630	595	820	865
	20	620	555	875	825
	19	635	540	840	755
	18	620	645	855	775
	17	515	675	895	915
	16	445	660	990	875
	15	430	525	965	795
	14	420	485	945	785
	13	341	515	930	755
	12	375	395	905	585
	11	320	410	910	430
	10	275	335	830	415
	9	281	295	780	295
	8	230	400	715	235
	7	227	260	540	130
	6	207	215	300	75
	5	225	260	130	65
	4	180	171	85	38
	3	140	115	34	35
	2	160	190	32	37
	1	105	720	29	32
	0	80	860	30	35
		0	1	2	3

Radial Distance (cm)

Values are Temperature, degrees Celsius
Case Beta (Φ = 1.5, Br = 0.53)

Table 7.3 Experimental Data, Case Beta

Axial Distance (cm)	0	1	2	3
35	830	865	960	830
34	845	835	945	845
33	845	850	920	865
32	812	820	895	858
31	795	825	905	830
30	805	812	930	845
29	818	788	925	845
28	765	795	960	832
27	780	780	945	815
26	735	765	925	755
25	685	748	948	765
24	715	735	905	760
23	700	720	915	735
22	710	735	932	832
21	620	715	895	748
20	628	715	880	730
19	615	708	935	785
18	575	685	960	785
17	580	748	947	740
16	573	750	925	755
15	545	735	958	730
14	568	727	930	715
13	525	688	915	685
12	495	695	880	720
11	435	745	895	667
10	425	713	868	515
9	375	635	825	480
8	340	725	715	335
7	340	618	640	345
6	263	595	485	215
5	195	415	165	135
4	215	475	125	115
3	180	635	88	55
2	155	715	55	33
1	135	947	48	28
0	95	725	30	29

Radial Distance (cm)

Values are Temperature, degrees Celsius
Case Chi (Φ = 1.0, Br = 0.44)

Table 7.4 Experimental Data, Case Chi

Axial Distance (cm)	0	1	2	3
35	765	840	915	896
34	774	815	905	905
33	740	828	945	895
32	735	840	950	876
31	690	825	968	890
30	705	790	940	877
29	700	735	935	905
28	695	730	908	942
27	715	745	915	920
26	660	690	900	895
25	655	685	878	715
24	638	648	920	785
23	680	650	890	835
22	630	635	935	850
21	665	565	940	875
20	615	589	1001	910
19	547	570	1008	915
18	520	615	965	865
17	475	535	915	775
16	420	540	940	780
15	365	530	935	735
14	354	478	912	680
13	350	460	896	538
12	348	435	875	430
11	335	375	910	415
10	270	415	785	275
9	285	390	695	285
8	255	365	546	225
7	238	385	485	140
6	240	245	320	98
5	215	235	495	85
4	185	165	115	33
3	195	115	60	32
2	140	385	33	34
1	112	845	34	31
0	100	830	31	30

Radial Distance (cm)

Values are Temperature, degrees Celsius
Case Delta ($\Phi = 1.5$, $Br = 0.44$)

Table 7.5 Experimental Data, Case Delta

8.0 CONCLUSIONS

1. The CFD package employed for the investigation was able to clearly recreate the effects of the characteristic regions of flow on the recirculation zone of a single bluff body obstruction, seen through the recreation of the work of Huang and Lin (1994).

2. The computational model for the single bluff body configuration was extended to include propane, and it was found that this configuration demonstrated poor mixing characteristics at all but the weakest prepenetration conditions. The propane tends to pierce through the recirculation zone in a jet column, yielding little fuel-oxidant mixing in the recirculation zone.

3. The double concentric bluff body flameholder was computationally modeled under cold flow conditions, and it was found that this configuration creates an additional recirculation zone (when compared to a single bluff body configuration), the central zone. The central zone causes an overall increase in the amount of mixing in the entire recirculation region.

4. The double concentric bluff body flameholder was computationally modeled under combustion conditions, and it was found that a stable flame is produced, with the effects of annular recirculation zone clearly present. Significant amounts of mixing and combustion takes place in the annular zone, resulting in very high temperature in that region. The effects of the central recirculation zone are also seen, as it serves to increase

the temperature of the incoming fuel, effectively preheating it, a potential increase in combustion efficiency.

5. An experimental analysis was performed on a double concentric bluff body flameholder under combustion conditions, in order to determine the validity of the computational models. The results of the experimental analysis showed a very stable flame for all cases, with a good degree of correlation between CFD and experimental for the size and shape of the flame, but only a fair correlation for temperature accuracy. The annular recirculation zone was clearly seen in the testing, and the beneficial effects of the central zone preheating are present in the results.

6. The double concentric bluff body configuration clearly shows potential benefits for operation in a combustion chamber. It demonstrates all the benefits of the classical annular recirculation zone, with added benefits from a central recirculation zone unique to this configuration. Benefits to flame stability are present due to the nature of the flameholder to decrease axial momentum of the inlet jets (for both fuel and air), and benefits to combustion efficiency are present in the effects of increased mixing and fuel preheating.

REFERENCES:

Huang, R.F. and C.L. Lin, 1994 "Visualized Flow Patterns of Double Concentric Jets at Low Annulus Velocities", AIAA Journal Vol. 32, No. 9, pp. 1868-1874

Isaac, J.J., M.S. Chidananda, and K. Shridhara, 1976, "Oil Flow Visualization Studies of the Characteristics of Flow around Bluff Body Flameholders," National Aeronautical Laboratory, TM-PR-202/2-76, Bangalore

Lefebvre, A.H., 1983, "Gas Turbine Combustion," Hemisphere Publishing Corporation, New York

Li, X. and R.S. Tankin, 1987, "A Study of Cold and Combusting Flows Around Bluff-Body Combustors," Combustion Science and Technology, Vol. 52, pp.173-206

Nikjooy, M., R.M.C. So, and R.E. Peck, 1988 "Modelling of Jet- and Swirl Stabilized Reacting Flows in Axisymmetric Combustors," Combustion Science and Technology, Vol. 58, pp. 135-153

Pan, J.C., W.J Schmoll and D.R. Ballal, 1992, "Turbulent Combustion Properties Behind a Confined Conical Stabilizer," Journal of Engineering for Gas Turbines and Power, Vol. 114, pp. 33-38

Shefer, R.W., M. Namazian. and J. Kelly, 1994, "Velocity Measurements in Turbulent Bluff-Body Stabilized Flows," AIAA Journal, Vol. 32, No. 9, pp. 1844-1851

Shefer, R.W., M. Namazian. and J. Kelly, 1989, "Comparison of Turbulent-Jet and Bluff-Body Stabilized Flames," Combustion Science and Technology, Vol. 67, pp. 123-146

APPENDIX A: CFDS-Flow3D Command Files

Appendix A-1: Sample Command File for Single Bluff Body Analysis

```
>> FLOW3D
  >> SET LIMITS
    TOTAL INTEGER WORK SPACE 10000000
    TOTAL REAL WORK SPACE 10000000
    END

  >> OPTIONS
    TWO DIMENSIONS
    TURBULENT FLOW
    HEAT TRANSFER
    COMPRESSIBLE FLOW
    MASS FRACTION EQUATIONS 1
    END

>> MODEL TOPOLOGY
  >> INPUT TOPOLOGY
    READ GEOMETRY FILE
    END

  >> CREATE PATCH
    PATCH NAME '#1'
    PATCH TYPE 'SOLID'
    BLOCK NAME 'BLOCK-NUMBER-1'
    PATCH LOCATION 1 15 1 15 1 1
    END

  >> CREATE PATCH
    PATCH NAME '#2'
    PATCH TYPE 'SOLID'
    BLOCK NAME 'BLOCK-NUMBER-1'
    PATCH LOCATION 27 28 1 14 1 1
    END

  >> CREATE PATCH
    PATCH NAME '#3'
    PATCH TYPE 'SOLID'
    BLOCK NAME 'BLOCK-NUMBER-1'
    PATCH LOCATION 21 28 15 15 1 1
    END

  >> CREATE PATCH
    PATCH NAME '#4'
    PATCH TYPE 'SOLID'
    BLOCK NAME 'BLOCK-NUMBER-1'
    PATCH LOCATION 33 40 15 15 1 1
    END

  >> CREATE PATCH
    PATCH NAME '#5'
    PATCH TYPE 'SOLID'
    BLOCK NAME 'BLOCK-NUMBER-1'
```

```
  PATCH LOCATION 33 34 1 14 1 1
  END

>> CREATE PATCH
  PATCH NAME '#6'
  PATCH TYPE 'SOLID'
  BLOCK NAME 'BLOCK-NUMBER-1'
  PATCH LOCATION 46 60 1 15 1 1
  END

>> CREATE PATCH
  PATCH NAME 'PRIMARY-L'
  PATCH TYPE 'INLET'
  BLOCK NAME 'BLOCK-NUMBER-1'
  PATCH LOCATION 16 26 1 1 1 1
  LOW J
  END

>> CREATE PATCH
  PATCH NAME 'PRIMARY-R'
  PATCH TYPE 'INLET'
  BLOCK NAME 'BLOCK-NUMBER-1'
  PATCH LOCATION 35 45 1 1 1 1
  LOW J
  END

>> CREATE PATCH
  PATCH NAME 'CENTRAL'
  PATCH TYPE 'INLET'
  BLOCK NAME 'BLOCK-NUMBER-1'
  PATCH LOCATION 29 32 1 1 1 1
  LOW J
  END

>> CREATE PATCH
  PATCH NAME 'LEFT-WALL'
  PATCH TYPE 'PRESSURE BOUNDARY'
  BLOCK NAME 'BLOCK-NUMBER-1'
  PATCH LOCATION 1 1 16 100 1 1
  LOW I
  END

>> CREATE PATCH
  PATCH NAME 'RIGHT-WALL'
  PATCH TYPE 'PRESSURE BOUNDARY'
  BLOCK NAME 'BLOCK-NUMBER-1'
  PATCH LOCATION 60 60 16 100 1 1
  HIGH I
  END

>> CREATE PATCH
  PATCH NAME 'TOP'
  PATCH TYPE 'MASS FLOW BOUNDARY'
  BLOCK NAME 'BLOCK-NUMBER-1'
```

```
    HIGH J
    END

>> MODEL DATA
 >> PHYSICAL PROPERTIES
  >> FLUID PARAMETERS
    PHASE NAME 'FUEL'
    VISCOSITY 0.0001072
    DENSITY 2.0
    END

  >> STANDARD FLUID
    FLUID 'AIR'
    STANDARD FLUID REFERENCE TEMPERATURE 293.0
    END

  >> MASS TRANSFER PARAMETERS
    >> MOLECULAR WEIGHTS
      MASS FRACTION1 44.10
      END

    >> DIFFUSIVITIES
      MASS FRACTION1 0.000015
      END

    >> SPECIFIC HEATS
      MASS FRACTION1 1600
      END

 >> AMBIENT VARIABLES
    MASS FRACTION1 0.0
    END

>> SOLVER DATA
  >> PROGRAM CONTROL
    MAXIMUM NUMBER OF ITERATIONS 200
    END

>> CREATE GRID
  >> INPUT GRID
    READ GRID FILE
    END

>> MODEL BOUNDARY CONDITIONS

  >> SET VARIABLES
    PATCH NAME 'CENTRAL'
    MASS FRACTION1 1.0
    V VELOCITY 1.28
    K 0.00329
    EPSILON 0.184992
    TEMPERATURE 293.0
    END
```

```
>> SET VARIABLES
  PATCH NAME 'PRIMARY-L'
  MASS FRACTION1 0.0
  V VELOCITY 0.75
  TEMPERATURE 293.0
  END

>> SET VARIABLES
  PATCH NAME 'PRIMARY-R'
  MASS FRACTION1 0.0
  V VELOCITY 0.75
  TEMPERATURE 293.0
  END

>> SET VARIABLES
  PATCH NAME 'LEFT-WALL'
  PRESSURE 000.0
  END

>> SET VARIABLES
  PATCH NAME 'RIGHT-WALL'
  PRESSURE 000.0
  END

>> STOP
```

Appendix A-2: Sample Command File for Double Bluff Body Cold Flow Analysis

```
>> FLOW3D
  >> SET LIMITS
    TOTAL INTEGER WORK SPACE 10000000
    TOTAL REAL WORK SPACE 10000000
    END

  >> OPTIONS
    TWO DIMENSIONS
    TURBULENT FLOW
    HEAT TRANSFER
    COMPRESSIBLE FLOW
    MASS FRACTION EQUATIONS 1
    END

>> MODEL TOPOLOGY
  >> INPUT TOPOLOGY
    READ GEOMETRY FILE
    END

  >> CREATE PATCH
    PATCH NAME '#1'
    PATCH TYPE 'SOLID'
    BLOCK NAME 'BLOCK-NUMBER-1'
    PATCH LOCATION 1 24 1 30 1 1
    END

  >> CREATE PATCH
    PATCH NAME '#2'
    PATCH TYPE 'SOLID'
    BLOCK NAME 'BLOCK-NUMBER-1'
    PATCH LOCATION 47 50 1 28 1 1
    END

  >> CREATE PATCH
    PATCH NAME '#3'
    PATCH TYPE 'SOLID'
    BLOCK NAME 'BLOCK-NUMBER-1'
    PATCH LOCATION 33 50 29 30 1 1
    END

  >> CREATE PATCH
    PATCH NAME '#4'
    PATCH TYPE 'SOLID'
    BLOCK NAME 'BLOCK-NUMBER-1'
    PATCH LOCATION 57 60 1 29 1 1
    END

  >> CREATE PATCH
    PATCH NAME '#5'
    PATCH TYPE 'SOLID'
    BLOCK NAME 'BLOCK-NUMBER-1'
```

```
    PATCH LOCATION 53 60 30 30 1 1
    END

  >> CREATE PATCH
    PATCH NAME 'PRIMARY'
    PATCH TYPE 'INLET'
    BLOCK NAME 'BLOCK-NUMBER-1'
    PATCH LOCATION 25 46 1 1 1 1
    LOW J
    END

  >> CREATE PATCH
    PATCH NAME 'CENTRAL'
    PATCH TYPE 'INLET'
    BLOCK NAME 'BLOCK-NUMBER-1'
    PATCH LOCATION 51 56 1 1 1 1
    LOW J
    END

  >> CREATE PATCH
    PATCH NAME 'LEFT-WALL'
    PATCH TYPE 'PRESSURE BOUNDARY'
    BLOCK NAME 'BLOCK-NUMBER-1'
    PATCH LOCATION 1 1 31 200 1 1
    LOW I
    END

  >> CREATE PATCH
    PATCH NAME 'RIGHT-WALL'
    PATCH TYPE 'SYMMETRY PLANE'
    BLOCK NAME 'BLOCK-NUMBER-1'
    PATCH LOCATION 60 60 31 200 1 1
    HIGH I
    END

  >> CREATE PATCH
    PATCH NAME 'TOP'
    PATCH TYPE 'MASS FLOW BOUNDARY'
    BLOCK NAME 'BLOCK-NUMBER-1'
    HIGH J
    END

>> MODEL DATA
 >> PHYSICAL PROPERTIES
  >> FLUID PARAMETERS
    PHASE NAME 'FUEL'
    VISCOSITY 0.0001072
    DENSITY 2.0
    END

  >> STANDARD FLUID
    FLUID 'AIR'
    STANDARD FLUID REFERENCE TEMPERATURE 293.0
    END
```

```
>> MASS TRANSFER PARAMETERS
  >> MOLECULAR WEIGHTS
    MASS FRACTION1 44.10
    END

  >> DIFFUSIVITIES
    MASS FRACTION1 0.000015
    END

  >> SPECIFIC HEATS
    MASS FRACTION1 1600
    END

>> AMBIENT VARIABLES
  MASS FRACTION1 0.0
  END

>> SOLVER DATA
  >> PROGRAM CONTROL
  MAXIMUM NUMBER OF ITERATIONS 200
  END

>> CREATE GRID
  >> INPUT GRID
  READ GRID FILE
  END

>> MODEL BOUNDARY CONDITIONS

  >> SET VARIABLES
  PATCH NAME 'CENTRAL'
  MASS FRACTION1 1.0
  V VELOCITY 2.282
  K 0.0149
  EPSILON 0.217
  TEMPERATURE 293.0
  END

  >> SET VARIABLES
  PATCH NAME 'PRIMARY'
  MASS FRACTION1 0.0
  V VELOCITY 2.732
  TEMPERATURE 293.0
  END

  >> SET VARIABLES
  PATCH NAME 'LEFT-WALL'
  PRESSURE 000.0
  END

>> STOP
```

Appendix A-3: Sample Command File for Double Bluff Body Combustion Analysis

```
>> FLOW3D
  >> SET LIMITS
    TOTAL INTEGER WORK SPACE 6000000
    TOTAL REAL WORK SPACE 7000000
    END

  >> OPTIONS
    TWO DIMENSIONS
    TURBULENT FLOW
    HEAT TRANSFER
    STEADY STATE
    COMPRESSIBLE FLOW
    BUOYANT FLOW
    MIXED IS BURNT COMBUSTION MODEL
    DOUBLE DELTA FUNCTION
    END

>> MODEL TOPOLOGY
  >> INPUT TOPOLOGY
    READ GEOMETRY FILE
    END

  >> CREATE PATCH
    PATCH NAME '#1'
    PATCH TYPE 'SOLID'
    BLOCK NAME 'BLOCK-NUMBER-1'
    PATCH LOCATION 87 90 1 28 1 1
    END

  >> CREATE PATCH
    PATCH NAME '#2'
    PATCH TYPE 'SOLID'
    BLOCK NAME 'BLOCK-NUMBER-1'
    PATCH LOCATION 73 90 29 30 1 1
    END

  >> CREATE PATCH
    PATCH NAME '#3'
    PATCH TYPE 'SOLID'
    BLOCK NAME 'BLOCK-NUMBER-1'
    PATCH LOCATION 97 100 1 29 1 1
    END

  >> CREATE PATCH
    PATCH NAME '#4'
    PATCH TYPE 'SOLID'
    BLOCK NAME 'BLOCK-NUMBER-1'
    PATCH LOCATION 93 100 30 30 1 1
    END

  >> CREATE PATCH
```

```
  PATCH NAME '#5'
  PATCH TYPE 'SOLID'
  BLOCK NAME 'BLOCK-NUMBER-1'
  PATCH LOCATION 1 64 1 30 1 1
  END

>> CREATE PATCH
  PATCH NAME 'WALL-1'
  PATCH TYPE 'WALL'
  BLOCK NAME 'BLOCK-NUMBER-2'
  PATCH LOCATION 73 90 1 1 1 1
  LOW J
  END

>> CREATE PATCH
  PATCH NAME 'PRIMARY'
  PATCH TYPE 'INLET'
  BLOCK NAME 'BLOCK-NUMBER-1'
  PATCH LOCATION 65 86 1 1 1 1
  LOW J
  END

>> CREATE PATCH
  PATCH NAME 'GAS'
  PATCH TYPE 'INLET'
  BLOCK NAME 'BLOCK-NUMBER-1'
  PATCH LOCATION 91 96 1 1 1 1
  LOW J
  END

>> CREATE PATCH
  PATCH NAME 'PRESSURE'
  PATCH TYPE 'INLET'
  BLOCK NAME 'BLOCK-NUMBER-2'
  LOW I
  END

>> CREATE PATCH
  PATCH NAME 'PRESSURE'
  PATCH TYPE 'INLET'
  BLOCK NAME 'BLOCK-NUMBER-3'
  LOW I
  END

>> CREATE PATCH
  PATCH NAME 'TOP'
  PATCH TYPE 'MASS FLOW BOUNDARY'
  BLOCK NAME 'BLOCK-NUMBER-3'
  HIGH J
  END

>> CREATE PATCH
  PATCH NAME 'SYMM-2'
  PATCH TYPE 'SYMMETRY PLANE'
```

```
    BLOCK NAME 'BLOCK-NUMBER-2'
    HIGH I
    END

  >> CREATE PATCH
    PATCH NAME 'SYMM-3'
    PATCH TYPE 'SYMMETRY PLANE'
    BLOCK NAME 'BLOCK-NUMBER-3'
    HIGH I
    END

>> MODEL DATA
  >> PHYSICAL PROPERTIES
    >> FLUID PARAMETERS
      VISCOSITY 1.81E-5
      END

    >> HEAT TRANSFER PARAMETERS
      COMBUSTION THERMAL DIFFUSIVITY 2.5857E-5
      END

    >> BUOYANCY PARAMETERS
      GRAVITY VECTOR 0.0 -9.81 0.0
      END

    >> COMBUSTION PARAMETERS
      >> MIXED IS BURNT
        >> MASS FRACTIONS OF FUEL
          METHANE 0.0
          ETHANE 0.0
          PROPANE 1.0
          BUTANE 0.0
          CARBON MONOXIDE 0.0
          CARBON DIOXIDE 0.0
          HYDROGEN 0.0
          END

        >> MASS FRACTION OF OXIDANT
          OXYGEN 0.22
          END

>> SOLVER DATA
  >> PROGRAM CONTROL
    MAXIMUM NUMBER OF ITERATIONS 400
    END

  >> DEFERRED CORRECTION
    EPSILON START 0
    EPSILON END 350
    K START 0
    EPSILON END 350
    END

>> CREATE GRID
```

```
  >> INPUT GRID
    READ GRID FILE
    END

>> MODEL BOUNDARY CONDITIONS
  >> SET VARIABLES
    PATCH NAME 'PRIMARY'
    V VELOCITY 2.732
    K 0.0149
    EPSILON .217
    TEMPERATURE 293.0
    COMBUSTION SCALAR1 0.0
    COMBUSTION SCALAR2 0.0
    END

  >> SET VARIABLES
    PATCH NAME 'GAS'
    V VELOCITY 2.282
    TEMPERATURE 293.0
    COMBUSTION SCALAR1 1.0
    COMBUSTION SCALAR2 0.0
    END

  >> SET VARIABLES
    PATCH NAME 'PRESSURE'
    U VELOCITY 0.001
    TEMPERATURE 293.0
    COMBUSTION SCALAR1 0.0
    COMBUSTION SCALAR2 0.0
    END

>>STOP
```

APPENDIX B: Sample CFD Output File (Edited to Contain Only Temperature Data)

```
CFDS-FLOW3D 3.3 started on Sat Mar 11 15:25:57 EST 1995

This job was run on : spawn
The command line was: /export/home/CFDS_dir/scripts/SUN/runf3d -rel 3.3 -dir /export/home/spawn/peter/cfds/combustx .f3d_tmpdir -enviro 33
c m33.fc -geom m05.geo

PERMANENT WORKSPACE ALLOCATED
  TYPE     TOTAL SET  TOTAL USED  REMAINING
 REAL       7000000    2819535    4180465
 INTEGER    6000000    1363011    4636989
 CHARACTER     1000        528        472

 FRONTEND MODULE ENTERED

 CONSTRUCTING INTEGER LISTS

COMMENCING TO COMPUTE TOPOLOGY STACK

 - FRONTEND CHECKING OF WALLS     -

 - END OF CHECKING, NO ERRORS FOUND -
   2-DIMENSIONAL SINGLE-PHASE FLOW PREDICTION USING CFDS-FLOW3D

FLOW OPTIONS
    TURBULENT FLOW
    STEADY STATE
    COMPRESSIBLE FLOW
    ADDITIONAL HEAT EQUATION
    DEGREE OF POLYNOMIAL DEPENDENCE ON T =   3
    NO. OF MASS FRACTION EQUATIONS    =   3
    NO. OF COMBUSTION SCALARS         =   2
    BUOYANT FLOW, GRAVITY VECTOR =    0.000E+00  -9.810E+00   0.000E+00
          BUOYANCY REFERENCE DENSITY  =  1.185E+00

  FLUID FLOW PROPERTIES
    UNIVERSAL GAS CONSTANT  =  8.314E+03
    REFERENCE PRESSURE          =  1.013E+05
    REFERENCE TEMPERATURE       =  2.880E+02
    MINIMUM CFDS-FLOW3D PRESSURE  = -9.117E+04
    MINIMUM TEMPERATURE         =  1.000E+02
    WEAKLY COMPRESSIBLE FLOW
    LAMINAR VISCOSITY =  1.810E-05   SET BY >> FLUID PARAMETERS

  HEAT AND MASS TRANSFER PROPERTIES
    THERMALLY PERFECT FLUID
    COMBUSTION THERMAL DIFFUSIVITY  =  2.586E-05
    DIFFUSIVITY OF COMBUSTION SCALAR1       2.586E-05
    DIFFUSIVITY OF COMBUSTION SCALAR2       2.586E-05

  TURBULENCE PROPERTIES
    TURBULENCE MODEL DETAILS
    MODEL = STANDARD K-EPSILON

    TURBULENT PRANDTL NUMBERS AND LOG LAYER CONSTANTS

    VARIABLE                PRT      ELOG     XYPLUS
    ____________            ___      ____     ______
    VELOCITY                1.000E+00  9.793E+00  1.123E+01
    ENTHALPY                9.000E-01  3.446E+00  1.123E+01
    COMBUSTION SCALAR1        9.000E-01  3.446E+00  1.123E+01
    COMBUSTION SCALAR2        9.000E-01  3.446E+00  1.123E+01
    K                  1.000E+00
    EPSILON                1.217E+00
    MODEL PARAMETERS
      C1   =  1.440   C2   =  1.920   C3   =  0.000
      CMU  =  0.090   CAPPA =  0.419

 COMBUSTION PROPERTIES
   GASEOUS COMBUSTION MODEL
   MIXED-IS-BURNT: DOUBLE DELTA FUNCTION PDF
   HEAT OF FUEL =  4.633000E+07
```

```
 CG1 = 2.222222E+00, CG2 = 2.000000E+00
 STOICHIOMETRIC MIXTURE FRACTION = 5.704856E-02
 SPECIFIC HEAT COEFFICIENTS:
   FUEL      = 6.677600E+01 6.245760E+00 -2.775600E-03 4.440000E-07
   OXIDANT   = 9.277986E+02 2.651890E-01 -3.765960E-05 -4.615999E-09
   PRODUCT   = 9.679108E+02 3.851845E-01 -6.437380E-05 -3.377653E-09
 FUEL MOLECULAR WEIGHT      = 4.400000E+01
 OXIDANT MOLECULAR WEIGHT   = 2.879177E+01
 PRODUCT MOLECULAR WEIGHT   = 2.829347E+01
 FUEL MASS FRACTIONS:
   NITROGEN      = 0.000000E+00
   METHANE       = 0.000000E+00
   ETHANE        = 0.000000E+00
   PROPANE       = 1.000000E+00
   BUTANE        = 0.000000E+00
   CARBON MONOXIDE = 0.000000E+00
   CARBON DIOXIDE = 0.000000E+00
   HYDROGEN      = 0.000000E+00
 OXIDANT MASS FRACTIONS:
   NITROGEN      = 7.800000E-01
   OXYGEN        = 2.200000E-01
 PRODUCT MASS FRACTIONS:
   NITROGEN      = 7.355021E-01
   CARBON DIOXIDE = 1.711457E-01
   WATER         = 9.335219E-02

WALL BOUNDARY CONDITIONS
  SYNTHETIC BOUNDARY CONDITIONS
  LOGARITHMIC WALL PROFILES
  DEFAULT NO SLIP BOUNDARY CONDITIONS

GEOMETRY AND GRID
  NON-ORTHOGONAL MODE
  CARTESIAN COORDINATES IN PHYSICAL SPACE

SOLUTION PROCEDURE OPTIONS
  SIMPLE ALGORITHM
  USING SIMPLEC CORRECTION, ALPHA = 1.000000
  DENSITY UPWINDED IN CONVECTION COEFFICIENTS

    FDS = DIFFERENCING SCHEME      RDFC = RESIDUAL REDUCTION FACTOR
    URF = UNDER RELAXATION FACTOR  MNSL = MINIMUM NUMBER OF ITERATIONS
    DTF = FALSE TIME STEP          MXSL = MAXIMUM NUMBER OF ITERATIONS
    METH = SOLVER METHOD           MOL = DIFFERENCE MOLECULE IN SOLVER

  EQUATION            FDS   URF   DTF    METH
  ----------          ---   ---   ---    ----
  U VELOCITY          HDS   0.65  0.0E+00 ST3D
  V VELOCITY          HDS   0.65  0.0E+00 ST3D
  PRESSURE            CDS   1.00  0.0E+00 ICCG
  K                   HDS   0.70  0.0E+00 LRLX
  EPSILON             HDS   0.70  0.0E+00 LRLX
  ENTHALPY            HDS   0.70  0.0E+00 ST3D
  COMBUSTION SCALAR1  HDS   0.70  0.0E+00 ST3D
  COMBUSTION SCALAR2  HDS   0.70  0.0E+00 ST3D
  TEMPERATURE               0.70
  DENSITY                   0.05

  EQUATION            RDFC  MNSL  MXSL  MOL
  ----------          ----  ----  ----  ---
  U VELOCITY          0.250   1     5   7-PT
  V VELOCITY          0.250   1     5   7-PT
  PRESSURE            0.100   1    30   7-PT
  K                   0.250   1     5   7-PT
  EPSILON             0.250   1     5   7-PT
  ENTHALPY            0.100   1    30   7-PT
  COMBUSTION SCALAR1  0.100   1    30   7-PT
  COMBUSTION SCALAR2  0.100   1    30   7-PT

NO ARTIFICIAL DISSIPATION USED.
```

```
 RHIE CHOW SWITCH:
   MODEL USED = IMPROV
   MULTIPHASE DAMPING OF THE RHIE-CHOW CORRECTION TERM

   RESIDUAL MASS FLOW =     1.000E-06

PATCH  IST  IFN  JST  JFN  KST  KFN  WALL BLOCK LABEL   TYPE NAME
  1   65   86    1    1    1    1 LOW J    1    1 INLET  PRIMARY
  2   91   96    1    1    1    1 LOW J    1    1 INLET  GAS
  3    1    1    1   40    1    1 LOW I    2    1 INLET  PRESSURE
  4    1    1    1   40    1    1 LOW I    3    1 INLET  PRESSURE
  5    1  100   40   40    1    1 HIGH J   3    1 OUTLET TOP
  6  100  100    1   40    1    1 HIGH I   2    1 SYMMET SYMM-2
  7  100  100    1   40    1    1 HIGH I   3    1 SYMMET SYMM-3
  8    1  100    1   30    1    1 HIGH K   1    1 SYMMET SYMMETRY PLANE
  9    1  100    1   30    1    1 LOW K    1    1 SYMMET SYMMETRY PLANE
 10    1  100    1   40    1    1 HIGH K   2    1 SYMMET SYMMETRY PLANE
 11    1  100    1   40    1    1 LOW K    2    1 SYMMET SYMMETRY PLANE
 12    1  100    1   40    1    1 HIGH K   3    1 SYMMET SYMMETRY PLANE
 13    1  100    1   40    1    1 LOW K    3    1 SYMMET SYMMETRY PLANE
 14   73   90    1    1    1    1 LOW J    2    1 WALL   WALL-1
 15   72   72   29   30    1    1 HIGH I   1    1 WALL   WALL
 16   86   86    1   28    1    1 HIGH I   1    1 WALL   WALL
 17   92   92   30   30    1    1 HIGH I   1    1 WALL   WALL
 18   96   96    1   29    1    1 HIGH I   1    1 WALL   WALL
 19   73   86   28   28    1    1 HIGH J   1    1 WALL   WALL
 20   93   96   29   29    1    1 HIGH J   1    1 WALL   WALL
 21   65   65    1   30    1    1 LOW I    1    1 WALL   WALL
 22   91   91    1   30    1    1 LOW I    1    1 WALL   WALL
 23    1   64    1    1    1    1 LOW J    2    1 WALL   WALL
 24   93  100    1    1    1    1 LOW J    2    1 WALL   WALL
 25    1  100   30   30    1    1 HIGH J   1    1 BLKBDY GLUE-PATCH—1HIGH-J-BLK—1-
 26    1  100    1    1    1    1 LOW J    2    1 BLKBDY GLUE-PATCH—2-LOW-J-BLK—2-
 27    1  100   40   40    1    1 HIGH J   2    1 BLKBDY GLUE-PATCH—3HIGH-J-BLK—2-
 28    1  100    1    1    1    1 LOW J    3    1 BLKBDY GLUE-PATCH—4-LOW-J-BLK—3-
 29   87   90    1   28    1    1        1    1 SOLID  #1
 30   73   90   29   30    1    1        1    1 SOLID  #2
 31   97  100    1   29    1    1        1    1 SOLID  #3
 32   93  100   30   30    1    1        1    1 SOLID  #4
 33    1   64    1   30    1    1        1    1 SOLID  #5


 NO. OF INTERBLOCK BOUNDARIES =    2
 INTER-BLOCK BOUNDARY NO.    1
 1ST. PATCH NAME = GLUE-PATCH—1HIGH-J-BLK—1-
 2ND. PATCH NAME = GLUE-PATCH—2-LOW-J-BLK—2-
 ORIENTATION CHANGE = HIGH I  HIGH J  HIGH K

 INTER-BLOCK BOUNDARY NO.    2
 1ST. PATCH NAME = GLUE-PATCH—3HIGH-J-BLK—2-
 2ND. PATCH NAME = GLUE-PATCH—4-LOW-J-BLK—3-
 ORIENTATION CHANGE = HIGH I  HIGH J  HIGH K

 INITIALISATION COMPLETE

 MONITORING POINT AT (50,15, 1) IN BLOCK: BLOCK-NUMBER-1
 ITER I————ABSOLUTE RESIDUAL SOURCE SUMS————I I————FIELD VALUES AT MONITORING POINT———
 I
   NO.  UMOM  VMOM  MASS  TKIN  EDIS  ENTH  MIXF  U VEL.  V VEL.  PRESS.   K     EPS.   ENTH.  MIX-FR
        CFLU                          CN-FLU  MFFUEL  MPOXID  MFPROD
   1 1.38E-8 6.90E-5 5.13E-5 6.11E-5 9.83E+4 2.90E+2 6.26E-6  0.000E+00 0.000E+00 0.000E+00 0.000E+00 0.000E+00-2.779E+05
 0.000E+00
       7.93E-8                          0.000E+00 0.000E+00 1.000E+00 0.000E+00

   2 3.41E-4 5.87E-4 1.31E-4 5.06E-5 2.34E+4 2.90E+2 6.26E-6  0.000E+00 0.000E+00 0.000E+00 0.000E+00 0.000E+00-2.779E+05
 0.000E+00
       7.82E-8                          0.000E+00 0.000E+00 1.000E+00 0.000E+00

   3 2.19E-4 3.47E-4 1.04E-4 6.50E-5 2.44E+4 2.90E+2 6.26E-6  0.000E+00 0.000E+00 0.000E+00 0.000E+00 0.000E+00-2.779E+05
 0.000E+00
       5.56E-8                          0.000E+00 0.000E+00 1.000E+00 0.000E+00
```

4 1.89E-4 3.26E-4 8.22E-5 8.17E-5 2.43E+4 2.90E+2 6.26E-6 0.000E+00 0.000E+00 0.000E+00 0.000E+00 0.000E+00-2.779E+05
0.000E+00
4.49E-8 0.000E+00 0.000E+00 1.000E+00 0.000E+00

5 1.57E-4 3.04E-4 6.46E-5 9.22E-5 2.13E+4 2.90E+2 6.26E-6 0.000E+00 0.000E+00 0.000E+00 0.000E+00 0.000E+00-2.779E+05
0.000E+00
3.74E-8 0.000E+00 0.000E+00 1.000E+00 0.000E+00

6 1.48E-4 3.00E-4 5.63E-5 1.01E-4 2.09E+4 2.90E+2 6.26E-6 0.000E+00 0.000E+00 0.000E+00 0.000E+00 0.000E+00-2.779E+05
0.000E+00
3.20E-8 0.000E+00 0.000E+00 1.000E+00 0.000E+00

7 1.44E-4 3.05E-4 6.60E-5 1.11E-4 2.08E+4 2.90E+2 6.26E-6 0.000E+00 0.000E+00 0.000E+00 0.000E+00 0.000E+00-2.779E+05
0.000E+00
2.81E-8 0.000E+00 0.000E+00 1.000E+00 0.000E+00

8 1.44E-4 3.06E-4 6.15E-5 1.28E-4 2.09E+4 2.90E+2 6.27E-6 0.000E+00 0.000E+00 0.000E+00 0.000E+00 0.000E+00-2.779E+05
0.000E+00
2.58E-8 0.000E+00 0.000E+00 1.000E+00 0.000E+00

9 1.48E-4 3.13E-4 5.32E-5 1.46E-4 2.20E+4 2.91E+2 6.28E-6 0.000E+00 0.000E+00 0.000E+00 0.000E+00 0.000E+00-2.779E+05
0.000E+00
2.64E-8 0.000E+00 0.000E+00 1.000E+00 0.000E+00

10 1.63E-4 3.27E-4 5.16E-5 1.64E-4 2.26E+4 2.90E+2 6.27E-6 0.000E+00 0.000E+00 0.000E+00 0.000E+00 0.000E+00-2.779E+05
0.000E+00
3.15E-8 0.000E+00 0.000E+00 1.000E+00 0.000E+00

11 1.74E-4 3.41E-4 4.62E-5 1.82E-4 2.29E+4 2.90E+2 6.27E-6 0.000E+00 0.000E+00 0.000E+00 0.000E+00 0.000E+00-2.779E+05
0.000E+00
4.46E-8 0.000E+00 0.000E+00 1.000E+00 0.000E+00

12 1.91E-4 3.58E-4 4.40E-5 2.03E-4 2.36E+4 2.91E+2 6.28E-6 0.000E+00 0.000E+00 0.000E+00 0.000E+00 0.000E+00-2.779E+05
0.000E+00
6.92E-8 0.000E+00 0.000E+00 1.000E+00 0.000E+00

13 2.05E-4 3.76E-4 4.25E-5 2.22E-4 2.43E+4 2.91E+2 6.28E-6 0.000E+00 0.000E+00 0.000E+00 0.000E+00 0.000E+00-2.779E+05
0.000E+00
1.08E-7 0.000E+00 0.000E+00 1.000E+00 0.000E+00

[Editors Note, middle iterations deleted for brevity]

220 3.36E-5 5.61E-5 1.18E-6 3.06E-5 4.96E+1 9.92E+1 2.14E-6 0.000E+00 0.000E+00 0.000E+00 0.000E+00 0.000E+00-2.779E+05
0.000E+00
1.72E-7 0.000E+00 0.000E+00 1.000E+00 0.000E+00

221 3.33E-5 5.58E-5 1.17E-6 3.02E-5 3.89E+1 9.90E+1 2.14E-6 0.000E+00 0.000E+00 0.000E+00 0.000E+00 0.000E+00-2.779E+05
0.000E+00
1.70E-7 0.000E+00 0.000E+00 1.000E+00 0.000E+00

222 3.34E-5 5.52E-5 1.11E-6 3.00E-5 4.07E+1 9.86E+1 2.13E-6 0.000E+00 0.000E+00 0.000E+00 0.000E+00 0.000E+00-2.779E+05
0.000E+00
1.68E-7 0.000E+00 0.000E+00 1.000E+00 0.000E+00

223 3.36E-5 5.49E-5 1.12E-6 2.99E-5 4.05E+1 9.83E+1 2.12E-6 0.000E+00 0.000E+00 0.000E+00 0.000E+00 0.000E+00-2.779E+05
0.000E+00
1.66E-7 0.000E+00 0.000E+00 1.000E+00 0.000E+00

224 3.38E-5 5.42E-5 1.15E-6 3.03E-5 5.74E+1 9.78E+1 2.11E-6 0.000E+00 0.000E+00 0.000E+00 0.000E+00 0.000E+00-2.779E+05
0.000E+00
1.65E-7 0.000E+00 0.000E+00 1.000E+00 0.000E+00

225 3.43E-5 5.38E-5 1.12E-6 2.98E-5 3.73E+1 9.73E+1 2.10E-6 0.000E+00 0.000E+00 0.000E+00 0.000E+00 0.000E+00-2.779E+05
0.000E+00
1.63E-7 0.000E+00 0.000E+00 1.000E+00 0.000E+00

226 3.43E-5 5.29E-5 1.07E-6 2.89E-5 4.41E+1 9.66E+1 2.08E-6 0.000E+00 0.000E+00 0.000E+00 0.000E+00 0.000E+00-2.779E+05
0.000E+00
1.62E-7 0.000E+00 0.000E+00 1.000E+00 0.000E+00

227 3.50E-5 5.23E-5 1.05E-6 2.83E-5 3.88E+1 9.58E+1 2.07E-6 0.000E+00 0.000E+00 0.000E+00 0.000E+00 0.000E+00-2.779E-05 0.000E+00
1.61E-7 0.000E+00 0.000E+00 1.000E+00 0.000E+00

228 3.50E-5 5.14E-5 1.01E-6 2.79E-5 3.17E+1 9.48E-1 2.05E-6 0.000E+00 0.000E+00 0.000E+00 0.000E+00 0.000E+00-2.779E-05 0.000E+00
1.60E-7 0.000E+00 0.000E+00 1.000E+00 0.000E+00

229 3.58E-5 5.06E-5 9.98E-7 2.75E-5 3.16E+1 9.39E+1 2.02E-6 0.000E+00 0.000E+00 0.000E+00 0.000E+00 0.000E+00-2.779E-05 0.000E+00
1.58E-7 0.000E+00 0.000E+00 1.000E+00 0.000E+00

AVERAGE REDUCTION FACTOR ACHIEVED BY LINEAR SOLVERS

U MOMENTUM RESIDUALS	1.9E-02
V MOMENTUM RESIDUALS	1.9E-02
MASS SOURCE RESIDUALS	1.5E-01
TURBULENCE ENERGY RESIDUALS	1.1E-01
ENERGY DISSIPATION RESIDUALS	1.5E-05
ENTHALPY RESIDUALS	2.8E-02
MIXTURE FRACTION RESIDUALS	2.8E-02
CONC. FLUCTUATION RESIDUALS	2.3E-02

CONVERGENCE IN 229 ITERATIONS

--*- BLOCK-NUMBER-1 PLANE K = 1 TEMPERATURE (KELVIN) -*-*-*-*-*-*-*-*-*-*-*-*-*-*-*-*-*-*-*

J													
0	2.88E+02	2.93E+02	2.93E+02	2.93E+02	2.93E+02	2.93E+02	2.93E+02	2.93E+02	2.94E+02	2.94E+02	2.94E+02	2.94E+02	
30	2.88E+02	1.00E+02	1.00E+02	1.00E+02	1.00E+02	1.00E+02	1.00E+02	1.00E+02	1.00E+02	1.00E+02	1.00E+02	1.00E+02	1.00E+02
29	2.88E+02	1.00E+02	1.00E+02	1.00E+02	1.00E+02	1.00E+02	1.00E+02	1.00E+02	1.00E+02	1.00E+02	1.00E+02	1.00E+02	1.00E+02
28	2.88E+02	1.00E+02	1.00E+02	1.00E+02	1.00E+02	1.00E+02	1.00E+02	1.00E+02	1.00E+02	1.00E+02	1.00E+02	1.00E+02	1.00E+02
27	2.88E+02	1.00E+02	1.00E+02	1.00E+02	1.00E+02	1.00E+02	1.00E+02	1.00E+02	1.00E+02	1.00E+02	1.00E+02	1.00E+02	1.00E+02
26	2.88E+02	1.00E+02	1.00E+02	1.00E+02	1.00E+02	1.00E+02	1.00E+02	1.00E+02	1.00E+02	1.00E+02	1.00E+02	1.00E+02	1.00E+02
25	2.88E+02	1.00E+02	1.00E+02	1.00E+02	1.00E+02	1.00E+02	1.00E+02	1.00E+02	1.00E+02	1.00E+02	1.00E+02	1.00E+02	1.00E+02
24	2.88E+02	1.00E+02	1.00E+02	1.00E+02	1.00E+02	1.00E+02	1.00E+02	1.00E+02	1.00E+02	1.00E+02	1.00E+02	1.00E+02	1.00E+02
23	2.88E+02	1.00E+02	1.00E+02	1.00E+02	1.00E+02	1.00E+02	1.00E+02	1.00E+02	1.00E+02	1.00E+02	1.00E+02	1.00E+02	1.00E+02
22	2.88E+02	1.00E+02	1.00E+02	1.00E+02	1.00E+02	1.00E+02	1.00E+02	1.00E+02	1.00E+02	1.00E+02	1.00E+02	1.00E+02	1.00E+02
21	2.88E+02	1.00E+02	1.00E+02	1.00E+02	1.00E+02	1.00E+02	1.00E+02	1.00E+02	1.00E+02	1.00E+02	1.00E+02	1.00E+02	1.00E+02
20	2.88E+02	1.00E+02	1.00E+02	1.00E+02	1.00E+02	1.00E+02	1.00E+02	1.00E+02	1.00E+02	1.00E+02	1.00E+02	1.00E+02	1.00E+02
19	2.88E+02	1.00E+02	1.00E+02	1.00E+02	1.00E+02	1.00E+02	1.00E+02	1.00E+02	1.00E+02	1.00E+02	1.00E+02	1.00E+02	1.00E+02
18	2.88E+02	1.00E+02	1.00E+02	1.00E+02	1.00E+02	1.00E+02	1.00E+02	1.00E+02	1.00E+02	1.00E+02	1.00E+02	1.00E+02	1.00E+02
17	2.88E+02	1.00E+02	1.00E+02	1.00E+02	1.00E+02	1.00E+02	1.00E+02	1.00E+02	1.00E+02	1.00E+02	1.00E+02	1.00E+02	1.00E+02
16	2.88E+02	1.00E+02	1.00E+02	1.00E+02	1.00E+02	1.00E+02	1.00E+02	1.00E+02	1.00E+02	1.00E+02	1.00E+02	1.00E+02	1.00E+02
15	2.88E+02	1.00E+02	1.00E+02	1.00E+02	1.00E+02	1.00E+02	1.00E+02	1.00E+02	1.00E+02	1.00E+02	1.00E+02	1.00E+02	1.00E+02
14	2.88E+02	1.00E+02	1.00E+02	1.00E+02	1.00E+02	1.00E+02	1.00E+02	1.00E+02	1.00E+02	1.00E+02	1.00E+02	1.00E+02	1.00E+02
13	2.88E+02	1.00E+02	1.00E+02	1.00E+02	1.00E+02	1.00E+02	1.00E+02	1.00E+02	1.00E+02	1.00E+02	1.00E+02	1.00E+02	1.00E+02
12	2.88E+02	1.00E+02	1.00E+02	1.00E+02	1.00E+02	1.00E+02	1.00E+02	1.00E+02	1.00E+02	1.00E+02	1.00E+02	1.00E+02	1.00E+02
11	2.88E+02	1.00E+02	1.00E+02	1.00E+02	1.00E+02	1.00E+02	1.00E+02	1.00E+02	1.00E+02	1.00E+02	1.00E+02	1.00E+02	1.00E+02
10	2.88E+02	1.00E+02	1.00E+02	1.00E+02	1.00E+02	1.00E+02	1.00E+02	1.00E+02	1.00E+02	1.00E+02	1.00E+02	1.00E+02	1.00E+02
9	2.88E+02	1.00E+02	1.00E+02	1.00E+02	1.00E+02	1.00E+02	1.00E+02	1.00E+02	1.00E+02	1.00E+02	1.00E+02	1.00E+02	1.00E+02
8	2.88E+02	1.00E+02	1.00E+02	1.00E+02	1.00E+02	1.00E+02	1.00E+02	1.00E+02	1.00E+02	1.00E+02	1.00E+02	1.00E+02	1.00E+02
7	2.88E+02	1.00E+02	1.00E+02	1.00E+02	1.00E+02	1.00E+02	1.00E+02	1.00E+02	1.00E+02	1.00E+02	1.00E+02	1.00E+02	1.00E+02
6	2.88E+02	1.00E+02	1.00E+02	1.00E+02	1.00E+02	1.00E+02	1.00E+02	1.00E+02	1.00E+02	1.00E+02	1.00E+02	1.00E+02	1.00E+02
5	2.88E+02	1.00E+02	1.00E+02	1.00E+02	1.00E+02	1.00E+02	1.00E+02	1.00E+02	1.00E+02	1.00E+02	1.00E+02	1.00E+02	1.00E+02
4	2.88E+02	1.00E+02	1.00E+02	1.00E+02	1.00E+02	1.00E+02	1.00E+02	1.00E+02	1.00E+02	1.00E+02	1.00E+02	1.00E+02	1.00E+02
3	2.88E+02	1.00E+02	1.00E+02	1.00E+02	1.00E+02	1.00E+02	1.00E+02	1.00E+02	1.00E+02	1.00E+02	1.00E+02	1.00E+02	1.00E+02
2	2.88E+02	1.00E+02	1.00E+02	1.00E+02	1.00E+02	1.00E+02	1.00E+02	1.00E+02	1.00E+02	1.00E+02	1.00E+02	1.00E+02	1.00E+02
1	2.88E+02	1.00E+02	1.00E+02	1.00E+02	1.00E+02	1.00E+02	1.00E+02	1.00E+02	1.00E+02	1.00E+02	1.00E+02	1.00E+02	1.00E+02
0	2.88E+02	2.88E+02	2.88E+02	2.88E+02	2.88E+02	2.88E+02	2.88E+02	2.88E+02	2.88E+02	2.88E+02	2.88E+02	2.88E+02	2.88E+02
I=	0	1	2	3	4	5	6	7	8	9	10	11	

J													
0	2.94E+02	2.94E+02	2.94E+02	2.94E+02	2.94E+02	2.94E+02	2.94E+02	2.94E+02	2.94E+02	2.94E+02	2.94E+02	2.94E+02	
30	1.00E+02	1.00E+02	1.00E+02	1.00E+02	1.00E+02	1.00E+02	1.00E+02	1.00E+02	1.00E+02	1.00E+02	1.00E+02	1.00E+02	1.00E+02
29	1.00E+02	1.00E+02	1.00E+02	1.00E+02	1.00E+02	1.00E+02	1.00E+02	1.00E+02	1.00E+02	1.00E+02	1.00E+02	1.00E+02	1.00E+02
28	1.00E+02	1.00E+02	1.00E+02	1.00E+02	1.00E+02	1.00E+02	1.00E+02	1.00E+02	1.00E+02	1.00E+02	1.00E+02	1.00E+02	1.00E+02
27	1.00E+02	1.00E+02	1.00E+02	1.00E+02	1.00E+02	1.00E+02	1.00E+02	1.00E+02	1.00E+02	1.00E+02	1.00E+02	1.00E+02	1.00E+02

26	1.00E+02	1.00E+02	1.00E+02	1.00E+02	1.00E+02	1.00E+02	1.00E+02	1.00E+02	1.00E+02	1.00E+02	1.00E+02	1.00E+02	1.00E+02
25	1.00E+02	1.00E+02	1.00E+02	1.00E+02	1.00E+02	1.00E+02	1.00E+02	1.00E+02	1.00E+02	1.00E+02	1.00E+02	1.00E+02	1.00E+02
24	1.00E+02	1.00E+02	1.00E+02	1.00E+02	1.00E+02	1.00E+02	1.00E+02	1.00E+02	1.00E+02	1.00E+02	1.00E+02	1.00E+02	1.00E+02
23	1.00E+02	1.00E+02	1.00E+02	1.00E+02	1.00E+02	1.00E+02	1.00E+02	1.00E+02	1.00E+02	1.00E+02	1.00E+02	1.00E+02	1.00E+02
22	1.00E+02	1.00E+02	1.00E+02	1.00E+02	1.00E+02	1.00E+02	1.00E+02	1.00E+02	1.00E+02	1.00E+02	1.00E+02	1.00E+02	1.00E+02
21	1.00E+02	1.00E+02	1.00E+02	1.00E+02	1.00E+02	1.00E+02	1.00E+02	1.00E+02	1.00E+02	1.00E+02	1.00E+02	1.00E+02	1.00E+02
20	1.00E+02	1.00E+02	1.00E+02	1.00E+02	1.00E+02	1.00E+02	1.00E+02	1.00E+02	1.00E+02	1.00E+02	1.00E+02	1.00E+02	1.00E+02
19	1.00E+02	1.00E+02	1.00E+02	1.00E+02	1.00E+02	1.00E+02	1.00E+02	1.00E+02	1.00E+02	1.00E+02	1.00E+02	1.00E+02	1.00E+02
18	1.00E+02	1.00E+02	1.00E+02	1.00E+02	1.00E+02	1.00E+02	1.00E+02	1.00E+02	1.00E+02	1.00E+02	1.00E+02	1.00E+02	1.00E+02
17	1.00E+02	1.00E+02	1.00E+02	1.00E+02	1.00E+02	1.00E+02	1.00E+02	1.00E+02	1.00E+02	1.00E+02	1.00E+02	1.00E+02	1.00E+02
16	1.00E+02	1.00E+02	1.00E+02	1.00E+02	1.00E+02	1.00E+02	1.00E+02	1.00E+02	1.00E+02	1.00E+02	1.00E+02	1.00E+02	1.00E+02
15	1.00E+02	1.00E+02	1.00E+02	1.00E+02	1.00E+02	1.00E+02	1.00E+02	1.00E+02	1.00E+02	1.00E+02	1.00E+02	1.00E+02	1.00E+02
14	1.00E+02	1.00E+02	1.00E+02	1.00E+02	1.00E+02	1.00E+02	1.00E+02	1.00E+02	1.00E+02	1.00E+02	1.00E+02	1.00E+02	1.00E+02
13	1.00E+02	1.00E+02	1.00E+02	1.00E+02	1.00E+02	1.00E+02	1.00E+02	1.00E+02	1.00E+02	1.00E+02	1.00E+02	1.00E+02	1.00E+02
12	1.00E+02	1.00E+02	1.00E+02	1.00E+02	1.00E+02	1.00E+02	1.00E+02	1.00E+02	1.00E+02	1.00E+02	1.00E+02	1.00E+02	1.00E+02
11	1.00E+02	1.00E+02	1.00E+02	1.00E+02	1.00E+02	1.00E+02	1.00E+02	1.00E+02	1.00E+02	1.00E+02	1.00E+02	1.00E+02	1.00E+02
10	1.00E+02	1.00E+02	1.00E+02	1.00E+02	1.00E+02	1.00E+02	1.00E+02	1.00E+02	1.00E+02	1.00E+02	1.00E+02	1.00E+02	1.00E+02
9	1.00E+02	1.00E+02	1.00E+02	1.00E+02	1.00E+02	1.00E+02	1.00E+02	1.00E+02	1.00E+02	1.00E+02	1.00E+02	1.00E+02	1.00E+02
8	1.00E+02	1.00E+02	1.00E+02	1.00E+02	1.00E+02	1.00E+02	1.00E+02	1.00E+02	1.00E+02	1.00E+02	1.00E+02	1.00E+02	1.00E+02
7	1.00E+02	1.00E+02	1.00E+02	1.00E+02	1.00E+02	1.00E+02	1.00E+02	1.00E+02	1.00E+02	1.00E+02	1.00E+02	1.00E+02	1.00E+02
6	1.00E+02	1.00E+02	1.00E+02	1.00E+02	1.00E+02	1.00E+02	1.00E+02	1.00E+02	1.00E+02	1.00E+02	1.00E+02	1.00E+02	1.00E+02
5	1.00E+02	1.00E+02	1.00E+02	1.00E+02	1.00E+02	1.00E+02	1.00E+02	1.00E+02	1.00E+02	1.00E+02	1.00E+02	1.00E+02	1.00E+02
4	1.00E+02	1.00E+02	1.00E+02	1.00E+02	1.00E+02	1.00E+02	1.00E+02	1.00E+02	1.00E+02	1.00E+02	1.00E+02	1.00E+02	1.00E+02
3	1.00E+02	1.00E+02	1.00E+02	1.00E+02	1.00E+02	1.00E+02	1.00E+02	1.00E+02	1.00E+02	1.00E+02	1.00E+02	1.00E+02	1.00E+02
2	1.00E+02	1.00E+02	1.00E+02	1.00E+02	1.00E+02	1.00E+02	1.00E+02	1.00E+02	1.00E+02	1.00E+02	1.00E+02	1.00E+02	1.00E+02
1	1.00E+02	1.00E+02	1.00E+02	1.00E+02	1.00E+02	1.00E+02	1.00E+02	1.00E+02	1.00E+02	1.00E+02	1.00E+02	1.00E+02	1.00E+02
0	2.88E+02	2.88E+02	2.88E+02	2.88E+02	2.88E+02	2.88E+02	2.88E+02	2.88E+02	2.88E+02	2.88E+02	2.88E+02	2.88E+02	2.88E+02
I =	12	13	14	15	16	17	18	19	20	21	22	23	

J

0	2.94E+02	2.94E+02	2.94E+02	2.94E+02	2.94E+02	2.94E+02	2.94E+02	2.94E+02	2.95E+02	2.95E+02	2.95E+02	2.95E+02	
30	1.00E+02	1.00E+02	1.00E+02	1.00E+02	1.00E+02	1.00E+02	1.00E+02	1.00E+02	1.00E+02	1.00E+02	1.00E+02	1.00E+02	
29	1.00E+02	1.00E+02	1.00E+02	1.00E+02	1.00E+02	1.00E+02	1.00E+02	1.00E+02	1.00E+02	1.00E+02	1.00E+02	1.00E+02	
28	1.00E+02	1.00E+02	1.00E+02	1.00E+02	1.00E+02	1.00E+02	1.00E+02	1.00E+02	1.00E+02	1.00E+02	1.00E+02	1.00E+02	
27	1.00E+02	1.00E+02	1.00E+02	1.00E+02	1.00E+02	1.00E+02	1.00E+02	1.00E+02	1.00E+02	1.00E+02	1.00E+02	1.00E+02	
26	1.00E+02	1.00E+02	1.00E+02	1.00E+02	1.00E+02	1.00E+02	1.00E+02	1.00E+02	1.00E+02	1.00E+02	1.00E+02	1.00E+02	
25	1.00E+02	1.00E+02	1.00E+02	1.00E+02	1.00E+02	1.00E+02	1.00E+02	1.00E+02	1.00E+02	1.00E+02	1.00E+02	1.00E+02	
24	1.00E+02	1.00E+02	1.00E+02	1.00E+02	1.00E+02	1.00E+02	1.00E+02	1.00E+02	1.00E+02	1.00E+02	1.00E+02	1.00E+02	
23	1.00E+02	1.00E+02	1.00E+02	1.00E+02	1.00E+02	1.00E+02	1.00E+02	1.00E+02	1.00E+02	1.00E+02	1.00E+02	1.00E+02	
22	1.00E+02	1.00E+02	1.00E+02	1.00E+02	1.00E+02	1.00E+02	1.00E+02	1.00E+02	1.00E+02	1.00E+02	1.00E+02	1.00E+02	
21	1.00E+02	1.00E+02	1.00E+02	1.00E+02	1.00E+02	1.00E+02	1.00E+02	1.00E+02	1.00E+02	1.00E+02	1.00E+02	1.00E+02	
20	1.00E+02	1.00E+02	1.00E+02	1.00E+02	1.00E+02	1.00E+02	1.00E+02	1.00E+02	1.00E+02	1.00E+02	1.00E+02	1.00E+02	
19	1.00E+02	1.00E+02	1.00E+02	1.00E+02	1.00E+02	1.00E+02	1.00E+02	1.00E+02	1.00E+02	1.00E+02	1.00E+02	1.00E+02	
18	1.00E+02	1.00E+02	1.00E+02	1.00E+02	1.00E+02	1.00E+02	1.00E+02	1.00E+02	1.00E+02	1.00E+02	1.00E+02	1.00E+02	
17	1.00E+02	1.00E+02	1.00E+02	1.00E+02	1.00E+02	1.00E+02	1.00E+02	1.00E+02	1.00E+02	1.00E+02	1.00E+02	1.00E+02	
16	1.00E+02	1.00E+02	1.00E+02	1.00E+02	1.00E+02	1.00E+02	1.00E+02	1.00E+02	1.00E+02	1.00E+02	1.00E+02	1.00E+02	
15	1.00E+02	1.00E+02	1.00E+02	1.00E+02	1.00E+02	1.00E+02	1.00E+02	1.00E+02	1.00E+02	1.00E+02	1.00E+02	1.00E+02	
14	1.00E+02	1.00E+02	1.00E+02	1.00E+02	1.00E+02	1.00E+02	1.00E+02	1.00E+02	1.00E+02	1.00E+02	1.00E+02	1.00E+02	
13	1.00E+02	1.00E+02	1.00E+02	1.00E+02	1.00E+02	1.00E+02	1.00E+02	1.00E+02	1.00E+02	1.00E+02	1.00E+02	1.00E+02	
12	1.00E+02	1.00E+02	1.00E+02	1.00E+02	1.00E+02	1.00E+02	1.00E+02	1.00E+02	1.00E+02	1.00E+02	1.00E+02	1.00E+02	
11	1.00E+02	1.00E+02	1.00E+02	1.00E+02	1.00E+02	1.00E+02	1.00E+02	1.00E+02	1.00E+02	1.00E+02	1.00E+02	1.00E+02	
10	1.00E+02	1.00E+02	1.00E+02	1.00E+02	1.00E+02	1.00E+02	1.00E+02	1.00E+02	1.00E+02	1.00E+02	1.00E+02	1.00E+02	
9	1.00E+02	1.00E+02	1.00E+02	1.00E+02	1.00E+02	1.00E+02	1.00E+02	1.00E+02	1.00E+02	1.00E+02	1.00E+02	1.00E+02	
8	1.00E+02	1.00E+02	1.00E+02	1.00E+02	1.00E+02	1.00E+02	1.00E+02	1.00E+02	1.00E+02	1.00E+02	1.00E+02	1.00E+02	
7	1.00E+02	1.00E+02	1.00E+02	1.00E+02	1.00E+02	1.00E+02	1.00E+02	1.00E+02	1.00E+02	1.00E+02	1.00E+02	1.00E+02	
6	1.00E+02	1.00E+02	1.00E+02	1.00E+02	1.00E+02	1.00E+02	1.00E+02	1.00E+02	1.00E+02	1.00E+02	1.00E+02	1.00E+02	
5	1.00E+02	1.00E+02	1.00E+02	1.00E+02	1.00E+02	1.00E+02	1.00E+02	1.00E+02	1.00E+02	1.00E+02	1.00E+02	1.00E+02	
4	1.00E+02	1.00E+02	1.00E+02	1.00E+02	1.00E+02	1.00E+02	1.00E+02	1.00E+02	1.00E+02	1.00E+02	1.00E+02	1.00E+02	
3	1.00E+02	1.00E+02	1.00E+02	1.00E+02	1.00E+02	1.00E+02	1.00E+02	1.00E+02	1.00E+02	1.00E+02	1.00E+02	1.00E+02	
2	1.00E+02	1.00E+02	1.00E+02	1.00E+02	1.00E+02	1.00E+02	1.00E+02	1.00E+02	1.00E+02	1.00E+02	1.00E+02	1.00E+02	
1	1.00E+02	1.00E+02	1.00E+02	1.00E+02	1.00E+02	1.00E+02	1.00E+02	1.00E+02	1.00E+02	1.00E+02	1.00E+02	1.00E+02	
0	2.88E+02	2.88E+02	2.88E+02	2.88E+02	2.88E+02	2.88E+02	2.88E+02	2.88E+02	2.88E+02	2.88E+02	2.88E+02	2.88E+02	
I =	24	25	26	27	28	29	30	31	32	33	34	35	

J

0	2.95E+02	2.95E+02	2.95E+02	2.95E+02	2.95E+02	2.95E+02	2.95E+02	2.95E+02	2.95E+02	2.95E+02	2.95E+02	2.95E+02	
30	1.00E+02	1.00E+02	1.00E+02	1.00E+02	1.00E+02	1.00E+02	1.00E+02	1.00E+02	1.00E+02	1.00E+02	1.00E+02	1.00E+02	
29	1.00E+02	1.00E+02	1.00E+02	1.00E+02	1.00E+02	1.00E+02	1.00E+02	1.00E+02	1.00E+02	1.00E+02	1.00E+02	1.00E+02	
28	1.00E+02	1.00E+02	1.00E+02	1.00E+02	1.00E+02	1.00E+02	1.00E+02	1.00E+02	1.00E+02	1.00E+02	1.00E+02	1.00E+02	

28	1.00E+02	1.00E+02	1.00E+02	1.00E+02	1.00E+02	2.93E+02	2.93E+02	2.93E+02	2.93E+02	2.93E+02	2.93E+02	2.93E+02
27	1.00E+02	1.00E+02	1.00E+02	1.00E+02	1.00E+02	2.93E+02	2.93E+02	2.93E+02	2.93E+02	2.93E+02	2.93E+02	2.93E+02
26	1.00E+02	1.00E+02	1.00E+02	1.00E+02	1.00E+02	2.93E+02	2.93E+02	2.93E+02	2.93E+02	2.93E+02	2.93E+02	2.93E+02
25	1.00E+02	1.00E+02	1.00E+02	1.00E+02	1.00E+02	2.93E+02	2.93E+02	2.93E+02	2.93E+02	2.93E+02	2.93E+02	2.93E+02
24	1.00E+02	1.00E+02	1.00E+02	1.00E+02	1.00E+02	2.93E+02	2.93E+02	2.93E+02	2.93E+02	2.93E+02	2.93E+02	2.93E+02
23	1.00E+02	1.00E+02	1.00E+02	1.00E+02	1.00E+02	2.93E+02	2.93E+02	2.93E+02	2.93E+02	2.93E+02	2.93E+02	2.93E+02
22	1.00E+02	1.00E+02	1.00E+02	1.00E+02	1.00E+02	2.93E+02	2.93E+02	2.93E+02	2.93E+02	2.93E+02	2.93E+02	2.93E+02
21	1.00E+02	1.00E+02	1.00E+02	1.00E+02	1.00E+02	2.93E+02	2.93E+02	2.93E+02	2.93E+02	2.93E+02	2.93E+02	2.93E+02
20	1.00E+02	1.00E+02	1.00E+02	1.00E+02	1.00E+02	2.93E+02	2.93E+02	2.93E+02	2.93E+02	2.93E+02	2.93E+02	2.93E+02
19	1.00E+02	1.00E+02	1.00E+02	1.00E+02	1.00E+02	2.93E+02	2.93E+02	2.93E+02	2.93E+02	2.93E+02	2.93E+02	2.93E+02
18	1.00E+02	1.00E+02	1.00E+02	1.00E+02	1.00E+02	2.93E+02	2.93E+02	2.93E+02	2.93E+02	2.93E+02	2.93E+02	2.93E+02
17	1.00E+02	1.00E+02	1.00E+02	1.00E+02	1.00E+02	2.93E+02	2.93E+02	2.93E+02	2.93E+02	2.93E+02	2.93E+02	2.93E+02
16	1.00E+02	1.00E+02	1.00E+02	1.00E+02	1.00E+02	2.93E+02	2.93E+02	2.93E+02	2.93E+02	2.93E+02	2.93E+02	2.93E+02
15	1.00E+02	1.00E+02	1.00E+02	1.00E+02	1.00E+02	2.93E+02	2.93E+02	2.93E+02	2.93E+02	2.93E+02	2.93E+02	2.93E+02
14	1.00E+02	1.00E+02	1.00E+02	1.00E+02	1.00E+02	2.93E+02	2.93E+02	2.93E+02	2.93E+02	2.93E+02	2.93E+02	2.93E+02
13	1.00E+02	1.00E+02	1.00E+02	1.00E+02	1.00E+02	2.93E+02	2.93E+02	2.93E+02	2.93E+02	2.93E+02	2.93E+02	2.93E+02
12	1.00E+02	1.00E+02	1.00E+02	1.00E+02	1.00E+02	2.93E+02	2.93E+02	2.93E+02	2.93E+02	2.93E+02	2.93E+02	2.93E+02
11	1.00E+02	1.00E+02	1.00E+02	1.00E+02	1.00E+02	2.93E+02	2.93E+02	2.93E+02	2.93E+02	2.93E+02	2.93E+02	2.93E+02
10	1.00E+02	1.00E+02	1.00E+02	1.00E+02	1.00E+02	2.93E+02	2.93E+02	2.93E+02	2.93E+02	2.93E+02	2.93E+02	2.93E+02
9	1.00E+02	1.00E+02	1.00E+02	1.00E+02	1.00E+02	2.93E+02	2.93E+02	2.93E+02	2.93E+02	2.93E+02	2.93E+02	2.93E+02
8	1.00E+02	1.00E+02	1.00E+02	1.00E+02	1.00E+02	2.93E+02	2.93E+02	2.93E+02	2.93E+02	2.93E+02	2.93E+02	2.93E+02
7	1.00E+02	1.00E+02	1.00E+02	1.00E+02	1.00E+02	2.93E+02	2.93E+02	2.93E+02	2.93E+02	2.93E+02	2.93E+02	2.93E+02
6	1.00E+02	1.00E+02	1.00E+02	1.00E+02	1.00E+02	2.93E+02	2.93E+02	2.93E+02	2.93E+02	2.93E+02	2.93E+02	2.93E+02
5	1.00E+02	1.00E+02	1.00E+02	1.00E+02	1.00E+02	2.93E+02	2.93E+02	2.93E+02	2.93E+02	2.93E+02	2.93E+02	2.93E+02
4	1.00E+02	1.00E+02	1.00E+02	1.00E+02	1.00E+02	2.93E+02	2.93E+02	2.93E+02	2.93E+02	2.93E+02	2.93E+02	2.93E+02
3	1.00E+02	1.00E+02	1.00E+02	1.00E+02	1.00E+02	2.93E+02	2.93E+02	2.93E+02	2.93E+02	2.93E+02	2.93E+02	2.93E+02
2	1.00E+02	1.00E+02	1.00E+02	1.00E+02	1.00E+02	2.93E+02	2.93E+02	2.93E+02	2.93E+02	2.93E+02	2.93E+02	2.93E+02
1	1.00E+02	1.00E+02	1.00E+02	1.00E+02	1.00E+02	2.93E+02	2.93E+02	2.93E+02	2.93E+02	2.93E+02	2.93E+02	2.93E+02
0	2.88E+02	2.88E+02	2.88E+02	2.88E+02	2.88E+02	2.93E+02	2.93E+02	2.93E+02	2.93E+02	2.93E+02	2.93E+02	2.93E+02
I =	60	61	62	63	64	65	66	67	68	69	70	71

J

0	3.59E+02	1.04E+03	1.58E+03	1.38E+03	1.37E+03	1.36E+03	1.34E+03	1.31E+03	1.28E+03	1.26E+03	1.23E+03	1.20E+03
30	3.01E+02	1.00E+02	1.00E+02	1.00E+02	1.00E+02	1.00E+02	1.00E+02	1.00E+02	1.00E+02	1.00E+02	1.00E+02	1.00E+02
29	2.93E+02	1.00E+02	1.00E+02	1.00E+02	1.00E+02	1.00E+02	1.00E+02	1.00E+02	1.00E+02	1.00E+02	1.00E+02	1.00E+02
28	2.93E+02	2.93E+02	2.93E+02	2.93E+02	2.93E+02	2.93E+02	2.93E+02	2.93E+02	2.93E+02	2.93E+02	2.93E+02	2.93E+02
27	2.93E+02	2.93E+02	2.93E+02	2.93E+02	2.93E+02	2.93E+02	2.93E+02	2.93E+02	2.93E+02	2.93E+02	2.93E+02	2.93E+02
26	2.93E+02	2.93E+02	2.93E+02	2.93E+02	2.93E+02	2.93E+02	2.93E+02	2.93E+02	2.93E+02	2.93E+02	2.93E+02	2.93E+02
25	2.93E+02	2.93E+02	2.93E+02	2.93E+02	2.93E+02	2.93E+02	2.93E+02	2.93E+02	2.93E+02	2.93E+02	2.93E+02	2.93E+02
24	2.93E+02	2.93E+02	2.93E+02	2.93E+02	2.93E+02	2.93E+02	2.93E+02	2.93E+02	2.93E+02	2.93E+02	2.93E+02	2.93E+02
23	2.93E+02	2.93E+02	2.93E+02	2.93E+02	2.93E+02	2.93E+02	2.93E+02	2.93E+02	2.93E+02	2.93E+02	2.93E+02	2.93E+02
22	2.93E+02	2.93E+02	2.93E+02	2.93E+02	2.93E+02	2.93E+02	2.93E+02	2.93E+02	2.93E+02	2.93E+02	2.93E+02	2.93E+02
21	2.93E+02	2.93E+02	2.93E+02	2.93E+02	2.93E+02	2.93E+02	2.93E+02	2.93E+02	2.93E+02	2.93E+02	2.93E+02	2.93E+02
20	2.93E+02	2.93E+02	2.93E+02	2.93E+02	2.93E+02	2.93E+02	2.93E+02	2.93E+02	2.93E+02	2.93E+02	2.93E+02	2.93E+02
19	2.93E+02	2.93E+02	2.93E+02	2.93E+02	2.93E+02	2.93E+02	2.93E+02	2.93E+02	2.93E+02	2.93E+02	2.93E+02	2.93E+02
18	2.93E+02	2.93E+02	2.93E+02	2.93E+02	2.93E+02	2.93E+02	2.93E+02	2.93E+02	2.93E+02	2.93E+02	2.93E+02	2.93E+02
17	2.93E+02	2.93E+02	2.93E+02	2.93E+02	2.93E+02	2.93E+02	2.93E+02	2.93E+02	2.93E+02	2.93E+02	2.93E+02	2.93E+02
16	2.93E+02	2.93E+02	2.93E+02	2.93E+02	2.93E+02	2.93E+02	2.93E+02	2.93E+02	2.93E+02	2.93E+02	2.93E+02	2.93E+02
15	2.93E+02	2.93E+02	2.93E+02	2.93E+02	2.93E+02	2.93E+02	2.93E+02	2.93E+02	2.93E+02	2.93E+02	2.93E+02	2.93E+02
14	2.93E+02	2.93E+02	2.93E+02	2.93E+02	2.93E+02	2.93E+02	2.93E+02	2.93E+02	2.93E+02	2.93E+02	2.93E+02	2.93E+02
13	2.93E+02	2.93E+02	2.93E+02	2.93E+02	2.93E+02	2.93E+02	2.93E+02	2.93E+02	2.93E+02	2.93E+02	2.93E+02	2.93E+02
12	2.93E+02	2.93E+02	2.93E+02	2.93E+02	2.93E+02	2.93E+02	2.93E+02	2.93E+02	2.93E+02	2.93E+02	2.93E+02	2.93E+02
11	2.93E+02	2.93E+02	2.93E+02	2.93E+02	2.93E+02	2.93E+02	2.93E+02	2.93E+02	2.93E+02	2.93E+02	2.93E+02	2.93E+02
10	2.93E+02	2.93E+02	2.93E+02	2.93E+02	2.93E+02	2.93E+02	2.93E+02	2.93E+02	2.93E+02	2.93E+02	2.93E+02	2.93E+02
9	2.93E+02	2.93E+02	2.93E+02	2.93E+02	2.93E+02	2.93E+02	2.93E+02	2.93E+02	2.93E+02	2.93E+02	2.93E+02	2.93E+02
8	2.93E+02	2.93E+02	2.93E+02	2.93E+02	2.93E+02	2.93E+02	2.93E+02	2.93E+02	2.93E+02	2.93E+02	2.93E+02	2.93E+02
7	2.93E+02	2.93E+02	2.93E+02	2.93E+02	2.93E+02	2.93E+02	2.93E+02	2.93E+02	2.93E+02	2.93E+02	2.93E+02	2.93E+02
6	2.93E+02	2.93E+02	2.93E+02	2.93E+02	2.93E+02	2.93E+02	2.93E+02	2.93E+02	2.93E+02	2.93E+02	2.93E+02	2.93E+02
5	2.93E+02	2.93E+02	2.93E+02	2.93E+02	2.93E+02	2.93E+02	2.93E+02	2.93E+02	2.93E+02	2.93E+02	2.93E+02	2.93E+02
4	2.93E+02	2.93E+02	2.93E+02	2.93E+02	2.93E+02	2.93E+02	2.93E+02	2.93E+02	2.93E+02	2.93E+02	2.93E+02	2.93E+02
3	2.93E+02	2.93E+02	2.93E+02	2.93E+02	2.93E+02	2.93E+02	2.93E+02	2.93E+02	2.93E+02	2.93E+02	2.93E+02	2.93E+02
2	2.93E+02	2.93E+02	2.93E+02	2.93E+02	2.93E+02	2.93E+02	2.93E+02	2.93E+02	2.93E+02	2.93E+02	2.93E+02	2.93E+02
1	2.93E+02	2.93E+02	2.93E+02	2.93E+02	2.93E+02	2.93E+02	2.93E+02	2.93E+02	2.93E+02	2.93E+02	2.93E+02	2.93E+02
0	2.93E+02	2.93E+02	2.93E+02	2.93E+02	2.93E+02	2.93E+02	2.93E+02	2.93E+02	2.93E+02	2.93E+02	2.93E+02	2.93E+02
I =	72	73	74	75	76	77	78	79	80	81	82	83

J

0	1.16E+03	1.14E+03	1.11E+03	1.09E+03	1.07E+03	1.05E+03	8.47E+02	3.38E+02	3.10E+02	3.62E+02	3.80E+02	3.80E+02
30	1.00E+02	1.00E+02	1.00E+02	1.00E+02	1.00E+02	1.00E+02	1.00E+02	3.02E+02	2.98E+02	1.00E+02	1.00E+02	1.00E+02

29	1.00E+02	1.00E+02	1.00E+02	1.00E+02	1.00E+02	1.00E+02	1.00E+02	2.98E+02	2.98E+02	2.97E+02	2.97E+02	2.96E+02
28	2.93E+02	2.93E+02	2.93E+02	1.00E+02	1.00E+02	1.00E+02	1.00E+02	2.98E+02	2.97E+02	2.97E+02	2.97E+02	2.96E+02
27	2.93E+02	2.93E+02	2.93E+02	1.00E+02	1.00E+02	1.00E+02	1.00E+02	2.97E+02	2.97E+02	2.97E+02	2.97E+02	2.97E+02
26	2.93E+02	2.93E+02	2.93E+02	1.00E+02	1.00E+02	1.00E+02	1.00E+02	2.97E+02	2.97E+02	2.97E+02	2.97E+02	2.97E+02
25	2.93E+02	2.93E+02	2.93E+02	1.00E+02	1.00E+02	1.00E+02	1.00E+02	2.97E+02	2.97E+02	2.97E+02	2.97E+02	2.97E+02
24	2.93E+02	2.93E+02	2.93E+02	1.00E+02	1.00E+02	1.00E+02	1.00E+02	2.97E+02	2.97E+02	2.97E+02	2.97E+02	2.97E+02
23	2.93E+02	2.93E+02	2.93E+02	1.00E+02	1.00E+02	1.00E+02	1.00E+02	2.97E+02	2.97E+02	2.97E+02	2.96E+02	2.96E+02
22	2.93E+02	2.93E+02	2.93E+02	1.00E+02	1.00E+02	1.00E+02	1.00E+02	2.97E+02	2.97E+02	2.97E+02	2.96E+02	2.96E+02
21	2.93E+02	2.93E+02	2.93E+02	1.00E+02	1.00E+02	1.00E+02	1.00E+02	2.96E+02	2.97E+02	2.97E+02	2.96E+02	2.96E+02
20	2.93E+02	2.93E+02	2.93E+02	1.00E+02	1.00E+02	1.00E+02	1.00E+02	2.96E+02	2.96E+02	2.96E+02	2.96E+02	2.96E+02
19	2.93E+02	2.93E+02	2.93E+02	1.00E+02	1.00E+02	1.00E+02	1.00E+02	2.96E+02	2.96E+02	2.96E+02	2.96E+02	2.95E+02
18	2.93E+02	2.93E+02	2.93E+02	1.00E+02	1.00E+02	1.00E+02	1.00E+02	2.96E+02	2.96E+02	2.96E+02	2.95E+02	2.95E+02
17	2.93E+02	2.93E+02	2.93E+02	1.00E+02	1.00E+02	1.00E+02	1.00E+02	2.95E+02	2.96E+02	2.96E+02	2.95E+02	2.95E+02
16	2.93E+02	2.93E+02	2.93E+02	1.00E+02	1.00E+02	1.00E+02	1.00E+02	2.95E+02	2.96E+02	2.96E+02	2.95E+02	2.95E+02
15	2.93E+02	2.93E+02	2.93E+02	1.00E+02	1.00E+02	1.00E+02	1.00E+02	2.95E+02	2.96E+02	2.96E+02	2.96E+02	2.95E+02
14	2.93E+02	2.93E+02	2.93E+02	1.00E+02	1.00E+02	1.00E+02	1.00E+02	2.95E+02	2.95E+02	2.95E+02	2.96E+02	2.95E+02
13	2.93E+02	2.93E+02	2.93E+02	1.00E+02	1.00E+02	1.00E+02	1.00E+02	2.95E+02	2.95E+02	2.95E+02	2.95E+02	2.95E+02
12	2.93E+02	2.93E+02	2.93E+02	1.00E+02	1.00E+02	1.00E+02	1.00E+02	2.94E+02	2.95E+02	2.95E+02	2.95E+02	2.95E+02
11	2.93E+02	2.93E+02	2.93E+02	1.00E+02	1.00E+02	1.00E+02	1.00E+02	2.94E+02	2.95E+02	2.95E+02	2.95E+02	2.95E+02
10	2.93E+02	2.93E+02	2.93E+02	1.00E+02	1.00E+02	1.00E+02	1.00E+02	2.94E+02	2.94E+02	2.94E+02	2.95E+02	2.94E+02
9	2.93E+02	2.93E+02	2.93E+02	1.00E+02	1.00E+02	1.00E+02	1.00E+02	2.94E+02	2.94E+02	2.94E+02	2.94E+02	2.94E+02
8	2.93E+02	2.93E+02	2.93E+02	1.00E+02	1.00E+02	1.00E+02	1.00E+02	2.94E+02	2.94E+02	2.94E+02	2.94E+02	2.94E+02
7	2.93E+02	2.93E+02	2.93E+02	1.00E+02	1.00E+02	1.00E+02	1.00E+02	2.93E+02	2.94E+02	2.94E+02	2.94E+02	2.94E+02
6	2.93E+02	2.93E+02	2.93E+02	1.00E+02	1.00E+02	1.00E+02	1.00E+02	2.93E+02	2.94E+02	2.94E+02	2.94E+02	2.94E+02
5	2.93E+02	2.93E+02	2.93E+02	1.00E+02	1.00E+02	1.00E+02	1.00E+02	2.93E+02	2.94E+02	2.93E+02	2.93E+02	2.94E+02
4	2.93E+02	2.93E+02	2.93E+02	1.00E+02	1.00E+02	1.00E+02	1.00E+02	2.93E+02	2.93E+02	2.93E+02	2.93E+02	2.93E+02
3	2.93E+02	2.93E+02	2.93E+02	1.00E+02	1.00E+02	1.00E+02	1.00E+02	2.93E+02	2.93E+02	2.93E+02	2.93E+02	2.93E+02
2	2.93E+02	2.93E+02	2.93E+02	1.00E+02	1.00E+02	1.00E+02	1.00E+02	2.93E+02	2.93E+02	2.93E+02	2.93E+02	2.93E+02
1	2.93E+02	2.93E+02	2.93E+02	1.00E+02	1.00E+02	1.00E+02	1.00E+02	2.93E+02	2.93E+02	2.93E+02	2.93E+02	2.93E+02
0	2.93E+02	2.93E+02	2.93E+02	2.88E+02	2.88E+02	2.88E+02	2.88E+02	2.93E+02	2.93E+02	2.93E+02	2.93E+02	2.93E+02
I =	84	85	86	87	88	89	90	91	92	93	94	95

J

0	3.80E+02	3.82E+02	3.83E+02	3.84E+02	3.82E+02	2.88E+02
30	1.00E+02	1.00E+02	1.00E+02	1.00E+02	1.00E+02	2.88E+02
29	2.96E+02	1.00E+02	1.00E+02	1.00E+02	1.00E+02	2.88E+02
28	2.94E+02	1.00E+02	1.00E+02	1.00E+02	1.00E+02	2.88E+02
27	2.95E+02	1.00E+02	1.00E+02	1.00E+02	1.00E+02	2.88E+02
26	2.95E+02	1.00E+02	1.00E+02	1.00E+02	1.00E+02	2.88E+02
25	2.96E+02	1.00E+02	1.00E+02	1.00E+02	1.00E+02	2.88E+02
24	2.95E+02	1.00E+02	1.00E+02	1.00E+02	1.00E+02	2.88E+02
23	2.95E+02	1.00E+02	1.00E+02	1.00E+02	1.00E+02	2.88E+02
22	2.96E+02	1.00E+02	1.00E+02	1.00E+02	1.00E+02	2.88E+02
21	2.95E+02	1.00E+02	1.00E+02	1.00E+02	1.00E+02	2.88E+02
20	2.95E+02	1.00E+02	1.00E+02	1.00E+02	1.00E+02	2.88E+02
19	2.95E+02	1.00E+02	1.00E+02	1.00E+02	1.00E+02	2.88E+02
18	2.95E+02	1.00E+02	1.00E+02	1.00E+02	1.00E+02	2.88E+02
17	2.94E+02	1.00E+02	1.00E+02	1.00E+02	1.00E+02	2.88E+02
16	2.94E+02	1.00E+02	1.00E+02	1.00E+02	1.00E+02	2.88E+02
15	2.94E+02	1.00E+02	1.00E+02	1.00E+02	1.00E+02	2.88E+02
14	2.94E+02	1.00E+02	1.00E+02	1.00E+02	1.00E+02	2.88E+02
13	2.95E+02	1.00E+02	1.00E+02	1.00E+02	1.00E+02	2.88E+02
12	2.94E+02	1.00E+02	1.00E+02	1.00E+02	1.00E+02	2.88E+02
11	2.94E+02	1.00E+02	1.00E+02	1.00E+02	1.00E+02	2.88E+02
10	2.94E+02	1.00E+02	1.00E+02	1.00E+02	1.00E+02	2.88E+02
9	2.94E+02	1.00E+02	1.00E+02	1.00E+02	1.00E+02	2.88E+02
8	2.94E+02	1.00E+02	1.00E+02	1.00E+02	1.00E+02	2.88E+02
7	2.94E+02	1.00E+02	1.00E+02	1.00E+02	1.00E+02	2.88E+02
6	2.93E+02	1.00E+02	1.00E+02	1.00E+02	1.00E+02	2.88E+02
5	2.93E+02	1.00E+02	1.00E+02	1.00E+02	1.00E+02	2.88E+02
4	2.93E+02	1.00E+02	1.00E+02	1.00E+02	1.00E+02	2.88E+02
3	2.93E+02	1.00E+02	1.00E+02	1.00E+02	1.00E+02	2.88E+02
2	2.93E+02	1.00E+02	1.00E+02	1.00E+02	1.00E+02	2.88E+02
1	2.93E+02	1.00E+02	1.00E+02	1.00E+02	1.00E+02	2.88E+02
0	2.93E+02	2.88E+02	2.88E+02	2.88E+02	2.88E+02	2.88E+02
I =	96	97	98	99	100	0

--*- BLOCK-NUMBER-2 PLANE K = 1 TEMPERATURE (KELVIN) -*-*-*-

J

0	2.88E+02	2.93E+02	2.93E+02	2.93E+02	2.93E+02	2.93E+02	2.93E+02	2.93E+02	2.93E+02	2.94E+02	2.94E+02	2.94E+02
40	2.93E+02	2.93E+02	2.93E+02	2.93E+02	2.93E+02	2.93E+02	2.93E+02	2.93E+02	2.94E+02	2.94E+02	2.94E+02	2.95E+02
39	2.93E+02	2.93E+02	2.93E+02	2.93E+02	2.93E+02	2.93E+02	2.93E+02	2.94E+02	2.94E+02	2.94E+02	2.95E+02	2.95E+02
38	2.93E+02	2.93E+02	2.93E+02	2.93E+02	2.93E+02	2.93E+02	2.94E+02	2.94E+02	2.94E+02	2.95E+02	2.95E+02	2.95E+02
37	2.93E+02	2.93E+02	2.93E+02	2.93E+02	2.93E+02	2.94E+02	2.94E+02	2.94E+02	2.94E+02	2.95E+02	2.95E+02	2.95E+02
36	2.93E+02	2.93E+02	2.93E+02	2.93E+02	2.93E+02	2.94E+02	2.94E+02	2.94E+02	2.94E+02	2.95E+02	2.95E+02	2.95E+02
35	2.93E+02	2.93E+02	2.93E+02	2.93E+02	2.93E+02	2.94E+02	2.94E+02	2.94E+02	2.94E+02	2.94E+02	2.95E+02	2.95E+02
34	2.93E+02	2.93E+02	2.93E+02	2.93E+02	2.93E+02	2.94E+02	2.94E+02	2.94E+02	2.94E+02	2.94E+02	2.95E+02	2.95E+02
33	2.93E+02	2.93E+02	2.93E+02	2.93E+02	2.93E+02	2.93E+02	2.94E+02	2.94E+02	2.94E+02	2.94E+02	2.94E+02	2.95E+02
32	2.93E+02	2.93E+02	2.93E+02	2.93E+02	2.93E+02	2.93E+02	2.94E+02	2.94E+02	2.94E+02	2.94E+02	2.94E+02	2.94E+02
31	2.93E+02	2.93E+02	2.93E+02	2.93E+02	2.93E+02	2.93E+02	2.93E+02	2.94E+02	2.94E+02	2.94E+02	2.94E+02	2.94E+02
30	2.93E+02	2.93E+02	2.93E+02	2.93E+02	2.93E+02	2.93E+02	2.93E+02	2.93E+02	2.94E+02	2.94E+02	2.94E+02	2.94E+02
29	2.93E+02	2.93E+02	2.93E+02	2.93E+02	2.93E+02	2.93E+02	2.93E+02	2.93E+02	2.94E+02	2.94E+02	2.94E+02	2.94E+02
28	2.93E+02	2.93E+02	2.93E+02	2.93E+02	2.93E+02	2.93E+02	2.93E+02	2.93E+02	2.93E+02	2.94E+02	2.94E+02	2.94E+02
27	2.93E+02	2.93E+02	2.93E+02	2.93E+02	2.93E+02	2.93E+02	2.93E+02	2.93E+02	2.93E+02	2.93E+02	2.94E+02	2.94E+02
26	2.93E+02	2.93E+02	2.93E+02	2.93E+02	2.93E+02	2.93E+02	2.93E+02	2.93E+02	2.93E+02	2.93E+02	2.94E+02	2.94E+02
25	2.93E+02	2.93E+02	2.93E+02	2.93E+02	2.93E+02	2.93E+02	2.93E+02	2.93E+02	2.93E+02	2.93E+02	2.94E+02	2.94E+02
24	2.93E+02	2.93E+02	2.93E+02	2.93E+02	2.93E+02	2.93E+02	2.93E+02	2.93E+02	2.93E+02	2.93E+02	2.94E+02	2.94E+02
23	2.93E+02	2.93E+02	2.93E+02	2.93E+02	2.93E+02	2.93E+02	2.93E+02	2.93E+02	2.94E+02	2.94E+02	2.94E+02	2.94E+02
22	2.93E+02	2.93E+02	2.93E+02	2.93E+02	2.93E+02	2.93E+02	2.94E+02	2.94E+02	2.94E+02	2.94E+02	2.94E+02	2.94E+02
21	2.93E+02	2.93E+02	2.93E+02	2.93E+02	2.93E+02	2.94E+02	2.94E+02	2.94E+02	2.94E+02	2.94E+02	2.94E+02	2.94E+02
20	2.93E+02	2.93E+02	2.93E+02	2.93E+02	2.94E+02	2.94E+02	2.94E+02	2.94E+02	2.94E+02	2.94E+02	2.94E+02	2.94E+02
19	2.93E+02	2.93E+02	2.93E+02	2.94E+02	2.94E+02	2.94E+02	2.94E+02	2.94E+02	2.94E+02	2.94E+02	2.94E+02	2.94E+02
18	2.93E+02	2.93E+02	2.93E+02	2.94E+02	2.94E+02	2.94E+02	2.94E+02	2.94E+02	2.94E+02	2.94E+02	2.94E+02	2.95E+02
17	2.93E+02	2.93E+02	2.94E+02	2.94E+02	2.94E+02	2.94E+02	2.94E+02	2.94E+02	2.94E+02	2.94E+02	2.95E+02	2.95E+02
16	2.93E+02	2.93E+02	2.94E+02	2.94E+02	2.94E+02	2.94E+02	2.94E+02	2.94E+02	2.94E+02	2.94E+02	2.95E+02	2.95E+02
15	2.93E+02	2.93E+02	2.94E+02	2.94E+02	2.94E+02	2.94E+02	2.94E+02	2.94E+02	2.94E+02	2.94E+02	2.95E+02	2.95E+02
14	2.93E+02	2.93E+02	2.94E+02	2.94E+02	2.94E+02	2.94E+02	2.94E+02	2.94E+02	2.94E+02	2.94E+02	2.95E+02	2.95E+02
13	2.93E+02	2.93E+02	2.94E+02	2.94E+02	2.94E+02	2.94E+02	2.94E+02	2.94E+02	2.94E+02	2.94E+02	2.94E+02	2.95E+02
12	2.93E+02	2.93E+02	2.94E+02	2.94E+02	2.94E+02	2.94E+02	2.94E+02	2.94E+02	2.94E+02	2.94E+02	2.94E+02	2.95E+02
11	2.93E+02	2.93E+02	2.93E+02	2.94E+02	2.94E+02	2.94E+02	2.94E+02	2.94E+02	2.94E+02	2.94E+02	2.94E+02	2.94E+02
10	2.93E+02	2.93E+02	2.93E+02	2.94E+02	2.94E+02	2.94E+02	2.94E+02	2.94E+02	2.94E+02	2.94E+02	2.94E+02	2.94E+02
9	2.93E+02	2.93E+02	2.93E+02	2.94E+02	2.94E+02	2.94E+02	2.94E+02	2.94E+02	2.94E+02	2.94E+02	2.94E+02	2.94E+02
8	2.93E+02	2.93E+02	2.93E+02	2.93E+02	2.94E+02	2.94E+02	2.94E+02	2.94E+02	2.94E+02	2.94E+02	2.94E+02	2.94E+02
7	2.93E+02	2.93E+02	2.93E+02	2.93E+02	2.94E+02	2.94E+02	2.94E+02	2.94E+02	2.94E+02	2.94E+02	2.94E+02	2.94E+02
6	2.93E+02	2.93E+02	2.93E+02	2.93E+02	2.93E+02	2.93E+02	2.94E+02	2.94E+02	2.94E+02	2.94E+02	2.94E+02	2.94E+02
5	2.93E+02	2.93E+02	2.93E+02	2.93E+02	2.93E+02	2.93E+02	2.93E+02	2.93E+02	2.94E+02	2.94E+02	2.94E+02	2.94E+02
4	2.93E+02	2.93E+02	2.93E+02	2.93E+02	2.93E+02	2.93E+02	2.93E+02	2.93E+02	2.93E+02	2.94E+02	2.94E+02	2.94E+02
3	2.93E+02	2.93E+02	2.93E+02	2.93E+02	2.93E+02	2.93E+02	2.93E+02	2.93E+02	2.93E+02	2.93E+02	2.94E+02	2.94E+02
2	2.93E+02	2.93E+02	2.93E+02	2.93E+02	2.93E+02	2.93E+02	2.93E+02	2.93E+02	2.93E+02	2.93E+02	2.94E+02	2.94E+02
1	2.93E+02	2.93E+02	2.93E+02	2.93E+02	2.93E+02	2.93E+02	2.93E+02	2.93E+02	2.94E+02	2.94E+02	2.94E+02	2.94E+02
0	2.88E+02	1.00E+02	1.00E+02	1.00E+02	1.00E+02	1.00E+02	1.00E+02	1.00E+02	1.00E+02	1.00E+02	1.00E+02	1.00E+02
I=	0	1	2	3	4	5	6	7	8	9	10	11

J

0	2.95E+02	2.95E+02	2.96E+02	2.97E+02	2.98E+02	2.99E+02	3.01E+02	3.02E+02	3.04E+02	3.06E+02	3.09E+02	3.11E+02
40	2.95E+02	2.96E+02	2.97E+02	2.98E+02	2.99E+02	3.00E+02	3.02E+02	3.03E+02	3.05E+02	3.07E+02	3.09E+02	3.11E+02
39	2.96E+02	2.97E+02	2.97E+02	2.98E+02	3.00E+02	3.01E+02	3.02E+02	3.04E+02	3.05E+02	3.07E+02	3.09E+02	3.11E+02
38	2.96E+02	2.97E+02	2.98E+02	2.99E+02	3.00E+02	3.01E+02	3.02E+02	3.03E+02	3.05E+02	3.07E+02	3.08E+02	3.10E+02
37	2.96E+02	2.97E+02	2.97E+02	2.98E+02	2.99E+02	3.00E+02	3.01E+02	3.03E+02	3.04E+02	3.06E+02	3.07E+02	3.09E+02
36	2.96E+02	2.96E+02	2.97E+02	2.98E+02	2.99E+02	3.00E+02	3.01E+02	3.02E+02	3.03E+02	3.04E+02	3.06E+02	3.07E+02
35	2.96E+02	2.96E+02	2.97E+02	2.97E+02	2.98E+02	2.99E+02	3.00E+02	3.01E+02	3.02E+02	3.03E+02	3.04E+02	3.05E+02
34	2.95E+02	2.96E+02	2.96E+02	2.97E+02	2.97E+02	2.98E+02	2.99E+02	3.00E+02	3.00E+02	3.01E+02	3.02E+02	3.03E+02
33	2.95E+02	2.95E+02	2.96E+02	2.96E+02	2.97E+02	2.97E+02	2.98E+02	2.99E+02	2.99E+02	3.00E+02	3.01E+02	3.02E+02
32	2.95E+02	2.95E+02	2.95E+02	2.96E+02	2.96E+02	2.97E+02	2.97E+02	2.98E+02	2.98E+02	2.99E+02	2.99E+02	3.00E+02
31	2.94E+02	2.95E+02	2.95E+02	2.95E+02	2.96E+02	2.96E+02	2.96E+02	2.97E+02	2.97E+02	2.98E+02	2.98E+02	2.99E+02
30	2.94E+02	2.94E+02	2.95E+02	2.95E+02	2.95E+02	2.95E+02	2.96E+02	2.96E+02	2.97E+02	2.97E+02	2.97E+02	2.98E+02
29	2.94E+02	2.94E+02	2.94E+02	2.95E+02	2.95E+02	2.95E+02	2.95E+02	2.96E+02	2.96E+02	2.96E+02	2.97E+02	2.97E+02
28	2.94E+02	2.94E+02	2.94E+02	2.94E+02	2.94E+02	2.95E+02	2.95E+02	2.95E+02	2.95E+02	2.96E+02	2.96E+02	2.96E+02
27	2.94E+02	2.94E+02	2.94E+02	2.94E+02	2.94E+02	2.94E+02	2.95E+02	2.95E+02	2.95E+02	2.95E+02	2.95E+02	2.96E+02
26	2.94E+02	2.94E+02	2.94E+02	2.94E+02	2.94E+02	2.94E+02	2.94E+02	2.95E+02	2.95E+02	2.95E+02	2.95E+02	2.95E+02
25	2.94E+02	2.94E+02	2.94E+02	2.94E+02	2.94E+02	2.94E+02	2.94E+02	2.94E+02	2.95E+02	2.95E+02	2.95E+02	2.95E+02
24	2.94E+02	2.94E+02	2.94E+02	2.94E+02	2.94E+02	2.94E+02	2.94E+02	2.94E+02	2.94E+02	2.95E+02	2.95E+02	2.95E+02
23	2.94E+02	2.94E+02	2.94E+02	2.94E+02	2.94E+02	2.94E+02	2.94E+02	2.94E+02	2.94E+02	2.95E+02	2.95E+02	2.95E+02
22	2.94E+02	2.94E+02	2.94E+02	2.94E+02	2.94E+02	2.94E+02	2.94E+02	2.94E+02	2.95E+02	2.95E+02	2.95E+02	2.95E+02
21	2.94E+02	2.94E+02	2.94E+02	2.94E+02	2.94E+02	2.94E+02	2.95E+02	2.95E+02	2.95E+02	2.95E+02	2.95E+02	2.95E+02
20	2.94E+02	2.94E+02	2.94E+02	2.95E+02	2.95E+02	2.95E+02	2.95E+02	2.95E+02	2.95E+02	2.95E+02	2.95E+02	2.95E+02
19	2.94E+02	2.95E+02	2.95E+02	2.95E+02	2.95E+02	2.95E+02	2.95E+02	2.95E+02	2.95E+02	2.95E+02	2.95E+02	2.95E+02

18	2.95E+02	2.95E+02	2.95E+02	2.95E+02	2.95E+02	2.95E+02	2.95E+02	2.95E+02	2.95E+02	2.95E+02	2.95E+02	2.95E+02	2.96E-02
17	2.95E+02	2.95E+02	2.95E+02	2.95E+02	2.95E+02	2.95E+02	2.95E+02	2.95E+02	2.95E+02	2.95E+02	2.96E+02	2.96E-02	2.96E-02
16	2.95E+02	2.95E+02	2.95E+02	2.95E+02	2.95E-02	2.95E+02	2.95E+02	2.95E+02	2.95E+02	2.96E+02	2.96E+02	2.96E-02	2.96E-02
15	2.95E+02	2.95E+02	2.95E+02	2.95E+02	2.95E-02	2.95E+02	2.95E+02	2.95E-02	2.96E+02	2.96E+02	2.96E-02	2.96E-02	
14	2.95E+02	2.95E+02	2.95E+02	2.95E+02	2.95E+02	2.95E+02	2.95E+02	2.95E+02	2.96E+02	2.96E+02	2.96E-02	2.96E-02	
13	2.95E+02	2.95E+02	2.95E+02	2.95E+02	2.95E+02	2.95E-02	2.95E+02	2.95E+02	2.96E+02	2.96E-02	2.96E-02	2.96E-02	
12	2.95E+02	2.95E+02	2.95E+02	2.95E+02	2.95E-02	2.95E+02	2.95E-02	2.95E+02	2.95E+02	2.96E+02	2.96E+02	2.96E-02	
11	2.95E+02	2.95E+02	2.95E+02	2.95E+02	2.95E+02	2.95E+02	2.95E+02	2.95E+02	2.95E+02	2.95E+02	2.96E+02	2.96E-02	2.96E-02
10	2.94E+02	2.95E+02	2.95E+02	2.95E+02	2.95E+02	2.95E+02	2.95E+02	2.95E+02	2.95E+02	2.95E+02	2.95E-02	2.96E-02	2.96E-02
9	2.94E+02	2.94E+02	2.95E+02	2.95E+02	2.95E+02	2.95E+02	2.95E+02	2.95E+02	2.95E+02	2.95E+02	2.95E+02	2.95E+02	2.95E+02
8	2.94E+02	2.94E+02	2.94E+02	2.94E+02	2.95E+02	2.95E+02	2.95E+02	2.95E+02	2.95E+02	2.95E-02	2.95E-02	2.95E-02	
7	2.94E+02	2.94E+02	2.94E+02	2.94E+02	2.94E+02	2.94E+02	2.94E+02	2.95E+02	2.95E+02	2.95E+02	2.95E-02	2.95E-02	
6	2.94E+02	2.94E+02	2.94E+02	2.94E+02	2.94E+02	2.94E+02	2.94E+02	2.94E+02	2.94E+02	2.94E+02	2.95E+02	2.95E-02	
5	2.94E+02	2.94E+02	2.94E+02	2.94E+02	2.94E+02	2.94E+02	2.94E+02	2.94E+02	2.94E+02	2.94E+02	2.94E+02	2.94E-02	
4	2.94E+02	2.94E+02	2.94E+02	2.94E+02	2.94E+02	2.94E+02	2.94E+02	2.94E+02	2.94E+02	2.94E-02	2.94E+02	2.94E-02	
3	2.94E+02	2.94E+02	2.94E+02	2.94E+02	2.94E+02	2.94E+02	2.94E+02	2.94E+02	2.94E+02	2.94E+02	2.94E+02	2.94E+02	
2	2.94E+02	2.94E+02	2.94E+02	2.94E+02	2.94E+02	2.94E+02	2.94E+02	2.94E+02	2.94E+02	2.94E+02	2.94E+02	2.94E-02	
1	2.94E+02	2.94E+02	2.94E+02	2.94E+02	2.94E+02	2.94E+02	2.94E+02	2.94E+02	2.94E+02	2.94E+02	2.94E+02	2.94E-02	
0	1.00E+02	1.00E+02	1.00E+02	1.00E+02	1.00E+02	1.00E+02	1.00E+02	1.00E+02	1.00E+02	1.00E+02	1.00E+02	1.00E+02	
I =	12	13	14	15	16	17	18	19	20	21	22	23	

J

0	3.14E+02	3.16E+02	3.19E+02	3.23E+02	3.26E+02	3.30E+02	3.34E+02	3.38E+02	3.42E+02	3.46E+02	3.51E+02	3.56E+02	
40	3.14E+02	3.16E+02	3.19E+02	3.22E+02	3.25E+02	3.28E+02	3.32E+02	3.35E+02	3.39E+02	3.43E+02	3.47E+02	3.51E+02	
39	3.13E+02	3.16E+02	3.18E+02	3.21E+02	3.24E+02	3.27E+02	3.30E+02	3.33E+02	3.36E+02	3.40E+02	3.43E+02	3.47E+02	
38	3.12E+02	3.14E+02	3.17E+02	3.19E+02	3.22E+02	3.24E+02	3.27E+02	3.30E+02	3.33E+02	3.35E+02	3.38E+02	3.41E+02	
37	3.11E+02	3.13E+02	3.15E+02	3.17E+02	3.19E+02	3.21E+02	3.23E+02	3.26E+02	3.28E+02	3.31E+02	3.33E+02	3.36E+02	
36	3.09E+02	3.10E+02	3.12E+02	3.14E+02	3.16E+02	3.18E+02	3.20E+02	3.22E+02	3.24E+02	3.26E+02	3.28E+02	3.30E+02	
35	3.07E+02	3.08E+02	3.09E+02	3.11E+02	3.13E+02	3.14E+02	3.16E+02	3.18E+02	3.20E+02	3.21E+02	3.23E+02	3.25E+02	
34	3.04E+02	3.06E+02	3.07E+02	3.08E+02	3.10E+02	3.11E+02	3.12E+02	3.14E+02	3.15E+02	3.17E+02	3.19E+02	3.20E+02	
33	3.03E+02	3.04E+02	3.05E+02	3.06E+02	3.07E+02	3.08E+02	3.09E+02	3.11E+02	3.12E+02	3.13E+02	3.14E+02	3.16E+02	
32	3.01E+02	3.02E+02	3.03E+02	3.04E+02	3.04E+02	3.05E+02	3.06E+02	3.07E+02	3.09E+02	3.10E+02	3.11E+02	3.12E+02	
31	3.00E+02	3.00E+02	3.01E+02	3.02E+02	3.02E+02	3.03E+02	3.04E+02	3.05E+02	3.06E+02	3.07E+02	3.08E+02	3.09E+02	
30	2.98E+02	2.99E+02	3.00E+02	3.00E+02	3.01E+02	3.01E+02	3.02E+02	3.03E+02	3.04E+02	3.04E+02	3.05E+02	3.06E+02	
29	2.97E+02	2.98E+02	2.98E+02	2.99E+02	2.99E+02	3.00E+02	3.00E+02	3.01E+02	3.02E+02	3.02E+02	3.03E+02	3.04E+02	
28	2.97E+02	2.97E+02	2.97E+02	2.98E+02	2.98E+02	2.99E+02	2.99E+02	3.00E+02	3.00E+02	3.01E+02	3.01E+02	3.02E+02	
27	2.96E+02	2.96E+02	2.97E+02	2.97E+02	2.97E+02	2.98E+02	2.98E+02	2.99E+02	2.99E+02	2.99E+02	3.00E+02	3.00E+02	
26	2.96E+02	2.96E+02	2.96E+02	2.96E+02	2.97E+02	2.97E+02	2.97E+02	2.98E+02	2.98E+02	2.98E+02	2.99E+02	2.99E+02	
25	2.95E+02	2.95E+02	2.96E+02	2.96E+02	2.96E+02	2.96E+02	2.97E+02	2.97E+02	2.97E+02	2.98E+02	2.98E+02	2.98E+02	
24	2.95E+02	2.95E+02	2.95E+02	2.96E+02	2.96E+02	2.96E+02	2.96E+02	2.97E+02	2.97E+02	2.97E+02	2.97E+02	2.98E+02	
23	2.95E+02	2.95E+02	2.95E+02	2.95E+02	2.96E+02	2.96E+02	2.96E+02	2.96E+02	2.96E+02	2.97E+02	2.97E+02	2.97E+02	
22	2.95E+02	2.95E+02	2.95E+02	2.95E+02	2.96E+02	2.96E+02	2.96E+02	2.96E+02	2.96E+02	2.96E+02	2.97E+02	2.97E+02	
21	2.95E+02	2.95E+02	2.95E+02	2.95E+02	2.96E+02	2.96E+02	2.96E+02	2.96E+02	2.96E+02	2.96E+02	2.97E+02	2.97E+02	
20	2.95E+02	2.95E+02	2.95E+02	2.96E+02	2.96E+02	2.96E+02	2.96E+02	2.96E+02	2.96E+02	2.96E+02	2.97E+02	2.97E+02	
19	2.95E+02	2.96E+02	2.96E+02	2.96E+02	2.96E+02	2.96E+02	2.96E+02	2.96E+02	2.96E+02	2.96E+02	2.97E+02	2.97E+02	
18	2.96E+02	2.96E+02	2.96E+02	2.96E+02	2.96E+02	2.96E+02	2.96E+02	2.96E+02	2.96E+02	2.97E+02	2.97E+02	2.97E+02	
17	2.96E+02	2.96E+02	2.96E+02	2.96E+02	2.96E+02	2.96E+02	2.96E+02	2.97E+02	2.97E+02	2.97E+02	2.97E+02	2.97E+02	
16	2.96E+02	2.96E+02	2.96E+02	2.96E+02	2.96E+02	2.96E+02	2.97E+02	2.97E+02	2.97E+02	2.97E+02	2.97E+02	2.97E+02	
15	2.96E+02	2.96E+02	2.96E+02	2.96E+02	2.96E+02	2.97E+02	2.97E+02	2.97E+02	2.97E+02	2.97E+02	2.97E+02	2.97E+02	
14	2.96E+02	2.96E+02	2.96E+02	2.96E+02	2.96E+02	2.97E+02	2.97E+02	2.97E+02	2.97E+02	2.97E+02	2.97E+02	2.97E+02	
13	2.96E+02	2.96E+02	2.96E+02	2.96E+02	2.96E+02	2.97E+02	2.97E+02	2.97E+02	2.97E+02	2.97E+02	2.97E+02	2.97E+02	
12	2.96E+02	2.96E+02	2.96E+02	2.96E+02	2.96E+02	2.97E+02	2.97E+02	2.97E+02	2.97E+02	2.97E+02	2.97E+02	2.97E+02	
11	2.96E+02	2.96E+02	2.96E+02	2.96E+02	2.96E+02	2.97E+02	2.97E+02	2.97E+02	2.97E+02	2.97E+02	2.97E+02	2.97E+02	
10	2.96E+02	2.96E+02	2.96E+02	2.96E+02	2.96E+02	2.96E+02	2.97E+02	2.97E+02	2.97E+02	2.97E+02	2.97E+02	2.97E+02	
9	2.96E+02	2.96E+02	2.96E+02	2.96E+02	2.96E+02	2.96E+02	2.96E+02	2.96E+02	2.97E+02	2.97E+02	2.97E+02	2.97E+02	
8	2.95E+02	2.95E+02	2.96E+02	2.96E+02	2.96E+02	2.96E+02	2.96E+02	2.96E+02	2.96E+02	2.96E+02	2.97E+02	2.97E+02	
7	2.95E+02	2.95E+02	2.95E+02	2.95E+02	2.95E+02	2.96E+02	2.96E+02	2.96E+02	2.96E+02	2.96E+02	2.96E+02	2.96E+02	
6	2.95E+02	2.95E+02	2.95E+02	2.95E+02	2.95E+02	2.95E+02	2.95E+02	2.95E+02	2.96E+02	2.96E+02	2.96E+02	2.96E+02	
5	2.95E+02	2.95E+02	2.95E+02	2.95E+02	2.95E+02	2.95E+02	2.95E+02	2.95E+02	2.95E+02	2.95E+02	2.96E+02	2.96E+02	
4	2.94E+02	2.94E+02	2.94E+02	2.95E+02	2.95E+02	2.95E+02	2.95E+02	2.95E+02	2.95E+02	2.95E+02	2.95E+02	2.95E+02	
3	2.94E+02	2.94E+02	2.94E+02	2.94E+02	2.94E+02	2.95E+02	2.95E+02	2.95E+02	2.95E+02	2.95E+02	2.95E+02	2.95E+02	
2	2.94E+02	2.94E+02	2.94E+02	2.94E+02	2.94E+02	2.94E+02	2.95E+02	2.95E+02	2.95E+02	2.95E+02	2.95E+02	2.95E+02	
1	2.94E+02	2.94E+02	2.94E+02	2.94E+02	2.94E+02	2.94E+02	2.94E+02	2.94E+02	2.95E+02	2.95E+02	2.95E+02	2.95E+02	
0	1.00E+02	1.00E+02	1.00E+02	1.00E+02	1.00E+02	1.00E+02	1.00E+02	1.00E+02	1.00E+02	1.00E+02	1.00E+02	1.00E+02	
I =	24	25	26	27	28	29	30	31	32	33	34	35	

J

0	3.61E+02	3.66E+02	3.71E+02	3.76E+02	3.81E+02	3.86E+02	3.91E+02	3.96E+02	4.01E+02	4.05E+02	4.09E+02	4.13E+02	
40	3.55E+02	3.59E+02	3.64E+02	3.68E+02	3.72E+02	3.77E+02	3.81E+02	3.85E+02	3.89E+02	3.92E+02	3.96E+02	3.99E+02	

39	3.50E+02	3.54E+02	3.57E+02	3.61E+02	3.65E+02	3.68E+02	3.72E+02	3.75E+02	3.78E+02	3.81E+02	3.84E+02	3.87E+02
38	3.44E+02	3.48E+02	3.51E+02	3.54E+02	3.57E+02	3.60E+02	3.63E+02	3.65E+02	3.68E+02	3.71E+02	3.73E+02	3.75E+02
37	3.38E+02	3.41E+02	3.44E+02	3.46E+02	3.49E+02	3.51E+02	3.54E+02	3.56E+02	3.58E+02	3.61E+02	3.63E+02	3.65E+02
36	3.33E+02	3.35E+02	3.37E+02	3.39E+02	3.41E+02	3.44E+02	3.46E+02	3.48E+02	3.50E+02	3.51E+02	3.53E+02	3.55E+02
35	3.27E+02	3.29E+02	3.31E+02	3.33E+02	3.35E+02	3.36E+02	3.38E+02	3.40E+02	3.42E+02	3.43E+02	3.45E+02	3.46E+02
34	3.22E+02	3.23E+02	3.25E+02	3.27E+02	3.28E+02	3.30E+02	3.31E+02	3.33E+02	3.34E+02	3.36E+02	3.37E+02	3.38E+02
33	3.17E+02	3.19E+02	3.20E+02	3.21E+02	3.23E+02	3.24E+02	3.25E+02	3.27E+02	3.28E+02	3.29E+02	3.30E+02	3.32E+02
32	3.13E+02	3.14E+02	3.15E+02	3.17E+02	3.18E+02	3.19E+02	3.20E+02	3.21E+02	3.22E+02	3.24E+02	3.25E+02	3.26E+02
31	3.10E+02	3.11E+02	3.12E+02	3.13E+02	3.14E+02	3.15E+02	3.16E+02	3.17E+02	3.18E+02	3.19E+02	3.20E+02	3.21E+02
30	3.07E+02	3.08E+02	3.08E+02	3.09E+02	3.10E+02	3.11E+02	3.12E+02	3.13E+02	3.14E+02	3.14E+02	3.15E+02	3.16E+02
29	3.04E+02	3.05E+02	3.06E+02	3.06E+02	3.07E+02	3.08E+02	3.09E+02	3.09E+02	3.10E+02	3.11E+02	3.12E+02	3.13E+02
28	3.02E+02	3.03E+02	3.04E+02	3.04E+02	3.05E+02	3.05E+02	3.06E+02	3.07E+02	3.08E+02	3.08E+02	3.09E+02	3.10E+02
27	3.01E+02	3.01E+02	3.02E+02	3.02E+02	3.03E+02	3.04E+02	3.04E+02	3.05E+02	3.05E+02	3.06E+02	3.07E+02	3.07E+02
26	3.00E+02	3.00E+02	3.01E+02	3.01E+02	3.01E+02	3.02E+02	3.02E+02	3.03E+02	3.04E+02	3.04E+02	3.05E+02	3.05E+02
25	2.99E+02	2.99E+02	2.99E+02	3.00E+02	3.00E+02	3.01E+02	3.01E+02	3.02E+02	3.02E+02	3.03E+02	3.03E+02	3.04E+02
24	2.98E+02	2.98E+02	2.99E+02	2.99E+02	2.99E+02	3.00E+02	3.00E+02	3.01E+02	3.01E+02	3.01E+02	3.02E+02	3.02E+02
23	2.97E+02	2.98E+02	2.98E+02	2.98E+02	2.99E+02	2.99E+02	2.99E+02	3.00E+02	3.00E+02	3.01E+02	3.01E+02	3.01E+02
22	2.97E+02	2.97E+02	2.98E+02	2.98E+02	2.98E+02	2.99E+02	2.99E+02	2.99E+02	3.00E+02	3.00E+02	3.00E+02	3.01E+02
21	2.97E+02	2.97E+02	2.97E+02	2.98E+02	2.98E+02	2.98E+02	2.98E+02	2.99E+02	2.99E+02	2.99E+02	3.00E+02	3.00E+02
20	2.97E+02	2.97E+02	2.97E+02	2.98E+02	2.98E+02	2.98E+02	2.98E+02	2.98E+02	2.99E+02	2.99E+02	2.99E+02	3.00E+02
19	2.97E+02	2.97E+02	2.97E+02	2.97E+02	2.98E+02	2.98E+02	2.98E+02	2.98E+02	2.99E+02	2.99E+02	2.99E+02	2.99E+02
18	2.97E+02	2.97E+02	2.97E+02	2.97E+02	2.98E+02	2.98E+02	2.98E+02	2.98E+02	2.98E+02	2.99E+02	2.99E+02	2.99E+02
17	2.97E+02	2.97E+02	2.97E+02	2.98E+02	2.98E+02	2.98E+02	2.98E+02	2.98E+02	2.98E+02	2.99E+02	2.99E+02	2.99E+02
16	2.97E+02	2.97E+02	2.98E+02	2.98E+02	2.98E+02	2.98E+02	2.98E+02	2.98E+02	2.98E+02	2.99E+02	2.99E+02	2.99E+02
15	2.97E+02	2.97E+02	2.98E+02	2.98E+02	2.98E+02	2.98E+02	2.98E+02	2.98E+02	2.99E+02	2.99E+02	2.99E+02	2.99E+02
14	2.97E+02	2.98E+02	2.98E+02	2.98E+02	2.98E+02	2.98E+02	2.98E+02	2.98E+02	2.99E+02	2.99E+02	2.99E+02	2.99E+02
13	2.98E+02	2.98E+02	2.98E+02	2.98E+02	2.98E+02	2.98E+02	2.98E+02	2.99E+02	2.99E+02	2.99E+02	2.99E+02	2.99E+02
12	2.98E+02	2.98E+02	2.98E+02	2.98E+02	2.98E+02	2.98E+02	2.98E+02	2.99E+02	2.99E+02	2.99E+02	2.99E+02	2.99E+02
11	2.98E+02	2.98E+02	2.98E+02	2.98E+02	2.98E+02	2.98E+02	2.98E+02	2.99E+02	2.99E+02	2.99E+02	2.99E+02	2.99E+02
10	2.97E+02	2.98E+02	2.98E+02	2.98E+02	2.98E+02	2.98E+02	2.98E+02	2.99E+02	2.99E+02	2.99E+02	2.99E+02	2.99E+02
9	2.97E+02	2.97E+02	2.98E+02	2.98E+02	2.98E+02	2.98E+02	2.98E+02	2.98E+02	2.99E+02	2.99E+02	2.99E+02	2.99E+02
8	2.97E+02	2.97E+02	2.97E+02	2.97E+02	2.98E+02	2.98E+02	2.98E+02	2.98E+02	2.98E+02	2.98E+02	2.99E+02	2.99E+02
7	2.97E+02	2.97E+02	2.97E+02	2.97E+02	2.97E+02	2.97E+02	2.98E+02	2.98E+02	2.98E+02	2.98E+02	2.98E+02	2.98E+02
6	2.96E+02	2.96E+02	2.96E+02	2.97E+02	2.97E+02	2.97E+02	2.97E+02	2.97E+02	2.97E+02	2.98E+02	2.98E+02	2.98E+02
5	2.96E+02	2.96E+02	2.96E+02	2.96E+02	2.96E+02	2.96E+02	2.97E+02	2.97E+02	2.97E+02	2.97E+02	2.97E+02	2.97E+02
4	2.95E+02	2.96E+02	2.96E+02	2.96E+02	2.96E+02	2.96E+02	2.96E+02	2.96E+02	2.96E+02	2.97E+02	2.97E+02	2.97E+02
3	2.95E+02	2.95E+02	2.95E+02	2.95E+02	2.96E+02	2.96E+02	2.96E+02	2.96E+02	2.96E+02	2.96E+02	2.96E+02	2.96E+02
2	2.95E+02	2.95E+02	2.95E+02	2.95E+02	2.95E+02	2.95E+02	2.95E+02	2.96E+02	2.96E+02	2.96E+02	2.96E+02	2.96E+02
1	2.95E+02	2.95E+02	2.95E+02	2.95E+02	2.95E+02	2.95E+02	2.95E+02	2.95E+02	2.95E+02	2.95E+02	2.95E+02	2.95E+02
0	1.00E+02	1.00E+02	1.00E+02	1.00E+02	1.00E+02	1.00E+02	1.00E+02	1.00E+02	1.00E+02	1.00E+02	1.00E+02	1.00E+02
I =	36	37	38	39	40	41	42	43	44	45	46	47

J

0	4.16E+02	4.19E+02	4.22E+02	4.24E+02	4.25E+02	4.26E+02	4.27E+02	4.27E+02	4.26E+02	4.26E+02	4.24E+02	4.23E+02
40	4.02E+02	4.05E+02	4.07E+02	4.09E+02	4.10E+02	4.12E+02	4.12E+02	4.13E+02	4.13E+02	4.13E+02	4.12E+02	4.11E+02
39	3.89E+02	3.91E+02	3.93E+02	3.95E+02	3.96E+02	3.98E+02	3.98E+02	3.99E+02	3.99E+02	3.99E+02	3.98E+02	3.98E+02
38	3.77E+02	3.79E+02	3.81E+02	3.82E+02	3.84E+02	3.85E+02	3.85E+02	3.86E+02	3.86E+02	3.86E+02	3.86E+02	3.85E+02
37	3.66E+02	3.68E+02	3.70E+02	3.71E+02	3.72E+02	3.73E+02	3.74E+02	3.74E+02	3.74E+02	3.74E+02	3.74E+02	3.74E+02
36	3.57E+02	3.58E+02	3.59E+02	3.60E+02	3.61E+02	3.62E+02	3.63E+02	3.63E+02	3.64E+02	3.64E+02	3.64E+02	3.63E+02
35	3.48E+02	3.49E+02	3.50E+02	3.51E+02	3.52E+02	3.53E+02	3.54E+02	3.54E+02	3.54E+02	3.55E+02	3.55E+02	3.54E+02
34	3.40E+02	3.41E+02	3.42E+02	3.43E+02	3.44E+02	3.45E+02	3.45E+02	3.46E+02	3.46E+02	3.46E+02	3.47E+02	3.47E+02
33	3.33E+02	3.34E+02	3.35E+02	3.36E+02	3.37E+02	3.37E+02	3.38E+02	3.39E+02	3.39E+02	3.39E+02	3.40E+02	3.40E+02
32	3.27E+02	3.28E+02	3.29E+02	3.29E+02	3.30E+02	3.31E+02	3.32E+02	3.32E+02	3.33E+02	3.33E+02	3.34E+02	3.34E+02
31	3.21E+02	3.22E+02	3.23E+02	3.24E+02	3.25E+02	3.26E+02	3.26E+02	3.27E+02	3.28E+02	3.28E+02	3.29E+02	3.29E+02
30	3.17E+02	3.18E+02	3.19E+02	3.20E+02	3.20E+02	3.21E+02	3.22E+02	3.22E+02	3.23E+02	3.24E+02	3.24E+02	3.25E+02
29	3.13E+02	3.14E+02	3.15E+02	3.16E+02	3.16E+02	3.17E+02	3.18E+02	3.19E+02	3.19E+02	3.20E+02	3.20E+02	3.21E+02
28	3.10E+02	3.11E+02	3.12E+02	3.12E+02	3.13E+02	3.14E+02	3.15E+02	3.15E+02	3.16E+02	3.17E+02	3.17E+02	3.18E+02
27	3.08E+02	3.08E+02	3.09E+02	3.10E+02	3.10E+02	3.11E+02	3.12E+02	3.13E+02	3.13E+02	3.14E+02	3.15E+02	3.15E+02
26	3.06E+02	3.06E+02	3.07E+02	3.08E+02	3.08E+02	3.09E+02	3.10E+02	3.10E+02	3.11E+02	3.12E+02	3.12E+02	3.13E+02
25	3.04E+02	3.05E+02	3.05E+02	3.06E+02	3.07E+02	3.07E+02	3.08E+02	3.09E+02	3.09E+02	3.10E+02	3.11E+02	3.11E+02
24	3.03E+02	3.03E+02	3.04E+02	3.05E+02	3.05E+02	3.06E+02	3.06E+02	3.07E+02	3.08E+02	3.08E+02	3.09E+02	3.10E+02
23	3.02E+02	3.02E+02	3.03E+02	3.03E+02	3.04E+02	3.04E+02	3.05E+02	3.06E+02	3.06E+02	3.07E+02	3.08E+02	3.08E+02
22	3.01E+02	3.02E+02	3.02E+02	3.02E+02	3.03E+02	3.04E+02	3.04E+02	3.05E+02	3.05E+02	3.06E+02	3.07E+02	3.07E+02
21	3.00E+02	3.01E+02	3.01E+02	3.02E+02	3.02E+02	3.03E+02	3.03E+02	3.04E+02	3.04E+02	3.05E+02	3.06E+02	3.06E+02
20	3.00E+02	3.00E+02	3.01E+02	3.01E+02	3.02E+02	3.02E+02	3.03E+02	3.03E+02	3.04E+02	3.04E+02	3.05E+02	3.05E+02
19	3.00E+02	3.00E+02	3.00E+02	3.01E+02	3.01E+02	3.02E+02	3.02E+02	3.03E+02	3.03E+02	3.04E+02	3.04E+02	3.05E+02
18	3.00E+02	3.00E+02	3.00E+02	3.00E+02	3.01E+02	3.01E+02	3.02E+02	3.02E+02	3.03E+02	3.03E+02	3.04E+02	3.04E+02
17	2.99E+02	3.00E+02	3.00E+02	3.00E+02	3.01E+02	3.01E+02	3.01E+02	3.02E+02	3.02E+02	3.03E+02	3.03E+02	3.04E+02
16	2.99E+02	3.00E+02	3.00E+02	3.00E+02	3.00E+02	3.01E+02	3.01E+02	3.01E+02	3.02E+02	3.02E+02	3.03E+02	3.03E+02
15	2.99E+02	3.00E+02	3.00E+02	3.00E+02	3.00E+02	3.01E+02	3.01E+02	3.01E+02	3.02E+02	3.02E+02	3.02E+02	3.03E+02

14	2.99E+02	3.00E+02	3.00E+02	3.00E+02	3.00E+02	3.01E+02	3.01E+02	3.01E+02	3.01E+02	3.02E+02	3.02E+02	3.03E+02	
13	2.99E+02	3.00E+02	3.00E+02	3.00E+02	3.00E+02	3.01E+02	3.01E+02	3.01E+02	3.01E+02	3.02E+02	3.02E+02	3.02E+02	
12	2.99E+02	3.00E+02	3.00E+02	3.00E+02	3.00E+02	3.01E+02	3.01E+02	3.01E+02	3.01E+02	3.02E+02	3.02E+02	3.02E+02	
11	2.99E+02	3.00E+02	3.00E+02	3.00E+02	3.00E+02	3.00E+02	3.01E+02	3.01E+02	3.01E+02	3.02E+02	3.02E+02	3.02E+02	
10	2.99E+02	3.00E+02	3.00E+02	3.00E+02	3.00E+02	3.00E+02	3.01E+02	3.01E+02	3.01E+02	3.01E+02	3.02E+02	3.02E+02	
9	2.99E+02	2.99E+02	3.00E+02	3.00E+02	3.00E+02	3.00E+02	3.01E+02	3.01E+02	3.01E+02	3.01E+02	3.02E+02	3.02E+02	
8	2.99E+02	2.99E+02	2.99E+02	3.00E+02	3.00E+02	3.00E+02	3.00E+02	3.01E+02	3.01E+02	3.01E+02	3.01E+02	3.02E+02	
7	2.99E+02	2.99E+02	2.99E+02	2.99E+02	2.99E+02	3.00E+02	3.00E+02	3.00E+02	3.00E+02	3.01E+02	3.01E+02	3.01E+02	
6	2.98E+02	2.98E+02	2.99E+02	2.99E+02	2.99E+02	2.99E+02	2.99E+02	3.00E+02	3.00E+02	3.00E+02	3.00E+02	3.01E+02	
5	2.98E+02	2.98E+02	2.98E+02	2.98E+02	2.98E+02	2.99E+02	2.99E+02	2.99E+02	2.99E+02	2.99E+02	3.00E+02	3.00E+02	
4	2.97E+02	2.97E+02	2.97E+02	2.98E+02	2.98E+02	2.98E+02	2.98E+02	2.98E+02	2.99E+02	2.99E+02	2.99E+02	2.99E+02	
3	2.97E+02	2.97E+02	2.97E+02	2.97E+02	2.97E+02	2.97E+02	2.97E+02	2.98E+02	2.98E+02	2.98E+02	2.98E+02	2.98E+02	
2	2.96E+02	2.96E+02	2.96E+02	2.96E+02	2.96E+02	2.97E+02	2.97E+02	2.97E+02	2.97E+02	2.97E+02	2.97E+02	2.98E+02	
1	2.96E+02	2.96E+02	2.96E+02	2.96E+02	2.96E+02	2.96E+02	2.96E+02	2.96E+02	2.96E+02	2.96E+02	2.96E+02	2.97E+02	
0	1.00E+02	1.00E+02	1.00E+02	1.00E+02	1.00E+02	1.00E+02	1.00E+02	1.00E+02	1.00E+02	1.00E+02	1.00E+02	1.00E+02	
I=	48	49	50	51	52	53	54	55	56	57	58	59	

J

0	4.21E+02	4.19E+02	4.16E+02	4.13E+02	4.10E+02	4.07E+02	4.03E+02	4.00E+02	3.96E+02	3.92E+02	3.88E+02	3.84E+02	
40	4.10E+02	4.09E+02	4.07E+02	4.04E+02	4.02E+02	3.99E+02	3.96E+02	3.93E+02	3.90E+02	3.87E+02	3.84E+02	3.80E+02	
39	3.96E+02	3.95E+02	3.93E+02	3.91E+02	3.89E+02	3.87E+02	3.85E+02	3.82E+02	3.79E+02	3.77E+02	3.74E+02	3.71E+02	
38	3.84E+02	3.83E+02	3.81E+02	3.80E+02	3.78E+02	3.76E+02	3.74E+02	3.72E+02	3.70E+02	3.68E+02	3.65E+02	3.63E+02	
37	3.73E+02	3.72E+02	3.71E+02	3.70E+02	3.68E+02	3.67E+02	3.65E+02	3.63E+02	3.62E+02	3.60E+02	3.58E+02	3.56E+02	
36	3.63E+02	3.62E+02	3.61E+02	3.61E+02	3.59E+02	3.58E+02	3.57E+02	3.56E+02	3.54E+02	3.53E+02	3.51E+02	3.50E+02	
35	3.54E+02	3.54E+02	3.53E+02	3.52E+02	3.52E+02	3.51E+02	3.50E+02	3.49E+02	3.48E+02	3.47E+02	3.45E+02	3.44E+02	
34	3.47E+02	3.46E+02	3.46E+02	3.46E+02	3.45E+02	3.44E+02	3.44E+02	3.43E+02	3.42E+02	3.41E+02	3.40E+02	3.40E+02	
33	3.40E+02	3.40E+02	3.40E+02	3.40E+02	3.39E+02	3.39E+02	3.38E+02	3.38E+02	3.37E+02	3.37E+02	3.36E+02	3.36E+02	
32	3.34E+02	3.34E+02	3.34E+02	3.34E+02	3.34E+02	3.34E+02	3.34E+02	3.34E+02	3.33E+02	3.33E+02	3.33E+02	3.33E+02	
31	3.29E+02	3.30E+02	3.30E+02	3.30E+02	3.30E+02	3.30E+02	3.30E+02	3.30E+02	3.30E+02	3.30E+02	3.30E+02	3.30E+02	
30	3.25E+02	3.25E+02	3.26E+02	3.26E+02	3.26E+02	3.26E+02	3.27E+02	3.27E+02	3.27E+02	3.27E+02	3.27E+02	3.28E+02	
29	3.22E+02	3.22E+02	3.22E+02	3.23E+02	3.23E+02	3.23E+02	3.24E+02	3.24E+02	3.24E+02	3.24E+02	3.25E+02	3.26E+02	
28	3.19E+02	3.19E+02	3.20E+02	3.20E+02	3.20E+02	3.21E+02	3.21E+02	3.21E+02	3.22E+02	3.22E+02	3.23E+02	3.24E+02	
27	3.16E+02	3.17E+02	3.17E+02	3.18E+02	3.18E+02	3.19E+02	3.19E+02	3.19E+02	3.20E+02	3.20E+02	3.21E+02	3.22E+02	
26	3.14E+02	3.14E+02	3.15E+02	3.16E+02	3.16E+02	3.17E+02	3.17E+02	3.18E+02	3.18E+02	3.19E+02	3.19E+02	3.19E+02	
25	3.12E+02	3.13E+02	3.13E+02	3.14E+02	3.14E+02	3.15E+02	3.15E+02	3.16E+02	3.17E+02	3.17E+02	3.17E+02	3.17E+02	
24	3.10E+02	3.11E+02	3.12E+02	3.12E+02	3.13E+02	3.13E+02	3.14E+02	3.15E+02	3.15E+02	3.15E+02	3.15E+02	3.15E+02	
23	3.09E+02	3.10E+02	3.10E+02	3.11E+02	3.11E+02	3.12E+02	3.13E+02	3.13E+02	3.13E+02	3.14E+02	3.14E+02	3.14E+02	
22	3.08E+02	3.08E+02	3.09E+02	3.10E+02	3.10E+02	3.11E+02	3.11E+02	3.12E+02	3.12E+02	3.12E+02	3.12E+02	3.12E+02	
21	3.07E+02	3.07E+02	3.08E+02	3.08E+02	3.09E+02	3.10E+02	3.10E+02	3.11E+02	3.11E+02	3.11E+02	3.10E+02	3.10E+02	
20	3.06E+02	3.06E+02	3.07E+02	3.07E+02	3.08E+02	3.08E+02	3.09E+02	3.09E+02	3.10E+02	3.09E+02	3.09E+02	3.09E+02	
19	3.05E+02	3.06E+02	3.06E+02	3.07E+02	3.07E+02	3.08E+02	3.08E+02	3.08E+02	3.08E+02	3.08E+02	3.08E+02	3.07E+02	
18	3.05E+02	3.05E+02	3.05E+02	3.06E+02	3.06E+02	3.07E+02	3.07E+02	3.07E+02	3.07E+02	3.07E+02	3.06E+02	3.06E+02	
17	3.04E+02	3.04E+02	3.05E+02	3.05E+02	3.06E+02	3.06E+02	3.06E+02	3.07E+02	3.06E+02	3.06E+02	3.05E+02	3.04E+02	
16	3.04E+02	3.04E+02	3.04E+02	3.05E+02	3.05E+02	3.05E+02	3.06E+02	3.06E+02	3.06E+02	3.05E+02	3.04E+02	3.03E+02	
15	3.03E+02	3.04E+02	3.04E+02	3.04E+02	3.05E+02	3.05E+02	3.05E+02	3.05E+02	3.05E+02	3.04E+02	3.03E+02	3.02E+02	
14	3.03E+02	3.03E+02	3.04E+02	3.04E+02	3.04E+02	3.04E+02	3.05E+02	3.04E+02	3.04E+02	3.03E+02	3.02E+02	3.01E+02	
13	3.03E+02	3.03E+02	3.03E+02	3.04E+02	3.04E+02	3.04E+02	3.04E+02	3.04E+02	3.03E+02	3.02E+02	3.01E+02	3.00E+02	
12	3.03E+02	3.03E+02	3.03E+02	3.03E+02	3.04E+02	3.04E+02	3.04E+02	3.03E+02	3.02E+02	3.01E+02	3.00E+02	2.99E+02	
11	3.02E+02	3.03E+02	3.03E+02	3.03E+02	3.03E+02	3.03E+02	3.03E+02	3.03E+02	3.01E+02	3.00E+02	2.99E+02	2.98E+02	
10	3.02E+02	3.03E+02	3.03E+02	3.03E+02	3.03E+02	3.03E+02	3.03E+02	3.02E+02	3.00E+02	2.99E+02	2.98E+02	2.97E+02	
9	3.02E+02	3.02E+02	3.03E+02	3.03E+02	3.03E+02	3.03E+02	3.02E+02	3.01E+02	2.99E+02	2.98E+02	2.97E+02	2.96E+02	
8	3.02E+02	3.02E+02	3.02E+02	3.02E+02	3.03E+02	3.02E+02	3.01E+02	2.99E+02	2.98E+02	2.97E+02	2.95E+02	2.95E+02	
7	3.01E+02	3.02E+02	3.02E+02	3.02E+02	3.02E+02	3.01E+02	3.00E+02	2.98E+02	2.97E+02	2.95E+02	2.95E+02	2.94E+02	
6	3.01E+02	3.01E+02	3.01E+02	3.01E+02	3.01E+02	3.00E+02	2.98E+02	2.97E+02	2.96E+02	2.95E+02	2.94E+02	2.94E+02	
5	3.00E+02	3.00E+02	3.01E+02	3.01E+02	3.00E+02	2.99E+02	2.97E+02	2.96E+02	2.95E+02	2.94E+02	2.94E+02	2.94E+02	
4	2.99E+02	3.00E+02	3.00E+02	3.00E+02	2.99E+02	2.98E+02	2.96E+02	2.95E+02	2.94E+02	2.94E+02	2.94E+02	2.95E+02	
3	2.99E+02	2.99E+02	2.99E+02	2.99E+02	2.98E+02	2.96E+02	2.95E+02	2.94E+02	2.93E+02	2.93E+02	2.93E+02	2.95E+02	
2	2.98E+02	2.98E+02	2.98E+02	2.98E+02	2.98E+02	2.95E+02	2.94E+02	2.93E+02	2.93E+02	2.93E+02	2.94E+02	2.97E+02	
1	2.97E+02	2.97E+02	2.97E+02	2.97E+02	2.97E+02	2.94E+02	2.93E+02	2.93E+02	2.93E+02	2.93E+02	2.94E+02	2.99E+02	
0	1.00E+02	1.00E+02	1.00E+02	1.00E+02	1.00E+02	2.93E+02	2.93E+02	2.93E+02	2.93E+02	2.93E+02	2.93E+02	2.94E+02	
I=	60	61	62	63	64	65	66	67	68	69	70	71	

J

0	3.80E+02	3.76E+02	3.73E+02	3.71E+02	3.71E+02	3.75E+02	3.81E+02	3.91E+02	4.07E+02	4.29E+02	4.59E+02	5.02E+02
40	3.77E+02	3.73E+02	3.70E+02	3.67E+02	3.66E+02	3.68E+02	3.73E+02	3.81E+02	3.94E+02	4.13E+02	4.39E+02	4.76E+02
39	3.68E+02	3.65E+02	3.62E+02	3.61E+02	3.61E+02	3.65E+02	3.71E+02	3.80E+02	3.94E+02	4.13E+02	4.41E+02	4.80E+02
38	3.60E+02	3.58E+02	3.56E+02	3.56E+02	3.58E+02	3.62E+02	3.69E+02	3.79E+02	3.94E+02	4.14E+02	4.43E+02	4.84E+02
37	3.54E+02	3.52E+02	3.51E+02	3.52E+02	3.55E+02	3.60E+02	3.68E+02	3.79E+02	3.94E+02	4.15E+02	4.46E+02	4.89E+02
36	3.48E+02	3.47E+02	3.47E+02	3.49E+02	3.53E+02	3.58E+02	3.67E+02	3.78E+02	3.94E+02	4.17E+02	4.49E+02	4.95E+02

35	3.43E+02	3.43E+02	3.44E+02	3.47E+02	3.51E+02	3.57E+02	3.66E+02	3.78E+02	3.94E+02	4.18E+02	4.52E+02	5.01E+02	
34	3.39E+02	3.40E+02	3.42E+02	3.45E+02	3.49E+02	3.55E+02	3.64E+02	3.77E+02	3.94E+02	4.19E+02	4.55E+02	5.08E+02	
33	3.36E+02	3.37E+02	3.39E+02	3.43E+02	3.47E+02	3.54E+02	3.63E+02	3.76E+02	3.94E+02	4.20E+02	4.58E+02	5.16E+02	
32	3.34E+02	3.35E+02	3.37E+02	3.41E+02	3.45E+02	3.52E+02	3.61E+02	3.74E+02	3.93E+02	4.21E+02	4.62E+02	5.26E+02	
31	3.31E+02	3.33E+02	3.35E+02	3.38E+02	3.43E+02	3.50E+02	3.59E+02	3.73E+02	3.92E+02	4.22E+02	4.66E+02	5.37E+02	
30	3.29E+02	3.31E+02	3.33E+02	3.36E+02	3.41E+02	3.47E+02	3.57E+02	3.71E+02	3.91E+02	4.23E+02	4.71E+02	5.50E+02	
29	3.27E+02	3.28E+02	3.30E+02	3.33E+02	3.38E+02	3.44E+02	3.54E+02	3.68E+02	3.90E+02	4.24E+02	4.78E+02	5.49E+02	
28	3.25E+02	3.26E+02	3.28E+02	3.31E+02	3.35E+02	3.41E+02	3.51E+02	3.66E+02	3.89E+02	4.26E+02	4.85E+02	5.43E+02	
27	3.22E+02	3.23E+02	3.25E+02	3.28E+02	3.32E+02	3.38E+02	3.48E+02	3.64E+02	3.89E+02	4.28E+02	4.95E+02	5.38E+02	
26	3.20E+02	3.21E+02	3.22E+02	3.25E+02	3.29E+02	3.35E+02	3.45E+02	3.62E+02	3.88E+02	4.32E+02	4.92E+02	5.35E+02	
25	3.18E+02	3.19E+02	3.20E+02	3.22E+02	3.26E+02	3.32E+02	3.43E+02	3.60E+02	3.89E+02	4.38E+02	4.86E+02	5.35E+02	
24	3.16E+02	3.16E+02	3.17E+02	3.19E+02	3.23E+02	3.29E+02	3.40E+02	3.58E+02	3.90E+02	4.45E+02	4.83E+02	5.38E+02	
23	3.14E+02	3.14E+02	3.15E+02	3.17E+02	3.20E+02	3.27E+02	3.38E+02	3.58E+02	3.93E+02	4.40E+02	4.83E+02	5.44E+02	
22	3.12E+02	3.12E+02	3.13E+02	3.14E+02	3.18E+02	3.24E+02	3.36E+02	3.58E+02	3.99E+02	4.38E+02	4.87E+02	5.54E+02	
21	3.10E+02	3.10E+02	3.10E+02	3.12E+02	3.16E+02	3.22E+02	3.35E+02	3.60E+02	4.03E+02	4.39E+02	4.94E+02	5.67E+02	
20	3.08E+02	3.08E+02	3.09E+02	3.10E+02	3.14E+02	3.21E+02	3.35E+02	3.63E+02	4.03E+02	4.44E+02	5.05E+02	5.85E+02	
19	3.07E+02	3.06E+02	3.07E+02	3.08E+02	3.12E+02	3.20E+02	3.36E+02	3.70E+02	4.06E+02	4.53E+02	5.21E+02	6.06E+02	
18	3.05E+02	3.05E+02	3.05E+02	3.07E+02	3.11E+02	3.20E+02	3.39E+02	3.78E+02	4.12E+02	4.66E+02	5.41E+02	6.31E+02	
17	3.04E+02	3.03E+02	3.04E+02	3.06E+02	3.11E+02	3.21E+02	3.45E+02	3.83E+02	4.23E+02	4.85E+02	5.66E+02	6.58E+02	
16	3.03E+02	3.02E+02	3.03E+02	3.05E+02	3.11E+02	3.24E+02	3.55E+02	3.92E+02	4.40E+02	5.09E+02	5.95E+02	6.87E+02	
15	3.01E+02	3.01E+02	3.02E+02	3.05E+02	3.13E+02	3.30E+02	3.71E+02	4.06E+02	4.62E+02	5.38E+02	6.27E+02	7.14E+02	
14	3.00E+02	3.00E+02	3.01E+02	3.05E+02	3.17E+02	3.41E+02	3.83E+02	4.26E+02	4.91E+02	5.73E+02	6.62E+02	7.40E+02	
13	2.99E+02	2.99E+02	3.01E+02	3.08E+02	3.24E+02	3.60E+02	4.00E+02	4.53E+02	5.27E+02	6.13E+02	6.96E+02	7.60E+02	
12	2.98E+02	2.98E+02	3.01E+02	3.12E+02	3.38E+02	3.79E+02	4.24E+02	4.89E+02	5.70E+02	6.55E+02	7.28E+02	7.75E+02	
11	2.97E+02	2.98E+02	3.04E+02	3.22E+02	3.57E+02	4.02E+02	4.59E+02	5.36E+02	6.21E+02	7.00E+02	7.57E+02	7.86E+02	
10	2.96E+02	2.98E+02	3.09E+02	3.35E+02	3.78E+02	4.35E+02	5.09E+02	5.96E+02	6.78E+02	7.44E+02	7.83E+02	7.93E+02	
9	2.95E+02	3.00E+02	3.16E+02	3.52E+02	4.10E+02	4.86E+02	5.78E+02	6.66E+02	7.38E+02	7.87E+02	8.07E+02	8.09E+02	
8	2.95E+02	3.02E+02	3.27E+02	3.80E+02	4.60E+02	5.63E+02	6.65E+02	7.45E+02	8.00E+02	8.26E+02	8.26E+02	1.09E+03	
7	2.95E+02	3.07E+02	3.47E+02	4.25E+02	5.41E+02	6.71E+02	7.67E+02	8.29E+02	8.58E+02	8.61E+02	9.42E+02	1.35E+03	
6	2.96E+02	3.16E+02	3.82E+02	5.04E+02	6.70E+02	8.00E+02	8.75E+02	9.08E+02	9.10E+02	9.42E+02	1.23E+03	1.28E+03	
5	2.97E+02	3.34E+02	4.47E+02	6.46E+02	8.34E+02	9.35E+02	9.75E+02	9.75E+02	1.06E+03	1.25E+03	1.38E+03	1.22E+03	
4	3.00E+02	3.69E+02	5.78E+02	8.55E+02	1.00E+03	1.05E+03	1.16E+03	1.29E+03	1.44E+03	1.43E+03	1.30E+03	1.19E+03	
3	3.06E+02	4.45E+02	8.27E+02	1.07E+03	1.26E+03	1.49E+03	1.61E+03	1.51E+03	1.42E+03	1.34E+03	1.26E+03	1.18E+03	
2	3.20E+02	6.24E+02	1.14E+03	1.63E+03	1.59E+03	1.50E+03	1.44E+03	1.39E+03	1.34E+03	1.28E+03	1.23E+03	1.18E+03	
1	3.59E+02	1.04E+03	1.58E+03	1.38E+03	1.37E+03	1.36E+03	1.34E+03	1.31E+03	1.28E+03	1.26E+03	1.23E+03	1.20E+03	
0	3.01E+02	1.00E+02	1.00E+02	1.00E+02	1.00E+02	1.00E+02	1.00E+02	1.00E+02	1.00E+02	1.00E+02	1.00E+02	1.00E+02	
I =	72	73	74	75	76	77	78	79	80	81	82	83	

J

0	5.65E+02	6.58E+02	7.29E+02	7.65E+02	8.12E+02	8.68E+02	9.28E+02	9.83E+02	1.02E+03	1.26E+03	1.47E+03	1.27E+03	
40	5.29E+02	6.10E+02	7.11E+02	7.43E+02	7.88E+02	8.44E+02	9.07E+02	9.67E+02	1.01E+03	1.21E+03	1.48E+03	1.28E+03	
39	5.36E+02	6.21E+02	7.06E+02	7.41E+02	7.89E+02	8.48E+02	9.13E+02	9.73E+02	1.01E+03	1.26E+03	1.44E+03	1.24E+03	
38	5.44E+02	6.35E+02	7.01E+02	7.40E+02	7.92E+02	8.54E+02	9.21E+02	9.79E+02	1.01E+03	1.34E+03	1.40E+03	1.21E+03	
37	5.53E+02	6.52E+02	6.98E+02	7.41E+02	7.96E+02	8.62E+02	9.31E+02	9.85E+02	1.04E+03	1.42E+03	1.35E+03	1.18E+03	
36	5.64E+02	6.62E+02	6.96E+02	7.43E+02	8.03E+02	8.73E+02	9.43E+02	9.91E+02	1.10E+03	1.51E+03	1.31E+03	1.15E+03	
35	5.77E+02	6.56E+02	6.95E+02	7.47E+02	8.12E+02	8.85E+02	9.53E+02	9.93E+02	1.16E+03	1.48E+03	1.27E+03	1.12E+03	
34	5.91E+02	6.51E+02	6.95E+02	7.53E+02	8.23E+02	8.98E+02	9.62E+02	9.93E+02	1.24E+03	1.42E+03	1.23E+03	1.09E+03	
33	6.08E+02	6.48E+02	6.97E+02	7.60E+02	8.35E+02	9.11E+02	9.69E+02	9.90E+02	1.31E+03	1.37E+03	1.19E+03	1.05E+03	
32	6.06E+02	6.46E+02	7.01E+02	7.70E+02	8.49E+02	9.24E+02	9.74E+02	1.03E+03	1.40E+03	1.33E+03	1.16E+03	1.03E+03	
31	6.00E+02	6.46E+02	7.07E+02	7.81E+02	8.63E+02	9.35E+02	9.75E+02	1.09E+03	1.48E+03	1.28E+03	1.12E+03	9.99E+02	
30	5.95E+02	6.47E+02	7.14E+02	7.94E+02	8.77E+02	9.43E+02	9.73E+02	1.14E+03	1.44E+03	1.24E+03	1.09E+03	9.71E+02	
29	5.92E+02	6.50E+02	7.23E+02	8.07E+02	8.89E+02	9.48E+02	9.68E+02	1.21E+03	1.39E+03	1.20E+03	1.06E+03	9.43E+02	
28	5.91E+02	6.55E+02	7.34E+02	8.21E+02	9.00E+02	9.50E+02	9.61E+02	1.28E+03	1.34E+03	1.16E+03	1.02E+03	9.16E+02	
27	5.92E+02	6.62E+02	7.47E+02	8.36E+02	9.10E+02	9.50E+02	9.99E+02	1.36E+03	1.29E+03	1.12E+03	9.92E+02	8.90E+02	
26	5.96E+02	6.72E+02	7.62E+02	8.50E+02	9.17E+02	9.47E+02	1.05E+03	1.45E+03	1.25E+03	1.08E+03	9.61E+02	8.62E+02	
25	6.02E+02	6.85E+02	7.77E+02	8.62E+02	9.20E+02	9.40E+02	1.12E+03	1.40E+03	1.20E+03	1.05E+03	9.28E+02	8.34E+02	
24	6.11E+02	6.99E+02	7.92E+02	8.72E+02	9.21E+02	9.32E+02	1.19E+03	1.33E+03	1.15E+03	1.01E+03	8.94E+02	8.05E+02	
23	6.23E+02	7.16E+02	8.08E+02	8.80E+02	9.19E+02	9.32E+02	1.29E+03	1.27E+03	1.10E+03	9.66E+02	8.60E+02	7.75E+02	
22	6.39E+02	7.34E+02	8.22E+02	8.86E+02	9.13E+02	1.00E+03	1.41E+03	1.21E+03	1.05E+03	9.25E+02	8.25E+02	7.45E+02	
21	6.58E+02	7.53E+02	8.35E+02	8.88E+02	9.04E+02	1.09E+03	1.34E+03	1.15E+03	9.98E+02	8.81E+02	7.88E+02	7.13E+02	
20	6.78E+02	7.71E+02	8.44E+02	8.85E+02	8.92E+02	1.21E+03	1.26E+03	1.08E+03	9.44E+02	8.36E+02	7.50E+02	6.81E+02	
19	7.01E+02	7.88E+02	8.51E+02	8.79E+02	9.37E+02	1.38E+03	1.18E+03	1.02E+03	8.91E+02	7.91E+02	7.12E+02	6.49E+02	
18	7.24E+02	8.03E+02	8.53E+02	8.68E+02	1.07E+03	1.29E+03	1.10E+03	9.50E+02	8.35E+02	7.44E+02	6.73E+02	6.16E+02	
17	7.47E+02	8.14E+02	8.49E+02	8.52E+02	1.25E+03	1.19E+03	1.01E+03	8.82E+02	7.79E+02	6.98E+02	6.34E+02	5.85E+02	
16	7.67E+02	8.20E+02	8.39E+02	9.66E+02	1.29E+03	1.09E+03	9.34E+02	8.17E+02	7.25E+02	6.54E+02	5.98E+02	5.56E+02	
15	7.82E+02	8.19E+02	8.24E+02	1.19E+03	1.17E+03	9.91E+02	8.57E+02	7.54E+02	6.73E+02	6.11E+02	5.64E+02	5.29E+02	
14	7.92E+02	8.12E+02	9.16E+02	1.27E+03	1.05E+03	9.01E+02	7.85E+02	6.95E+02	6.26E+02	5.74E+02	5.35E+02	5.07E+02	
13	7.95E+02	7.98E+02	1.20E+03	1.13E+03	9.49E+02	8.18E+02	7.20E+02	6.44E+02	5.86E+02	5.43E+02	5.11E+02	4.88E+02	
12	7.90E+02	9.42E+02	1.21E+03	1.00E+03	8.57E+02	7.48E+02	6.66E+02	6.03E+02	5.55E+02	5.19E+02	4.93E+02	4.74E+02	
11	7.85E+02	1.29E+03	1.08E+03	9.14E+02	7.92E+02	6.99E+02	6.29E+02	5.75E+02	5.34E+02	5.02E+02	4.79E+02	4.62E+02	

10	1.02E+03	1.19E+03	9.94E+02	8.53E+02	7.48E+02	6.68E+02	6.07E+02	5.59E+02	5.21E+02	4.90E+02	4.67E+02	4.50E+02
9	1.32E+03	1.09E+03	9.34E+02	8.14E+02	7.22E+02	6.52E+02	5.97E+02	5.52E+02	5.12E+02	4.79E+02	4.54E+02	4.38E+02
8	1.22E+03	1.04E+03	8.98E+02	7.94E+02	7.13E+02	6.50E+02	5.98E+02	5.51E+02	5.05E+02	4.66E+02	4.39E+02	4.24E+02
7	1.15E+03	1.00E+03	8.83E+02	7.92E+02	7.19E+02	6.60E+02	6.07E+02	5.53E+02	4.94E+02	4.48E+02	4.22E+02	4.09E+02
6	1.12E+03	9.87E+02	8.86E+02	8.05E+02	7.38E+02	6.79E+02	6.21E+02	5.53E+02	4.74E+02	4.25E+02	4.02E+02	3.94E+02
5	1.10E+03	9.91E+02	9.05E+02	8.32E+02	7.68E+02	7.07E+02	6.36E+02	5.44E+02	4.42E+02	3.98E+02	3.83E+02	3.80E+02
4	1.10E+03	1.01E+03	9.39E+02	8.74E+02	8.12E+02	7.44E+02	6.55E+02	5.17E+02	4.00E+02	3.73E+02	3.70E+02	3.72E+02
3	1.11E+03	1.05E+03	9.89E+02	9.34E+02	8.76E+02	8.01E+02	6.86E+02	4.68E+02	3.60E+02	3.57E+02	3.64E+02	3.70E+02
2	1.13E+03	1.09E+03	1.05E+03	1.01E+03	9.61E+02	8.94E+02	7.52E+02	4.06E+02	3.29E+02	3.54E+02	3.69E+02	3.76E+02
1	1.16E+03	1.14E+03	1.11E+03	1.09E+03	1.07E+03	1.05E+03	8.47E+02	3.38E+02	3.10E+02	3.62E+02	3.80E+02	3.80E+02
0	1.00E+02	1.00E+02	1.00E+02	1.00E+02	1.00E+02	1.00E+02	1.00E+02	3.02E+02	2.98E+02	1.00E+02	1.00E+02	1.00E+02
I =	84	85	86	87	88	89	90	91	92	93	94	95

J

0	1.13E+03	1.03E+03	9.55E+02	9.08E+02	8.85E+02	2.88E+02
40	1.13E+03	1.02E+03	9.46E+02	8.97E+02	8.73E+02	8.73E+02
39	1.10E+03	1.00E+03	9.28E+02	8.81E+02	8.57E+02	8.57E+02
38	1.08E+03	9.80E+02	9.10E+02	8.64E+02	8.41E+02	8.41E+02
37	1.05E+03	9.59E+02	8.91E+02	8.47E+02	8.25E+02	8.25E+02
36	1.03E+03	9.38E+02	8.73E+02	8.30E+02	8.09E+02	8.09E+02
35	1.00E+03	9.16E+02	8.53E+02	8.12E+02	7.92E+02	7.92E+02
34	9.77E+02	8.94E+02	8.34E+02	7.94E+02	7.75E+02	7.75E+02
33	9.52E+02	8.73E+02	8.15E+02	7.77E+02	7.57E+02	7.57E+02
32	9.28E+02	8.52E+02	7.96E+02	7.58E+02	7.40E+02	7.40E+02
31	9.04E+02	8.30E+02	7.76E+02	7.40E+02	7.23E+02	7.23E+02
30	8.80E+02	8.09E+02	7.57E+02	7.22E+02	7.05E+02	7.05E+02
29	8.56E+02	7.88E+02	7.37E+02	7.04E+02	6.87E+02	6.87E+02
28	8.32E+02	7.66E+02	7.18E+02	6.85E+02	6.69E+02	6.69E+02
27	8.08E+02	7.45E+02	6.98E+02	6.67E+02	6.52E+02	6.52E+02
26	7.84E+02	7.23E+02	6.78E+02	6.48E+02	6.34E+02	6.34E+02
25	7.59E+02	7.01E+02	6.58E+02	6.29E+02	6.15E+02	6.15E+02
24	7.34E+02	6.78E+02	6.37E+02	6.11E+02	5.97E+02	5.97E+02
23	7.08E+02	6.56E+02	6.17E+02	5.92E+02	5.79E+02	5.79E+02
22	6.82E+02	6.32E+02	5.96E+02	5.73E+02	5.62E+02	5.62E+02
21	6.54E+02	6.09E+02	5.76E+02	5.55E+02	5.45E+02	5.45E+02
20	6.27E+02	5.86E+02	5.56E+02	5.37E+02	5.28E+02	5.28E+02
19	6.00E+02	5.63E+02	5.37E+02	5.20E+02	5.12E+02	5.12E+02
18	5.73E+02	5.41E+02	5.19E+02	5.04E+02	4.98E+02	4.98E+02
17	5.48E+02	5.21E+02	5.02E+02	4.90E+02	4.84E+02	4.84E+02
16	5.25E+02	5.02E+02	4.87E+02	4.77E+02	4.73E+02	4.73E+02
15	5.04E+02	4.86E+02	4.74E+02	4.66E+02	4.62E+02	4.62E+02
14	4.86E+02	4.72E+02	4.62E+02	4.56E+02	4.53E+02	4.53E+02
13	4.72E+02	4.60E+02	4.52E+02	4.47E+02	4.45E+02	4.45E+02
12	4.60E+02	4.50E+02	4.44E+02	4.40E+02	4.38E+02	4.38E+02
11	4.50E+02	4.41E+02	4.36E+02	4.32E+02	4.30E+02	4.30E+02
10	4.39E+02	4.32E+02	4.27E+02	4.25E+02	4.24E+02	4.24E+02
9	4.28E+02	4.23E+02	4.19E+02	4.18E+02	4.17E+02	4.17E+02
8	4.16E+02	4.12E+02	4.11E+02	4.10E+02	4.10E+02	4.10E+02
7	4.04E+02	4.02E+02	4.02E+02	4.03E+02	4.03E+02	4.03E+02
6	3.91E+02	3.92E+02	3.94E+02	3.96E+02	3.97E+02	3.97E+02
5	3.81E+02	3.84E+02	3.87E+02	3.90E+02	3.91E+02	3.91E+02
4	3.76E+02	3.80E+02	3.83E+02	3.86E+02	3.87E+02	3.87E+02
3	3.75E+02	3.79E+02	3.82E+02	3.84E+02	3.85E+02	3.85E+02
2	3.78E+02	3.80E+02	3.81E+02	3.82E+02	3.83E+02	3.83E+02
1	3.80E+02	3.82E+02	3.83E+02	3.84E+02	3.82E+02	3.82E+02
0	1.00E+02	1.00E+02	1.00E+02	1.00E+02	1.00E+02	2.88E+02
I =	96	97	98	99	100	0

--*- BLOCK-NUMBER-3 PLANE K = 1 TEMPERATURE (KELVIN) -*

J

0	2.88E+02	2.88E+02	2.88E+02	2.88E+02	2.88E+02	2.88E+02	2.88E+02	2.88E+02	2.88E+02	2.88E+02	2.88E+02	2.88E+02
40	2.93E+02	2.90E+02	2.89E+02	2.88E+02	2.88E+02	2.88E+02	2.88E+02	2.88E+02	2.88E+02	2.88E+02	2.88E+02	2.88E+02
39	2.93E+02	2.91E+02	2.90E+02	2.89E+02	2.88E+02	2.88E+02	2.88E+02	2.88E+02	2.88E+02	2.88E+02	2.88E+02	2.88E+02
38	2.93E+02	2.91E+02	2.90E+02	2.89E+02	2.89E+02	2.88E+02	2.88E+02	2.88E+02	2.88E+02	2.88E+02	2.88E+02	2.88E+02
37	2.93E+02	2.91E+02	2.90E+02	2.90E+02	2.89E+02	2.89E+02	2.88E+02	2.88E+02	2.88E+02	2.88E+02	2.88E+02	2.88E+02
36	2.93E+02	2.92E+02	2.90E+02	2.90E+02	2.89E+02	2.89E+02	2.88E+02	2.88E+02	2.88E+02	2.88E+02	2.88E+02	2.88E+02
35	2.93E+02	2.92E+02	2.91E+02	2.90E+02	2.89E+02	2.89E+02	2.89E+02	2.88E+02	2.88E+02	2.88E+02	2.88E+02	2.88E+02
34	2.93E+02	2.92E+02	2.91E+02	2.90E+02	2.89E+02	2.89E+02	2.89E+02	2.88E+02	2.88E+02	2.88E+02	2.88E+02	2.88E+02

33	2.93E+02	2.92E+02	2.91E+02	2.90E+02	2.90E+02	2.89E+02	2.89E+02	2.89E+02	2.88E+02	2.88E+02	2.88E+02	2.88E+02
32	2.93E+02	2.92E+02	2.91E+02	2.90E+02	2.90E+02	2.89E+02	2.89E+02	2.89E+02	2.89E+02	2.88E+02	2.89E+02	2.89E+02
31	2.93E+02	2.92E+02	2.91E+02	2.90E+02	2.90E+02	2.89E+02	2.89E+02	2.89E+02	2.89E+02	2.89E+02	2.89E+02	2.89E+02
30	2.93E+02	2.92E+02	2.91E+02	2.90E+02	2.90E+02	2.89E+02	2.89E+02	2.89E+02	2.89E+02	2.89E+02	2.89E+02	2.89E+02
29	2.93E+02	2.92E+02	2.91E+02	2.90E+02	2.90E+02	2.89E+02	2.89E+02	2.89E+02	2.89E+02	2.89E+02	2.89E+02	2.89E+02
28	2.93E+02	2.92E+02	2.91E+02	2.90E+02	2.90E+02	2.90E+02	2.89E+02	2.89E+02	2.89E+02	2.89E+02	2.89E+02	2.90E+02
27	2.93E+02	2.92E+02	2.91E+02	2.90E+02	2.90E+02	2.90E+02	2.89E+02	2.89E+02	2.89E+02	2.89E+02	2.90E+02	2.90E+02
26	2.93E+02	2.92E+02	2.91E+02	2.91E+02	2.90E+02	2.90E+02	2.90E+02	2.89E+02	2.89E+02	2.90E+02	2.90E+02	2.90E+02
25	2.93E+02	2.92E+02	2.91E+02	2.91E+02	2.90E+02	2.90E+02	2.90E+02	2.90E+02	2.90E+02	2.90E+02	2.90E+02	2.91E+02
24	2.93E+02	2.92E+02	2.91E+02	2.91E+02	2.90E+02	2.90E+02	2.90E+02	2.90E+02	2.90E+02	2.90E+02	2.91E+02	2.92E+02
23	2.93E+02	2.92E+02	2.91E+02	2.91E+02	2.90E+02	2.90E+02	2.90E+02	2.90E+02	2.90E+02	2.91E+02	2.91E+02	2.92E+02
22	2.93E+02	2.92E+02	2.91E+02	2.91E+02	2.91E+02	2.90E+02	2.90E+02	2.90E+02	2.91E+02	2.91E+02	2.92E+02	2.93E+02
21	2.93E+02	2.92E+02	2.91E+02	2.91E+02	2.91E+02	2.90E+02	2.90E+02	2.91E+02	2.91E+02	2.92E+02	2.93E+02	2.94E+02
20	2.93E+02	2.92E+02	2.92E+02	2.91E+02	2.91E+02	2.91E+02	2.91E+02	2.91E+02	2.91E+02	2.92E+02	2.93E+02	2.94E+02
19	2.93E+02	2.92E+02	2.92E+02	2.91E+02	2.91E+02	2.91E+02	2.91E+02	2.91E+02	2.92E+02	2.93E+02	2.94E+02	2.95E+02
18	2.93E+02	2.92E+02	2.92E+02	2.91E+02	2.91E+02	2.91E+02	2.91E+02	2.92E+02	2.92E+02	2.93E+02	2.94E+02	2.96E+02
17	2.93E+02	2.92E+02	2.92E+02	2.91E+02	2.91E+02	2.91E+02	2.92E+02	2.92E+02	2.93E+02	2.94E+02	2.95E+02	2.97E+02
16	2.93E+02	2.92E+02	2.92E+02	2.92E+02	2.91E+02	2.92E+02	2.92E+02	2.92E+02	2.93E+02	2.94E+02	2.96E+02	2.97E+02
15	2.93E+02	2.92E+02	2.92E+02	2.92E+02	2.92E+02	2.92E+02	2.92E+02	2.93E+02	2.93E+02	2.94E+02	2.96E+02	2.98E+02
14	2.93E+02	2.93E+02	2.92E+02	2.92E+02	2.92E+02	2.92E+02	2.92E+02	2.93E+02	2.94E+02	2.95E+02	2.97E+02	2.99E+02
13	2.93E+02	2.93E+02	2.92E+02	2.92E+02	2.92E+02	2.92E+02	2.93E+02	2.93E+02	2.94E+02	2.96E+02	2.97E+02	2.99E+02
12	2.93E+02	2.93E+02	2.92E+02	2.92E+02	2.92E+02	2.92E+02	2.93E+02	2.94E+02	2.95E+02	2.96E+02	2.97E+02	2.99E+02
11	2.93E+02	2.93E+02	2.92E+02	2.92E+02	2.92E+02	2.93E+02	2.93E+02	2.94E+02	2.95E+02	2.96E+02	2.98E+02	2.99E+02
10	2.93E+02	2.93E+02	2.93E+02	2.92E+02	2.93E+02	2.93E+02	2.93E+02	2.94E+02	2.95E+02	2.96E+02	2.98E+02	2.99E+02
9	2.93E+02	2.93E+02	2.93E+02	2.93E+02	2.93E+02	2.93E+02	2.93E+02	2.94E+02	2.95E+02	2.96E+02	2.97E+02	2.99E+02
8	2.93E+02	2.93E+02	2.93E+02	2.93E+02	2.93E+02	2.93E+02	2.93E+02	2.94E+02	2.95E+02	2.96E+02	2.97E+02	2.99E+02
7	2.93E+02	2.93E+02	2.93E+02	2.93E+02	2.93E+02	2.93E+02	2.93E+02	2.94E+02	2.95E+02	2.96E+02	2.97E+02	2.98E+02
6	2.93E+02	2.93E+02	2.93E+02	2.93E+02	2.93E+02	2.93E+02	2.93E+02	2.94E+02	2.94E+02	2.95E+02	2.96E+02	2.98E+02
5	2.93E+02	2.93E+02	2.93E+02	2.93E+02	2.93E+02	2.93E+02	2.93E+02	2.94E+02	2.94E+02	2.95E+02	2.96E+02	2.97E+02
4	2.93E+02	2.93E+02	2.93E+02	2.93E+02	2.93E+02	2.93E+02	2.93E+02	2.94E+02	2.94E+02	2.95E+02	2.95E+02	2.96E+02
3	2.93E+02	2.93E+02	2.93E+02	2.93E+02	2.93E+02	2.93E+02	2.93E+02	2.94E+02	2.94E+02	2.94E+02	2.95E+02	2.96E+02
2	2.93E+02	2.93E+02	2.93E+02	2.93E+02	2.93E+02	2.93E+02	2.93E+02	2.93E+02	2.94E+02	2.94E+02	2.94E+02	2.95E+02
1	2.93E+02	2.93E+02	2.93E+02	2.93E+02	2.93E+02	2.93E+02	2.93E+02	2.93E+02	2.93E+02	2.94E+02	2.94E+02	2.94E+02
0	2.88E+02	2.93E+02	2.93E+02	2.93E+02	2.93E+02	2.93E+02	2.93E+02	2.93E+02	2.93E+02	2.94E+02	2.94E+02	2.95E+02
I =	0	1	2	3	4	5	6	7	8	9	10	11

J

0	2.88E+02	2.88E+02	2.88E+02	2.88E+02	2.88E+02	2.88E+02	2.88E+02	2.88E+02	2.88E+02	2.88E+02	2.88E+02	2.88E+02
40	2.88E+02	2.88E+02	2.88E+02	2.88E+02	2.88E+02	2.88E+02	2.88E+02	2.88E+02	2.88E+02	2.88E+02	2.88E+02	2.88E+02
39	2.88E+02	2.88E+02	2.88E+02	2.88E+02	2.88E+02	2.88E+02	2.88E+02	2.88E+02	2.88E+02	2.88E+02	2.89E+02	2.89E+02
38	2.88E+02	2.88E+02	2.88E+02	2.88E+02	2.88E+02	2.88E+02	2.88E+02	2.88E+02	2.89E+02	2.89E+02	2.89E+02	2.90E+02
37	2.88E+02	2.88E+02	2.88E+02	2.88E+02	2.88E+02	2.88E+02	2.89E+02	2.89E+02	2.89E+02	2.90E+02	2.90E+02	2.91E+02
36	2.88E+02	2.88E+02	2.88E+02	2.88E+02	2.89E+02	2.89E+02	2.89E+02	2.89E+02	2.90E+02	2.90E+02	2.91E+02	2.92E+02
35	2.88E+02	2.88E+02	2.88E+02	2.89E+02	2.89E+02	2.89E+02	2.90E+02	2.90E+02	2.91E+02	2.91E+02	2.92E+02	2.94E+02
34	2.88E+02	2.89E+02	2.89E+02	2.89E+02	2.89E+02	2.90E+02	2.90E+02	2.91E+02	2.92E+02	2.93E+02	2.94E+02	2.95E+02
33	2.89E+02	2.89E+02	2.89E+02	2.89E+02	2.90E+02	2.90E+02	2.90E+02	2.91E+02	2.92E+02	2.93E+02	2.94E+02	2.95E+02
32	2.89E+02	2.89E+02	2.89E+02	2.90E+02	2.90E+02	2.91E+02	2.92E+02	2.93E+02	2.94E+02	2.95E+02	2.97E+02	2.99E+02
31	2.89E+02	2.89E+02	2.90E+02	2.90E+02	2.91E+02	2.92E+02	2.93E+02	2.94E+02	2.95E+02	2.97E+02	2.98E+02	3.00E+02
30	2.89E+02	2.90E+02	2.90E+02	2.91E+02	2.92E+02	2.92E+02	2.94E+02	2.95E+02	2.96E+02	2.98E+02	3.00E+02	3.03E+02
29	2.90E+02	2.90E+02	2.91E+02	2.91E+02	2.92E+02	2.93E+02	2.95E+02	2.96E+02	2.98E+02	3.00E+02	3.02E+02	3.05E+02
28	2.90E+02	2.91E+02	2.91E+02	2.92E+02	2.93E+02	2.94E+02	2.96E+02	2.98E+02	3.00E+02	3.02E+02	3.04E+02	3.07E+02
27	2.91E+02	2.91E+02	2.92E+02	2.93E+02	2.94E+02	2.96E+02	2.97E+02	2.99E+02	3.01E+02	3.04E+02	3.07E+02	3.10E+02
26	2.91E+02	2.92E+02	2.93E+02	2.94E+02	2.95E+02	2.97E+02	2.99E+02	3.01E+02	3.03E+02	3.06E+02	3.09E+02	3.13E+02
25	2.92E+02	2.93E+02	2.94E+02	2.95E+02	2.97E+02	2.98E+02	3.00E+02	3.03E+02	3.06E+02	3.09E+02	3.12E+02	3.16E+02
24	2.92E+02	2.93E+02	2.95E+02	2.96E+02	2.98E+02	3.00E+02	3.02E+02	3.05E+02	3.08E+02	3.11E+02	3.15E+02	3.19E+02
23	2.93E+02	2.94E+02	2.96E+02	2.97E+02	2.99E+02	3.02E+02	3.04E+02	3.07E+02	3.10E+02	3.14E+02	3.18E+02	3.23E+02
22	2.94E+02	2.95E+02	2.97E+02	2.99E+02	3.01E+02	3.03E+02	3.06E+02	3.09E+02	3.13E+02	3.17E+02	3.22E+02	3.27E+02
21	2.95E+02	2.96E+02	2.98E+02	3.00E+02	3.02E+02	3.05E+02	3.08E+02	3.12E+02	3.16E+02	3.20E+02	3.25E+02	3.31E+02
20	2.96E+02	2.97E+02	2.99E+02	3.02E+02	3.04E+02	3.07E+02	3.10E+02	3.14E+02	3.19E+02	3.23E+02	3.29E+02	3.35E+02
19	2.97E+02	2.98E+02	3.01E+02	3.03E+02	3.06E+02	3.09E+02	3.13E+02	3.17E+02	3.21E+02	3.26E+02	3.32E+02	3.39E+02
18	2.98E+02	2.99E+02	3.02E+02	3.04E+02	3.07E+02	3.11E+02	3.15E+02	3.19E+02	3.24E+02	3.29E+02	3.36E+02	3.42E+02
17	2.98E+02	3.01E+02	3.03E+02	3.06E+02	3.09E+02	3.13E+02	3.17E+02	3.21E+02	3.27E+02	3.32E+02	3.39E+02	3.46E+02
16	2.99E+02	3.01E+02	3.04E+02	3.07E+02	3.10E+02	3.14E+02	3.19E+02	3.23E+02	3.29E+02	3.35E+02	3.42E+02	3.49E+02
15	3.00E+02	3.02E+02	3.05E+02	3.08E+02	3.12E+02	3.16E+02	3.20E+02	3.25E+02	3.31E+02	3.37E+02	3.44E+02	3.51E+02
14	3.01E+02	3.03E+02	3.06E+02	3.09E+02	3.13E+02	3.17E+02	3.21E+02	3.26E+02	3.32E+02	3.39E+02	3.46E+02	3.53E+02
13	3.01E+02	3.04E+02	3.06E+02	3.10E+02	3.13E+02	3.17E+02	3.22E+02	3.27E+02	3.33E+02	3.39E+02	3.47E+02	3.54E+02
12	3.01E+02	3.04E+02	3.07E+02	3.10E+02	3.14E+02	3.18E+02	3.23E+02	3.28E+02	3.33E+02	3.40E+02	3.47E+02	3.54E+02
11	3.02E+02	3.04E+02	3.07E+02	3.10E+02	3.14E+02	3.18E+02	3.22E+02	3.28E+02	3.33E+02	3.39E+02	3.46E+02	3.54E+02
10	3.01E+02	3.04E+02	3.07E+02	3.10E+02	3.13E+02	3.17E+02	3.22E+02	3.27E+02	3.32E+02	3.38E+02	3.45E+02	3.52E+02
9	3.01E+02	3.04E+02	3.06E+02	3.09E+02	3.13E+02	3.16E+02	3.21E+02	3.25E+02	3.31E+02	3.36E+02	3.43E+02	3.49E+02

29	3.78E+02	3.87E+02	3.97E+02	4.07E+02	4.17E+02	4.28E+02	4.40E+02	4.51E+02	4.64E+02	4.77E+02	4.90E+02	5.04E-02	
28	3.87E+02	3.97E+02	4.07E+02	4.18E+02	4.29E-02	4.41E+02	4.53E+02	4.66E+02	4.80E+02	4.93E+02	5.08E+02	5.22E-02	
27	3.97E+02	4.07E-02	4.18E+02	4.30E+02	4.42E+02	4.55E+02	4.69E+02	4.82E+02	4.96E-02	5.11E+02	5.26E+02	5.41E-02	
26	4.07E+02	4.19E+02	4.31E+02	4.43E+02	4.57E+02	4.70E+02	4.84E+02	4.99E+02	5.14E+02	5.29E+02	5.44E-02	5.59E-02	
25	4.19E+02	4.31E+02	4.44E+02	4.58E+02	4.72E+02	4.86E+02	5.01E+02	5.16E+02	5.31E+02	5.46E+02	5.61E+02	5.75E-02	
24	4.31E+02	4.44E+02	4.58E+02	4.72E+02	4.87E+02	5.01E+02	5.17E+02	5.32E+02	5.47E+02	5.62E+02	5.76E+02	5.89E-02	
23	4.43E+02	4.57E+02	4.71E+02	4.86E+02	5.01E+02	5.16E+02	5.31E+02	5.47E+02	5.61E+02	5.75E+02	5.88E+02	6.01E-02	
22	4.55E+02	4.69E+02	4.84E+02	4.99E+02	5.15E+02	5.30E+02	5.45E+02	5.59E+02	5.73E+02	5.86E+02	5.98E-02	6.09E-02	
21	4.66E+02	4.81E+02	4.96E+02	5.11E+02	5.26E+02	5.41E+02	5.56E+02	5.69E+02	5.82E+02	5.94E+02	6.05E-02	6.14E-02	
20	4.77E+02	4.92E+02	5.07E+02	5.22E+02	5.36E+02	5.51E+02	5.64E+02	5.77E+02	5.89E+02	6.00E+02	6.09E+02	6.17E-02	
19	4.86E+02	5.01E+02	5.15E+02	5.30E+02	5.44E+02	5.57E+02	5.70E+02	5.82E+02	5.93E+02	6.03E+02	6.11E+02	6.17E-02	
18	4.93E+02	5.07E+02	5.22E+02	5.36E+02	5.49E+02	5.62E+02	5.74E+02	5.85E+02	5.95E+02	6.03E+02	6.10E+02	6.16E-02	
17	4.98E+02	5.12E+02	5.26E+02	5.39E+02	5.52E+02	5.64E+02	5.75E+02	5.85E+02	5.94E+02	6.02E+02	6.08E+02	6.13E-02	
16	5.02E+02	5.15E+02	5.28E+02	5.41E+02	5.53E+02	5.64E+02	5.75E+02	5.84E+02	5.92E+02	5.99E+02	6.05E+02	6.09E+02	
15	5.03E+02	5.16E+02	5.28E+02	5.40E+02	5.52E+02	5.63E+02	5.72E+02	5.81E+02	5.89E+02	5.95E+02	6.00E+02	6.04E+02	
14	5.02E+02	5.15E+02	5.27E+02	5.38E+02	5.49E+02	5.59E+02	5.68E+02	5.76E+02	5.84E+02	5.90E+02	5.95E+02	5.98E-02	
13	5.00E+02	5.11E+02	5.23E+02	5.34E+02	5.44E+02	5.54E+02	5.62E+02	5.70E+02	5.77E+02	5.83E+02	5.88E+02	5.91E+02	
12	4.95E+02	5.07E+02	5.18E+02	5.28E+02	5.38E+02	5.47E+02	5.55E+02	5.63E+02	5.69E+02	5.75E+02	5.79E+02	5.83E+02	
11	4.89E+02	5.00E+02	5.11E+02	5.20E+02	5.30E+02	5.39E+02	5.46E+02	5.54E+02	5.60E+02	5.65E+02	5.69E+02	5.73E-02	
10	4.82E+02	4.92E+02	5.02E+02	5.11E+02	5.20E+02	5.29E+02	5.36E+02	5.43E+02	5.49E+02	5.54E+02	5.58E+02	5.61E+02	
9	4.73E+02	4.82E+02	4.92E+02	5.01E+02	5.09E+02	5.17E+02	5.25E+02	5.31E+02	5.37E+02	5.42E+02	5.45E+02	5.48E+02	
8	4.62E+02	4.71E+02	4.80E+02	4.89E+02	4.97E+02	5.05E+02	5.12E+02	5.18E+02	5.23E+02	5.28E+02	5.32E+02	5.34E+02	
7	4.50E+02	4.59E+02	4.68E+02	4.76E+02	4.84E+02	4.91E+02	4.97E+02	5.03E+02	5.09E+02	5.13E+02	5.17E+02	5.19E+02	
6	4.37E+02	4.46E+02	4.54E+02	4.61E+02	4.69E+02	4.76E+02	4.82E+02	4.88E+02	4.93E+02	4.97E+02	5.01E+02	5.03E+02	
5	4.23E+02	4.31E+02	4.39E+02	4.46E+02	4.53E+02	4.60E+02	4.66E+02	4.71E+02	4.76E+02	4.80E+02	4.84E+02	4.87E+02	
4	4.08E+02	4.16E+02	4.23E+02	4.30E+02	4.36E+02	4.43E+02	4.49E+02	4.54E+02	4.59E+02	4.63E+02	4.67E+02	4.69E+02	
3	3.93E+02	4.00E+02	4.06E+02	4.13E+02	4.19E+02	4.25E+02	4.31E+02	4.36E+02	4.41E+02	4.45E+02	4.48E+02	4.52E+02	
2	3.77E+02	3.83E+02	3.89E+02	3.95E+02	4.01E+02	4.07E+02	4.12E+02	4.17E+02	4.22E+02	4.26E+02	4.29E+02	4.33E+02	
1	3.61E+02	3.66E+02	3.71E+02	3.76E+02	3.81E+02	3.86E+02	3.91E+02	3.96E+02	4.01E+02	4.05E+02	4.09E+02	4.13E+02	
0	3.55E+02	3.59E+02	3.64E+02	3.68E+02	3.72E+02	3.77E+02	3.81E+02	3.85E+02	3.89E+02	3.92E+02	3.96E+02	3.99E+02	
I =	36	37	38	39	40	41	42	43	44	45	46	47	

J

0	4.07E+02	4.19E+02	4.31E+02	4.43E+02	4.56E+02	4.70E+02	4.85E+02	5.01E+02	5.19E+02	5.38E+02	5.59E+02	5.82E+02
40	4.07E+02	4.19E+02	4.31E+02	4.43E+02	4.56E+02	4.70E+02	4.85E+02	5.01E+02	5.19E+02	5.38E+02	5.59E+02	5.82E+02
39	4.12E+02	4.23E+02	4.34E+02	4.47E+02	4.59E+02	4.73E+02	4.88E+02	5.04E+02	5.22E+02	5.41E+02	5.61E+02	5.83E+02
38	4.18E+02	4.28E+02	4.40E+02	4.51E+02	4.64E+02	4.78E+02	4.93E+02	5.09E+02	5.26E+02	5.45E+02	5.65E+02	5.86E+02
37	4.24E+02	4.35E+02	4.46E+02	4.58E+02	4.70E+02	4.84E+02	4.99E+02	5.15E+02	5.32E+02	5.50E+02	5.70E+02	5.90E+02
36	4.31E+02	4.41E+02	4.53E+02	4.65E+02	4.78E+02	4.92E+02	5.06E+02	5.22E+02	5.39E+02	5.57E+02	5.76E+02	5.96E+02
35	4.39E+02	4.50E+02	4.61E+02	4.73E+02	4.87E+02	5.01E+02	5.16E+02	5.32E+02	5.49E+02	5.67E+02	5.85E+02	6.03E+02
34	4.48E+02	4.59E+02	4.71E+02	4.84E+02	4.98E+02	5.12E+02	5.27E+02	5.44E+02	5.60E+02	5.77E+02	5.95E+02	6.12E+02
33	4.58E+02	4.70E+02	4.83E+02	4.96E+02	5.11E+02	5.25E+02	5.41E+02	5.57E+02	5.73E+02	5.90E+02	6.06E+02	6.22E+02
32	4.71E+02	4.83E+02	4.97E+02	5.11E+02	5.25E+02	5.41E+02	5.56E+02	5.72E+02	5.88E+02	6.03E+02	6.18E+02	6.33E+02
31	4.85E+02	4.98E+02	5.12E+02	5.27E+02	5.42E+02	5.57E+02	5.73E+02	5.88E+02	6.02E+02	6.17E+02	6.30E+02	6.43E+02
30	5.01E+02	5.15E+02	5.30E+02	5.45E+02	5.60E+02	5.75E+02	5.89E+02	6.03E+02	6.17E+02	6.29E+02	6.41E+02	6.51E+02
29	5.19E+02	5.33E+02	5.48E+02	5.63E+02	5.78E+02	5.92E+02	6.05E+02	6.18E+02	6.29E+02	6.40E+02	6.49E+02	6.57E+02
28	5.37E+02	5.52E+02	5.67E+02	5.81E+02	5.95E+02	6.08E+02	6.20E+02	6.30E+02	6.40E+02	6.48E+02	6.54E+02	6.59E+02
27	5.56E+02	5.70E+02	5.84E+02	5.98E+02	6.10E+02	6.21E+02	6.31E+02	6.40E+02	6.47E+02	6.52E+02	6.56E+02	6.58E+02
26	5.73E+02	5.87E+02	6.00E+02	6.12E+02	6.23E+02	6.32E+02	6.40E+02	6.46E+02	6.50E+02	6.53E+02	6.54E+02	6.53E+02
25	5.89E+02	6.01E+02	6.13E+02	6.23E+02	6.32E+02	6.39E+02	6.44E+02	6.48E+02	6.49E+02	6.50E+02	6.48E+02	6.45E+02
24	6.02E+02	6.13E+02	6.23E+02	6.31E+02	6.37E+02	6.42E+02	6.45E+02	6.46E+02	6.46E+02	6.43E+02	6.40E+02	6.35E+02
23	6.12E+02	6.21E+02	6.29E+02	6.35E+02	6.39E+02	6.42E+02	6.43E+02	6.42E+02	6.39E+02	6.35E+02	6.30E+02	6.23E+02
22	6.18E+02	6.26E+02	6.32E+02	6.36E+02	6.38E+02	6.39E+02	6.38E+02	6.35E+02	6.31E+02	6.26E+02	6.19E+02	6.11E+02
21	6.22E+02	6.28E+02	6.32E+02	6.35E+02	6.35E+02	6.35E+02	6.32E+02	6.28E+02	6.23E+02	6.16E+02	6.09E+02	6.00E+02
20	6.23E+02	6.28E+02	6.31E+02	6.32E+02	6.31E+02	6.29E+02	6.26E+02	6.21E+02	6.15E+02	6.08E+02	6.00E+02	5.91E+02
19	6.22E+02	6.26E+02	6.27E+02	6.28E+02	6.26E+02	6.23E+02	6.19E+02	6.14E+02	6.08E+02	6.00E+02	5.92E+02	5.83E+02
18	6.20E+02	6.23E+02	6.24E+02	6.23E+02	6.21E+02	6.18E+02	6.13E+02	6.08E+02	6.01E+02	5.94E+02	5.86E+02	5.77E+02
17	6.17E+02	6.19E+02	6.19E+02	6.18E+02	6.16E+02	6.12E+02	6.08E+02	6.02E+02	5.96E+02	5.89E+02	5.81E+02	5.72E+02
16	6.12E+02	6.14E+02	6.14E+02	6.13E+02	6.11E+02	6.07E+02	6.03E+02	5.97E+02	5.91E+02	5.84E+02	5.76E+02	5.67E+02
15	6.07E+02	6.08E+02	6.09E+02	6.07E+02	6.05E+02	6.02E+02	5.97E+02	5.92E+02	5.86E+02	5.79E+02	5.71E+02	5.62E+02
14	6.01E+02	6.02E+02	6.02E+02	6.01E+02	5.99E+02	5.95E+02	5.91E+02	5.86E+02	5.79E+02	5.72E+02	5.64E+02	5.55E+02
13	5.94E+02	5.95E+02	5.95E+02	5.94E+02	5.91E+02	5.88E+02	5.83E+02	5.78E+02	5.72E+02	5.65E+02	5.56E+02	5.47E+02
12	5.85E+02	5.86E+02	5.86E+02	5.85E+02	5.82E+02	5.79E+02	5.74E+02	5.69E+02	5.62E+02	5.55E+02	5.47E+02	5.38E+02
11	5.75E+02	5.76E+02	5.75E+02	5.74E+02	5.72E+02	5.68E+02	5.63E+02	5.58E+02	5.51E+02	5.44E+02	5.35E+02	5.26E+02
10	5.63E+02	5.64E+02	5.63E+02	5.62E+02	5.59E+02	5.56E+02	5.51E+02	5.45E+02	5.39E+02	5.31E+02	5.23E+02	5.14E+02
9	5.50E+02	5.51E+02	5.50E+02	5.48E+02	5.46E+02	5.42E+02	5.37E+02	5.32E+02	5.25E+02	5.18E+02	5.10E+02	5.02E+02
8	5.36E+02	5.36E+02	5.36E+02	5.34E+02	5.32E+02	5.28E+02	5.23E+02	5.18E+02	5.12E+02	5.05E+02	4.98E+02	4.90E+02
7	5.21E+02	5.21E+02	5.21E+02	5.19E+02	5.17E+02	5.14E+02	5.10E+02	5.05E+02	4.99E+02	4.93E+02	4.86E+02	4.80E+02
6	5.05E+02	5.06E+02	5.06E+02	5.04E+02	5.02E+02	5.00E+02	4.96E+02	4.92E+02	4.87E+02	4.81E+02	4.76E+02	4.70E+02
5	4.89E+02	4.90E+02	4.90E+02	4.89E+02	4.88E+02	4.85E+02	4.83E+02	4.79E+02	4.75E+02	4.70E+02	4.65E+02	4.60E+02

8	3.01E+02	3.03E+02	3.05E-02	3.08E+02	3.12E-02	3.15E-02	3.19E-02	3.24E+02	3.28E+02	3.34E+02	3.40E-02	3.46E-02
7	3.00E+02	3.02E-02	3.04E+02	3.07E+02	3.10E+02	3.13E+02	3.17E-02	3.21E-02	3.26E-02	3.31E-02	3.36E-02	3.42E-02
6	2.99E+02	3.01E+02	3.03E+02	3.06E+02	3.08E+02	3.11E+02	3.15E-02	3.19E+02	3.23E+02	3.27E+02	3.32E-02	3.37E-02
5	2.98E+02	3.00E+02	3.02E+02	3.04E+02	3.06E+02	3.09E+02	3.12E+02	3.15E+02	3.19E+02	3.23E+02	3.28E-02	3.32E-02
4	2.97E+02	2.99E+02	3.00E+02	3.02E+02	3.04E+02	3.07E+02	3.09E+02	3.12E-02	3.15E-02	3.19E+02	3.23E+02	3.27E-02
3	2.97E+02	2.98E+02	2.99E+02	3.00E+02	3.02E+02	3.04E+02	3.07E+02	3.09E+02	3.12E-02	3.15E+02	3.18E-02	3.22E-02
2	2.96E+02	2.97E+02	2.98E+02	2.99E+02	3.00E+02	3.02E+02	3.04E+02	3.06E+02	3.08E+02	3.11E+02	3.13E+02	3.16E-02
1	2.95E+02	2.95E+02	2.96E+02	2.97E+02	2.98E+02	2.99E+02	3.01E+02	3.02E+02	3.04E+02	3.06E-02	3.09E-02	3.11E-02
0	2.95E-02	2.96E+02	2.97E+02	2.98E+02	2.99E+02	3.00E+02	3.02E+02	3.03E-02	3.05E-02	3.07E-02	3.09E-02	3.11E-02
I =	12	13	14	15	16	17	18	19	20	21	22	23

J

0	2.88E+02	2.88E+02	2.88E+02	2.88E+02	2.88E+02	2.88E+02	2.88E+02	2.88E+02	2.88E+02	2.88E+02	2.88E+02	2.88E+02
40	2.88E+02	2.89E+02	2.89E+02	2.89E+02	2.89E+02	2.90E+02	2.91E+02	2.91E+02	2.92E+02	2.94E+02	2.95E+02	2.97E+02
39	2.89E+02	2.90E+02	2.90E+02	2.91E+02	2.92E+02	2.93E+02	2.94E+02	2.96E+02	2.98E+02	3.00E+02	3.03E-02	3.06E+02
38	2.90E+02	2.91E+02	2.92E+02	2.93E+02	2.94E+02	2.96E+02	2.98E+02	3.00E+02	3.03E+02	3.06E+02	3.10E+02	3.14E+02
37	2.92E+02	2.93E+02	2.94E+02	2.95E+02	2.97E+02	2.99E+02	3.02E+02	3.05E+02	3.08E+02	3.12E+02	3.16E+02	3.21E+02
36	2.93E+02	2.95E+02	2.96E+02	2.98E+02	3.00E+02	3.03E+02	3.06E+02	3.09E+02	3.13E+02	3.17E+02	3.22E+02	3.27E+02
35	2.95E+02	2.97E+02	2.98E+02	3.01E+02	3.03E+02	3.06E+02	3.10E+02	3.13E+02	3.18E+02	3.22E+02	3.27E+02	3.33E+02
34	2.97E+02	2.99E+02	3.01E+02	3.03E+02	3.06E+02	3.10E+02	3.13E+02	3.17E+02	3.22E+02	3.27E+02	3.32E+02	3.38E+02
33	2.99E+02	3.01E+02	3.03E+02	3.06E+02	3.09E+02	3.13E+02	3.17E+02	3.22E+02	3.26E+02	3.32E+02	3.38E+02	3.44E+02
32	3.01E+02	3.03E+02	3.06E+02	3.09E+02	3.13E+02	3.17E+02	3.21E+02	3.26E+02	3.31E+02	3.37E+02	3.43E+02	3.49E+02
31	3.03E+02	3.06E+02	3.09E+02	3.12E+02	3.16E+02	3.20E+02	3.25E+02	3.30E+02	3.36E+02	3.42E+02	3.49E+02	3.56E+02
30	3.05E+02	3.08E+02	3.12E+02	3.15E+02	3.20E+02	3.24E+02	3.30E+02	3.35E+02	3.41E+02	3.48E+02	3.55E+02	3.62E+02
29	3.08E+02	3.11E+02	3.15E+02	3.19E+02	3.24E+02	3.29E+02	3.34E+02	3.40E+02	3.47E+02	3.54E+02	3.62E+02	3.70E+02
28	3.11E+02	3.14E+02	3.18E+02	3.23E+02	3.28E+02	3.34E+02	3.40E+02	3.46E+02	3.53E+02	3.61E+02	3.69E+02	3.78E+02
27	3.14E+02	3.18E+02	3.22E+02	3.27E+02	3.33E+02	3.39E+02	3.45E+02	3.52E+02	3.60E+02	3.68E+02	3.77E+02	3.87E+02
26	3.17E+02	3.21E+02	3.26E+02	3.32E+02	3.38E+02	3.44E+02	3.51E+02	3.59E+02	3.68E+02	3.77E+02	3.86E+02	3.96E+02
25	3.20E+02	3.25E+02	3.31E+02	3.37E+02	3.43E+02	3.50E+02	3.58E+02	3.67E+02	3.76E+02	3.85E+02	3.96E+02	4.07E+02
24	3.24E+02	3.30E+02	3.36E+02	3.42E+02	3.49E+02	3.57E+02	3.65E+02	3.75E+02	3.84E+02	3.95E+02	4.06E+02	4.18E+02
23	3.28E+02	3.34E+02	3.41E+02	3.48E+02	3.55E+02	3.64E+02	3.73E+02	3.83E+02	3.93E+02	4.05E+02	4.17E+02	4.30E+02
22	3.33E+02	3.39E+02	3.46E+02	3.53E+02	3.62E+02	3.71E+02	3.81E+02	3.91E+02	4.03E+02	4.15E+02	4.28E+02	4.41E+02
21	3.37E+02	3.44E+02	3.51E+02	3.59E+02	3.68E+02	3.78E+02	3.89E+02	4.00E+02	4.12E+02	4.25E+02	4.38E+02	4.52E+02
20	3.41E+02	3.49E+02	3.57E+02	3.65E+02	3.75E+02	3.85E+02	3.96E+02	4.08E+02	4.21E+02	4.34E+02	4.48E+02	4.62E+02
19	3.46E+02	3.53E+02	3.62E+02	3.71E+02	3.81E+02	3.92E+02	4.04E+02	4.16E+02	4.29E+02	4.43E+02	4.57E+02	4.71E+02
18	3.50E+02	3.58E+02	3.67E+02	3.77E+02	3.87E+02	3.98E+02	4.10E+02	4.23E+02	4.36E+02	4.50E+02	4.64E+02	4.79E+02
17	3.54E+02	3.62E+02	3.72E+02	3.82E+02	3.92E+02	4.04E+02	4.16E+02	4.29E+02	4.42E+02	4.56E+02	4.70E+02	4.84E+02
16	3.57E+02	3.66E+02	3.75E+02	3.86E+02	3.97E+02	4.08E+02	4.21E+02	4.34E+02	4.47E+02	4.60E+02	4.74E+02	4.88E+02
15	3.60E+02	3.69E+02	3.78E+02	3.89E+02	4.00E+02	4.12E+02	4.24E+02	4.37E+02	4.50E+02	4.63E+02	4.76E+02	4.90E+02
14	3.62E+02	3.71E+02	3.80E+02	3.91E+02	4.02E+02	4.14E+02	4.26E+02	4.38E+02	4.51E+02	4.64E+02	4.77E+02	4.89E+02
13	3.63E+02	3.72E+02	3.81E+02	3.92E+02	4.03E+02	4.14E+02	4.26E+02	4.38E+02	4.50E+02	4.63E+02	4.75E+02	4.87E+02
12	3.63E+02	3.72E+02	3.81E+02	3.91E+02	4.02E+02	4.13E+02	4.24E+02	4.36E+02	4.48E+02	4.60E+02	4.72E+02	4.84E+02
11	3.62E+02	3.70E+02	3.80E+02	3.90E+02	4.00E+02	4.11E+02	4.22E+02	4.33E+02	4.44E+02	4.56E+02	4.67E+02	4.78E+02
10	3.60E+02	3.68E+02	3.77E+02	3.86E+02	3.96E+02	4.07E+02	4.17E+02	4.28E+02	4.39E+02	4.50E+02	4.60E+02	4.71E+02
9	3.57E+02	3.65E+02	3.73E+02	3.82E+02	3.92E+02	4.01E+02	4.11E+02	4.21E+02	4.32E+02	4.42E+02	4.52E+02	4.63E+02
8	3.53E+02	3.60E+02	3.68E+02	3.77E+02	3.86E+02	3.95E+02	4.04E+02	4.14E+02	4.23E+02	4.33E+02	4.43E+02	4.53E+02
7	3.48E+02	3.55E+02	3.63E+02	3.70E+02	3.78E+02	3.87E+02	3.96E+02	4.05E+02	4.14E+02	4.23E+02	4.32E+02	4.41E+02
6	3.43E+02	3.49E+02	3.56E+02	3.63E+02	3.70E+02	3.78E+02	3.86E+02	3.95E+02	4.03E+02	4.12E+02	4.20E+02	4.29E+02
5	3.37E+02	3.43E+02	3.49E+02	3.55E+02	3.62E+02	3.69E+02	3.76E+02	3.84E+02	3.91E+02	3.99E+02	4.07E+02	4.16E+02
4	3.31E+02	3.36E+02	3.41E+02	3.47E+02	3.53E+02	3.59E+02	3.65E+02	3.72E+02	3.79E+02	3.86E+02	3.94E+02	4.01E+02
3	3.25E+02	3.30E+02	3.34E+02	3.39E+02	3.44E+02	3.49E+02	3.55E+02	3.61E+02	3.67E+02	3.73E+02	3.79E+02	3.86E+02
2	3.20E+02	3.23E+02	3.27E+02	3.31E+02	3.35E+02	3.40E+02	3.44E+02	3.49E+02	3.55E+02	3.60E+02	3.66E+02	3.71E+02
1	3.14E+02	3.16E+02	3.19E+02	3.23E+02	3.26E+02	3.30E+02	3.34E+02	3.38E+02	3.42E+02	3.46E+02	3.51E+02	3.56E+02
0	3.14E+02	3.16E+02	3.19E+02	3.22E+02	3.25E+02	3.28E+02	3.32E+02	3.35E+02	3.39E+02	3.43E+02	3.47E+02	3.51E+02
I =	24	25	26	27	28	29	30	31	32	33	34	35

J

0	2.88E+02	2.88E+02	2.88E+02	2.88E+02	2.88E+02	2.88E+02	3.38E+02	3.50E+02	3.62E+02	3.73E+02	3.85E+02	3.96E+02
40	2.99E+02	3.03E+02	3.06E+02	3.11E+02	3.18E+02	3.27E+02	3.38E+02	3.50E+02	3.62E+02	3.73E+02	3.85E+02	3.96E+02
39	3.10E+02	3.15E+02	3.20E+02	3.26E+02	3.33E+02	3.41E+02	3.50E+02	3.60E+02	3.70E+02	3.80E+02	3.90E+02	4.01E+02
38	3.19E+02	3.24E+02	3.30E+02	3.37E+02	3.44E+02	3.52E+02	3.60E+02	3.69E+02	3.78E+02	3.88E+02	3.97E+02	4.07E+02
37	3.26E+02	3.32E+02	3.39E+02	3.45E+02	3.53E+02	3.61E+02	3.69E+02	3.77E+02	3.86E+02	3.95E+02	4.04E+02	4.14E+02
36	3.33E+02	3.39E+02	3.46E+02	3.53E+02	3.60E+02	3.68E+02	3.76E+02	3.84E+02	3.93E+02	4.02E+02	4.11E+02	4.21E+02
35	3.39E+02	3.45E+02	3.52E+02	3.59E+02	3.67E+02	3.75E+02	3.83E+02	3.91E+02	4.00E+02	4.09E+02	4.19E+02	4.28E+02
34	3.45E+02	3.51E+02	3.58E+02	3.66E+02	3.74E+02	3.82E+02	3.90E+02	3.99E+02	4.08E+02	4.17E+02	4.27E+02	4.37E+02
33	3.50E+02	3.57E+02	3.65E+02	3.73E+02	3.81E+02	3.89E+02	3.98E+02	4.07E+02	4.16E+02	4.26E+02	4.36E+02	4.47E+02
32	3.56E+02	3.64E+02	3.72E+02	3.80E+02	3.88E+02	3.97E+02	4.06E+02	4.16E+02	4.26E+02	4.36E+02	4.47E+02	4.59E+02
31	3.63E+02	3.71E+02	3.79E+02	3.88E+02	3.97E+02	4.06E+02	4.16E+02	4.26E+02	4.37E+02	4.48E+02	4.60E+02	4.72E+02
30	3.70E+02	3.79E+02	3.87E+02	3.97E+02	4.06E+02	4.16E+02	4.27E+02	4.38E+02	4.50E+02	4.62E+02	4.74E+02	4.87E+02

27	1.00E+02	1.00E+02	1.00E+02	1.00E+02	1.00E+02	1.00E+02	1.00E+02	1.00E+02	1.00E+02	1.00E+02	1.00E+02	1.00E+02	1.00E-02
26	1.00E+02	1.00E+02	1.00E+02	1.00E+02	1.00E+02	1.00E+02	1.00E+02	1.00E+02	1.00E+02	1.00E+02	1.00E+02	1.00E-02	1.00E-02
25	1.00E+02	1.00E+02	1.00E+02	1.00E+02	1.00E+02	1.00E+02	1.00E+02	1.00E+02	1.00E+02	1.00E+02	1.00E+02	1.00E-02	1.00E-02
24	1.00E+02	1.00E+02	1.00E+02	1.00E+02	1.00E+02	1.00E-02	1.00E+02	1.00E+02	1.00E+02	1.00E+02	1.00E+02	1.00E-02	1.00E-02
23	1.00E+02	1.00E+02	1.00E+02	1.00E+02	1.00E+02	1.00E+02	1.00E+02	1.00E+02	1.00E+02	1.00E+02	1.00E+02	1.00E-02	1.00E-02
22	1.00E+02	1.00E+02	1.00E+02	1.00E+02	1.00E+02	1.00E+02	1.00E+02	1.00E+02	1.00E+02	1.00E+02	1.00E+02	1.00E+02	1.00E-02
21	1.00E+02	1.00E+02	1.00E+02	1.00E+02	1.00E+02	1.00E+02	1.00E+02	1.00E+02	1.00E+02	1.00E+02	1.00E+02	1.00E-02	1.00E-02
20	1.00E+02	1.00E+02	1.00E+02	1.00E+02	1.00E+02	1.00E+02	1.00E+02	1.00E+02	1.00E+02	1.00E+02	1.00E+02	1.00E-02	1.00E-02
19	1.00E+02	1.00E+02	1.00E+02	1.00E+02	1.00E+02	1.00E+02	1.00E+02	1.00E+02	1.00E+02	1.00E+02	1.00E+02	1.00E-02	1.00E-02
18	1.00E+02	1.00E+02	1.00E+02	1.00E+02	1.00E+02	1.00E+02	1.00E+02	1.00E+02	1.00E+02	1.00E+02	1.00E+02	1.00E-02	1.00E+02
17	1.00E+02	1.00E+02	1.00E+02	1.00E+02	1.00E+02	1.00E+02	1.00E+02	1.00E+02	1.00E+02	1.00E+02	1.00E+02	1.00E+02	1.00E+02
16	1.00E+02	1.00E+02	1.00E+02	1.00E+02	1.00E+02	1.00E+02	1.00E+02	1.00E+02	1.00E+02	1.00E+02	1.00E+02	1.00E+02	1.00E+02
15	1.00E+02	1.00E+02	1.00E+02	1.00E+02	1.00E+02	1.00E+02	1.00E+02	1.00E+02	1.00E+02	1.00E+02	1.00E+02	1.00E-02	1.00E-02
14	1.00E+02	1.00E+02	1.00E+02	1.00E+02	1.00E+02	1.00E+02	1.00E+02	1.00E+02	1.00E+02	1.00E+02	1.00E+02	1.00E+02	1.00E-02
13	1.00E+02	1.00E+02	1.00E+02	1.00E+02	1.00E+02	1.00E+02	1.00E+02	1.00E+02	1.00E+02	1.00E+02	1.00E+02	1.00E+02	1.00E+02
12	1.00E+02	1.00E+02	1.00E+02	1.00E+02	1.00E+02	1.00E+02	1.00E+02	1.00E+02	1.00E+02	1.00E+02	1.00E+02	1.00E+02	1.00E+02
11	1.00E+02	1.00E+02	1.00E+02	1.00E+02	1.00E+02	1.00E+02	1.00E+02	1.00E+02	1.00E+02	1.00E+02	1.00E+02	1.00E+02	1.00E+02
10	1.00E+02	1.00E+02	1.00E+02	1.00E+02	1.00E+02	1.00E+02	1.00E+02	1.00E+02	1.00E+02	1.00E+02	1.00E+02	1.00E+02	1.00E+02
9	1.00E+02	1.00E+02	1.00E+02	1.00E+02	1.00E+02	1.00E+02	1.00E+02	1.00E+02	1.00E+02	1.00E+02	1.00E+02	1.00E+02	1.00E+02
8	1.00E+02	1.00E+02	1.00E+02	1.00E+02	1.00E+02	1.00E+02	1.00E+02	1.00E+02	1.00E+02	1.00E+02	1.00E+02	1.00E+02	1.00E+02
7	1.00E+02	1.00E+02	1.00E+02	1.00E+02	1.00E+02	1.00E+02	1.00E+02	1.00E+02	1.00E+02	1.00E+02	1.00E+02	1.00E+02	1.00E+02
6	1.00E+02	1.00E+02	1.00E+02	1.00E+02	1.00E+02	1.00E+02	1.00E+02	1.00E+02	1.00E+02	1.00E+02	1.00E+02	1.00E+02	1.00E+02
5	1.00E+02	1.00E+02	1.00E+02	1.00E+02	1.00E+02	1.00E+02	1.00E+02	1.00E+02	1.00E+02	1.00E+02	1.00E+02	1.00E+02	1.00E+02
4	1.00E+02	1.00E+02	1.00E+02	1.00E+02	1.00E+02	1.00E+02	1.00E+02	1.00E+02	1.00E+02	1.00E+02	1.00E+02	1.00E+02	1.00E+02
3	1.00E+02	1.00E+02	1.00E+02	1.00E+02	1.00E+02	1.00E+02	1.00E+02	1.00E+02	1.00E+02	1.00E+02	1.00E+02	1.00E+02	1.00E+02
2	1.00E+02	1.00E+02	1.00E+02	1.00E+02	1.00E+02	1.00E+02	1.00E+02	1.00E+02	1.00E+02	1.00E+02	1.00E+02	1.00E+02	1.00E+02
1	1.00E+02	1.00E+02	1.00E+02	1.00E+02	1.00E+02	1.00E+02	1.00E+02	1.00E+02	1.00E+02	1.00E+02	1.00E+02	1.00E+02	1.00E+02
0	2.88E+02	2.88E+02	2.88E+02	2.88E+02	2.88E+02	2.88E+02	2.88E+02	2.88E+02	2.88E+02	2.88E+02	2.88E+02	2.88E+02	2.88E+02
I =	36	37	38	39	40	41	42	43	44	45	46	47	

J

0	2.96E+02	2.96E+02	2.96E+02	2.96E+02	2.96E+02	2.96E+02	2.96E+02	2.96E+02	2.96E+02	2.96E+02	2.96E+02	2.96E+02	2.97E+02
30	1.00E+02	1.00E+02	1.00E+02	1.00E+02	1.00E+02	1.00E+02	1.00E+02	1.00E+02	1.00E+02	1.00E+02	1.00E+02	1.00E+02	1.00E+02
29	1.00E+02	1.00E+02	1.00E+02	1.00E+02	1.00E+02	1.00E+02	1.00E+02	1.00E+02	1.00E+02	1.00E+02	1.00E+02	1.00E+02	1.00E+02
28	1.00E+02	1.00E+02	1.00E+02	1.00E+02	1.00E+02	1.00E+02	1.00E+02	1.00E+02	1.00E+02	1.00E+02	1.00E+02	1.00E+02	1.00E+02
27	1.00E+02	1.00E+02	1.00E+02	1.00E+02	1.00E+02	1.00E+02	1.00E+02	1.00E+02	1.00E+02	1.00E+02	1.00E+02	1.00E+02	1.00E+02
26	1.00E+02	1.00E+02	1.00E+02	1.00E+02	1.00E+02	1.00E+02	1.00E+02	1.00E+02	1.00E+02	1.00E+02	1.00E+02	1.00E+02	1.00E+02
25	1.00E+02	1.00E+02	1.00E+02	1.00E+02	1.00E+02	1.00E+02	1.00E+02	1.00E+02	1.00E+02	1.00E+02	1.00E+02	1.00E+02	1.00E+02
24	1.00E+02	1.00E+02	1.00E+02	1.00E+02	1.00E+02	1.00E+02	1.00E+02	1.00E+02	1.00E+02	1.00E+02	1.00E+02	1.00E+02	1.00E+02
23	1.00E+02	1.00E+02	1.00E+02	1.00E+02	1.00E+02	1.00E+02	1.00E+02	1.00E+02	1.00E+02	1.00E+02	1.00E+02	1.00E+02	1.00E+02
22	1.00E+02	1.00E+02	1.00E+02	1.00E+02	1.00E+02	1.00E+02	1.00E+02	1.00E+02	1.00E+02	1.00E+02	1.00E+02	1.00E+02	1.00E+02
21	1.00E+02	1.00E+02	1.00E+02	1.00E+02	1.00E+02	1.00E+02	1.00E+02	1.00E+02	1.00E+02	1.00E+02	1.00E+02	1.00E+02	1.00E+02
20	1.00E+02	1.00E+02	1.00E+02	1.00E+02	1.00E+02	1.00E+02	1.00E+02	1.00E+02	1.00E+02	1.00E+02	1.00E+02	1.00E+02	1.00E+02
19	1.00E+02	1.00E+02	1.00E+02	1.00E+02	1.00E+02	1.00E+02	1.00E+02	1.00E+02	1.00E+02	1.00E+02	1.00E+02	1.00E+02	1.00E+02
18	1.00E+02	1.00E+02	1.00E+02	1.00E+02	1.00E+02	1.00E+02	1.00E+02	1.00E+02	1.00E+02	1.00E+02	1.00E+02	1.00E+02	1.00E+02
17	1.00E+02	1.00E+02	1.00E+02	1.00E+02	1.00E+02	1.00E+02	1.00E+02	1.00E+02	1.00E+02	1.00E+02	1.00E+02	1.00E+02	1.00E+02
16	1.00E+02	1.00E+02	1.00E+02	1.00E+02	1.00E+02	1.00E+02	1.00E+02	1.00E+02	1.00E+02	1.00E+02	1.00E+02	1.00E+02	1.00E+02
15	1.00E+02	1.00E+02	1.00E+02	1.00E+02	1.00E+02	1.00E+02	1.00E+02	1.00E+02	1.00E+02	1.00E+02	1.00E+02	1.00E+02	1.00E+02
14	1.00E+02	1.00E+02	1.00E+02	1.00E+02	1.00E+02	1.00E+02	1.00E+02	1.00E+02	1.00E+02	1.00E+02	1.00E+02	1.00E+02	1.00E+02
13	1.00E+02	1.00E+02	1.00E+02	1.00E+02	1.00E+02	1.00E+02	1.00E+02	1.00E+02	1.00E+02	1.00E+02	1.00E+02	1.00E+02	1.00E+02
12	1.00E+02	1.00E+02	1.00E+02	1.00E+02	1.00E+02	1.00E+02	1.00E+02	1.00E+02	1.00E+02	1.00E+02	1.00E+02	1.00E+02	1.00E+02
11	1.00E+02	1.00E+02	1.00E+02	1.00E+02	1.00E+02	1.00E+02	1.00E+02	1.00E+02	1.00E+02	1.00E+02	1.00E+02	1.00E+02	1.00E+02
10	1.00E+02	1.00E+02	1.00E+02	1.00E+02	1.00E+02	1.00E+02	1.00E+02	1.00E+02	1.00E+02	1.00E+02	1.00E+02	1.00E+02	1.00E+02
9	1.00E+02	1.00E+02	1.00E+02	1.00E+02	1.00E+02	1.00E+02	1.00E+02	1.00E+02	1.00E+02	1.00E+02	1.00E+02	1.00E+02	1.00E+02
8	1.00E+02	1.00E+02	1.00E+02	1.00E+02	1.00E+02	1.00E+02	1.00E+02	1.00E+02	1.00E+02	1.00E+02	1.00E+02	1.00E+02	1.00E+02
7	1.00E+02	1.00E+02	1.00E+02	1.00E+02	1.00E+02	1.00E+02	1.00E+02	1.00E+02	1.00E+02	1.00E+02	1.00E+02	1.00E+02	1.00E+02
6	1.00E+02	1.00E+02	1.00E+02	1.00E+02	1.00E+02	1.00E+02	1.00E+02	1.00E+02	1.00E+02	1.00E+02	1.00E+02	1.00E+02	1.00E+02
5	1.00E+02	1.00E+02	1.00E+02	1.00E+02	1.00E+02	1.00E+02	1.00E+02	1.00E+02	1.00E+02	1.00E+02	1.00E+02	1.00E+02	1.00E+02
4	1.00E+02	1.00E+02	1.00E+02	1.00E+02	1.00E+02	1.00E+02	1.00E+02	1.00E+02	1.00E+02	1.00E+02	1.00E+02	1.00E+02	1.00E+02
3	1.00E+02	1.00E+02	1.00E+02	1.00E+02	1.00E+02	1.00E+02	1.00E+02	1.00E+02	1.00E+02	1.00E+02	1.00E+02	1.00E+02	1.00E+02
2	1.00E+02	1.00E+02	1.00E+02	1.00E+02	1.00E+02	1.00E+02	1.00E+02	1.00E+02	1.00E+02	1.00E+02	1.00E+02	1.00E+02	1.00E+02
1	1.00E+02	1.00E+02	1.00E+02	1.00E+02	1.00E+02	1.00E+02	1.00E+02	1.00E+02	1.00E+02	1.00E+02	1.00E+02	1.00E+02	1.00E+02
0	2.88E+02	2.88E+02	2.88E+02	2.88E+02	2.88E+02	2.88E+02	2.88E+02	2.88E+02	2.88E+02	2.88E+02	2.88E+02	2.88E+02	2.88E+02
I =	48	49	50	51	52	53	54	55	56	57	58	59	

J

0	2.97E+02	2.97E+02	2.97E+02	2.97E+02	2.97E+02	2.94E+02	2.93E+02	2.93E+02	2.93E+02	2.93E+02	2.94E+02	2.99E+02	
30	1.00E+02	1.00E+02	1.00E+02	1.00E+02	1.00E+02	2.93E+02	2.93E+02	2.93E+02	2.93E+02	2.93E+02	2.93E+02	2.94E+02	
29	1.00E+02	1.00E+02	1.00E+02	1.00E+02	1.00E+02	2.93E+02	2.93E+02	2.93E+02	2.93E+02	2.93E+02	2.93E+02	2.93E+02	

4	4.72E+02	4.73E+02	4.74E+02	4.74E+02	4.73E+02	4.71E+02	4.69E+02	4.66E+02	4.63E+02	4.59E+02	4.55E+02	4.51E+02
3	4.54E+02	4.56E+02	4.57E+02	4.57E+02	4.57E+02	4.57E+02	4.55E+02	4.53E+02	4.51E+02	4.48E+02	4.45E+02	4.42E+02
2	4.36E+02	4.38E+02	4.40E+02	4.41E+02	4.41E+02	4.41E+02	4.41E+02	4.40E+02	4.39E+02	4.37E+02	4.35E+02	4.33E+02
1	4.16E+02	4.19E+02	4.22E+02	4.24E+02	4.25E+02	4.26E+02	4.27E+02	4.27E+02	4.26E+02	4.26E+02	4.24E+02	4.23E+02
0	4.02E+02	4.05E+02	4.07E+02	4.09E+02	4.10E+02	4.12E+02	4.12E+02	4.13E+02	4.13E+02	4.13E+02	4.12E+02	4.11E+02
I =	48	49	50	51	52	53	54	55	56	57	58	59

J

0	6.07E+02	6.33E+02	6.61E+02	6.91E+02	7.22E+02	7.54E+02	7.88E+02	8.23E+02	8.58E+02	8.95E+02	9.33E+02	9.71E+02
40	6.07E+02	6.33E+02	6.61E+02	6.91E+02	7.22E+02	7.54E+02	7.88E+02	8.23E+02	8.58E+02	8.95E+02	9.33E+02	9.71E+02
39	6.07E+02	6.32E+02	6.58E+02	6.85E+02	7.14E+02	7.43E+02	7.73E+02	8.04E+02	8.36E+02	8.68E+02	9.01E+02	9.34E+02
38	6.08E+02	6.32E+02	6.56E+02	6.82E+02	7.08E+02	7.34E+02	7.61E+02	7.88E+02	8.16E+02	8.44E+02	8.72E+02	9.01E+02
37	6.11E+02	6.33E+02	6.56E+02	6.79E+02	7.03E+02	7.27E+02	7.51E+02	7.75E+02	7.99E+02	8.22E+02	8.46E+02	8.70E+02
36	6.16E+02	6.37E+02	6.58E+02	6.79E+02	7.00E+02	7.21E+02	7.42E+02	7.63E+02	7.83E+02	8.03E+02	8.23E+02	8.43E+02
35	6.22E+02	6.41E+02	6.61E+02	6.80E+02	6.98E+02	7.17E+02	7.35E+02	7.52E+02	7.69E+02	7.85E+02	8.01E+02	8.18E+02
34	6.30E+02	6.47E+02	6.64E+02	6.81E+02	6.97E+02	7.13E+02	7.28E+02	7.42E+02	7.55E+02	7.68E+02	7.81E+02	7.94E+02
33	6.38E+02	6.54E+02	6.69E+02	6.83E+02	6.96E+02	7.09E+02	7.20E+02	7.31E+02	7.41E+02	7.51E+02	7.60E+02	7.71E+02
32	6.47E+02	6.60E+02	6.72E+02	6.84E+02	6.94E+02	7.04E+02	7.12E+02	7.20E+02	7.27E+02	7.33E+02	7.40E+02	7.48E+02
31	6.54E+02	6.65E+02	6.75E+02	6.83E+02	6.91E+02	6.97E+02	7.02E+02	7.07E+02	7.10E+02	7.14E+02	7.19E+02	7.25E+02
30	6.60E+02	6.68E+02	6.75E+02	6.80E+02	6.85E+02	6.88E+02	6.90E+02	6.91E+02	6.92E+02	6.94E+02	6.97E+02	7.03E+02
29	6.63E+02	6.68E+02	6.72E+02	6.74E+02	6.76E+02	6.76E+02	6.75E+02	6.74E+02	6.73E+02	6.73E+02	6.75E+02	6.81E+02
28	6.63E+02	6.65E+02	6.66E+02	6.65E+02	6.63E+02	6.61E+02	6.57E+02	6.54E+02	6.52E+02	6.51E+02	6.54E+02	6.61E+02
27	6.59E+02	6.58E+02	6.56E+02	6.53E+02	6.48E+02	6.43E+02	6.38E+02	6.34E+02	6.30E+02	6.30E+02	6.33E+02	6.42E+02
26	6.51E+02	6.48E+02	6.43E+02	6.37E+02	6.31E+02	6.24E+02	6.18E+02	6.13E+02	6.10E+02	6.10E+02	6.15E+02	6.26E+02
25	6.41E+02	6.35E+02	6.28E+02	6.21E+02	6.13E+02	6.05E+02	5.98E+02	5.93E+02	5.91E+02	5.92E+02	5.99E+02	6.12E+02
24	6.28E+02	6.21E+02	6.12E+02	6.04E+02	5.95E+02	5.87E+02	5.80E+02	5.76E+02	5.74E+02	5.77E+02	5.85E+02	5.98E+02
23	6.15E+02	6.06E+02	5.97E+02	5.88E+02	5.79E+02	5.71E+02	5.65E+02	5.61E+02	5.60E+02	5.64E+02	5.72E+02	5.86E+02
22	6.02E+02	5.93E+02	5.84E+02	5.74E+02	5.65E+02	5.58E+02	5.52E+02	5.48E+02	5.48E+02	5.51E+02	5.60E+02	5.73E+02
21	5.91E+02	5.82E+02	5.72E+02	5.63E+02	5.54E+02	5.46E+02	5.41E+02	5.37E+02	5.37E+02	5.40E+02	5.48E+02	5.60E+02
20	5.82E+02	5.72E+02	5.63E+02	5.53E+02	5.45E+02	5.37E+02	5.31E+02	5.27E+02	5.26E+02	5.29E+02	5.36E+02	5.48E+02
19	5.74E+02	5.65E+02	5.55E+02	5.46E+02	5.37E+02	5.29E+02	5.22E+02	5.18E+02	5.16E+02	5.18E+02	5.24E+02	5.34E+02
18	5.68E+02	5.59E+02	5.49E+02	5.39E+02	5.30E+02	5.21E+02	5.14E+02	5.09E+02	5.06E+02	5.07E+02	5.12E+02	5.21E+02
17	5.63E+02	5.54E+02	5.44E+02	5.33E+02	5.23E+02	5.14E+02	5.06E+02	4.99E+02	4.96E+02	4.96E+02	4.99E+02	5.08E+02
16	5.58E+02	5.48E+02	5.38E+02	5.27E+02	5.16E+02	5.06E+02	4.97E+02	4.90E+02	4.85E+02	4.84E+02	4.87E+02	4.94E+02
15	5.52E+02	5.42E+02	5.31E+02	5.20E+02	5.09E+02	4.98E+02	4.88E+02	4.80E+02	4.75E+02	4.73E+02	4.75E+02	4.81E+02
14	5.46E+02	5.35E+02	5.24E+02	5.12E+02	5.00E+02	4.89E+02	4.79E+02	4.70E+02	4.65E+02	4.62E+02	4.63E+02	4.68E+02
13	5.37E+02	5.27E+02	5.15E+02	5.03E+02	4.91E+02	4.80E+02	4.69E+02	4.61E+02	4.55E+02	4.52E+02	4.52E+02	4.56E+02
12	5.28E+02	5.17E+02	5.06E+02	4.94E+02	4.82E+02	4.71E+02	4.61E+02	4.52E+02	4.46E+02	4.42E+02	4.42E+02	4.44E+02
11	5.17E+02	5.06E+02	4.95E+02	4.84E+02	4.73E+02	4.62E+02	4.53E+02	4.44E+02	4.38E+02	4.34E+02	4.33E+02	4.34E+02
10	5.05E+02	4.95E+02	4.85E+02	4.75E+02	4.65E+02	4.55E+02	4.46E+02	4.38E+02	4.31E+02	4.27E+02	4.24E+02	4.25E+02
9	4.93E+02	4.84E+02	4.75E+02	4.66E+02	4.57E+02	4.48E+02	4.40E+02	4.32E+02	4.26E+02	4.21E+02	4.18E+02	4.17E+02
8	4.82E+02	4.74E+02	4.66E+02	4.58E+02	4.50E+02	4.42E+02	4.35E+02	4.27E+02	4.21E+02	4.16E+02	4.12E+02	4.10E+02
7	4.72E+02	4.65E+02	4.58E+02	4.51E+02	4.44E+02	4.37E+02	4.30E+02	4.23E+02	4.17E+02	4.12E+02	4.07E+02	4.04E+02
6	4.63E+02	4.57E+02	4.51E+02	4.45E+02	4.38E+02	4.32E+02	4.26E+02	4.20E+02	4.14E+02	4.08E+02	4.04E+02	4.00E+02
5	4.55E+02	4.50E+02	4.44E+02	4.39E+02	4.33E+02	4.28E+02	4.22E+02	4.16E+02	4.11E+02	4.06E+02	4.01E+02	3.96E+02
4	4.47E+02	4.42E+02	4.37E+02	4.33E+02	4.28E+02	4.23E+02	4.18E+02	4.13E+02	4.08E+02	4.03E+02	3.98E+02	3.93E+02
3	4.38E+02	4.35E+02	4.31E+02	4.26E+02	4.22E+02	4.18E+02	4.13E+02	4.09E+02	4.04E+02	4.00E+02	3.95E+02	3.90E+02
2	4.30E+02	4.27E+02	4.23E+02	4.20E+02	4.16E+02	4.13E+02	4.09E+02	4.05E+02	4.00E+02	3.96E+02	3.92E+02	3.88E+02
1	4.21E+02	4.19E+02	4.16E+02	4.13E+02	4.10E+02	4.07E+02	4.03E+02	4.00E+02	3.96E+02	3.92E+02	3.88E+02	3.84E+02
0	4.10E+02	4.09E+02	4.07E+02	4.04E+02	4.02E+02	3.99E+02	3.96E+02	3.93E+02	3.90E+02	3.87E+02	3.84E+02	3.80E+02
I =	60	61	62	63	64	65	66	67	68	69	70	71

J

0	1.01E+03	1.05E+03	1.09E+03	1.13E+03	1.18E+03	1.23E+03	1.25E+03	1.22E+03	1.20E+03	1.18E+03	1.16E+03	1.15E+03
40	1.01E+03	1.05E+03	1.09E+03	1.13E+03	1.18E+03	1.23E+03	1.25E+03	1.22E+03	1.20E+03	1.18E+03	1.16E+03	1.15E+03
39	9.68E+02	1.00E+03	1.04E+03	1.08E+03	1.12E+03	1.16E+03	1.22E+03	1.20E+03	1.18E+03	1.16E+03	1.14E+03	1.14E+03
38	9.30E+02	9.59E+02	9.90E+02	1.02E+03	1.06E+03	1.10E+03	1.16E+03	1.18E+03	1.16E+03	1.14E+03	1.13E+03	1.13E+03
37	8.95E+02	9.20E+02	9.47E+02	9.77E+02	1.01E+03	1.05E+03	1.11E+03	1.16E+03	1.14E+03	1.12E+03	1.12E+03	1.13E+03
36	8.63E+02	8.85E+02	9.09E+02	9.36E+02	9.70E+02	1.01E+03	1.07E+03	1.14E+03	1.12E+03	1.11E+03	1.11E+03	1.13E+03
35	8.35E+02	8.53E+02	8.74E+02	9.01E+02	9.34E+02	9.78E+02	1.04E+03	1.12E+03	1.11E+03	1.10E+03	1.11E+03	1.13E+03
34	8.08E+02	8.24E+02	8.44E+02	8.70E+02	9.04E+02	9.51E+02	1.02E+03	1.10E+03	1.10E+03	1.10E+03	1.11E+03	1.13E+03
33	7.82E+02	7.97E+02	8.17E+02	8.43E+02	8.81E+02	9.32E+02	1.00E+03	1.09E+03	1.09E+03	1.10E+03	1.12E+03	1.14E+03
32	7.58E+02	7.72E+02	7.93E+02	8.22E+02	8.63E+02	9.20E+02	9.97E+02	1.09E+03	1.09E+03	1.10E+03	1.12E+03	1.14E+03
31	7.35E+02	7.50E+02	7.72E+02	8.05E+02	8.51E+02	9.14E+02	9.97E+02	1.08E+03	1.09E+03	1.10E+03	1.12E+03	1.15E+03
30	7.13E+02	7.29E+02	7.55E+02	7.92E+02	8.43E+02	9.11E+02	9.98E+02	1.08E+03	1.09E+03	1.10E+03	1.12E+03	1.15E+03
29	6.93E+02	7.12E+02	7.41E+02	7.82E+02	8.37E+02	9.08E+02	9.99E+02	1.08E+03	1.09E+03	1.10E+03	1.12E+03	1.15E+03
28	6.74E+02	6.96E+02	7.29E+02	7.73E+02	8.31E+02	9.05E+02	9.97E+02	1.07E+03	1.08E+03	1.10E+03	1.12E+03	1.15E+03
27	6.58E+02	6.83E+02	7.18E+02	7.64E+02	8.23E+02	8.98E+02	9.91E+02	1.07E+03	1.08E+03	1.09E+03	1.12E+03	1.14E+03
26	6.44E+02	6.71E+02	7.07E+02	7.54E+02	8.14E+02	8.88E+02	9.80E+02	1.06E+03	1.07E+03	1.09E+03	1.11E+03	1.13E+03

25	6.31E+02	6.59E+02	6.95E+02	7.42E+02	8.01E+02	8.75E-02	9.66E+02	1.05E+03	1.06E+03	1.08E-03	1.10E-03	1.13E-03	
24	6.18E+02	6.46E+02	6.82E+02	7.28E+02	7.86E-02	8.58E+02	9.48E+02	1.04E-03	1.05E+03	1.07E+03	1.09E-03	1.12E-03	
23	6.06E+02	6.33E+02	6.68E+02	7.13E+02	7.69E+02	8.39E-02	9.26E-02	1.03E+03	1.04E-03	1.06E+03	1.08E-03	1.11E-03	
22	5.92E+02	6.18E+02	6.52E+02	6.95E+02	7.50E+02	8.18E+02	9.02E+02	1.01E+03	1.03E-03	1.05E+03	1.07E-03	1.10E-03	
21	5.79E+02	6.03E+02	6.36E+02	6.77E+02	7.29E+02	7.94E+02	8.76E+02	9.77E+02	1.02E+03	1.04E-03	1.06E+03	1.08E-03	
20	5.65E+02	5.88E+02	6.18E+02	6.58E+02	7.07E+02	7.69E+02	8.47E+02	9.45E+02	1.00E-03	1.02E+03	1.04E-03	1.07E-03	
19	5.50E+02	5.72E+02	6.01E+02	6.37E+02	6.84E-02	7.43E+02	8.17E+02	9.10E+02	9.90E-02	1.01E+03	1.03E+03	1.05E-03	
18	5.35E+02	5.56E+02	5.82E+02	6.17E+02	6.61E+02	7.16E+02	7.86E+02	8.74E+02	9.74E+02	9.89E-02	1.01E-03	1.04E-03	
17	5.21E-02	5.39E+02	5.64E+02	5.96E+02	6.37E+02	6.89E-02	7.54E+02	8.37E+02	9.42E+02	9.72E+02	9.93E-02	1.02E-03	
16	5.06E+02	5.22E+02	5.45E+02	5.75E+02	6.13E-02	6.61E+02	7.22E+02	7.99E+02	8.97E+02	9.53E+02	9.73E-02	9.99E-02	
15	4.91E+02	5.06E-02	5.27E+02	5.54E+02	5.89E+02	6.33E+02	6.89E+02	7.61E-02	8.53E+02	9.34E-02	9.53E-02	9.78E-02	
14	4.77E+02	4.90E+02	5.09E+02	5.33E+02	5.65E-02	6.05E+02	6.57E+02	7.23E+02	8.08E+02	9.14E-02	9.31E-02	9.56E-02	
13	4.63E+02	4.75E+02	4.91E+02	5.13E+02	5.42E+02	5.78E+02	6.26E+02	6.86E+02	7.64E-02	8.65E+02	9.09E+02	9.33E-02	
12	4.51E+02	4.61E+02	4.75E+02	4.94E-02	5.20E-02	5.53E+02	5.95E+02	6.50E+02	7.21E+02	8.13E+02	8.87E-02	9.09E-02	
11	4.39E+02	4.47E+02	4.59E+02	4.76E+02	4.99E+02	5.28E+02	5.66E+02	6.15E+02	6.79E+02	7.63E-02	8.64E+02	8.85E-02	
10	4.28E+02	4.35E+02	4.45E+02	4.59E+02	4.79E+02	5.05E+02	5.38E+02	5.82E+02	6.40E+02	7.16E+02	8.17E+02	8.61E+02	
9	4.19E+02	4.23E+02	4.32E+02	4.44E+02	4.61E+02	4.83E+02	5.13E+02	5.52E+02	6.03E+02	6.71E+02	7.62E+02	8.37E-02	
8	4.10E+02	4.14E+02	4.20E+02	4.30E+02	4.44E+02	4.63E+02	4.89E+02	5.23E+02	5.69E+02	6.29E+02	7.10E+02	8.13E+02	
7	4.03E+02	4.05E+02	4.09E+02	4.17E+02	4.29E+02	4.45E+02	4.68E+02	4.98E+02	5.37E+02	5.91E+02	6.63E+02	7.62E-02	
6	3.98E+02	3.98E+02	4.00E+02	4.06E+02	4.16E+02	4.29E+02	4.49E+02	4.74E+02	5.09E+02	5.55E+02	6.19E+02	7.07E+02	
5	3.93E+02	3.92E+02	3.93E+02	3.97E+02	4.04E+02	4.15E+02	4.31E+02	4.53E+02	4.83E+02	5.24E+02	5.79E+02	6.57E-02	
4	3.89E+02	3.87E+02	3.86E+02	3.88E+02	3.94E+02	4.03E+02	4.16E+02	4.35E+02	4.60E+02	4.95E+02	5.44E+02	6.11E+02	
3	3.86E+02	3.83E+02	3.81E+02	3.82E+02	3.85E+02	3.92E+02	4.03E+02	4.18E+02	4.40E+02	4.70E+02	5.12E+02	5.70E+02	
2	3.83E+02	3.79E+02	3.77E+02	3.76E+02	3.78E+02	3.83E+02	3.91E+02	4.04E+02	4.22E+02	4.48E+02	4.84E+02	5.34E+02	
1	3.80E+02	3.76E+02	3.73E+02	3.71E+02	3.71E+02	3.75E+02	3.81E+02	3.91E+02	4.07E+02	4.29E+02	4.59E+02	5.02E+02	
0	3.77E+02	3.73E+02	3.70E+02	3.67E+02	3.66E+02	3.68E+02	3.73E+02	3.81E+02	3.94E+02	4.13E+02	4.39E+02	4.76E+02	
I=	72	73	74	75	76	77	78	79	80	81	82	83	

J

0	1.15E+03	1.16E+03	1.18E+03	1.20E+03	1.22E+03	1.25E+03	1.34E+03	1.45E+03	1.61E+03	1.73E+03	1.63E+03	1.54E+03	
40	1.15E+03	1.16E+03	1.18E+03	1.20E+03	1.22E+03	1.25E+03	1.34E+03	1.45E+03	1.61E+03	1.73E+03	1.63E+03	1.54E+03	
39	1.15E+03	1.16E+03	1.18E+03	1.20E+03	1.22E+03	1.26E+03	1.34E+03	1.46E+03	1.63E+03	1.73E+03	1.63E+03	1.53E+03	
38	1.14E+03	1.16E+03	1.18E+03	1.21E+03	1.23E+03	1.27E+03	1.35E+03	1.48E+03	1.64E+03	1.72E+03	1.62E+03	1.52E+03	
37	1.14E+03	1.16E+03	1.19E+03	1.21E+03	1.24E+03	1.28E+03	1.37E+03	1.49E+03	1.66E+03	1.72E+03	1.61E+03	1.51E+03	
36	1.15E+03	1.17E+03	1.20E+03	1.22E+03	1.24E+03	1.29E+03	1.38E+03	1.51E+03	1.68E+03	1.71E+03	1.60E-03	1.50E+03	
35	1.15E+03	1.18E+03	1.20E+03	1.23E+03	1.25E+03	1.30E+03	1.39E+03	1.52E+03	1.70E+03	1.70E+03	1.59E+03	1.49E+03	
34	1.16E+03	1.18E+03	1.21E+03	1.23E+03	1.25E+03	1.31E+03	1.41E+03	1.54E+03	1.72E+03	1.69E+03	1.57E+03	1.47E-03	
33	1.16E+03	1.19E+03	1.21E+03	1.24E+03	1.25E+03	1.32E+03	1.42E+03	1.55E+03	1.74E+03	1.67E+03	1.56E+03	1.46E+03	
32	1.17E+03	1.19E+03	1.22E+03	1.24E+03	1.26E+03	1.33E+03	1.43E+03	1.57E+03	1.76E+03	1.66E+03	1.54E+03	1.44E+03	
31	1.17E+03	1.20E+03	1.22E+03	1.24E+03	1.26E+03	1.33E+03	1.44E+03	1.58E+03	1.75E+03	1.64E+03	1.53E+03	1.43E+03	
30	1.17E+03	1.20E+03	1.22E+03	1.24E+03	1.26E+03	1.34E+03	1.44E+03	1.59E+03	1.74E+03	1.63E+03	1.51E+03	1.41E+03	
29	1.17E+03	1.19E+03	1.22E+03	1.23E+03	1.26E+03	1.34E+03	1.45E+03	1.60E+03	1.73E+03	1.61E+03	1.50E+03	1.39E+03	
28	1.17E+03	1.19E+03	1.21E+03	1.23E+03	1.26E+03	1.34E+03	1.45E+03	1.60E+03	1.71E+03	1.60E+03	1.48E+03	1.38E+03	
27	1.16E+03	1.19E+03	1.21E+03	1.22E+03	1.25E+03	1.33E+03	1.45E+03	1.60E+03	1.70E+03	1.58E+03	1.47E+03	1.36E+03	
26	1.16E+03	1.18E+03	1.20E+03	1.22E+03	1.25E+03	1.33E+03	1.44E+03	1.60E+03	1.69E+03	1.57E+03	1.45E+03	1.35E+03	
25	1.15E+03	1.17E+03	1.19E+03	1.21E+03	1.24E+03	1.32E+03	1.43E+03	1.60E+03	1.68E+03	1.56E+03	1.44E+03	1.34E+03	
24	1.14E+03	1.16E+03	1.19E+03	1.20E+03	1.23E+03	1.31E+03	1.42E+03	1.59E+03	1.67E+03	1.55E+03	1.43E+03	1.32E+03	
23	1.13E+03	1.16E+03	1.18E+03	1.19E+03	1.21E+03	1.29E+03	1.41E+03	1.58E+03	1.66E+03	1.54E+03	1.42E+03	1.31E+03	
22	1.12E+03	1.14E+03	1.17E+03	1.18E+03	1.20E+03	1.27E+03	1.39E+03	1.56E+03	1.66E+03	1.53E+03	1.41E+03	1.30E+03	
21	1.11E+03	1.13E+03	1.15E+03	1.17E+03	1.19E+03	1.26E+03	1.37E+03	1.54E+03	1.65E+03	1.52E+03	1.40E+03	1.29E+03	
20	1.09E+03	1.12E+03	1.14E+03	1.16E+03	1.18E+03	1.23E+03	1.35E+03	1.52E+03	1.65E+03	1.52E+03	1.39E+03	1.28E+03	
19	1.08E+03	1.10E+03	1.13E+03	1.15E+03	1.16E+03	1.21E+03	1.32E+03	1.49E+03	1.65E+03	1.51E+03	1.38E+03	1.28E+03	
18	1.06E+03	1.09E+03	1.11E+03	1.14E+03	1.15E+03	1.19E+03	1.30E+03	1.46E+03	1.65E+03	1.51E+03	1.38E+03	1.27E+03	
17	1.05E+03	1.07E+03	1.10E+03	1.12E+03	1.14E+03	1.16E+03	1.27E+03	1.43E+03	1.65E+03	1.51E+03	1.37E+03	1.26E+03	
16	1.03E+03	1.05E+03	1.08E+03	1.11E+03	1.13E+03	1.14E+03	1.23E+03	1.40E+03	1.64E+03	1.51E+03	1.37E+03	1.26E+03	
15	1.01E+03	1.04E+03	1.06E+03	1.09E+03	1.11E+03	1.13E+03	1.20E+03	1.36E+03	1.60E+03	1.51E+03	1.37E+03	1.25E+03	
14	9.84E+02	1.01E+03	1.04E+03	1.07E+03	1.10E+03	1.11E+03	1.17E+03	1.32E+03	1.56E+03	1.51E+03	1.37E+03	1.25E+03	
13	9.62E+02	9.92E+02	1.02E+03	1.05E+03	1.08E+03	1.10E+03	1.13E+03	1.28E+03	1.51E+03	1.52E+03	1.37E+03	1.25E+03	
12	9.38E+02	9.69E+02	1.00E+03	1.03E+03	1.06E+03	1.09E+03	1.10E+03	1.24E+03	1.47E+03	1.53E+03	1.37E+03	1.25E+03	
11	9.13E+02	9.45E+02	9.79E+02	1.01E+03	1.04E+03	1.07E+03	1.09E+03	1.20E+03	1.42E+03	1.53E+03	1.37E+03	1.25E+03	
10	8.88E+02	9.20E+02	9.55E+02	9.90E+02	1.02E+03	1.05E+03	1.08E+03	1.16E+03	1.37E+03	1.54E+03	1.38E+03	1.25E+03	
9	8.62E+02	8.94E+02	9.30E+02	9.67E+02	1.00E+03	1.04E+03	1.06E+03	1.11E+03	1.33E+03	1.56E+03	1.38E+03	1.25E+03	
8	8.37E+02	8.68E+02	9.04E+02	9.43E+02	9.82E+02	1.02E+03	1.05E+03	1.07E+03	1.28E+03	1.57E+03	1.39E+03	1.25E+03	
7	8.12E+02	8.42E+02	8.78E+02	9.19E+02	9.60E+02	1.00E+03	1.03E+03	1.06E+03	1.23E+03	1.56E+03	1.40E+03	1.25E+03	
6	7.87E+02	8.16E+02	8.52E+02	8.93E+02	9.37E+02	9.80E+02	1.02E+03	1.05E+03	1.19E+03	1.51E+03	1.41E+03	1.25E+03	
5	7.65E+02	7.90E+02	8.25E+02	8.67E+02	9.13E+02	9.60E+02	1.00E+03	1.03E+03	1.14E+03	1.46E+03	1.42E+03	1.26E+03	
4	7.08E+02	7.66E+02	7.99E+02	8.41E+02	8.88E+02	9.38E+02	9.86E+02	1.02E+03	1.10E+03	1.41E+03	1.43E+03	1.26E+03	
3	6.54E+02	7.44E+02	7.74E+02	8.15E+02	8.63E+02	9.15E+02	9.67E+02	1.01E+03	1.05E+03	1.36E+03	1.44E+03	1.26E+03	
2	6.07E+02	7.15E+02	7.50E+02	7.89E+02	8.37E+02	8.92E+02	9.48E+02	9.97E+02	1.03E+03	1.31E+03	1.45E+03	1.27E+03	
1	5.65E+02	6.58E+02	7.29E+02	7.65E+02	8.12E+02	8.68E+02	9.28E+02	9.83E+02	1.02E+03	1.26E+03	1.47E+03	1.27E+03	

```
 0  5.29E+02 6.10E+02 7.11E+02 7.43E+02 7.88E+02 8.44E-02 9.07E+02 9.67E-02 1.01E-03 1.21E-03 1.48E-03 1.28E-03
 I =   84     85     86     87     88     89     90     91     92     93     94     95


 J
  0  1.46E-03 1.39E+03 1.34E+03 1.31E+03 1.29E+03 2.88E+02
 40  1.46E+03 1.39E+03 1.34E+03 1.31E+03 1.29E+03 1.29E+03
 39  1.45E+03 1.38E+03 1.33E+03 1.30E+03 1.28E+03 1.28E+03
 38  1.44E-03 1.37E+03 1.32E+03 1.28E+03 1.26E-03 1.26E-03
 37  1.43E+03 1.36E+03 1.31E+03 1.27E+03 1.25E+03 1.25E+03
 36  1.42E+03 1.35E+03 1.29E+03 1.26E+03 1.24E-03 1.24E+03
 35  1.40E+03 1.33E+03 1.28E+03 1.24E+03 1.22E+03 1.22E+03
 34  1.39E+03 1.32E+03 1.26E+03 1.23E+03 1.21E+03 1.21E+03
 33  1.37E+03 1.30E+03 1.25E+03 1.21E+03 1.19E+03 1.19E+03
 32  1.36E+03 1.29E+03 1.23E+03 1.20E+03 1.18E+03 1.18E+03
 31  1.34E+03 1.27E+03 1.22E+03 1.19E+03 1.17E+03 1.17E+03
 30  1.32E+03 1.26E+03 1.21E+03 1.17E+03 1.15E+03 1.15E+03
 29  1.31E+03 1.24E+03 1.19E+03 1.16E+03 1.14E+03 1.14E+03
 28  1.29E+03 1.23E+03 1.18E+03 1.15E+03 1.13E+03 1.13E+03
 27  1.28E+03 1.21E+03 1.17E+03 1.13E+03 1.12E+03 1.12E+03
 26  1.27E+03 1.20E+03 1.15E+03 1.12E+03 1.11E+03 1.11E+03
 25  1.25E+03 1.19E+03 1.14E+03 1.11E+03 1.09E+03 1.09E+03
 24  1.24E+03 1.18E+03 1.13E+03 1.10E+03 1.08E+03 1.08E+03
 23  1.23E+03 1.17E+03 1.12E+03 1.09E+03 1.07E+03 1.07E+03
 22  1.22E+03 1.16E+03 1.11E+03 1.08E+03 1.06E+03 1.06E+03
 21  1.21E+03 1.15E+03 1.10E+03 1.07E+03 1.05E+03 1.05E+03
 20  1.20E+03 1.14E+03 1.09E+03 1.06E+03 1.05E+03 1.05E+03
 19  1.19E+03 1.13E+03 1.08E+03 1.05E+03 1.04E+03 1.04E+03
 18  1.18E+03 1.12E+03 1.07E+03 1.04E+03 1.03E+03 1.03E+03
 17  1.18E+03 1.11E+03 1.07E+03 1.04E+03 1.02E+03 1.02E+03
 16  1.17E+03 1.11E+03 1.06E+03 1.03E+03 1.01E+03 1.01E+03
 15  1.17E+03 1.10E+03 1.05E+03 1.02E+03 1.00E+03 1.00E+03
 14  1.16E+03 1.09E+03 1.04E+03 1.01E+03 9.97E+02 9.97E+02
 13  1.16E+03 1.09E+03 1.04E+03 1.00E+03 9.89E+02 9.89E+02
 12  1.15E+03 1.08E+03 1.03E+03 9.98E+02 9.81E+02 9.81E+02
 11  1.15E+03 1.08E+03 1.02E+03 9.90E+02 9.74E+02 9.74E+02
 10  1.15E+03 1.07E+03 1.02E+03 9.83E+02 9.66E+02 9.66E+02
  9  1.14E+03 1.07E+03 1.01E+03 9.75E+02 9.58E+02 9.58E+02
  8  1.14E+03 1.06E+03 1.00E+03 9.68E+02 9.50E+02 9.50E+02
  7  1.14E+03 1.06E+03 9.98E+02 9.60E+02 9.42E+02 9.42E+02
  6  1.14E+03 1.05E+03 9.92E+02 9.53E+02 9.33E+02 9.33E+02
  5  1.14E+03 1.05E+03 9.85E+02 9.44E+02 9.25E+02 9.25E+02
  4  1.13E+03 1.04E+03 9.78E+02 9.36E+02 9.15E+02 9.15E+02
  3  1.13E+03 1.04E+03 9.71E+02 9.27E+02 9.06E+02 9.06E+02
  2  1.13E+03 1.03E+03 9.63E+02 9.18E+02 8.95E+02 8.95E+02
  1  1.13E+03 1.03E+03 9.55E+02 9.08E+02 8.85E+02 8.85E+02
  0  1.13E+03 1.02E+03 9.46E+02 8.97E+02 8.73E+02 2.88E+02
 I =   96     97     98     99     100    0

 TOTAL REAL     WORKSPACE USED =  4524027
 TOTAL INTEGER  WORKSPACE USED =  1575997
 TOTAL CHARACTER WORKSPACE USED =      731


 TOTAL CPU TIME =   6.293E+03 SECONDS

 CFDS-FLOW3D 3.3 finished on Sat Mar 11 17:14:00 EST 1995
```